DEVELOPMENT OF NOVEL APPROACHES FOR THE SYNTHESIS OF GLYCATED/GLYCOSYLATED PROTEINS OF POTENTIAL APPLICATIONS AS FOOD INGREDIENTS AND NUTRACEUTICALS

by

Sooyoun Seo

Department of Food Science and Agricultural Chemistry

Macdonald Campus, McGill University

Quebec, Canada

April, 2014

A thesis submitted to McGill University in partial fulfillment of the requirements of the degree of Doctor of Philosophy in Food Science and Agricultural Chemistry

SUGGESTED SHORT TITLE

Synthesis of Glycated/Glycosylated Proteins with Improved Functional Properties

ABSTRACT

Lysozymes (LZM) conjugated with galactose, galactooligosaccharides (GOS), and galactan through the Maillard reaction were produced. Mass spectrometry analyses revealed the formation of LZM conjugated to up to 8 galactose moieties and to up to 4 GOS. LZM was conjugated to 3 galactan. The produced LZM:galactan conjugates exhibited higher solubility, thermal stability and emulsion stability as compared to the native LZM. LZM:GOS conjugates demonstrated most improvement in emulsifying properties. The immunoreactivity of all conjugates decreased as compared to the native LZM. The optimization of the production of LZM:GOS conjugates by response surface methodology revealed that molar ratio and temperature were the most significant variables affecting the glycation of LZM with GOS.

Patatin (PTT) conjugated with galactose, GOS, and galactan through the Maillard reaction were produced. The results revealed important changes in tertiary structure and in total secondary structures upon glycation with GOS (61.2%) and galactan (36.7%). Upon glycation, more heat stable forms of PTT, with higher unfolding temperature (70–90°C), were obtained compared to the native protein (50–70°C). The conjugates exhibited also higher antioxidant activity (IC_{50} of 11.25–49.6 μM) than the native PTT (93.1 μM). PTT demonstrated an increase in immunoreactivity when it was conjugated to galactose and to GOS as compared to the native protein (IC_{50} of 0.70, 0.38, 1.19 μg/ml, respectively). The digestion of the PTT conjugates (14.2–29.5%) was less effective than the native PTT (59.6%), leading to significantly smaller decreases (2.76–4.90 μg/ml) in the immunoreactivity as compared to the native PTT (7.75 μg/ml). Selected Maillard reaction inhibitors, including aminoguanidine, cysteine, pyridoxamine, and sodium bisulfite, were evaluated for the efficient production of low cross-linked PTT:carbohydrate conjugates. The results revealed 65.1 and 67.2% decreases in protein cross-linking and 60.2 and 2.6% increases in the percent blocked lysine of PTT:GOS and PTT:xylooligosaccharides conjugates in the presence of cysteine and aminoguanidine, respectively. The use of these inhibitors led to an increase in the protein digestibility (0.4–9.3% per 5% blocked lysine). Given the success of the use of Maillard reaction inhibitors for the production of PTT:carbohydrate conjugates, the production of PTT:galactose/xylose was optimized through response surface methodology using a mixture of cysteine and sodium bisulfite. The incubation time was identified as the most important parameter affecting the percent blocked lysine, whereas the

cysteine to sodium bisulfite inhibitor ratio was identified as the most important parameter affecting the particle size distribution of conjugates.

The galactosylated serine/threonine derivatives were synthesized through *Escherichia coli* β-galactosidase-catalyzed glycosylation. The highest yield (23.2%) of transgalactosylated *N*-carboxy benzyl serine methyl ester was achieved in heptane:buffer biphasic reaction system, when *o*-nitrophenyl-β-galactoside was used as donor. The results also revealed the importance of protecting groups of amino acid derivatives for the improvement of their transgalactosylation yields. The binding of the investigated serine and threonine derivatives to the enzyme's active site were stronger (-4.6–-7.9 kcal/mol) than the natural leaving group, glucose. For *N*-*tert*-butoxy carbonyl serine methyl ester (6.8%) and *N*-carboxy benzyl serine benzyl ester (3.4%), their binding affinities and the distances between their hydroxyl side chain and the 1'-OH group of galactose moiety were in good accordance with the quantified transgalactosylation yields. However, the high bioconversion yield obtained with *N*-carboxy benzyl serine methyl ester (23.2%) despite its unfavorable theoretical predictions by the docking simulations demonstrated the importance of the thermodynamically driven nature of the transgalactosylation reaction.

RÉSUMÉ

Les lysozymes (LZM), conjugués avec le galactose, les galactooligosaccharides (GOS), et la galactane par la réaction de Maillard, ont été produits. Les analyses par la spectrométrie de masse ont révélé que les LZM ont été conjugués avec un maximum de 8 substituents de galactose et de 4 GOS. Trois galactanes ont été conjuguées à la LZM. Le conjugué LZM:galactane a démontré une grande solubilité, une bonne stabilité thermique et une grande stabilité de l'émulsion formée par rapport aux protéines natives. L'immuno-réactivité de tous les produits conjugués a diminué par rapport à celle d'un LZM naturel. L'optimisation de la production des conjugués LZM:GOS par la méthodologie de surface des réponses a révélée que le rapport molaire et la température sont les variables les plus importantes qui affectent les paramètres de la glycation de la LZM avec les GOS.

Les patatines (PTT) conjuguées avec le galactose, les GOS et la galactane par la réaction de Maillard ont été produites. Les résultats ont révélé des changements importants dans les structures secondaires totales causés par la glycation avec les GOS (61,2 %) et avec la galactane (36,7 %). Après la glycation, des formes de PTT conjugées thermostables ont été obtenues avec une température de dénaturation plus élevée (70–90°C) que celle de la protéine native (50–70°C). Les PTT conjuguées ont aussi démontré une activité anti-oxydante supérieure (IC_{50} de 11,25–49,6 μM) que celle de la PTT native (93,1 μM). Bien que l'immuno-réactivité a diminué après un traitement thermique de la PTT native (IC_{50} de 2,77 μg/ml), elle a augmenté lorsque la PTT a été conjuguée avec les GOS (0,03 μg/ml). Des inhibiteurs de la réaction de Maillard sélectionnés, tels que l'aminoguanidine, la cystéine, la pyridoxamine, et le bisulfite de sodium, ont été évalués pour produire, d'une façon plus efficace, des conjugués PTT. Les résultats ont révélé des diminutions de 65.1 et de 67.2% de réticulation des protéines et des augmentations de 60.2 à 2.6% des lysines bloquées des conjugués PTT:GOS and PTT:xylooligosaccharides en présence de la cystéine et de l'aminoguanidine, respectivement. Vue le succès de l'utilisation des inhibiteurs de la réaction de Maillard pour la production de conjugués de PTT:glucides, la production des conjugués PTT:galactose/xylose a été optimisée, avec la méthodologie de surface de réponse, en utilisant une combinaison de la cystéine et du bisulfite de sodium. Le temps d'incubation a été identifié comme étant le paramètre le plus important qui affecte le pourcentage

des lysines bloquées, et le rapport des inhibiteurs a été identifié comme étant le paramètre le plus important qui influence la taille des particules.

Les dérivés galactosylées de la sérine/thréonine ont été synthétisés à travers une réaction de transgalactosylation catalysée par une *β*-galactosidase de l'*Escherichia coli*. Le rendement le plus élevé (23,2%) d'ester méthylique de serine benzyle carboxylique galactosylée a été obtenu dans un système réactionnel biphasique composé de l'heptane et de la solution tampon lors de l'utilisation de l'*o*-nitrophényl-*β*-galactoside en tant que donneur. L'affinité de fixation des dérivés de sérine et de thréonine au site actif de l'enzyme a été généralement plus élevée (4,6 à 7,9 kcal/mol) que celle du groupe naturel, le glucose. Pour l'ester méthylique de serine butoxyle carbonylique (6,8%) et l'ester benzylique de serine benzyle carboxylique (3,4%), leurs affinités de fixation au site actif de l'enzyme et les distances entre leurs chaînes latérales hydroxyle et le groupe 1'-OH du fragment du galactose ont été en accord avec les rendements de transgalactosylation quantifiés. Toutefois, le haut rendement de bioconversion obtenu avec l'ester méthylique de serine benzyle carboxylique (23,2%) malgré ses prédictions théoriques défavorables par la simulation interactive de l'assemblage moléculaire a démontré l'importance de la nature thermodynamique de la réaction de transgalactosylation.

STATEMENT FROM THE THESIS OFFICE

According to the regulations of the Faculty of Graduate Studies and Research of McGill University, Guidelines for Thesis Preparation include:

Candidates have the option of including, as part of the thesis, the text of one or more papers submitted, or to be submitted, for publication, or the clearly-duplicated text of one or more published papers. These texts must conform to the "Guidelines for Thesis Preparation" and must be bound together as an integral part of the thesis.

The thesis must be more than a collection of manuscripts. All components must be integrated into a cohesive unit with a logical progression from one chapter to the next. In order to ensure that the thesis has continuity, connecting texts that provide logical bridges between the different papers are mandatory.

The thesis must conform to all other requirements of the "Guidelines for Thesis Preparation" in addition to the manuscripts.

As manuscripts for publication are frequently very concise documents, where appropriate, additional material must be provided in sufficient detail to allow a clear and precise judgement to be made of the importance and originality of the research reported in the thesis.

In general when co-authored papers are included in a thesis, the candidate must have made a substantial contribution to all papers included in the thesis. In addition, the candidate is required to make an explicit statement in the thesis as to who contributed to such work and to what extent. This statement should appear in a single section entitled "Contribution of Authors" as a preface of the thesis.

When previously published copyright material is presented in a thesis, the candidate must obtain, if necessary, signed waivers from the co-authors and publishers and submit these to the Thesis Office with the final deposition.

CONTRIBUTION OF AUTHORS

The present thesis consists of eleven chapters.

Chapter I provides a general introduction and a short literature review on the field, and outlines the objectives of the study.

Chapter II reports on the literature review of protein:carbohydrate conjugate production through the Maillard reaction and through the enzymatic glycosylation. An explanation of the chemistry involved in the Maillard reaction, the factors affecting the Maillard reaction, and the Maillard reaction inhibitors are provided. A brief explanation of the transgalactosylation mechanism of β-galactosidase is presented and the computational docking analysis method for the structural analysis of the enzyme and its substrates is introduced. The functional properties that can be improved upon carbohydrate conjugation are outlined. The target proteins that will be investigated in this study are presented. The chapter ends by demonstrating some of the analytical techniques used to characterize protein–carbohydrate conjugates.

Chapter III to IX are presented in the form of manuscripts, and have been or will be submitted for publication. The connecting statements in between the chapters provide the rationale linking the different chapters presented in this study. Chapter III covers the production of lysozyme (LZM):carbohydrate conjugates and their structural and functional properties. Chapter IV describes the optimization of the production of LZM:carbohydrate conjugates. Chapter V presents the production of patatin (PTT):carbohydrate conjugates and their structural and functional properties. Chapter VI deals with the effect of PTT glycation on its immunoreactivity. Chapter VII demonstrates the effect of Maillard reaction inhibitors on the production of PTT:carbohydrate conjugates. Chapter VIII covers the optimization of the production of PTT:carbohydrate conjugates using Maillard reaction inhibitors. Finally, Chapter IX reports on the production of galactosylated serine/threonine derivatives through β-galactosidase-catalyzed glycosylation.

Chapter X provides a general conclusion to the thesis with a summary of major findings.

Chapter XI outlines the contribution of this study to the field and gives recommendations regarding the direction of future research in the topic of protein:carbohydrate conjugate production.

Sooyoun Seo, the author, was responsible for the experimental work and the preparation of the manuscripts for publication and dissertation.

Dr. Salwa Karboune, the supervisor of the author's PhD work, guided all the research and critically revised the manuscripts prior to their submission.

Dr. Lamia L'Hocine, the fourth author of manuscripts #1 (Chapter IV), the third author of manuscript #2 (Chapters III), and the second author of manuscript #4 (Chapter VI), guided the research work related to the immunoreactivity of the proteins. She was involved in the revision of manuscript#4.

Dr. Varoujan Yalayan, the third author of manuscripts #1 (Chapter IV) and the fourth author of manuscript #2 (Chapter III) reviewed the manuscripts before their submission for publication.

Dr. Alain Archelas, the third author of manuscript #3 (Chapter V), provided technical support for the structural analysis of proteins.

Dr. Josef Rebehmed and Dr. Alexandre de Brevern, the co-authors of manuscript #7 (Chapter IX), performed the computational analysis.

PUBLICATIONS

1. **Seo, S.**, Karboune, S., Yaylayan, V. A., & L'Hocine, L. (2012). Glycation of lysozyme with galactose, galactooligosaccharides and potato galactan through the Maillard reaction and optimization of the production of prebiotic glycoproteins. *Process Biochemistry, 47*(2), 297–304.

2. **Seo, S.**, Karboune, S., L'Hocine, L., & Yaylayan, V. (2013). Characterization of glycated lysozyme with galactose, galactooligosaccharides and galactan: Effect of glycation on structural and functional properties of conjugates. *LWT – Food Science and Technology, 53*(1), 44–53.

3. **Seo, S.**, Karboune, S., & Archelas, A. (2014). Production and characterization of potato patatin:galactose, galatooligosaccharides, and galactan conjugates of great potential as functional ingredients. *Food Chemistry, 158*(1), 480–489.

4. **Seo, S.**, L'Hocine, L., & Karboune, S. (2014). Allergenicity of potato proteins and of their conjugates with galactose, galactooligosaccharides, and galactan in native, heated, and digested forms. *Journal of Agricultural and Food Chemistry, 62*(16), 3591-3598.

5. **Seo, S.**, & Karboune, S. (2014). Investigation of the use of Maillard reaction inhibitors for the production of patatin:carbohydrate conjugates. (To be Submitted).

6. **Seo, S.**, & Karboune, S. (2014). Optimization of the production of patatin-galatose/xylose conjugates, by the combined use of L-cysteine and sodium bisulfite inhibitors, through response surface methodology. (To be Submitted).

7. **Seo, S.**, Rebehmed, J., de Brevern, A., Karboune, S. (2014) Enzymatic synthesis of galactosylated serine/threonine derivatives using *β*-galactosidase from *Escherichia coli*. (To be submitted).

ACKNOWLEDGEMENTS

First of all, I would like to express my utmost gratitude to my supervisor Dr. Salwa Karboune, for her support and guidance during my graduate studies.

I would like to thank Dr. Lamia L'Hocine for her guidance for the research work related to the assessement of the immunoreactivity and Ms. Mélanie Pitre for her support during my time working at the Food Research and Development Centre in St-Hyacinthe, Qc.

I am thankful to Dr. Alan Archelas for his help and to his research team at ISM2 (University of Aix-Marseille) for making me feel at home during my stay in Marseille, France.

I would like to thank Dr. Rebehmed and Dr. de Brevern at INSERM for their help with the molecular docking analysis.

I am extremely grateful to the present and past administrative staff at the Department of Food Science and Agricultural Chemistry, particularly Ms. Leslie Ann LaDuke and Ms. Diane Chan-Hum, for their help throughout my graduate studies.

I wish to thank all my previous and present colleages, Jessica Couto, Lotthida Inthanavong, Dr. Feng Tian, Nastaran Khodaei, Amanda Waglay, Juan Tamayo, Andrea Hill, Mengxi Li, Jin Li, Afshan Malick, Dr. Maryam Khodadadi and also my previous interns, Adeline Bayle, Francine Gabrielle Ngaleu, and Elaine Chan for their constant technical and moral support, and for their friendship during my graduate studies. They were there for me when I was going through difficult times and they have immensely contributed towards my growth as a better person.

I am infinitely thankful to my sister and to my parents for giving me their unconditional love. And finally, to my significant other, thank you.

TABLE OF CONTENTS

LIST OF FIGURES

CHAPTER II

CHAPTER III

CHAPTER IV

CHAPTER V

CHAPTER VI

CHAPTER VIII

CHAPTER IX

LIST OF TABLES

CHAPTER VII

CHAPTER VIII

CHAPTER IX

NOMENCLATURE/LIST OF ABBREVIATIONS

a_w	Water activity
Amu	Atomic mass unit
ANOVA	Analysis of variance
Arg	Arginine
CCD	Central composite design
CCRD	Central composite rotatable design
Cys	Cysteine
DP	Degree of polymerization
DPPH	2,2-Diphenyl-1-picrylhydrazyl
EC number	Enzyme classification number
ESI	Electrospray ionization
FPLC	Fast protein liquid chromatography
His	Histidine
HPLC	High-performance liquid chromatography
Glu	Glutamic acid
GOS	Galactooligosaccharides
kDa	Kilodalton
IC_{50}	Half maximal inhibitory concentration
Lys	Lysine
LZM	Lysozyme
MALDI	Matrix-assisted laser desorption/ionization
MS	Mass spectrometry
MW	Molecular weight
N-Boc-Ser-OMe	*N*-*tert*-butoxy-carbonyl L-serine methyl ester
N-Boc-Ser-OH	*N*-*tert*-butoxy-carbonyl L-serine
N-Boc-Ser-OBzl	*N*-*tert*-butoxy-carbonyl L-serine benzyl ester
N-Fmoc-Ser-OH	Fluorenyl-methyloxy-carbonyl L-serine
N-Z-Ser-OBzl	*N*-carboxy-benzyl L-serine benzyl ester
N-Z-Ser-OMe	*N*-carboxy-benzyl L-serine methyl ester
N-*Z*-Thr-OH	*N*-carboxy-benzyloxy L-threonine

N-*Z*-Thr-OMe	*N*-carboxy-benzyl L-threonine methyl ester
PI	Polydispersity index
PIs	Protease inhibitors
PTT	Patatin
Pyro-glu	Pyroglutamic acid
RSM	Response surface methodology
SDS–PAGE	Sodiutm dodecyl sulfate polyacrylamide gel electrophoresis
Ser	Serine
Ser-Glu	Serine-glutamic acid
Thr	Threonine
TLC	Thin-layer chromatography
TNBSA	2,4,6–rinitrobenzenesulfonic acid
Trp	Tryptophan
XOS	Xylooligosaccharides

CHAPTER I

GENERAL INTRODUCTION

Innovative research efforts to improve the functional properties of food proteins are needed to meet the increased demands for multifunctional food ingredients that can be easily incorporated into a wide range of processed food products. While many genetic-, chemical-, and physical-based modification methods (Ali et al., 2010; Jegouic et al., 1997; Nakamura et al., 1993; Park et al., 2000) have already provided the capability to generate a variety of modified proteins, there have been only few successful developments of food proteins with improved functional properties. The carbohydrate conjugation to proteins, through the Maillard reaction or by the enzymatic glycosylation, has emerged as a highly promising modification approach to improve the functional properties of food proteins. The functional properties of proteins are improved upon conjugation with carbohydrates as a result of changes in their charge, solvation, and/or conformation (Darewicz & Dziuba, 2001; Khan et al., 1999). Conjugation of proteins with carbohydrates can lead to a more heat stable form of the protein (Shu et al., 1996) and to an increase in the protein solubility (Saeki & Inoue, 1997). In addition, the improvements in the emulsifying properties have been reported with protein:carbohydrate conjugates (Wong et al., 2011). The protein glycation was also found to be a very efficient approach to decrease, *in vivo*, the allergenicity of proteins (Arita et al., 2001). Moreover, the conjugation of prebiotic oligosaccharides with a protein could potentially increase their colonic persistence, allowing them to reach the distal colonic region, where most of chronic gut disorders originate (Gibson et al., 2004).

The Maillard reaction comprises complex series of naturally-occurring reactions in which the formation of protein:carbohydrate conjugates occurs during the early stage, where the free amino group of a protein reacts with the carbonyl group of carbohydrates to form Amadori products. During the advanced stages of the reaction, the products resulting from the degradation of the Amadori products can undergo numerous transformations under various pathways giving rise to peptide-bound adducts, to protein cross-linking, and to the formation of brown and polymeric materials (Horvat & Jakas, 2004). To limit the Maillard reaction to its early stages, its parameters (protein:carbohydrate ratio, temperature, incubation time, pH, a_w) need to be controlled. Although many studies (Jakas et al., 2008; Jiménez-Castaño et al., 2005; van Boekel, 2001) have provided a good understanding of the effects of Maillard reaction parameters on the glycation rate, only few of them have looked at the interactive effects of these parameters on the glycation rate. To our knowledge, the glycation of proteins with oligosaccharides have been little

investigated (Sanz et al., 2005; Trofimova & de Jongh, 2004; Zheng et al., 2013). Moreover, there are no systematic studies comparing the effects of type (pentose/hexose) and size (mono, oligo/ polysaccharide) of carbohydrates on the glycation rate and on the functional properties of the produced protein conjugates. Considering the conflicting results reported in the literature (Groubet et al., 1999; Kato et al., 1998; Matsudomi et al., 1994), there is a need to further elucidate the effects of carbohydrate and binding numbers on the structural and the functional properties of the glycoproteins. Moreover, due to the complexity of the Maillard reaction, the use of inhibitors is required to better control its progress and to limit the protein cross-linking. To our knowledge, to date, no literature has systematically compared the efficiency of selected inhibitors, aminoguanidine, cysteine, pyridoxamine, and sodium bisulfite, for the purpose of producing functional protein:carbohydrate conjugates. In addition, the effects of the carbohydrate structure (chain length; pentose/hexose) on the efficiency of these inhibitors have not been studied. The understandings of the mechanisms behind the improvements in functional properties of glycated food proteins, upon the modulation of the Maillard reaction parameters and the use of inhibitors, are expected to result in a more effective production of glycated proteins with enhanced functional properties.

The enzymatic glycosylation of amino acids/peptides/proteins can be catalyzed by glycosidases. The glycosidases naturally catalyze the cleavage of glycosidic bond; however, they can also form glycosidic bonds under thermodynamically and/or kinetically favored conditions. *β*-Galactosidase is a commonly used catalyst in the food industry (Husain, 2010) that has demonstrated a promising transgalatosylating activity (Johansson et al., 1991). However, only limited studies have investigated the production of galactosylated amino acid/peptide derivatives using *β*-galactosidase and reported poor transgalactosylation yields (Attal et al., 1992; Becker & Kuhl, 1999; Layer & Fischer, 2006). In order to improve the transgalactosylation yields, the elucidation of the binding affinity, interactions and orientations of amino acids and peptides as acceptor substrates in the *β*-galactosidase's active site would be necessary. Such molecular mechanistic study is expected to contribute to a better understanding of the enzyme's transgalactosylating specificity towards different acceptors and subsequently to the identification of more suitable acceptor substrates.

Lysozyme (LZM), derived from hen egg white protein, and patatin (PTT), being a major potato protein, were selected as the model proteins because they are well characterized and have many desirable properties. Indeed, the desirable properties of LZM as a food protein include antimicrobial activity and heat stability (Lesnierowski & Kijowski, 2007); however, LZM has poor functional emulsifying properties and it is known to be one of the most important allergenic food ingredients (Frémont et al., 1997). In addition to its antioxidant activity (Liu et al., 2003), its high nutritional values (Camire et al., 2009), and antiproliferative activity against cancer cells (Sun et al., 2013), PTT has excellent foaming (Ralet & Gueguen, 2001), gelling (Creusot et al., 2010), and emulsifying properties (Ralet & Gueguen, 2000). However, due to its very high exposed hydrophobicity (Creusot et al., 2010), PTT exhibits limited solubility at increased ionic strength. Furthermore, the denaturation temperature of PTT has been shown to be around 59ºC (Creusot et al., 2010), which is lower than those of other animal proteins being used as food ingredients. In order to make better use of LZM and of PTT as functional ingredients and to broaden their applications, the improvement of their functional properties through protein modifications is of great interest.

Given this, the overall objective of the present study is to develop novel approaches for the synthesis of glycated/glycosylated proteins of potential applications as food ingredients and nutraceuticals. The carbohydrate conjugation to the target proteins will lead to improvements in different functional properties.

The specific objectives of this study were as follows:

1. Production and structural characterization of LZM conjugated with galactose, galactooligosaccharide (GOS), and galactan through the Maillard reaction and the investigation of the conjugation effect on its functional properties.
2. Investigation and optimization of the interactions between the glycation parameters for the production of LZM conjugated with prebiotic GOS using response surface methodology.
3. Study the effects of carbohydrate type (pentose, hexose) and length (galactose/xylose/GOS/XOS/galactan/xylan) on the conjugation and the cross-linking levels of PTT and characterization of the structural and functional properties of PTT conjugates.

4. Investigation of the effect of carbohydrate conjugation on the digestibility and the allergenicity (immunoreactivity) of PTT.
5. Investigation of the effectiveness of selected Maillard reaction inhibitors to maximize the conjugation level of PTT conjugates and to minimize the protein cross-linking.
6. Optimization of the synthesis of PTT:galactose/xylose conjugates, through the Maillard reaction, by the combined use of L-cysteine and sodium bisulfite as inhibitors.
7. Synthesis of galactosylated serine/threonine derivatives through β-galactosidase-catalyzed transgalactosylation reaction and understanding of the mechanism involved through molecular docking simulations.

CHAPTER II

LITERATURE REVIEW

2.1. Introduction

Due to the increase in demand for food proteins with desirable functionalities, many methods have been developed in order to modify proteins to improve their functional properties. This literature review will cover one of these protein modifications, the carbohydrate conjugation to proteins and peptides through glycation (Maillard reaction) and through enzymatic glycosylation. In addition, the different functional properties of food proteins that have been improved upon carbohydrate conjugation and the analytical techniques that have been used to investigate the produced protein:carbohydrate conjugates are summarized.

2.2. Proteins as Functional Ingredients

The increasing demand for foods possessing aesthetic and organoleptic appeal has placed great emphasis on the need for proteins with multiple functional properties. Therefore, in addition to having acceptable intrinsic properties, such as flavor, color, and nutritional value, proteins as food ingredients also need to have appropriate functional properties for the variety of intended applications (Kinsella, 1979). Functional properties of proteins are those physicochemical properties that affect the behavior of proteins in food systems during preparation, processing, storage, and consumption (Kinsella & Melachouris, 1976). Depending on the use of these proteins, the importance placed on these properties may vary. For example, foaming activity might be more desired in proteins used in dessert toppings and emulsification could be looked for in proteins added in coffee creamers. Functional properties are governed by physical attributes of the protein (amino acid composition, size, charge distribution, protein conformation, hydrophobicity/hydrophilicity), by interactions with food components (water, ions, proteins, lipids, carbohydrates), and by the environment (temperature, pH, ionic strength) (Kinsella, 1979).

2.3. Modifications of Proteins

The adoption of many novel proteins as food ingredients, especially those that have been isolated from industrial waste, is impeded by the lack of the requisite functional properties (Kinsella & Melachouris, 1976; Kristinsson & Rasco, 2000). Therefore, the development of methods for the modification of these nonfunctional proteins to impart the needed functional attributes has been ongoing. Protein modification usually refers to the intentional changes in protein structure through physical, enzymatic, or chemical agents to improve functional properties (Kinsella &

Melachouris, 1976). Common examples of protein modification include thermal extrusion (Camire, 1991), hydrolysis (Kristinsson & Rasco, 2000), proteolysis (Kester & Richardson, 1984), and carbohydrate conjugation (Oliver et al., 2006a). The carbohydrate conjugation to proteins and peptides has demonstrated to be an effective method to improve various functional properties and it can be achieved through the Maillard reaction or through enzymatic methods.

2. 3.1. Protein Glycation through the Maillard Reaction

The Maillard reaction is one of the most important and complex reactions between reducing sugars and amino acids/peptides/proteins that may spontaneously occur in living organisms and during food processing, prolonged storage, and domestic cooking. The reaction is known for its enhancing effects on food properties through color, aroma and flavor changes (Finot, 2005). Both beneficial and detrimental effects have been attributed to the Maillard reaction products. Some compounds such as reductones and melanoidins have shown antioxidant activity (Borrelli et al., 2002; Xu et al., 2007), whereas the advanced glycation end products (AGEs) include a variety of protein adducts implicated in inflammatory reactions and tissue damage (Brownlee et al., 1984; Horie et al., 1997). From the standpoint of food technology, the coupling of carbohydrates to proteins through the Maillard reaction has been reported to improve their functional properties (Kato et al., 1993; Wooster & Augustin, 2006) (Scheme 2.1).

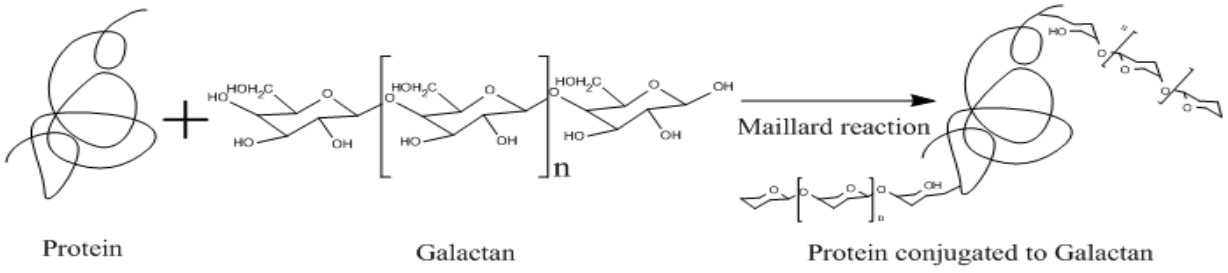

Scheme 2.1 Simplified schematic demonstrating the conjugation of galactan polysaccharide to a protein through the Maillard reaction

The Maillard reaction is a spontaneous and naturally occurring reaction which is greatly accelerated by heat without any extraneous chemicals. Therefore, the Maillard reaction is probably one of the most promising approaches to create protein:carbohydrate conjugates for food purposes. The use of these conjugates in food systems is more desirable when compared to chemically modified food ingredients, as it does not pose the problem of residual chemicals in

the food systems (Kato et al., 1996). However, the application of heat induced products in the food systems as functional ingredients will require precise reaction conditions, and evaluation methods to ensure product quality and consistency. The reaction products formed through the Maillard reaction are not a single species. They consist of various glycoforms and are produced in combination with a vast array of predominantly poorly–characterized products. The types and yields of Maillard reaction products are further influenced by various reaction conditions, including temperature, pH, substrates ratio, relative humidity and the intrinsic properties of the reactants (Labuza & Baisier, 1992; van Boekel, 2001).

2.3.1.1. Chemistry

The Maillard reaction can be divided into three stages: early, intermediate, and advanced. The early stage of the Maillard reaction (initial glycation reaction) is well characterized (Scheme 2.2). A condensation reaction takes place between the carbonyl group of a reducing sugar with an available, unprotonated amine group, forming a Schiff base with the release of water (Ames, 1992). The Schiff base that is formed cyclizes to the corresponding *N*–glycosylamine, which then undergoes an irreversible Amadori rearrangement to produce the Amadori product (1-amino-1-deoxy-2-ketose) (Ames, 1992). With ketoses, such as fructose, the Heyn's rearrangement changes ketosylamine to a corresponding Heyn's product (2-amino-2-deoxyaldose) (Martins et al., 2000). The kinetics of the initial nucleophilic attack of the carbonyl carbon of the reducing sugars by the amino groups of proteins depend on temperature, water activity (a_w), and the proportion of the reducing sugar in the acyclic form (Davies et al., 1998; Labuza & Saltmarch, 1981; Yaylayan et al., 1993). The *pKa* of the protein amino groups, as well as their location within the protein structure (effect of neighboring amino acid residues and accessibility of the amino group) can also influence the initial kinetics (Baynes et al., 1989). No color is produced at this stage of the reaction.

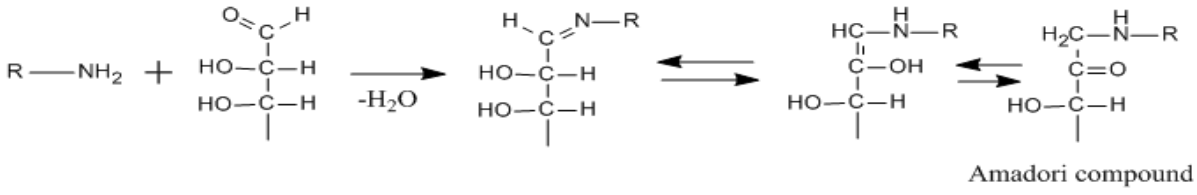

Scheme 2.2 Simplified reaction schematic of the early Maillard reaction

The intermediate stage begins with the degradation of the Amadori/Heyn's product(s) which can undergo numerous transformations involving various divergent pathways (Scheme 2.3). These include oxidation, fragmentation, enolization, dehydration, acid hydrolysis, and free radical reactions producing a multiplicity of compounds (Friedman, 1996; Ledl & Schleicher, 1990). Although some color is produced at this stage, most of the color is not produced until the final stage which leads to the formation of (a) highly reactive compounds that may decompose into small volatile flavor compounds or polymerize to form high molecular weight brown pigments called melanoidins and (b) the formation of fluorescent compounds that can be measured to monitor the Maillard reaction in food or model systems (Morales et al., 1996; Moreaux & BirlouezAragon, 1997).

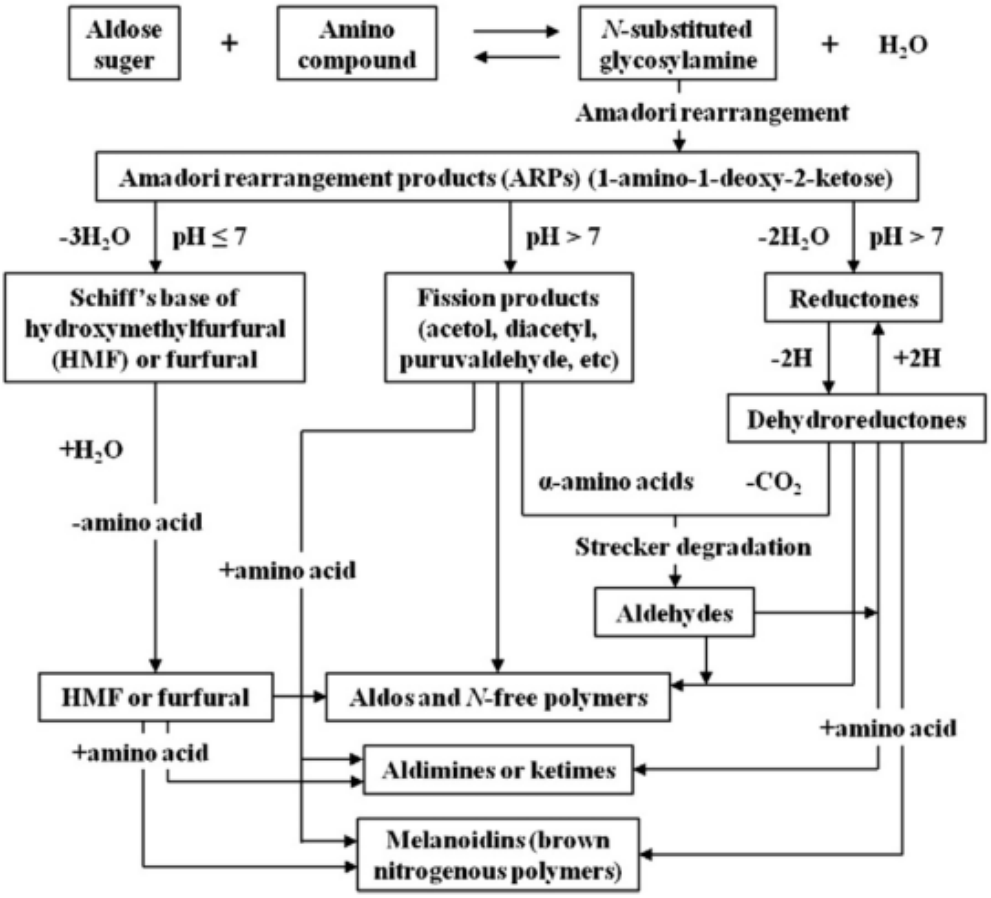

Scheme 2.3 General schematic of the Maillard reaction by Liu et al. (2012a) adapted from Hodge (1953)

In contrast to earlier stages, the high degree of complexity of the advanced stages of the Maillard reaction has made the accurate chemical description a difficult challenge. So far the details of this stage are unresolved although the results, in terms of cooking reactions that give color and flavor changes, can be easily recognized. The reactions that should be considered for the purpose of producing protein:carbohydrate conjugates are those that occur during the early and intermediate stages of the Maillard reaction involving proteins and carbohydrates, and in which the protein is still recognizable. These reactions are the initial condensation reaction to form Amadori or Heyn's products, and inter- and intra-molecular cross-linking reactions that form insoluble polymers. Ideally, a glycoconjugate destined for incorporation into food will possess improved functionality with minimal color or flavor development. This requires that the Maillard reaction be performed under carefully controlled conditions to prevent the later stage color and flavor changes.

2.3.1.2. Site Specificity

The vast majority of existing synthetic strategies for the conjugation of carbohydrates with proteins rely on the formation of covalent linkages with lysine's free amino groups on the protein. It was demonstrated in studies of glycation of RNAse under physiological conditions that the lysine residues in basic sequences or regions of the proteins were preferentially glycated (Erbersdobler & Somoza, 2007; Watkins et al., 1987). This preference was explained by the binding of phosphate ions to the cationic pocket of the basic sequence or region of the protein causing local catalysis of the Amadori rearrangement of the lysine residues. Also, the presence of acidic residues in the vicinity of protein amino groups may catalyze the Amadori rearrangement process, especially, under neutral and slightly basic conditions. Hydrophobic residues in the microenvironment of lysine residues may also reduce the a_w of the local environment and increase the rate of glycation. Lysine is one of the most abundant amino acids occurring in proteins, and most of these polar residues are located on the protein surface (Creighton & Freeman, 1983; Khmelnitsky, 2004). For this reason, any chemical modifications targeting lysine amino groups in proteins almost invariably give a broad distribution of products, differing in the degree of modification of the amino groups. The heterogeneity of the product mixture can be significantly reduced by using a very high excess of the modifying reagent, resulting in complete modification of all available amino groups (Yoshida & Lee, 1994).

2.3.1.3. Effects of Reaction Parameters

The complexity of the Maillard reaction can be explained by the effects of numerous parameters such as the nature, concentration and proportion of the reactants, a_w, heating time, temperature, pH, buffer type, and presence of oxygen (Ames, 1992; Yeboah et al., 1999). The modulation of all these factors is necessary to control the Maillard reaction progress.

The Maillard reaction can take place in both "wet" and "dry" conditions, but it has been reported that the optimum a_w for the reaction is between 0.5–0.8 (Labuza & Baisier, 1992; van Boekel, 2001). The use of "dry" conditions for the preparation of protein:carbohydrate conjugates is of great interest because both protein denaturation/aggregation and Maillard secondary reaction products are prevented to some extent by controlling the reaction conditions (Fenaille et al., 2003). In addition, "dry" products have long-term stability and are easier to store and to handle. Some have reported that reaction specificity can be influenced by a_w (Wu et al., 1990). There is evidence that different buffer systems can affect the rate of reaction and the specificity of the different amino groups of proteins (Baynes et al., 1989). Indeed, the effect of buffer ions on the initial rate of reaction is influenced by their interaction with the β-hydrogen of the sugar moiety of the Schiff base to speed up or to slow down the Amadori rearrangement process. Anionic buffer ions, such as phosphate and carbonate ions, catalyze the Amadori rearrangement reaction by enabling the abstraction of β-hydrogen of the sugar moiety of the Schiff base to form an enaminol (Watkins et al., 1987). Cationic buffer ions on the other hand, can suppress the abstraction of the β-hydrogen, therefore can slow down the Amadori rearrangement process. The specificity of glycation of certain amino groups can also be influenced by anionic buffer by anchoring to other polar amino acid residues in the microenvironment of the target amino group through hydrogen bonding or electrostatic interaction, thus bringing them in close proximity to the target amino group (Watkins et al., 1987). The presence of oxygen in the reaction system also influences the rate and specificity of reaction during the early stage (Yeboah et al., 1999). Yeboah et al. (1999) investigated the glycation of bovine serum albumin and lysozyme by D-glucose and D-fructose under dry heating, and limiting sugar conditions. They demonstrated that the initial rate of glycation was lower in the presence of oxygen than in its absence. Selectivity of the amino groups of the proteins towards glycation could be also seen in the presence of oxygen. Similar observations were made by another group in a glycation study conducted in solution (Hayase et al., 1990). The lower initial rate of glycation and the selectivity in the glycation of the

amino groups of proteins in the presence of oxygen was explained by the parallel competitive glycoxidation reactions of the reducing sugars (Yeboah et al., 1999). The competitive glycoxidation reactions can reduce the effective concentration of the reducing sugar in the reaction system, which results in reduction in the rate of glycation. In the presence of oxygen, aldoses readily undergo oxidation and form more reactive oxidation products, such as glyoxal and glucosone (Hayase et al., 1990; Yaylayan & Huyghues-Despointes, 1994). These glycoxidation products are more effective at glycating primary amino groups. It was also suggested by Yeboah et al. (2000) that the observed selectivity in glycation during the initial stages of the reaction in the presence of oxygen was due to the decrease in concentration of the reducing sugars caused by competing side reactions leading to the glycation of the most reactive amino groups of the proteins first.

The other major factors influencing the rate and extent of protein glycation are temperature, and nature and amount of the reducing sugars (Davies et al., 1998; Labuza & Saltmarch, 1981). It has been demonstrated that the glycation efficiency of peptides/proteins increases at higher sugar concentrations and at higher temperatures. Glycation efficiency also increases at higher pH; however, this could result from denaturation of protein and the resultant exposure of potential glycation sites (Davis & Williams, 1998). Efficiency of the glycation process is time dependent but reaches a maximum when all the glycation sites are saturated. The initial kinetics of glycation are also dependent on the proportion of the reducing sugars existing in the acyclic or active form under the reaction conditions, and on the electrophilicity of the sugar carbonyl group (Bunn & Higgins, 1981; Labuza & Baisier, 1992; Yaylayan et al., 1993). It is widely accepted that aldoses are intrinsically more reactive than ketoses; however, there has been conflicting reports on the reactivities of glucose and fructose. Several researchers have reported that fructose is more reactive than glucose (Suarez et al., 1995). Other researchers have reported glucose to be more reactive (Naranjo et al., 1998). It has also been reported that fructose is more effective in causing protein cross-linking and in generating protein bound Maillard fluorescence than glucose (Suarez et al., 1991). The discrepancies in the literature may be related to differences in the conditions under which the Maillard reactions were conducted and the methods used to monitor the reaction.

2.3.1.4. Effect of Carbohydrate Length on Glycation

Higher degree of polymerization of carbohydrate can lead to a slower rate of the Maillard reaction and as a result, to a lower level of glycation (Chevalier et al., 2001b; Nacka et al., 1998; Oliver et al., 2006a). Corzo-Martínez et al. (2010b) reported the sugar reactivity towards the glycation of sodium caseinate as being galactose > lactose > dextran. Indeed, the smaller the degree of polymerization of the sugar, the more acyclic forms exist and the more reactive is the sugar with the free amino groups of the proteins (Corzo-Martínez et al., 2010b). On the other hand, the steric hindrance of longer carbohydrate chains or the extensive branching might block reducing groups from reacting with free amino groups on the protein (Aminlari et al., 2005). Many studies have reported on the glycation of proteins with small carbohydrates, such as galactose, glucose, and fructose (Corzo-Martínez et al., 2010b; Gu et al., 2010b; Yeboah et al., 1999), and polysaccharides, such as dextran, galactomannan, and chitosan (Liu et al., 2012b; Nakamura et al., 1992; Song et al., 2002); however, fewer number of studies on the glycation of proteins with oligosaccharides have been carried out to date (Oliver et al., 2006b; Sanz et al., 2005; Trofimova & de Jongh, 2004; Zheng et al., 2013; Zhong et al., 2013).

2.3.1.5. Protein Cross-linking during the Maillard Reaction

Protein cross-linking is the formation of covalent bonds between polypeptide chains within a protein or between proteins (Feeney & Whitaker, 1988). The Maillard reaction, which is a complex cascade of chemical reactions, involves protein cross-linking as a subset of the many reaction products and the cross-linking of food proteins by the Maillard reaction is well established (Gerrard et al., 2003; Hill & Easa, 1998; Mohammed et al., 2008). The characterization of some of these cross-links has been accomplished and these include petosidine, glucosepane, glyoxal lysine dimer, methylglyoxal lysine dimer, lysine arginine dimer, methylglyoxal lysine arginine dimer, and glyoxal lysine arginine dimer (Biemel et al., 2001; Chellan & Nagaraj, 1999; Nagaraj et al., 1996). There is evidence that the sugar-derived dicarbonyl compounds, such as methylglyoxal, 3–deoxyosones or glyoxal (Biemel et al., 2002; Chellan & Nagaraj, 1999; Lederer et al., 1998; Meade et al., 2003) get attached to lysine and arginine residues on the protein by one of their bifunctional groups which in turn favor the polymerization of the protein through the second functional group binding with the remaining lysine and arginine residues on the protein (Glomb & Tschirnich, 2001; Hollnagel & Kroh, 2000) (Scheme 2.4). The introduction of protein cross–links produces substantial changes in the

structure of proteins, and therefore creates changes in the functional (Singh, 1991) and nutritional (Friedman, 1996) properties. The precise chemical structures of these cross–links, however, are less understood (Gerrard, 2002). Protein cross–linking can influence many functional properties of food proteins, including texture, viscosity, solubility, emulsification and gelling properties (Motoki & Kumazawa, 2000). Since protein cross–linking takes place during the intermediate/advanced stages of the Maillard reaction (Mauron, 1990), it is a good indication of the Maillard reaction progress and it has to be inhibited for the purposes of protein:carbohydrate conjugates production. It has been described that by controlling the extent of protein cross–linking associated with the intermediate/advanced stages of the Maillard reaction, it is possible to obtain protein:carbohydrate conjugates with increased solubility, but without excessive color formation (Oliver et al., 2006a). There are different ways to inhibit the progress of Maillard reaction: by adding sulfite or sulfhydryl containing compounds (Friedman, 1996) or by adding trapping agents such as aminoguanidine or pyridoxamine (Scheme 2.5).

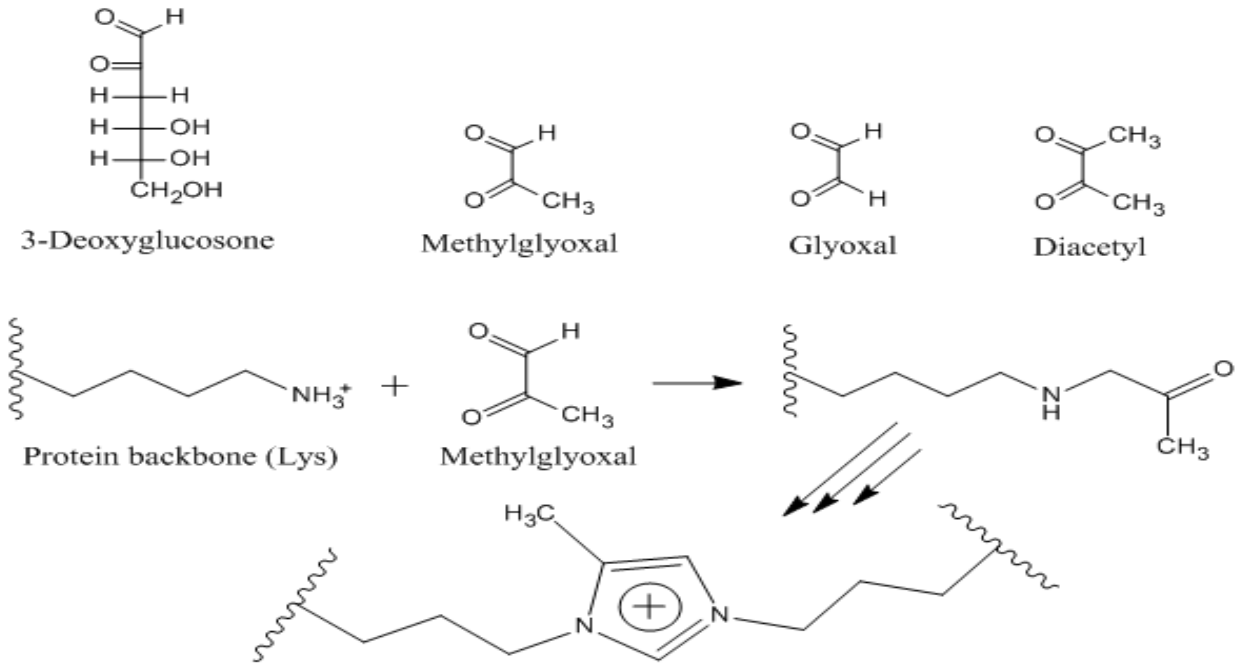

Scheme 2.4 Structure of some *α*–dicarbonyls generated during the Maillard reaction and possible protein cross–linking reaction pathway for lysine modification by methylglyoxal (Miller et al., 2003)

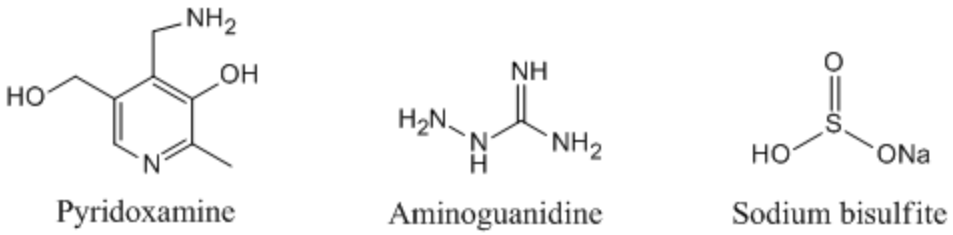

Scheme 2.5 Maillard reaction inhibitors

Sulfite is regarded as an effective inhibitor of the advanced stages of the Maillard reaction, which is currently used in the food industry (Nursten, 2005). The effectiveness of sulfites in controlling the Maillard reaction probably depends on distinct chemical reactions involving its participation with carbonylic intermediates formed during the Maillard reaction. The dicarbonyl compounds with the addition of sulfite in the reaction, are more likely to favor the formation of bisulfite adduct. An example of a bisulfite adduct is 1–alkyl–2–formyl–3,4–diglycosylpyrroles formed from 3–deoxyosone and the Amadori product followed by irreversible reaction of sulfite ion with the electrophilic carbons of 1–alkyl–2–formyl–3,4–diglycosylpyrroles to form 1–alkyl–2–formyl–3,4–diglycosylpyrroles/bisulfite adducts which are blocked from reacting with other proteins (Farmar et al., 1988). Scaman et al. (2006) demonstrated that the progress of the Maillard reaction can be controlled effectively using sodium bisulfite for the production of lysozyme–galactomannan/mannan conjugates.

Brownlee et al. (1986) showed that aminoguanidine can effectively inhibit protein cross–linking caused by the Maillard reaction. The gradual increase in fluorescence associated with cross–linking during the Maillard reaction was able to be inhibited by 90% upon addition of aminoguanidine. Its nucleophilic hydrazine group (–$NHNH_2$) and the dicarbonyl–directing guanidino group (–NH–C(=NH)NH_2) provide a reactive bifunctional scavenging of α, β–dicarbonyls. It has also been demonstrated that aminoguanidine has little to no effect on the conjugate/Amadori product formation (Edelstein & Brownlee, 1992). Oimomi et al. (1989) were able to demonstrate that incubation of the 3–deoxyglucosone with bovine serum albumin increased the fluorescence associated with cross–linking by 10–fold, whereas preincubation of the 3–deoxyglucosone with aminoguanidine brought the fluorescence down by a factor of almost

5. Their results suggested that aminoguanidine inhibits the advanced stage of the Maillard reaction and Maillard reaction induced protein cross–linking by reacting with 3–deoxyglucosone. Pyridoxamine which is a natural intermediate of vitamin B_6 metabolism, has been demonstrated to be an adequate *in vitro* and *in vivo* inhibitor of the transformation of the Amadori compounds to AGEs acting on several pathways of the Maillard reaction (Amarnath et al., 2004; Booth et al., 1996; Voziyan et al., 2002). Booth et al. (1996) demonstrated that pyridoxamine is significantly more effective at inhibiting the glucose–derived AGEs formation than aminoguanidine. The mechanism of inhibition of the Maillard reaction by pyridoxamine is difficult to study because the advanced stages of Maillard reaction involve multiple pathways leading to AGEs and pyridoxamine is believed to be involved in different steps. It was suggested that pyridoxamine has a different mechanism than aminoguanidine in order to prevent the advanced stages of Maillard reaction since it inhibited the formation of AGE N^{ε}–(carboxymethyl)lysine (CML) from the isolated protein–Amadori intermediate, which could not be achieved with aminoguanidine (Booth et al., 1997). Pyridoxamine has also been shown to scavenge reactive carbonyl species that act as precursors of AGEs and of advanced lipoxidation end products (ALEs) (Amarnath et al., 2004; Nagaraj et al., 2002; Voziyan et al., 2002). Recently, Corzo-Martinez et al. (2008) used pyridoxamine to inhibit the advanced stages of Maillard reaction during production of *β*–lactoglobulin:galactose/tagatose conjugates for food purposes. They concluded that pyridoxamine also competes with the free amino groups of *β*–lactoglobulin for the carbonyl group of the carbohydrates, thus delaying the formation of the Amadori/Heyns compounds, preventing additional cross–linking reactions and the formation of protein aggregates.

The suggested mechanisms of action of aminoguanidine and of pyridoxamine found in the literature have been summarized in Table 2.1.

Table 2.1 The suggested mechanisms of action of aminoguanidine and of pyridoxamine

References	Inhibitor	Mechanism of action
(Voziyan et al., 2002)	Pyridoxamine	Competes with protein lysine residues for dicarbonyl and α-hydroxycarbonyl moieties of GO and GLA to form cyclic aminal derivatives
(Chetyrkin et al., 2008)	Pyridoxamine	Transient reversible adduction of 3-deoxyglucosone by pyridoxamine followed by irreversible pyridoxamine-mediated oxidative cleavage of 3-deoxyglucosone to give nonreactive products
(Adrover et al., 2008)	Pyridoxamine	The inhibition of post-Amadori reactions is due to the metal ion sequestering effect of pyridoxamine
(Edelstein & Brownlee, 1992)	Aminoguanidine	Aminoguanidine reacts with Amadori-derived fragmentation products
(Thornalley et al., 2000)	Aminoguanidine	Aminoguanidine reacts with α-oxoaldehydes glyoxal, methylglyoxal, and 3-deoxyglucosone to form 3-amino-1,2,4-triazine derivatives
(Hirsch et al., 1995)	Aminoguanidine	Aminoguanidine reacts with glucose to form β-D-glucopyranosyl aminoguanidine
(Requena et al., 1993)	Aminoguanidine	Early glycation of albumin was inhibited

2.3.2. Protein Glycosylation through Enzymatic Approach

Another method for the synthesis of protein:carbohydrate conjugates is through enzymatic reactions. Among the enzymes that can be used for the production of these conjugates, glycosidases (EC. 3.2.1) and glycosyltransferases (EC. 2.4) are the most investigated so far. The easy accessibility and the broad substrate range of glycosidases make them interesting candidates for the production of protein:carbohydrate conjugates compared to glycosyltransferases, which are less available and require the use of expensive sugar nucleotides.

2.3.2.1. Glycosidases-catalyzed Glycosylation of Amino Acids and Peptides

The glycosidases naturally catalyze the cleavage of glycosidic bond. These enzymes can be divided into two groups: the exoglycosidases which cleave glycosidic bonds at the terminal end of the carbohydrates and the endoglycosidases which cleave internal glycosidic linkages (Ichikawa et al., 1992; Nilsson, 1988; Toone et al., 1989). Although glycosidases are hydrolytic enzymes, under controlled conditions, glycosidases can be used to synthesize glycosidic bonds rather than for cleavage. As such, they have been employed as catalysts in oligosaccharide synthesis (Sinnott, 1990). Two general protocols for glycosidase–based synthesis have been reported. The equilibrium controlled synthesis reverses the hydrolysis reaction by combining a free monosaccharide and a nucleophile. The reaction requires high concentration of substrate and high temperature because the equilibrium favors the hydrolysis reaction. The yield of oligosaccharide remains low, from 20 to 30%. Several examples of synthesis using glycosidases have been reported (Johansson et al., 1991; Johansson et al., 1989). However, improved yields can often be achieved under kinetic conditions (transglycosylation), usually employing an activated glycosyl donor, organic cosolvent, or using a transglycosidase that prefers transglycosidation to hydrolysis. In general, only simple glycosides can be prepared, and product yields are still greatly decreased when compared to those of glycosyltransferase–catalyzed reactions. Glycosidases exhibit a less pronounced selectivity than the glycosyltransferases for the acceptor structure. They are highly selective for the anomeric configuration of the newly synthesized linkage. Generally, it is selective for the primary hydroxyl group of the acceptor, forming (1,6)–linkage between donor and acceptor. Thus, the use of glycosidases for the transglycosylation reactions presents several advantages: the enzymes are readily available and inexpensive, sugar nucleotides and cofactors are not required (Ichikawa et al., 1992; Jenkins & Curling, 1994; Nilsson, 1988).

2.3.2.2. β–Galactosidase-catalyzed galactosylations

β–Galactosidase is a commonly used catalyst in the food industry (Husain, 2010) to improve sweetness, solubility, flavor and digestibility of dairy products. *β*–Galactosidases work in a broad pH range: enzymes from fungal origin act between pH 2.5–5.4, yeast and bacterial enzymes act between pH 6.0–7.0. *β*–Galactosidases can use a variety of acceptors for the transgalactosylation reactions. It has been demonstrated that formation of a glycosidic bond between galactose and L–serine was possible using *β*–galactosidase, as long as both the amino and carboxyl groups of serine were protected (Holla et al., 1992; Johansson et al., 1991; Layer & Fischer, 2006) (Scheme 2.6). Sauerbrei and Thiem (1992) were able to galactosylate unprotected serine using *ortho*–nitrophenyl *β*–galactoside and *β*–galactosidase from *Aspergillus oryzae*. A transgalactosylation of a protected dipeptide has also been demonstrated using lactose as a donor and *β*–galactosidase from *Escherichia coli* as catalyst (Attal et al., 1992). Leparoux et al. (1996) have also demonstrated galactosylation of *N*–protected dipeptide using the *Achatina achatina* digestive juice and lactose as donor and obtained better yields than those using the *E. coli* *β*–galactosidase.

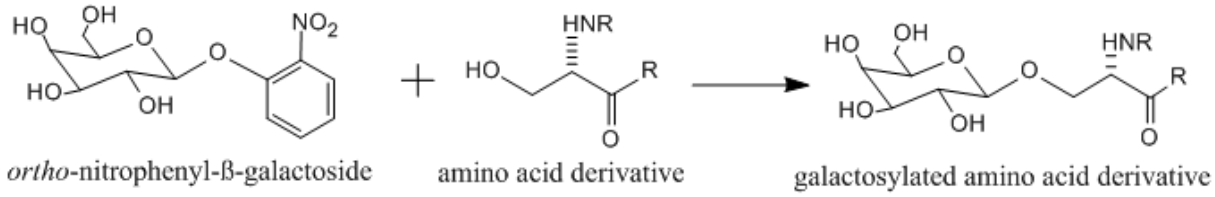

Scheme 2.6 *β*–Galactosidase–catalyzed galactosylation of an amino acid derivative

The *β*–galactosidase from *E. coli* has been widely used for various biotechnological applications and its amino acid and nucleotide sequences and its structure have been well characterized. The enzyme is a homotetramer, each monomer weighing 116 353 Da and having 1023 amino–acid residues in five sequential domains, with an extended segment at the amino terminus. The three–dimentional structure of *β*–galactosidase shows that the active site is located in a deep pocket within a distorted "TIM" barrel. Divalent and monovalent cations are required for full catalytic efficiency: Mg2+ or Mn2+ cations leads to 5–100–fold activation depending on the substrate level. The active site has two subsites: the first is highly specific for the galactose moiety, whereas the second lacks the specificity (Jacobson et al., 1994; Juers et al., 2001; Juers et al., 2000). This lack of specificity allows the binding of a wide variety of substrates.

β–Galactosidase from *E. coli* is a retaining glycosidase and therefore maintains the initial conformation on the anomeric carbon. The proposed catalytic mechanism of the enzyme occurs through a double–displacement reaction involving galactosylation and degalactosylation steps, with the reaction proceeding through a covalent galactosyl–enzyme intermediate (Crout & Vic, 1998) (Scheme 2.7). The active site consists of two carboxylic acid residues (Glu461 as proton–donor, Glu537 as catalytic nucleophile) that are approximately 5.5 Å apart (Juers et al., 2001). The first mechanistic step is characterized by the departure of the glucose group. The second step involves the attack of the covalent carbohydrate–enzyme intermediate by a sugar molecule, concomitantly with or followed by the transfer of a proton from sugar to the proton donor, in a reverse mode of the first step. The literature suggests that both transition states have substantial oxocarbenium ion character (Namchuk et al., 2000).

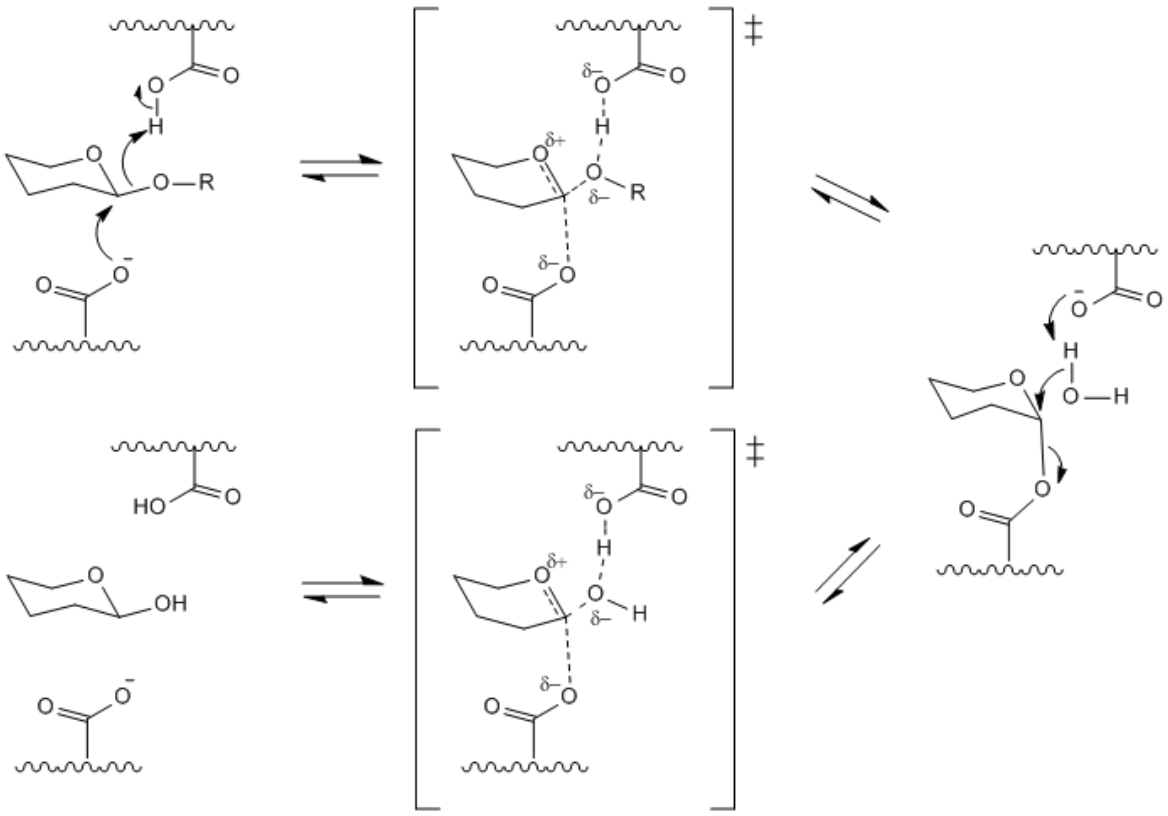

Scheme 2.7 General mechanism for retaining glycosidases such as *β*–galactosidase from *E. coli* (Rye & Withers, 2000)

2.3.2.3. Computational Analysis for Enzymatic Glycosylation: Molecular Docking

The goals of a computational study of an enzymatic reaction are the elucidation of its chemical mechanism, the identification of specific interactions stabilizing the intermediate/transition state(s), and the understanding of the effects produced by an enzyme's conformational fluctuations, especially over the reaction rates (Lonsdale et al., 2010). Comprehensive analysis of experimental and computational binding data can provide new insights into the nature of the interactions between the substrates and the enzyme (Honarparvar et al., 2014). Some of these computer–based techniques include free binding energy calculations (Brandsdal et al., 2003), molecular mechanics (Brás et al., 2010), molecular dynamic simulations (Karplus & McCammon, 2002), homology modeling (Yoo & Medina-Franco, 2011), and molecular docking (Udatha et al., 2012). Molecular docking, among other computational methods, can provide an understanding of the binding modes between substrates and an enzyme. It is used for both exploring the possible conformations of a substrate inside the binding site of an enzyme as well as for the estimation of the strength of substrate-enzyme interaction (Honarparvar et al., 2014). Molecular docking relies upon the preexistence of X-ray crystallography structures of the particular enzyme of interest (Honarparvar et al., 2014). In order to improve the yield of the protein:carbohydrate conjugates through enzymatic glycosylation, the interactions between the enzyme and the substrates need to be well-characterized. Since the goal of molecular docking is to understand and predict molecular recognition by finding likely binding modes, and by energetically predicting the binding affinity (Morris & Lim-Wilby, 2008), it may be a useful tool to improve the yield of the protein:carbohydrate conjugates through *β*–galactosidase–catalyzed glycosylation by aiding in the selection of the right substrate. Selecting compounds *in silico* that bind to an enzyme's active site is challenging because the method must find the optimum binding orientation and substrate conformation. Another challenge is that the method must score the compound so that its relative affinity can be judged compared to other compounds (Morris & Lim-Wilby, 2008). Therefore, all docking programs have an algorithm that first performs a "docking" (substrate binding orientation/conformational search) followed by a scoring function that ranks the substrates in terms of intermolecular binding energy (Udatha et al., 2012). Most docking software makes use of force field calculations that approximate the binding energy based on both high-level calculated quantum mechanics and the experimental data. The binding affinities of various substrates to the enzyme are compared and may provide a correlation between the bioconversion yield and the substrates used (Honarparvar et al., 2014). During the

docking process, the x, y, z coordinates of the individual substrate and the enzyme are used to predict the best–fit conformation for the resulting enzyme–substrate complex. The binding mode of a substrate can be defined by its state variables, such as its position and its conformation. Each of these state variables will contribute one degree of freedom in a multidimensional search space. The search methods can be divided into two main categories: systematic and stochastic (Morris & Lim-Wilby, 2008). In systematic search, the outcome of the search is deterministic, but the quality of the solution depends on the granularity of sampling of the search space. Stochastic methods rely on an element of randomness with varying outcomes. Systematic search methods are commonly used in cases with lower degrees of freedom with programs such as DOT (Morris & Lim-Wilby, 2008), GRAMM (Tovchigrechiko & Vakser, 2006), and ZDOCK (Chen & Weng, 2002). Stochastic search methods are more suitable for more complex problems and can be performed using algorithms such as Monte Carlo simulated annealing (MCSA) (Goodsell & Olson, 1990), genetic algorithms, and hybrid global-local search methods (Morris et al., 1998). Scoring functions can be empirical, knowledge based, or molecular mechanics based (Taylor et al., 2002). Two criteria need to be considered when evaluating the quality of docking results; 1) how well does the binding mode predicted by the docking match the known structural data, and 2) how did the docking procedure rank the substrates and does the ranking match the experimental data? (Morris & Lim-Wilby, 2008). Brás et al. (2010) have used computational methods to study the catalytic mechanism of transglycosylation reaction of retaining *E.coli β*–galactosidase using lactose as the substrate. They have used the ONIOM method (molecular mechanics/quantum mechanical method) to account for the stereochemistry of the reactive residues and the long-range enzyme-lactose interactions. They have found that the formation of *β*(1–6) glycosidic bonds, therefore the formation of allolactose, is favored and have confirmed their results experimentally. Pérez-Sánchez et al. (2011) have used Autodock 4 software for their molecular docking procedures followed by molecular dynamics simulations with GROMACS software to explain the transgalactosylating activity boost of *E. coli β*–galactosidase in glycerol-based solvents. They have concluded that the better disposition of the substrate in the active site originating from the different solvation effects may explain the observed behavior.

2.4. Improvements in Functional Properties of Protein Conjugates

Selected functional properties of proteins can be improved by conjugating with carbohydrates as a result of changes in their charge, solvation, and/or conformation (Darewicz & Dziuba, 2001; Kato et al., 1993; Khan et al., 1999; Morgan et al., 1999a; Nakamura et al., 1994). The most important functional properties that are affected by protein:carbohydrate conjugation are protein solubility, heat stability, emulsifying properties, allergenicity, foam forming activity, and antioxidant activity. Table 2.2 lists some selected publications where improvements in protein functional properties were observed through carbohydrate conjugation to different proteins at different reaction conditions.

2.4.1. Protein Solubility

Earlier studies done by several researchers showed decrease in protein solubility after protein:carbohydrate conjugation (Kato et al., 1986); however, more recent studies demonstrate that there is an improvement in protein solubility after glycation/glycosylation. It has been suggested that the protein solubility is improved when there is a limited degree of conjugation (Oliver et al., 2006b). This implies that the conjugates formed by the Maillard reaction can have improved solubility due to the hydrating ability of the carbohydrate, but also the solubility can decrease since the advanced Maillard reaction favors the formation of protein cross–links. A study done by Saeki and Inoue (1997) demonstrated an improvement of fish myofibrillar protein solubility when just 17% of the available lysine residues were glycated with glucose. In contrast, Nishimura et al. (2011) obtained a decrease in solubility when chicken myofibrillar proteins were conjugated with glucose. Conjugating fenugreek gum, a galactomannan, to soy whey protein isolate led to an increase in solubility over a broad range of pH (3–8), which demonstrates that the conjugation of fenugreek gum led to a protective effect against protein aggregation even at the isoelectric point of the protein (Kasran et al., 2013). To obtain a net improvement in protein solubility by using the Maillard reaction conjugates, it would require very tight control of the reaction progress and of the rate of the glycation. On the other hand, such improvement would be more easily achieved with the enzymatic glycosylation since the rate of the reaction can be more easily controlled, and the protein cross–linking is not favored by the enzymatic glycosylation. For both methods, the protein solubility is likely to depend mostly on the molecular structure and chemistry of the protein and of the reacting sugars.

Table 2.2 Selected literature demonstrating improvements in functional properties through the carbohydrate conjugation to proteins

Reference	Conjugate	Reaction conditions	Improvements in functional properties
(Sarabia-Sainz et al., 2013)	Porcine serum albumin–GOS	1:2 (protein:carbohydrate) weight ratio Dry reaction at pH 8, 9 80°C and 90°C for 30 min	Inhibition of enterotoxic *E. coli* adhesion to piglet mucins *in vitro*
(Kato et al., 1990)	Ovalbumin–dextrose	1:5 (protein:carbohydrate) weight ratio Dry reaction (a_w = 0.65) 60°C for 3 weeks	Emulsion stability over a wide pH and temperature range
(Dickinson & Galazka, 1991)	*β*–Lactoglobulin–dextran	1:1 or 1:3 (protein:carbohydrate) weight ratio Dry reaction (a_w = 0.35–40) 60°C for 3 weeks	Enhanced emulsion stability and inhibition of serum and cream separation
(Wong et al., 2011)	Deamidated soluble isolated wheat protein–dextran	1:1 (protein:carbohydrate) mole ratio Dry reaction (a_w = 0.75) 60°C for 5 days	Improvement in emulsion stability by conjugation with larger dextran (64–76 kDa)
(Matemu et al., 2009)	Tofu whey protein–chitosan oligosaccharide/galactomannan/xyloglucan	1:1 (protein:carbohydrate) weight ratio Dry reaction at pH 7 (a_w = 0.65) 60°C for 7 days	Improvements in emulsion stability and water hydration capacity when larger protein (>3kDa) used for the conjugation
(Einhorn-Stoll et al., 2005)	Whey protein isolate–high or low methoxylated pectin	1:1, 1:3, or 1:5 (protein:carbohydrate) weight ratio Dry reaction at pH 5 or 7 (a_w = 65 or 80) 50, 60, or 65°C for 3 weeks	Emulsion activity and stability improved following conjugation
(Nakamura et al., 1991)	Lysozyme–dextran	1:5 (protein:carbohydrate) weight ratio Dry reaction (a_w = 78.9) 60°C for 0–3 weeks	Improvement in emulsifying properties and in antimicrobial activity
(Kato, 2000)	Lysozyme–galactomannan/xyloglucan Soy protein–galactomannan/xyloglucan	For conjugation with galactomannan: 1:4 (protein:carbohydrate) mole ratio Dry reaction (a_w = 65) 60°C for 2 weeks For conjugation with xyloglucan: 1:8 (protein:carbohydrate) mole ratio Dry reaction (a_w = 65) 60°C for 24h	Increase in heat stability, and in emulsifying properties after conjugation and decrease in immunoreactivity
(Chevalier et al., 2001a)	*β*–Lactoglobulin–galactose/glucose/lactose/rhamnose	1:1 mole ratio Wet reaction at pH 6.5 60°C for 72h	Improvements in heat stability and in emulsifying properties
(Kasran et al., 2013)	Soy whey protein isolate–fenugreek gum	1:3 (protein:carbohydrate) weight ratio Dry reaction (a_w = 0.75) 60°C for 3 days	Improvements in solubility of soy whey protein isolate after conjugation over pH 3–8 and in emulsifying properties

(Shepherd et al., 2000)	Casein–maltodextrin	2:1 (protein:carbohydrate) weight ratio Dry reaction (a_w = 0.79) 60°C for 0–120h	Improved emulsifying stability and solubility at pH <6
(O'Regan & Mulvihill, 2010)	Sodium caseinate–maltodextrin	2:1 (protein:carbohydrate) weight ratio Dry reaction (a_w = 0.79) 60°C for 0–96h	Improved solubility and emulsion stability
(Aoki et al., 1999)	Ovalbumin–glucuronic acid	2:1 (protein:carbohydrate) weight ratio Dry reaction at pH 7.5 (a_w = 0.65) 50°C for 0.5–3 days.	Improvements in heat stability and in emulsifying properties
(Akhtar & Dickinson, 2003)	Whey protein isolate–dextran	1:3 (protein:carbohydrate) weight ratio Dry reaction (a_w = 0.79) 80°C for 2h	Improved emulsifying properties at pH 3.2
(Medrano et al., 2009)	*β*–Lactoglobulin–lactose/glucose	1:10 and 1:100 (protein:carbohydrate) molar ratio Dry reaction at pH 7 (a_w = 0.65) 50°C for 51 and 96h	Improved foaming properties
(Gu et al., 2010a)	Casein–glucose	1:2 (protein:carbohydrate) weight ratio Wet reaction at pH 12 102°C for 130 min	Non–hydrolyzed reaction products exhibited highest reducing power, but peptic hydrolysates were more efficient in radical scavenging activity
(Dong et al., 2012)	Hydrolyzed *β*–lactoglobulin–glucose	1:1 mole ratio of free amino groups to sugar carboyl groups Wet reaction at pH 8 90°C for 18h	Improved DPPH· scavenging activity, reducing power, and iron chelating activity
(Joubran et al., 2013)	Lactoferrin–glucose/fructose	1:1 and 1:3 (protein:carbohydrate) mole ratios Dry reaction at pH 7 (a_w = 0.79) 60°C for 12 or 36h	Increase in antioxidant capacity only with glucose–based conjugates
(Jing et al., 2011)	Albumin/ovomucoid/lysozyme/casein–fructose/inulin	2:1 (protein:carbohydrate) weight ratio Dry reaction at pH 7 (a_w = 0.79) 60°C for 3 days	All conjugates demonstrated improvements in emulsion stability and DPPH· radical scavenging activity
(Amid & Mirhosseini, 2014)	Whey protein isolate–durian seed gum	1:3 (protein:carbohydrate) weight ratio Dry reaction (a_w = 0.80) 60°C for 48h	Partial conjugation of durian seed gum to whey protein isolate improved the characteristics of water in oil in water emulsion
(Li et al., 2013)	Rice protein–glucose/lactose/maltose/maltodextrin/dextran	1:1 (protein:carbohydrate) weight ratio Wet reaction at pH 11 100°C for 0–40min	Limited hydrolysis in addition to carbohydrate conjugation improved the solubility and the emulsifying activity of the protein

2.4.2. Heat Stability

There is evidence that conjugation of proteins with carbohydrates results in a more heat stable form. A study done by Shu et al. (1996) using lysozyme–polysaccharide conjugate demonstrated that the conjugates showed no aggregation up to 95ºC, whereas the turbidity of the native lysozyme increased at 85ºC and reached a maximum tubidity of 1.7 (OD_{500}) at 95 ºC. This result indicates an increase in thermal stability of lysozyme upon its conjugation with galactomannan. Lysozyme–xyloglycan conjugate was less heat stable as compared the one conjugated with galactomannan; however, it was still more heat stable than the native lysozyme. In another study, the conjugation of *β*–lactoglobulin with galactose, glucose, lactose, or rhamnose led to better heat stability as compared to the native protein (Chevalier et al., 2001a). Kato (2002) suggested that the carbohydrate that is conjugated to the protein may stabilize the protein in a manner that sterically protects its aggregation and since the unfolded protein–protein interaction is inhibited, it may enable the protein to reverse its denaturation.

2.4.3. Emulsifying Properties

Both protein and carbohydrate have a role in the stabilization of oil-in-water emulsions. Proteins adsorb at the oil–water interface during emulsification, while carbohydrates confer colloid stability through their gelation behavior in the aqueous phase (Scheme 2.8). Usually this is better achieved with polysaccharides since they have better hydrating capacity compared to shorter carbohydrates. Kato (2000) demonstrated that the conjugation of lysozyme with galactomannan having a molecular size of more than 6–12 kDa is essential for the improvement of the emulsifying properties. When xyloglucan, an oligosaccharide, was used for the conjugation with lysozyme, it did not lead to an improvement of the emulsifying properties. When the conjugation of fenugreek gum to soy whey protein isolate improved dramatically the emulsifying properties of the proteins (Kasran et al., 2013), this improvement was attributed to the inhibition of the unfolded protein–protein interaction due to the attached polysaccharide. Shepherd et al. (2000) investigated the emulsifying properties of casein conjugated with maltodextrins and demonstrated improvements in emulsifying properties, but they could not conclude if this improvement was only due to the increase in solubility of the conjugates. In other studies, the emulsifying properties either remain unchanged (Groubet et al., 1999) or decreased (Kato et al., 1992; Kato et al., 1990) when proteins were glycated with mono– or di– saccharides. However, Moreno et al. (2002) have shown that reaction of caseinomacropeptide with lactose improved

emulsifying activity of the native protein. Saeki and Inoue (1997) and Moreno et al. (2002) were able to explain these findings by associating the improvement in emulsifying properties of the conjugates with maximum decrease in rate of available lysine, which indicates that high degree of glycation can compensate for the shorter carbohydrate chain and the smaller hydrating effect. The effect of higher conjugation level on the improvement of emulsifying properties was also demonstrated by Kato (2000) when using lysozyme with galactomannan where the double conjugated lysozyme demonstrated better emulsifying activity than the single conjugated lysozyme.

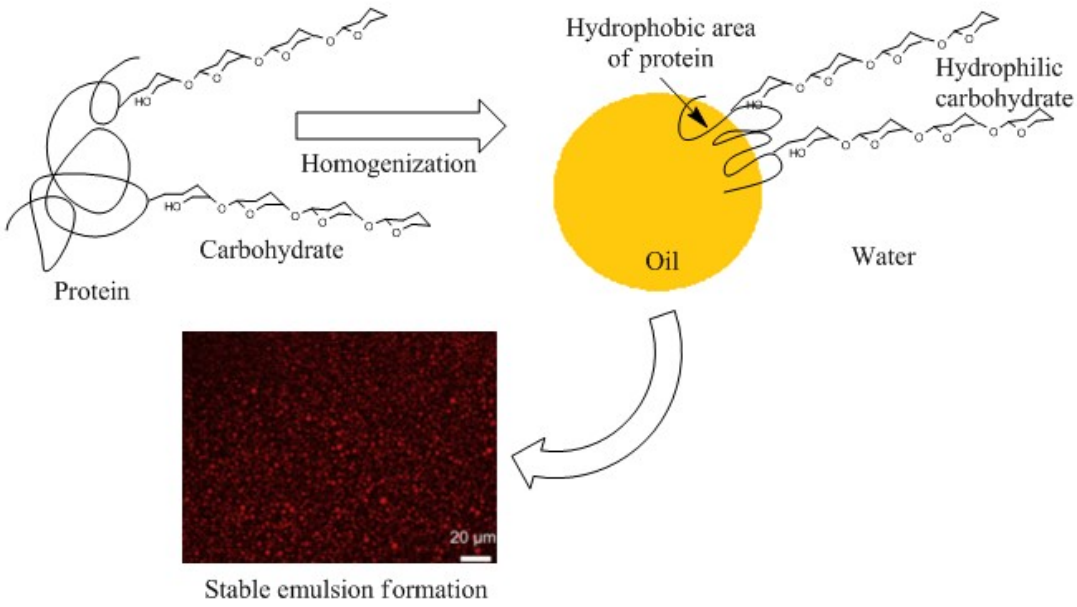

Scheme 2.8 Schematic of emulsion formation through proteins glycated with polysaccharides adapted from Wong et al. (2011)

2.4.4. Allergenicity

The conjugation of proteins with carbohydrates has been reported to be able to mask their allergenic structures. When compared with other methods of decreasing the allergenicity of food proteins, such as protease digestion and transglutaminase treatment, the polysaccharide conjugation was found to be the best method to reduce the allergenicity of soy protein (Babiker & Kato, 1998). The decrease in allergenicity could be the result of the destruction of conformational epitopes by denaturation of the protein or by glycation of the amino acid residues located on the epitopes that sterically inhibit some epitope binding (Arita et al., 2001). On the other hand, the Maillard reaction may increase the allergenicity of food allergens by contributing

to the formation of new epitopes or by exposing the buried epitopes (Gruber et al., 2005; Nakamura et al., 2005). Babiker et al. (1998) used 34 kDa soy protein, which is a well identified allergenic protein (Ogawa et al., 1993), to demonstrate that the binding affinities of antibody to soy protein conjugated with polysaccharides greatly decreased compared to the native protein. Another study demonstrated that glycation of soy protein with chitosan decreased the affinity of human immunoglobulin E (IgE) antibody from an allergic patient's serum compared to the native soy allergen (Usui et al., 2004). Arita et al. (2001) came to a similar conclusion using lysozyme in an *in vivo* system. They demonstrated that while the production of IgG was not suppressed, the production of IgE induced by the conjugates decreased significantly compared to the IgE production induced by the native protein and they concluded that the polysaccharide conjugation with allergenic proteins is a promising therapeutic approach.

2.4.5. Foam Forming Activity

Foaming characteristics of dispersions are important in many foods such as milk, mayonnaise, ice cream, etc which depend on the quality of the foam which determines the structure and contributes to sensory qualities. The foam stability depends on the properties of the surface–active components in the system (Rodríguez Patino et al., 2008). Several studies have demonstrated that carbohydrate conjugation of proteins can lead to an increase in protein diffusion at the air/water interface due to an increase in exposed hydrophobicity improving the protein's ability to form and stabilize foams. Chevalier et al. (2001a) demonstrated that moderately conjugated *β*–lactoglobulin with galactose or with glucose can be used to form foam with better stabilities and less drainage as compared to the native.

2.4.6. Antioxidant Activity

Many studies have demonstrated that alimentary proteins and peptides can interfere with radical reactions and act as primary or secondary antioxidants (Elias et al., 2008). Proteins can act as primary antioxidants by their electron or proton donor functionality or act as secondary antioxidants by retarding the oxidation through chelation of pro–oxidant transition metals such as iron and copper (Huang et al., 2005). There is evidence that the protein:carbohydrate conjugates produced through the Maillard reaction have improved radical scavenging properties (Dong et al., 2012; Gu et al., 2010b; Jing et al., 2011; Joubran et al., 2013). Sun et al. (2006) demonstrated that conjugation of ovalbumin to different D–aldohexoses could significantly increase the

antioxidant activity of ovalbumin. It has been numerously demonstrated that some advanced Maillard reaction products resulting from the numerous degradations of the initial substrates, such as reductones and melanoidins, are potent antioxidants (Borrelli et al., 2002; Manzocco et al., 2000; Xu et al., 2007). Although the mechanisms by which the Maillard reaction conjugates themselves exert their antioxidant activity are yet to be fully understood, the main structural characteristics of protein, required for an efficient radical scavenging activity, were reported to be the number of free radical scavenging amino acids and their solvent accessibility (Elias et al., 2008). It is likely that the different structural changes of the protein during carbohydrate conjugation can lead to an increased exposure of free radical scavenging amino acids within the protein, therefore increasing the antioxidant activity of the protein.

2.5. Target Proteins

The proteins that were used in this study to be conjugated to different carbohydrates were lysozyme and potato protein patatin. Although these proteins have been demonstrated to possess many interesting functional properties to be used as food ingredients, their application has been limited. This makes them suitable candidate proteins to be investigated for carbohydrate conjugation.

2.5.1. Lysozyme

Lysozyme from hen egg white has desirable properties as a food preservative since it has demonstrated bacteriostatic, bateriolytic, and bacteriocidal acitivity (Hughey & Johnson, 1987). Other desirable characteristic of lysozyme as a food ingredient is its very high heat stability; it has a denaturation temperature at around 80 °C (Tomizawa et al., 1994). It is a polypeptide of 129 amino acid residues with a molecular weight of 14.3 kDa. It is a strongly basic protein with an isoelectric point of 10–11 (Lesnierowski & Kijowski, 2007). Since it a well characterized protein, it is often used as model protein for the carbohydrate conjugation through the Maillard reaction. Lysozyme has 7 available free amino groups including the amino terminal of the protein and the most susceptible amino acid residue to glycation has been identified as Lys 97 (Shu et al., 1996). Song et al. (2002) have used chitosan to conjugate to lysozyme and demonstrated improvements in antimicrobial activity, solubility, and also emulsifying activity of the protein. Another study by Alahdad et al. (2009) conjugated dextran sulfate to lysozyme and have observed improvements in heat stability, solubility and, emulsifying activity. Their study

demonstrated that their conjugate, lysozyme–dextran sulfate, had lower antimicrobial activity against Gram–positive bacteria, such as *Staphylococcus aureus*, compared to the unconjugated lysozyme, but had higher antimicrobial activity against Gram–negative bacteria, such as *E. coli*, compared to the native protein. Shu et al. (1996) demonstrated that the improvements in functional properties of carbohydrate–conjugated lysozyme are dependent on the length of the carbohydrate. They obtained better emulsifying activity when lysozyme was conjugated to the 6–12 kDa galactomannan as compared to the smaller galactomannan. Since lysozyme is a known egg allergen (Frémont et al., 1997), the carbohydrate conjugation through the Maillard reaction to decrease its allergenicity has also been studied by other researchers (Arita et al., 2001).

2.5.2. Potato Protein: Patatin

Potato (*Solanum tuberosum*) is the world's fourth most important crop after rice, wheat and corn. More than 3 hundred million tons of potato are produced world–wide annually (FAO, 2008). Potato tuber proteins are classified into three groups: patatin, protease inhibitors, and other proteins (Pots et al., 1999b). Patatin (PTT) is a nonspecific lipid hydrolase that consists of approximately 25–40% of the total soluble protein in mature potato tubers (Sharma et al., 2004). The mature tuber PTT variants are dimers of 40 to 45 kDa subunits without disulfide bridges but carry from one to two N–linked glycans (Pots et al., 1999a). There are 25 available free amino groups on PTT. Its foaming (Ralet & Gueguen, 2001), gelling (Creusot et al., 2010), and emulsifying properties (Ralet & Gueguen, 2000) have already been reported. In addition to its many functional properties, the use of PTT as potential food ingredient is of great interest due to its high nutritional quality that is similar to egg proteins (Camire et al., 2009), its antioxidant activity, and its potential antiproliferative activity against cancer cells (Sun et al., 2013). So far, the application of PTT as a food ingredient has been limited by its very high exposed hydrophobicity (Creusot et al., 2010) leading to limited solubility at increased ionic strength. In addition, PTT has been shown to be denatured at around 59ºC (Creusot et al., 2010), which is lower than many proteins being used as food ingredients. Given its interesting functional properties and in order to broaden its applications, the improvement of its solubility and its heat stability through carbohydrate conjugation is of great interest. Although a patent has been granted on the production of carbohydrate conjugated enriched PTT fraction through the Maillard reaction to be used as a food ingredient to decrease the strong astringent taste of a food

product (Giuseppin et al., 2011), there are no published academic studies that have looked at the effect of this conjugation on the structure, and on the functional properties of PTT.

2.6. Analytical Methods

Different analytical methods have been used for the characterization of protein:carbohydrate conjugates and for the investigation of the reaction leading to the production of these conjugates. The major analytical methods found in the literature have been summarized in the following sections.

2.6.1. Progress of the Maillard Reaction: Percent Blocked Lysine

In order to quantify the protein:carbohydrate conjugates, the Amadori compounds, and the extent of early Maillard reaction, furosine assay can be used. The furosine assay remains the most sensitive and most accepted method for determining the extent of early Maillard reactions (Marconi et al., 2002). Furosine is formed during acid hydrolysis of the Amadori product (Erbersdobler & Somoza, 2007; Krause et al., 2003). The yield of furosine is constant under controlled conditions. Published yields range from 29 to 46% after hydrolysis in 8 M hydrochloric acid (Krause et al., 2003), therefore, a conversion factor for calculating the content of Amadori product from the furosine content needs to be selected based on the nature of the Amadori product and also the molarity of the hydrochloric acid used for the hydrolysis (Krause et al., 2003). Determination of furosine at low levels can be achieved using ion-pair HPLC with UV detection at 280 nm (Resmini et al., 1990). Krause et al. (2003) found the conversion factors for calculating the amount of Amadori-modified lysine from the furosine content under different acid concentrations (Table 2.3). They have determined that the molar yield of furosine is largely dependent on the concentration of the acid used for hydrolysis and also on the type of Amadori compound.

Table 2.3 Conversion factors for calculating the amount of Amadori-modified lysine from the furosine content taken from Krause et al. (2003)

Amadori compound	Conversion factor for hydrolysis in hydrochloric acid		
	6.0 M	8.0 M	7.3 M
Fructosyl-	3.1	2.2	2.4
Lactulosyl-, Maltulosyl-	2.9	2.0	Not determined
Tagatosyl-	2.4	2.4	2.4

Once the amount of Amadori product in a sample has been quantified, the percent blocked lysine indicating the extent of carbohydrate conjugation can be calculated using the amount of Amadori product and the amount of total lysine according to following equations (Marconi et al., 2002):

$$Blocked\ lysine = furosine \times conversion\ factor \quad (2.1)$$

$$\%\ Blocked\ lysine = (blocked\ lysine \times 100)/total\ lysine \quad (2.2)$$

The amount of total lysine of a sample can be found using different colorimetric methods that measure the free amino groups, such as TNBSA assay (Cayot & Tainturier, 1997) or the *ortho*-phthaldialdehyde assay (OPA) (Kosters et al., 2003). Compared to assessing the blocked amino groups on a protein after glycation which can result from carbohydrate conjugation but also from protein cross-linking by using these colorimetric assays, the calculation of percent blocked lysine using the quantity of furosine and of total lysine offers the advantage of measuring only the formation of protein:carbohydrate conjugate. Many studies, that have looked at the production of protein:carbohydrate conjugates with improved functional properties, have used the furosine assay or have calculated the blocked lysine based on the furosine assay to measure the level of carbohydrate conjugation and to determine the extent of early Maillard reaction (Jiménez-Castaño et al., 2007; Sanz et al., 2007; Wang & Ismail, 2012).

2.6.2. Structural Analysis

2.6.2.1. Mass Spectrometry

Mass spectrometry has been used for the characterization of protein glycation both in food and in biological systems. Soft-ionization methods, such as electrospray ionization (ESI) and matrix assisted laser induced desorption/ionization (MALDI), are the commonly used techniques due to their operability under atmospheric pressure conditions to generate intact molecular ions in the gas-phase (Yeboah & Yaylayan, 2001). The advantages of mass spectrometric techniques for the analysis of protein:carbohydrate conjugates include the accurate relative molecular mass measurement that can be obtained and the high sensitivity of the technique that allows for a quantitative measurements at femtomole levels (Yeboah & Yaylayan, 2001). These techniques allow for the distinction between the glycated and non-glycated species of specific protein and provides quantitative estimation of the level of glycation. When used in conjunction with enzymatic digestion, mass spectrometric analysis of the partial hydrolysates of protein:carbohydrate conjugates can identify the glycation sites on the protein (Frolov &

Hoffmann, 2010; Lapolla et al., 2000). The main differences between ESI and MALDI is the type of ions produced and the mass analyzer used. The single charging nature of MALDI results in the production of a simple mass spectrum of molecular species in a mixture; however, the molecular weight determinations are not as accurate as in ESI. The change in molecular weight during glycation with a hexose, such as glucose, is 162 units, and the sugar moiety of the conjugates can undergo further reactions, such as dehydration that can change the molecular weight by multiples of 18 units. These mass differences are at the resolution limit of MALDI-TOF, and it is difficult to obtain adequate resolution for quantitative analysis. Corzo-Martínez et al. (2008) determined the number of carbohydrate molecules linked to *β*-lactoglobulin through MALDI-TOF-MS. The mass spectra of *β*-lactoglobulin incubated with galactose or with tagatose were characterized by a broad peak shape due to the heterogeneity of the glycated forms of the protein. They calculated the average number of galactose or tagatose molecules bound to *β*-lactoglobulin by considering the maximum intensity. After 1 day of incubation at 40°C a_w of 0.44, 14 galactose and 3 tagatose molecules were linked to *β*-lactoglobulin. Since protein glycation usually results in the formation of a wide variety of glycoforms and at different extents of oxidation and dehydration of the sugar moieties, the multiple charging nature of ESI and the high resolving power of quadrupole mass analyzers is essential in identifying and in quantifying the different species found during glycation (Yeboah & Yaylayan, 2001). ter Haar et al. (2011) used glucose, maltotriose, maltoheptaose, rhamnose, arabinose, galacturonic acid, and trigalacturonic acid for the conjugation to *α*-lactalbumin through the Maillard reaction at 60°C at a_w of 0.65. They demonstrated that between 0–15 moieties of carbohydrates were attached per molecule of *α*-lactalbumin. The initial reactivity of the carbohydrates was arabinose > rhamnose > galacturonic acid > glucose > maltotriose > trigalacturonic acid > maltoheptaose. Although more precise in molecular weight determination, ESI does not permit the analysis of complicated mixtures due to the overlapping clusters of multiple charged peaks (Yeboah & Yaylayan, 2001), therefore, MALDI-TOF/MS could be a more suitable technique when analyzing such complex samples.

2.6.2.2. Fourier Transform Infrared Spectroscopy (FTIR)

FTIR spectroscopy is a valuable tool for the examination of protein secondary structure which makes it useful for the investigation of the effect of glycation/glycosylation on the secondary

structure of the protein. Since data obtained from X-ray crystallography cannot be easily extrapolated to the dynamic properties of the proteins in solutions, vibrational spectroscopic techniques, such as FTIR, are still important and commonly used techniques for protein structure and dynamic studies (Kong & Yu, 2007). FTIR measures wavelength and intensity of the absorption of IR radiation by a sample. The polypeptide and protein units give rise to nine characteristic IR absorption bands, namely, amide A, B, and I–VII. Among these, the amide I and II bands are the most prominent vibrational bands of the protein backbone (Surewicz & Mantsch, 1988; Susi & Byler, 1986). The amide I band (1700–1600 cm^{-1}), which is mostly due to the C=O stretch vibrations of the peptide linkages (80%), is the most sensitive spectral region to the protein secondary structural components. The amide II band is from in-plane N-H bending (40–60%) and from the C-N stretching vibration (18–40%) (Krimm & Bandekar, 1986) and is therefore less affected by the protein conformation than the amide I band. The advantages of FTIR over other techniques include the analysis of proteins in a wide range of environments, and the direct correlations between the amide I band frequencies and the secondary structure components that can be found. Since the observed amide I bands of proteins are usually overlapping, mathematical methods such as resolution-enhancing techniques are necessary to resolve the individual band component corresponding to a specific secondary structure. The mathematical methods increase the degree of separation by narrowing the half-bandwidth of individual components for better distinction, but also lead to a lower signal-to-noise ratio. The Fourier self-deconvolution (FSD) curve fitting and second derivative analysis are the most often used methods (Surewicz & Mantsch, 1988; Susi & Byler, 1983). The purpose of the FSD method is to find the conditions achieving the maximum band narrowing while keeping the increase in noise and the appearance of side-lobes at minimum. This method assumes that a spectrum of single bands is broadened. The second derivative spectra allow the identification of various secondary structures present in the protein (Susi & Byler, 1983) then a curve fitting procedure can be applied to calculate quantitatively the area of each component representing a type of secondary structure. The quantitative analysis of protein secondary structure assumes that protein can be considered as a linear sum of a few fundamental secondary structural elements and that the percentage of each element is only related to the spectral intensity (Kong & Yu, 2007). Assignments of the amide I band component to each secondary structure element are available

Table 2.4 Deconvoluted amide I band frequencies and assignments to secondary structure for protein in D_2O and H_2O media

H_2O*		D_2O*	
Mean frequencies	**Assignment**	**Mean frequencies**	**Assignment**
1624±1.0	β-sheet	1624±4.0	β-sheet
1627±2.0	β-sheet		
1633±2.0	β-sheet	1631±3.0	β-sheet
1638±2.0	β-sheet	1637±3.0	β-sheet
1642±1.0	β-sheet	1641±2.0	3_{10} helix
1648±2.0	Random	1645±4.0	Random
1656±2.0	α-helix	1653±4.0	α-helix
1663±3.0	3_{10} helix	1663±4.0	β-turn
1667±1.0	β-turn	1671±3.0	β-turn
1675±1.0	β-turn	1675±3.0	β-sheet
1680±2.0	β-turn	1683±2.0	β-turn
1685±2.0	β-turn	1689±2.0	β-turn
1691±2.0	β-sheet	1694±2.0	β-turn
1696±2.0	β-sheet		

*Data are from Kong and Yu (2007) adapted from Susi and Byler (Byler & Susi, 1986; Susi & Byler, 1983) and from Dong et al. (1992).

for proteins in both D_2O and H_2O and they are listed in Table 2.4. The subtraction of the H_2O is important since H_2O has strong IR absorbance around 3400 (O-H stretching), 2125 (water association), and 1645 cm^{-1} (H-O-H bending) (Kong & Yu, 2007). For this reason, it is much easier if the study is carried out in D_2O solution since it has no absorption spectrum in the region where amide I and II bands are found. To judge if obtained spectrum is adequate, first the bands originating from water vapor must be subtracted from the protein spectrum between 1800 and 1500 cm^{-1}, then a straight baseline must be obtained from 2000 to 1750 cm^{-1} (Dong et al., 1992). Jindal and Naeem (2013) investigated the secondary structural changes of κ-casein during glycation with fructose at 37°C for 15 days in sodium phosphate buffer. Through FTIR and with samples in D_2O, they have demonstrated that upon incubation for 15 days, there is a significant drop in absorbance along with the appearance of a broad peak at 1626 cm^{-1} which is suggestive of the intermolecular aggregated state (intermolecular β-sheets). On the other hand, Joubran et al. (2013) demonstrated that the glycation of bovine lactoferrin with glucose or fructose at 60°C for 12 or 36h at a_w of 0.79 did not lead to any marked changes in FTIR spectra in the amide I band. It has been previously demonstrated by other studies that under similarly moderate dry glycation conditions, changes in protein structure are significantly less pronounced than in studies performed in aqueous solution (Morgan et al., 1999b; Wong et al., 2011; Wooster & Augustin, 2007).

2.6.2.3. Tryptophan Fluorescence

The intrinsic fluorophore tryptophan is an excellent parameter to monitor the polarity of the tryptophan environment in the protein (Beechem & Brand, 1985). Tryptophan is usually found fully or partially buried in the hydrophobic core of protein interiors, at the interface between two protein domains, or at the subunit interface in oligomeric protein systems due to its aromatic character (Royer, 2006). Upon disruption of the protein's tertiary or quaternary structure during glycation/glycosylation, these side chains become more exposed to solvent. Due to the large excited-state dipole moment of the tryptophan, its emission maximum is quite sensitive to its local environment and roughly correlates with the degree of solvent exposure of the residue. The residues that are buried in the hydrophobic interior or interfaces of proteins will exhibit a blue-shift (decrease in wavelength) in emission maximum. Upon unfolding, the emission maximum of tryptophan residue will shift to red (increase in wavelength) (Royer, 2006). Typically, the information obtained from the interpretation of the fluorescence parameters is limited to the

degree of exposure of the fluorophore to the solvent and the extent of its local mobility. In protein folding studies, it is preferred to compare the observed fluorescence changes with circular dichroism, FTIR, or, NMR spectrum of the protein (Royer, 2006). Jindal and Naeem (2013) demonstrated that the emission spectra maxima of native *κ*-casein was at 345 nm and upon glycation with fructose for 12 days, there was a decrease in fluorescence intensity and a red shift of 5 nm (to 350 nm) indicating the aggregation of *κ*-casein. Corzo-Martínez et al. (2008) demonstrated that while the native *β*-lactoglobulin had a fluorescence emission maximum at 335 nm, the incubation of *β*-lactoglobulin with galactose or with tagatose at 50°C for 2 days led to a red shift of the emission maximum to 340 or to 338 nm, respectively. Their results suggest that the glycation at 50°C led to a disruption of the protein's tertiary structure towards a more aggregated state.

CONNECTING STATEMENT 1

A comprehensive literature review on the carbohydrate conjugation to proteins through the Maillard reaction and through the enzymatic glycosylation is provided in Chapter II. The production of LZM:carbohydrate conjugates through the Maillard reaction is reported in Chapter III. The progress of the Maillard reaction was studied with focus on the effects of the incubation time and on that of the carbohydrate chain length (galactose, GOS, galactan) on the glycation extent of LZM conjugates and on their protein cross-linking/browning level. LZM:carbohydrate conjugates were purified using cation exchange chromatography. The effects of carbohydrate conjugation on thermal stability, protein solubility, emulsifying properties, and immunoreactivity of LZM are also discussed in this chapter.

The results from this study were presented at the International Biotechnology Symposium and Exhibition and published in the journal of *LWT – Food Science and Technology*.

Seo, S., Karboune, S., Khodaei, N, & Yaylayan, V. (2010) *Preparation of potato galactooligosaccharide and galactan derivatives by Maillard-type glycation with lysozyme*. 14th International Biotechnology Symposium and Exhibition, Rimini, Italy, September 14–18.

Seo, S., Karboune, S., L'Hocine, L., & Yaylayan, V. (2013). Characterization of glycated lysozyme with galactose, galactooligosaccharides and galactan: Effect of glycation on structural and functional properties of conjugates. *LWT - Food Science and Technology, 53*(1), 44–53.

CHAPTER III

CHARACTERIZATION OF GLYCATED LYSOZYME WITH GALACTOSE, GALACTOOLIGOSACCHARIDES AND GALACTAN: EFFECT OF GLYCATION ON FUNCTIONAL PROPERTIES OF LYSOZYME

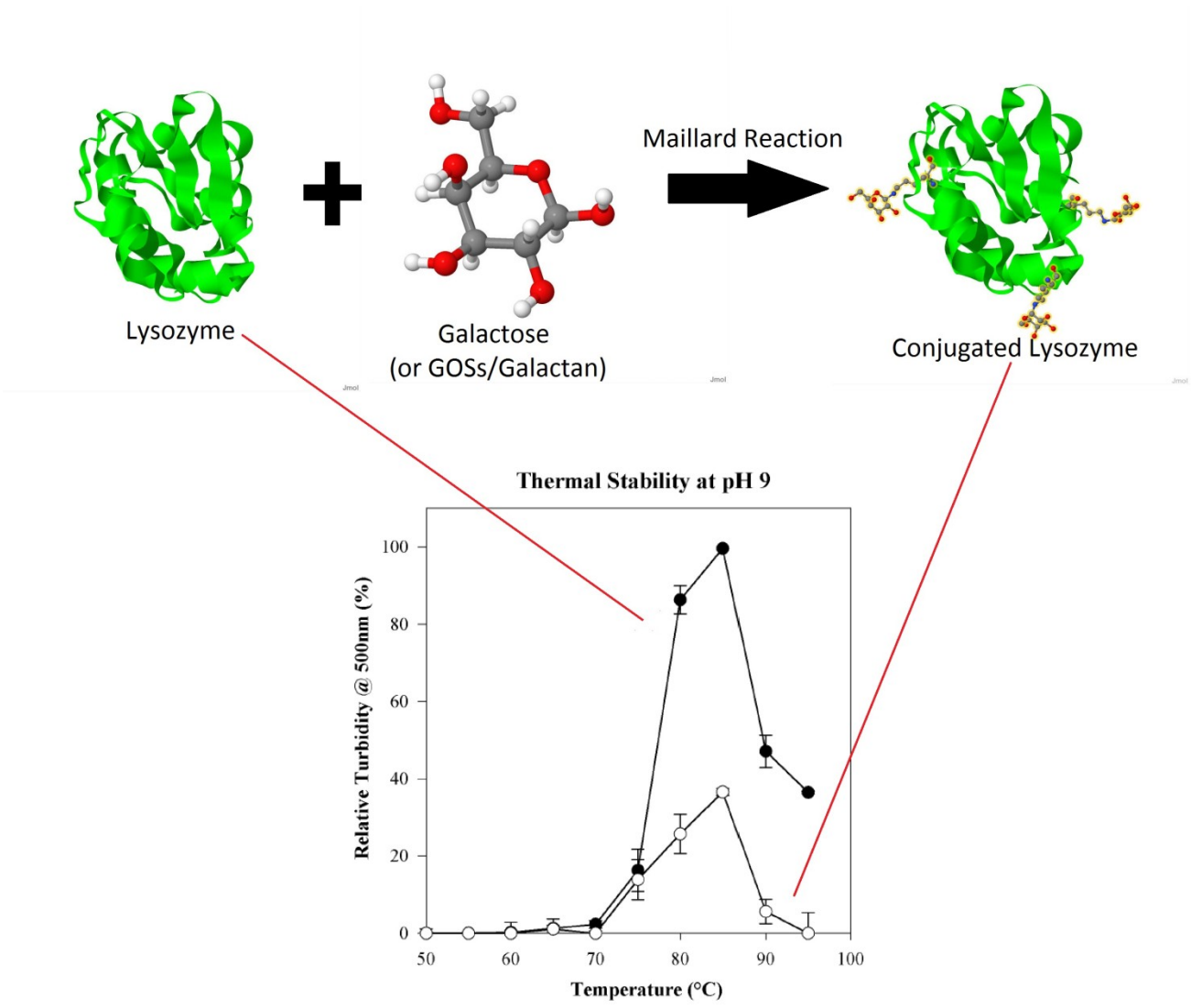

3.1. Abstract

Lysozyme (LZM) was conjugated with galactose-, galactooligosaccharides (GOS), and galactan through the Maillard reaction under controlled conditions. The reaction mixtures were investigated for the progress of the Maillard reaction, for the structural characteristics of the produced conjugates, and for the improvement in functional properties of the conjugates. The progress of the Maillard reaction revealed high initial reactivity of galactose to LZM compared to GOS and to galactan. The glycation reaction between LZM and GOS revealed the presence of oxidative side reactions that competed with the initial formation of Amadori products and that favored protein cross-linking. The longer chain carbohydrate galactan demonstrated the slowest progress of the Maillard reaction. The percentage distribution of LZM conjugates revealed the formation of different glycoforms. Glycated LZM containing up to eight galactose moieties were formed, while only mono- to tetraglycated LZM with GOS were detected. 2–3 moles of galactan were conjugated to one mole of LZM. In general, the proportion of glycoforms shifted toward the highly glycated LZM with an increase in incubation time. Galactan-conjugated LZM exhibited improvements in solubility at pH 9, in thermal stability and in emulsion stability as compared to the unmodified LZM and LZM:galactose conjugates. LZM conjugated with GOS demonstrated most improvement in emulsion stability among the conjugates. The glycation of LZM with galactose/GOS/galactan decreased its immunoreactivity.

3.2. Introduction

The Maillard reaction comprises of complex series of naturally-occurring reactions with the protein glycation reactions being the early and intermediates ones (Nursten, 2005). These glycation reactions include the initial condensation reaction between amino groups of proteins and the carbonyl group of a reducing carbohydrate to form Amadori/Heyns intermediate products, followed by dehydration of the sugar moieties, cross-linking and degradation of proteins (Davidek et al., 2002; Nursten, 2005). To control and limit the Maillard reaction to its early stages, the effects of selected parameters, including protein:carbohydrate ratio, temperature, pH, incubation time, and water activity (a_w), on the reaction rate have been studied by others (Jakas et al., 2008; Jiménez-Castaño et al., 2005).

Over the last years, there has been an increased interest in the use of Maillard reaction as a simple way to form protein:carbohydrate conjugates with improved functional properties.

Indeed, Maillard-type glycation under controlled conditions has been reported to improve emulsifying properties (Dickinson & Galazka, 1991), solubility (Niu et al., 2011), heat stability (Broersen et al., 2004), water/oil holding capacity (Matemu et al., 2009), and foam-forming properties (Fechner et al., 2007) of proteins. In addition, a decrease in the allergenicity of proteins, *in vivo,* upon glycation has also been reported (Arita et al., 2001). Moreover, the glycation of proteins with prebiotic oligosaccharides could lead to novel prebiotic products with an enhanced colonic persistence (Gibson et al., 2004). The structural modifications of proteins via the Maillard reaction are, therefore, expected to extend the use of proteins in many applications and to fulfill the current needs of high-quality multi-functional food ingredients.

In order to produce glycoproteins with improved properties via the Maillard reaction, proper understanding of the effects of carbohydrate moieties on the protein glycation extent and on the functional properties of resulting protein:carbohydrate conjugates are necessary. As an overall, it has been found that the carbohydrate reactivity in the Maillard reaction decreased as the chain length increased (Corzo-Martínez et al., 2010b; Li et al., 2009; Niu et al., 2011). However, conflicting results (Corzo-Martínez et al., 2010b; Li et al., 2009; Matemu et al., 2009; Shu et al., 1996) have been reported on the effects of the carbohydrate moieties (mono, oligo and polysaccharides) on the functional properties of conjugates. For instance, the emulsifying properties of protein:low molecular weight carbohydrate (mono-, di-, oligosaccharides) conjugates were reported to be unchanged, (Matemu et al., 2009; Niu et al., 2011), lower (Niu et al., 2011) or higher (Li et al., 2009; Matemu et al., 2009) as compared to native proteins and/or to proteins conjugated with higher molecular weight carbohydrates. Water and oil-binding capacities, which are dependent on the length/charge of carbohydrate moieties and on the glycation extent, have been identified as important factors for the emulsifying properties of conjugates (Matemu et al., 2009). The extent of the improvement of the solubility of proteins upon Maillard-type glycation was also dependent on the molecular weight of carbohydrates (Li et al., 2009; Niu et al., 2011). Low molecular weight carbohydrates (glucose, lactose) imparted better solubility to rice proteins upon glycation than higher molecular weight ones (dextrin, maltodextrin) (Li et al., 2009). In contrast, the glycation of wheat germ protein with high molecular weight dextran led to a more significant improvement in the protein solubility as compared to the glycation with smaller carbohydrates (glucose and xylose) (Niu et al., 2011).

Considering these conflicting results, there is a need to further elucidate the effect of carbohydrate chain length and binding numbers on the functional properties of the glycoproteins.

The present study was aimed at the investigation of the glycation of LZM with carbohydrates of different lengths, including mono- (galactose), prebiotic oligo- (potato GOS) and polysaccharides (potato galactan), through the Maillard reaction. LZM has many desirable properties as a food protein including antimicrobial activity (Hughey & Johnson, 1987) and heat stability (Tomizawa et al., 1994); however, LZM has poor functional emulsifying properties and it is known to be one of the most important allergenic food ingredients (Frémont et al., 1997). The specific objectives of this study were (a) to evaluate the glycation of LZM with galactose, GOS, and galactan, (b) to characterize the structures of glycated LZM, and (c) to investigate the functional properties of these conjugates such as protein solubility, heat stability and emulsifying capacity. The allergenicity of the glycated LZM was also evaluated indirectly by measuring their immunoreactivity.

3.3. Materials and Methods

3.3.1. Materials

LZM from chicken egg white (>96% purity), triolein, D-(+)-galactose, TNBSA (2,4,6-trinitrobenzene sulfonic acid) and salts were purchased from Sigma Chemical Co. (St-Louis, MO). Biogel P2 extra fine, Bradford reagent and low range SDS-PAGE standards were purchased from Bio-Rad (Philadelphia, PA). Furosine standard was purchased from Neosystem Lab. (Strasbourg, France). Potato galactan (~100 kDa) and endo-1→4-*β*-D-galactanase from *Aspergillus niger* were purchased from Megazyme (Wicklow, Ireland).

3.3.2. Preparation of Galactooligosaccharides

Potato galactan was enzymatically hydrolyzed to produce GOS. Endo-1→4-*β*-D-galactanase (25 U/l) was added to potato galactan solution (1 g/l) in 0.1 M sodium acetate buffer (pH 4.5). After 23 h incubation at 40ºC, the reaction mixture was ultrafiltered using a stirred ultrafiltration unit (Amicon system, Millipore, Billerica, MA) fitted with a 3 kDa molecular mass cut-off membrane. The recovered filtrate was fractionated by size exclusion chromatography on Biogel P2 column using 20 mM ammonium carbonate buffer (pH 7.0) as a mobile phase at a flow rate of 0.3 ml/min. Fractions of 1 ml were collected using a fraction collector (LKB FRAC-100, Pharmacia, Uppsala, Sweden) and subjected to analysis by thin layer chromatography (TLC).

TLC on silica-gel 60 F_{254} plates (EMD Chemicals, Gibbstown, NJ) was performed with butanol/acetic acid/water (4: 5: 2, v/v/v) as the developing mobile phase. For carbohydrate detection, the TLC plates were sprayed with 2 % (v/v) sulfuric acid in methanol and heated at 90^{o}C for the development of orange spots. The fractions containing GOS were pooled and lyophilized. The lyophilized powder was desalted by elution with water using the same Biogel P2 column. The molar mass of the obtained GOS was determined by taking the average of the distribution of the different GOS determined from ESI-MS analysis (1990.9 g/mol, data not shown).

3.3.3. Preparation of Conjugates

LZM and carbohydrates (galactose or GOS or galactan) were dissolved in 0.1 % (w/v) of 0.05 M sodium phosphate buffer (pH 7.0) at the molar ratio of 1:7, and were lyophilized at -25°C. The powder mixtures were incubated in sealed glass dessicators at 60ºC for various periods (1, 3, 5, 7 days) under controlled a_w values of 0.65 (saturated potassium iodide) for LZM:galactan mixtures and 0.45 (saturated magnesium nitrate) for LZM:galactose/GOS mixtures. The mixtures were stored at -20ºC after incubation until further analyses.

3.3.4. Determination of the Extent of Glycation of Lysozyme with Selected Carbohydrates

3.3.4.1. Measurement of Proportion of Free Amino Groups

The free amino groups of LZM after glycation with selected carbohydrates was determined using trinitrobenzene sulfonic acid (TNBSA) assay (Goodwin & Choi, 1970). 0.25 ml of 0.01 % (v/v) TNBSA was added to 0.5 ml of LZM conjugate solutions (10 mg/ml) in 0.1 M sodium bicarbonate buffer (pH 8.5) then incubated at 37°C for 2 h. 0.25 ml of 10 % (w/v) sodium dodecyl sulfate (SDS) and 0.125 ml of 1 N hydrochloric acid were added to solubilize the protein and to avoid their precipitation. The absorbance of the reaction mixtures was measured spectrophotometrically (DU 800, Beckman Coulter, Fuellerton, CA) at 335 nm against a buffer blank. The standard curve was constructed using L-leucine. The percentage of unavailable amino groups was calculated as the concentration of the initial free amino acids of LZM minus the concentration of free amino acids of LZM upon glycation, divided by the initial value. All assays were run in triplicates.

3.3.4.2. Furosine Analysis

To estimate the degree of glycation, the ε-N-2-(furoylmethyl)-L-lysine (furosine) was determined using a modified method of Moreno et al. (2002). Four hundred microliters of LZM conjugates (2–4 mg of protein) was added to 1.1 ml of 8 N hydrochloric acid, and were incubated at 110°C for 23 h under nitrogen. The recovered hydrolysates were centrifuged at 14,000 x *g* for 10 min before applying 1 ml to a previously activated Sep-pak C18 cartridge (Waters Corp., Milford, MA). Three milliliters of 3 N hydrochloric acid was used for the elution of furosine. The eluate was evaporated until dryness under nitrogen. Furosine concentration was determined using high-pressure-liquid chromatography (HPLC) according to the method described by Resmini et al. (1990). A Beckman HPLC System equipped with a programmable solvent module (model 126), a photodiode array detector and a system Gold software for data collection, was used. Thermo Hypersil-Keystone Prism RPN (250 x 3 mm, 5μm, Thermo Scientific, Waltham, MA, US) column was used for the separation. 0.06 M sodium acetate buffer (pH 4.3) was used as the mobile phase at an isocratic mode for 30 min at a flow rate of 0.4 ml/min. Injected sample volume was 20 µl and the detection of furosine was performed at 280 nm. The calibration curve was constructed using furosine standard. All assays were run in duplicates with quadruplicate injections with or without internal standard.

3.3.4.3. Measurement of Browning Index

The extent of the brown polymer formation occurring during the advanced stages of Maillard reaction was estimated spectrophotometrically by measuring the browning index at 420 nm (Wijewickreme et al., 1997). All assays were run in triplicates.

3.3.4.4. SDS-PAGE Analysis

Sodium dodecyl sulfate-polyacrylamide gel electrophoresis (SDS-PAGE) was carried out according to the method of Laemmli (1970) using 5 and 15% (v/v) acrylamide content in the stacking and resolving gels, respectively. Sample loading (LZM / LZM conjugates at 0.5 mg/ml) was achieved in a mini protein gel apparatus with a 1.5 mm-thick gel. The electrophoresis was conducted at a constant voltage of 120 mV. The gels were then stained for 2 h with a staining solution containing 1 g of Coomassie brilliant blue R250 in methanol: water: acetic acid (45: 45: 10, v/v/v), followed by destaining in methanol: acetic acid: water (1: 1: 8, v/v/v). A low range of protein standards (14.4 to 97.4 kDa, Bio-Rad) was used. Alphaview software (version 3.3.1, Cell Biociences, Santa Clara, CA) was used to analyze the band densities.

3.3.5. Fractionation of LZM Conjugates through Cation Exchange Chromatography

LZM:galactose and LZM:GOS conjugates at day 1 of incubation and LZM:galactan conjugates at day 5 of incubation were passed through a 0.2 μm filter (Millipore) before being subjected to cation exchange chromatography on CM Sepharose FF column (Pharmacia). First, the insoluble protein was removed by centrifugation at 4000 × g for 5 min. One mililiter of LZM conjugates (10 mg protein) was loaded on the column (20 ml) previously equilibrated with 10 mM ammonium carbonate buffer at pH 7.0. LZM conjugates were eluted stepwise with the same buffer containing 0, 0.1 and 0.2 M of sodium chloride. Fractions of 1 ml were collected using a fraction collector and subjected to total glycoside and protein content analyses using the phenol sulfuric acid method (Dubois et al., 1956) and the Bradford Microassay (Bradford, 1976), respectively. The final glycoside concentration was corrected for the unconjugated glycoside eluted at fraction 1 and 2 by injecting the controls containing the unincubated mixtures of LZM and galactose/GOS/galactan. The fractions containing purified glycated LZM were collected, dialyzed against distilled water overnight at 4ºC and used for the assessment of the functional properties. LZM:galactose and LZM:galactan conjugates at day 7 were assessed for their elution profile at advanced stages of the Maillard reaction.

3.3.6. Structural Characterization of Lysozyme Conjugates

3.3.6.1. Mass Spectrometry

A triple-quadrupole mass spectrometer equipped with a Surveyor LC pump, an LCQ advantage mass spectrometer (ion trap) with Xcalibur software to control the system acquisition and data processing was used to obtain the mass spectra of LZM:galactose and LZM:GOS conjugates. Samples were infused at a rate of 1 µl/min into the spectrospray ion source (fused silica capillary of 100 μm i.d.) from a low-pressure infusion pump (model 22, Harvard Apparatus, South Natick, MA). The following equation was used to identify different peaks corresponding to the different species of the conjugates where M is the molecular weight of LZM (~14.3 kDa), N is the number of attached galactose molecules and W is the number of dehydrated water molecules:

$$m/z = (M + N\ x\ 180 - N * 18 - W\ x\ 18 + 12)/12 \qquad (3.1)$$

The relative proportions of different species of conjugates were estimated from the relative intensities of their corresponding peak in the mass spectrum as a ratio of the total intensity of all identified peaks of conjugates and expressed as percentage distribution of glycoforms.

3.3.6.2. Size Exclusion Chromatography

Gel filtration with a 25 ml Superose 12 (GE Healthcare, Piscataway, NJ) column was used to estimate the molecular weight of the LZM:galactan conjugates. 20 μl of the purified LZM:galactan conjugates (5 mg/ml) was applied to the column using a FPLC system (GE Healthcare). 0.05 M sodium phosphate buffer at pH 7.0 containing 0.15 M of sodium chloride was used to carry out the elution at a flow rate of 0.5 ml/min. The sample was detected at 280 nm with a UV-MII detector (Pharmacia). A mixture of protein standards consisting of bovine serum albumin (67 kDa), ovalbumin (44 kDa) and ribonuclease A (13.7 kDa) was used. The standard curve was constructed by plotting the log of the molecular weight of the standards versus the elution volume. The column void volume was determined using blue dextran 2000.

3.3.7. Functional Properties of Conjugates

3.3.7.1. Protein Solubility

Protein solubility was assessed according to the method of Abtahi and Aminlari (1997). Ten miligrams of conjugates were dissolved in 1 ml of 0.1 M appropriate buffer (sodium acetate at pH 5.0; sodium phosphate at pH 7.0 or 9.0), mixed thoroughly and assessed for their total protein content using the Bradford method (Bradford, 1976). The conjugate solutions were then centrifuged at 2700 x *g* for 15 min and the protein content of their supernatant was measured. Protein solubility was expressed as the percentage of protein content in the supernatant with respect to the total protein content.

3.3.7.2. Thermal Stability

Thermal stability of unmodified and glycated LZM was assessed, using a modified method of Shu et al. (1996), by measuring the turbidity of protein solutions (10 mg/ml, 0.1 M sodium phosphate pH 7.0 or 9.0) at intervals of 5ºC from 50 to 95ºC. The temperature was increased approximately 1ºC/ 2 min. After reaching a given temperature, the turbidity of the sample was measured spectrophotometrically at 500 nm. Heat stability was expressed as the percentage of relative turbidity calculated by comparing the developed turbidity of a sample with the highest turbidity obtained with unmodified LZM (at pH 9, 85°C).

3.3.7.3. Emulsifying Property

Thirty percent solution of triolein containing unmodified or glycated LZM (1 mg/ml) was homogenized for 3 min using a sonic dismembrator (Model 550, Fisher Scientific, Pittsburgh,

PA). The droplet size distribution of the emulsions was measured at 25ºC using a Delsa Nano C particle size analyzer (Beckman Coulter). The particle size (nm) was reported for individual droplets in the emulsion as a mean of a distribution of 70 measurements. To assess the emulsion stability, the emulsions were heated at 65ºC for 2 h and their absorbance was measured spectrophotometrically at 500 nm after dilution with 0.1% SDS (Alahdad et al., 2009).

3.3.7.4. ELISA Assessment of Immunoreactivity of the Conjugates

A slightly modified procedure of the Ridascreen FAST egg ELISA (R-Biopharm AG, Darmstadt, Germany) was used to assess the impact of glycation on the binding of LZM to specific IgG. The test, which is an enzyme linked immunosorbent assay (ELISA) for the rapid detection of egg white proteins, was calibrated against unmodified LZM standard. Unmodified and glycated LZM samples were dissolved in the extraction buffer (provided with the kit) and diluted to a final protein concentration of 100 mg/l. The samples were incubated for 10 min at 60^{o}C, centrifuged at 2500 x *g* for 10 min, and then tested. Briefly, 100 μl of each sample were placed in wells coated with antibodies against egg proteins. After 10 min of incubation, the wells were washed and 100 µl of enzyme conjugated antibody was added, followed by an incubation period of 10 min at 37^{o}C. After a last washing step, substrate solution was added. Finally the colorimetric reaction was stopped with 2 M of sulfuric acid and absorbance was measured at 450 nm using a Bench Mark Plus Microplate Reader controlled by Microplate Manager Software (Bio-Rad). Duplicate analyses were performed for each sample. ELISA data were statistically evaluated by one-way analysis of variance (ANOVA) using the SAS software 9.2 (SAS Institute Inc., Cary, NC). Significant differences between means were determined by the multiple comparison Waller Duncan K-ratio t-Test procedure at the 5% significance level.

3.4. Results and Discussion

3.4.1. Glycation of Lysozyme with Selected Carbohydrates

The glycation of LZM with galactose/GOS/galactan was quantified by measuring the percentage of unavailable amino groups and the concentration of the formed furosine (Table 3.1). Since the percent unavailable amino groups could be due to protein glycation (Cayot & Tainturier, 1997), inter/intramolecular cross-linking and subsequent degradation reactions (Bubnis & Ofner III, 1992), it can be used as an indicator in assessing the early and intermediate stages of the Maillard reaction. On the other hand, furosine, formed upon the acid hydrolysis of tagatosyl-lysine

Amadori compounds, is a better parameter for determining the glycation extent of LZM occurring during the early stages of the Maillard reaction (Resmini et al., 1990). The tagatosyl-lysine Amadori compounds are known to generated about 42% furosine upon 8 N acid hydrolysis (Krause et al., 2003). A general scheme of the early Maillard reaction and of furosine formation has been reported by Yaylayan and Huyghues-Despointes (1994). As compared to GOS and galactan, galactose showed clearly a faster initial rate of glycation with the ε-amino groups of LZM lysine residues with 51% of unavailable amino groups and 0.32 μmol of furosine after 1 day of reaction (Table 3.1). The higher reactivity of galactose may be due (a) to its high affinity for the LZM glycation binding sites by virtue of its smaller size and its higher proportion in the open-ring form, (b) to its ability to undergo glycoxidation leading to the generation of dicarbonyls that may have favored the involvement of arginine residues in the glycation reaction and/or (c) to the release of the degradation products that may have increased the rate of glycation (Fu et al., 1994; Kroh et al., 1996; Yeboah et al., 2000). The high reactivity of shorter-chain carbohydrates in the Maillard reaction has been previously reported (Corzo-Martínez et al., 2010b; Li et al., 2009; Niu et al., 2011). ter Haar et al. (2011) have highlighted that saccharide reactivity and lysine accessibility are the most determining factors for the rate of the Maillard reaction.

The maximum level of unavailable amino groups was obtained at day 3, 5 and 7 for LZM:galactose (75%), LZM:GOS (80%), and LZM:galactan (39%), respectively (Table 3.1). Beyond these reaction times, the percentage of unavailable amino groups decreased; these results may be attributed to the occurrence of the degradation reactions and hence the release of amino groups (Oliyai et al., 1994). The extent of degradation reactions was reported to be dependent on the incubation time and the stability and dehydration of the involved saccharides (ter Haar et al., 2011; Yeboah et al., 2000). The results also show that the maximum level of furosine was obtained at day 1 for LZM:galactose conjugate and at day 7 for LZM:GOS and LZM: galactan conjugates. The concerted increase of the percent unavailable amino groups of LZM:galactose conjugate with the decrease of its furosine concentration, after day 1 of reaction, confirm the very rapid progress of the Maillard reaction with galactose, resulting in the degradation of the Amadori products and in the protein cross-linking (Meade et al., 2003). However, the parallel increase of the percentage of unavailable amino groups of LZM:GOS conjugate and its furosine

Table 3.1 Percentage of unavailable amino groups and the formation of furosine upon glycation of LZM with galactose, GOS and galactan through the Maillard reaction

Conjugates	Incubation time (Days)	Unavailable amino groups [a] (%)	Furosine [b] (μmol/10 mg protein)
LZM:Galactose	1	51.0 (± 2.9)	0.32
	3	74.9 (± 6.4)	0.19
	5	62.3 (± 4.9)	0.19
	7	52.8 (± 1.7)	0.13
LZM:GOS	1	15.3 (± 5.2)	0.16
	3	78.2 (± 3.4)	0.13
	5	80.4 (± 1.9)	0.17
	7	74.1 (± 0.6)	0.48
LZM:Galactan	1	19.6 (± 1.5)	0.06
	3	27.8 (± 1.7)	0.01
	5	28.0 (± 0.2)	0.15
	7	39.1 (± 0.6)	0.46

[a] Percentage of unavailable amino groups was measured by the quantification of free amino groups.
[b] Experimental results are averages of quadruplicates and the standard deviations are less than 3%.

concentration at day 7 reveals that the protein cross-linking at the early stage of the Maillard reaction was not significantly due to the degradation of the Amadori products. The protein cross-linking observed with GOS could possibly be due to their initial degradation through autoxidation/glycoxidation leading to the formation of reactive dicarbonyls (Hollnagel & Kroh, 2000) that favor protein cross-linking (Meade et al., 2003). As indicated by the low amount of formed furosine at day 1 to day 5, the side autoxidation/glycoxidation reactions of GOS may have also reduced the effective concentration of GOS available for reacting with free amino groups of LZM; however, at day 7, the rate of glycation increased, resulting in a high formation of furosine (0.48 μmol/10 mg protein). The results may be explained by the high accumulation of oxidation products at the early stages (Yeboah et al., 2000). Contrary to the shorter carbohydrates (galactose and GOS), the reaction with galactan demonstrated a slower rate of glycation with low level of protein cross-linking. The low reaction rate with galactan may be related to the lower accessibility of this more bulky carbohydrate to the available lysine moieties of LZM.

Fig. 3.1 shows the SDS–PAGE electrophoretic patterns of LZM and conjugates with galactose/GOS/galactan at day 1 of incubation. As compared to the unmodified LZM (lane 1), dimeric and trimeric forms were observed with all conjugates, indicating that glycation of LZM promoted its polymerization (lanes 2–4). Similar results were previously described (Al-Hakkak & Al-Hakkak, 2010; Choi et al., 2005) and attributed to the prevalence of a covalent polymerization of the LZM monomers by reacting with dicarbonyls formed during the Maillard reaction (Meade et al., 2003) and during the glycoxidation/autoxidation of the carbohydrates (Thornalley et al., 1984). The protein cross-links resulting from the reaction of dicarbonyls with arginine and lysine residues of proteins are well documented (Biemel et al., 2001). The electrophoretic patterns of LZM:GOS conjugates showed higher percentage of dimeric (25 % ≈ 30 kDa) and trimeric (22 % ≈ 44kDa) cross-linked forms than the highly cross-linked forms (12 % > 100 kDa), as compared to LZM:galactose conjugates (18% ≈ 30 kDa, 17% ≈ 44 kDa, 39% > 100 kDa). The limited polymerization of LZM:GOS conjugates may be due to their glycation extent (Table 3.1). However, a higher proportion (39%) of very high molecular weight polymers (near the loading end of the gel) were obtained with LZM:galactose conjugates; the high molecular weight protein polymers in the galactose and LZM reaction are probably originated

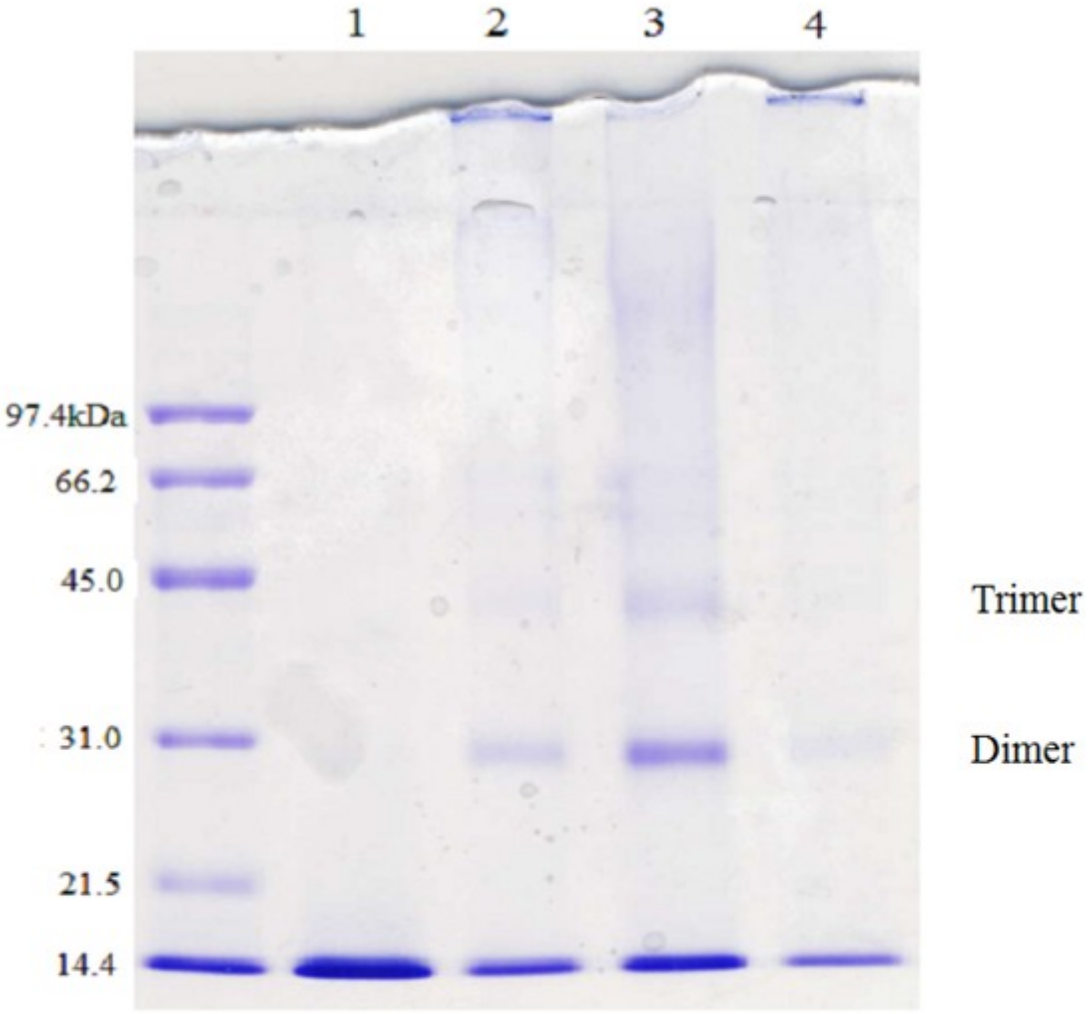

Figure 3.1 SDS-PAGE analysis of unmodified LZM (lane 1), and LZM:galactose (lane 2), LZM:GOS (lane 3) and LZM:galactan (lane 4) conjugates

from the extensive cross-linking of conjugated proteins that is favored during the intermediate and advanced stages of the Maillard reaction (Meade et al., 2003). The high molecular weight species formed (60% > 100 kDa) during the LZM:galactan reactions are the conjugates.

3.4.2. Fractionation and Identification of Lysozyme Conjugates

Fig. 3.2 shows the elution profiles of the conjugates upon fractionation by cationic exchange chromatography. While the unmodified LZM was eluted at 0.2 M sodium chloride (Fig. 3.2C), LZM conjugates were eluted at 0 and 0.1 M sodium chloride (Fig. 3.2A, B, D). LZM has seven free amino groups, three of which (Lys-1, Lys-98, Lys-33) have been shown to be particularly reactive for conjugation with a carbohydrate (Aminlari et al., 2005). The low affinity of LZM conjugates for binding to the cation exchange column could be explained by the decrease in the number of free positively charged Lys residues, leading to a decrease in the protein's isoelectric point (Fenaille et al., 2003). As expected, carbohydrate:protein content ratios of the conjugates eluted at 0 M sodium chloride are higher as compared to those eluted at 0.1 M sodium chloride. This fact confirms the heavy glycation of the conjugates eluted at 0 M sodium chloride.

The overall results indicate the multiplicity of conjugated derivatives obtained upon the glycation of LZM. This multiplicity could be due to the presence of multiple forms with different numbers of carbohydrates attached to each molecule of LZM, to the extensive variability in the conjugate conformation and to the presence of protein-protein interactions. For LZM:galactose conjugates (Fig. 3.2A), two main fractions and three minor ones with one being highly glycated (eluted at 0 M sodium chloride) were obtained. The fractionation of the LZM:galactan conjugates (Fig. 3.2D) resulted in, four fractions with the main ones being highly glycated. Longer incubation times of LZM:galactose and LZM:galactan mixtures resulted in the presence of highly glycated conjugates eluted at 0 M sodium chloride over the less glycated ones (insert, Fig. 3.2A, D). As compared to LZM:galactose and LZM:galactan conjugates, no fraction of LZM:GOS conjugates could be detected at 0 M sodium chloride even upon longer incubation time (Fig. 3.2B). These results confirm our results in Table 3.1 where a high level of protein cross-linking was observed for the reaction between LZM and GOS at longer incubation times. Such cross-linked proteins were removed during the centrifugation step before the fractionation. Even though LZM:galactan conjugates at day 5 of incubation had a similar furosine level compared to LZM:GOS at day 1 of

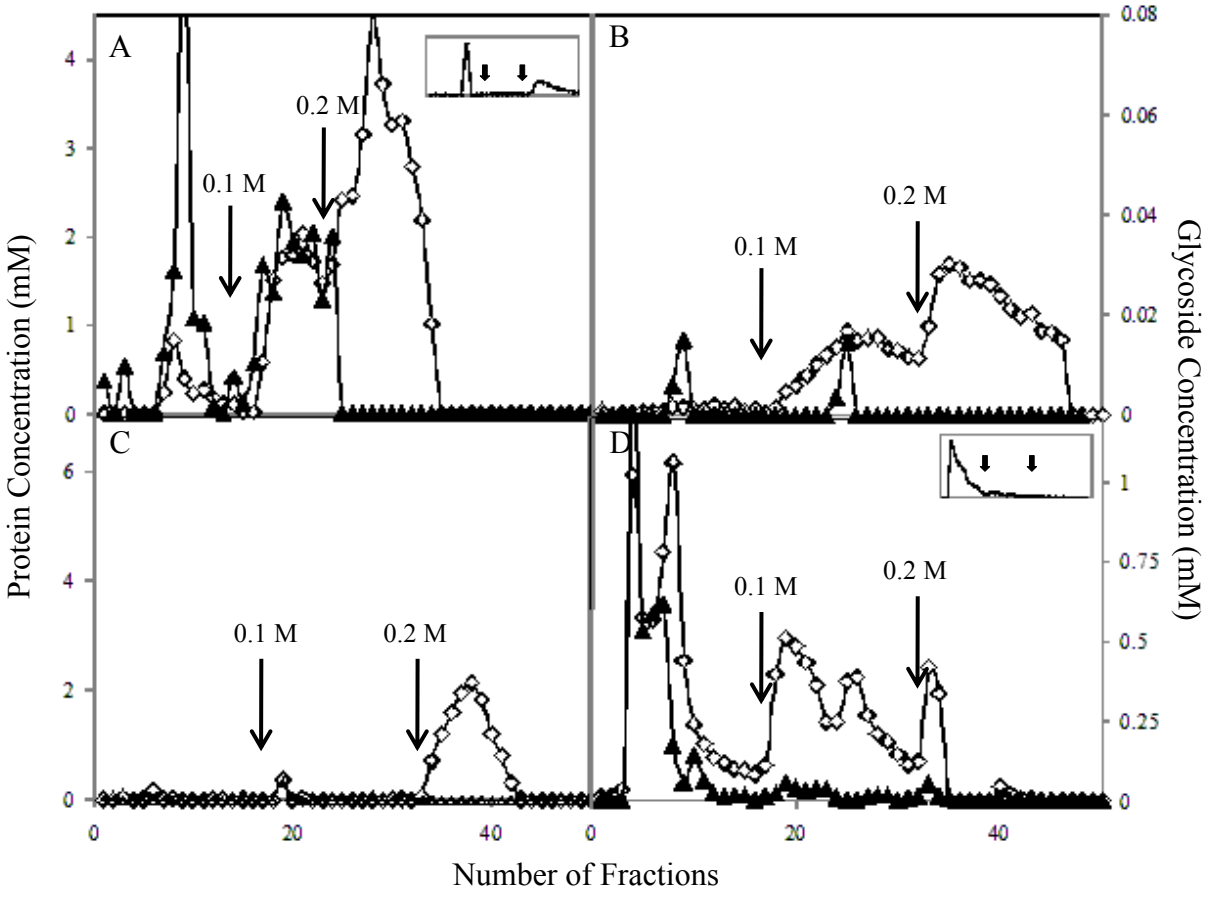

Figure 3.2 Cation exchange chromatography of LZM:galactose (A), LZM:GOS (B), unmodified LZM (C), and LZM:galactan (D) conjugates: protein (◇) and carbohydrate (▲) concentrations. Inserted graph: conjugated LZM at advanced reaction. The arrows indicate the change in sodium chloride concentration (0, 0.1, 0.2 M).

incubation (Table 3.1), the difference in their elution profiles demonstrate that the elution at 0 M sodium chloride of LZM:galactan conjugates cannot solely be explained by the bigger decrease in number of free Lys residues, but also by the spatial arrangement of the bulky galactan chains conjugated to LZM interfering with the interaction of the protein with the column. From the elution profile and from the protein:carbohydrate ratio, the conjugation level of purified LZM:galactose, LZM:GOS, and LZM:galactan conjugates were estimated to be 1–8, 1–2, and 2–3 moles of carbohydrates conjugated to 1 mole of protein, respectively. These purified conjugates were further assessed for their functional properties.

3.4.3. Structural Characterization of Lysozyme Conjugates

To analyze the heterogeneous pool of LZM glycoforms produced during the Maillard reaction, the percentage distribution of glycation species (Fig. 3.3) at selected incubation times was estimated from the intensity of the peaks in the ESI-MS spectra. Yeboah and Yaylayan (2001) have demonstrated that limited glycation has no to little effect on the ionization state of proteins and that the molecular ion distribution profile of glycoforms is representative of their corresponding species. At longer reaction times (5 to 7 days), new molecular ion peaks, separating each other by 18 atomic mass unit (amu), appeared beside the main peak of glycoforms, indicating the dehydration of the Amadori products (data not shown). However, over the investigated reaction time course, the mass distribution of the conjugates was adequately dispersed allowing an accurate interpretation of the results. After one day of incubation, LZM glycated with two and three galactoses were predominant (18.7-21.7%), whereas the glycoforms with the highest level of glycation, hexa-, hepta and octogalactosylated LZMs, represented the lowest proportion (<10.4%). By the fifth day of incubation, the predominant glycoform became the tetragalactosylated LZM (20.0%). Upon reaching the seventh day of incubation, the most observed glycoform was LZM glycated with more than five galactose moieties, representing 55.5% of total glycoforms. It can be observed that the relative proportion of the predominant glycoform at day 1, the digalactosylated LZM, gradually decreased to the second lowest observed glycoform at day 7 (9.7%). In overall, there was a shift in the distribution of LZM glycoforms toward the highly glycated forms with longer incubation time. Similar results have been reported by Yeboah et al. (2000) where the proportion of glycoforms of LZM with higher number of conjugated fructose moieties increased with incubation time.

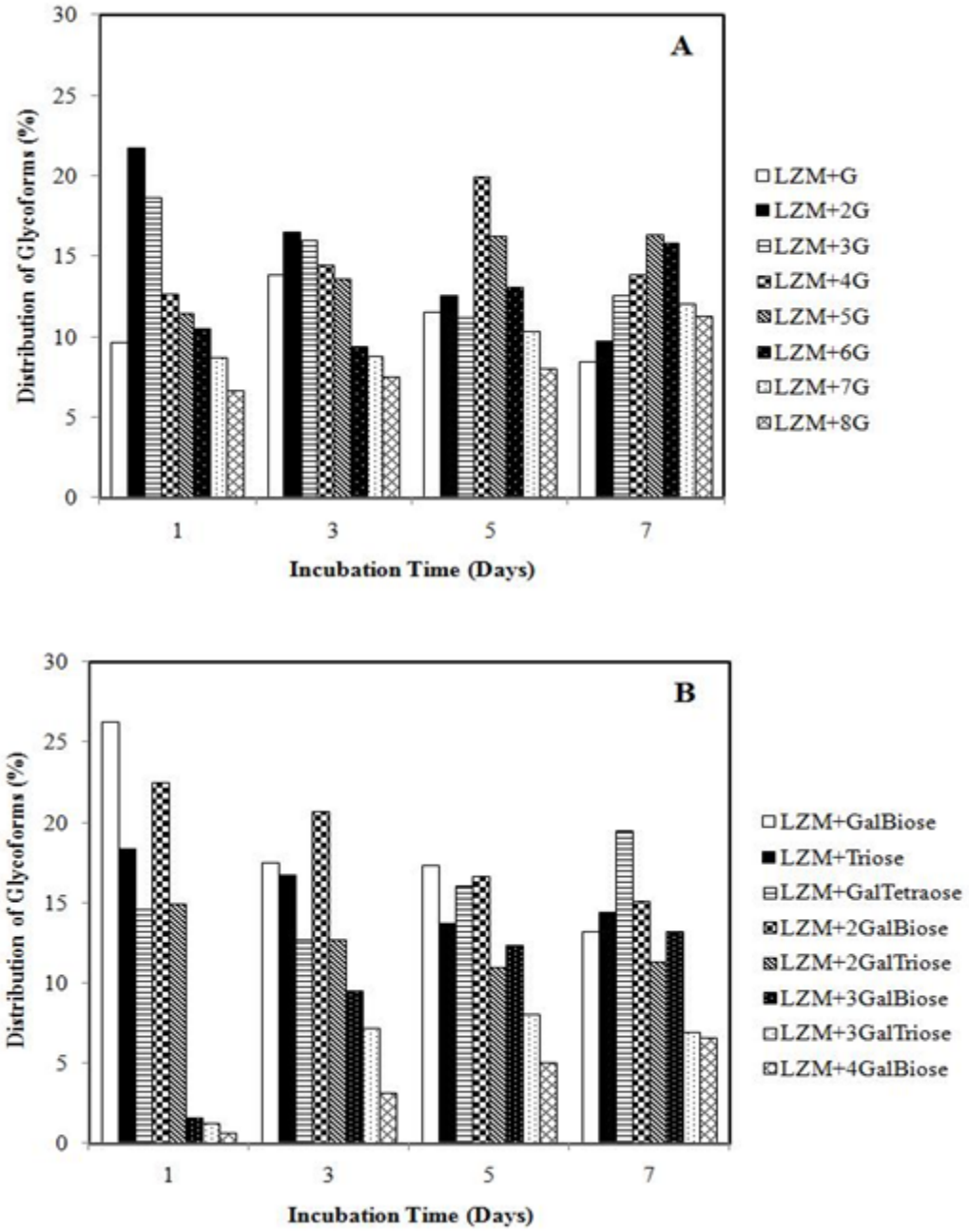

Figure 3.3 Percentage distribution of glycoforms of LZM:galactose (A) and LZM:GOS (B) conjugates at selected reaction times.

The results (Fig. 3.3B) show that both the incubation time and the chain length of GOS affect the percent distribution of glycoforms of LZM:GOS conjugates. The shorter galactobiose exhibited a faster initial rate of conjugation with LZM, resulting in the highest percent distribution of 26.3% at day 1, whereas the longer galactotetraose was slower to react with LZM reaching the highest proportion of 19.4% only at day 7. However, the monoglycated form of LZM:galactobiose conjugates gradually decreased in proportion as incubation time increased; in parallel, there was an increase in the relative percentage distribution of multi-glycated forms with longer incubation time. As compared to other LZM:GOS conjugates, LZM:galactobiose conjugates reached the highest level of glycation (up to four galactobiose) and were the most predominant glycoforms at day 1, 3, and 5 of incubation. The galactotriose was also able to multiglycate LZM with up to three galactotrioses; however, the proportions of multiglycated forms of LZM:galactotrioses were lower as compared to those of LZM:galactobioses conjugates within the glycation time course. Contrary to other GOS, The galactotetraose could only monoglycate LZM. The high reactivity of shorter chain GOS may be due to their high open chain form, their high mobility and their low bulkiness, increasing their accessibility and binding to the LZM glycation sites with high affinity. The ability of shorter chain GOS to undergo glycoxidation can also be an explanation of their high glycation rate (Yeboah et al., 2000). Similarly, ter Haar et al. (2011) have reported that the glycation rate of lactalbumin decreased when the saccharide size was increased. Moreover, the same authors have shown that using a dipeptide, the effect of a carbohydrate length on the glycation decreased with an increase in the length, revealing that the saccharide reactivity is the major important factor for the observed effect rather than the mobility of protein.

The molecular weight of LZM:galactan conjugates after day 1 of incubation was found to be at around 300 kDa by SEC on Superose 12 (data not shown). These results indicated that 2-3 moles of galactan (average MW of 100 kDa) were covalently linked to one mole of LZM. Similarly, Aminlari et al. (2005) have reported that one mole of LZM was conjugated with 2 to 3 moles of dextran. The structural characterization of LZM conjugates were in accordance with the glycation level obtained from the fractionation of LZM conjugates (Fig. 3.2).

3.4.4. Functional Properties of Conjugates

3.4.4.1. Protein Solubility

The effect of glycation on LZM solubility at different pH is shown in Table 3.2. While the unmodified LZM was highly soluble at pH 5 (93.1%) and 7 (91.1%), it exhibited low solubility at pH 9 (49.6%) closest to its isolectric point (pH 11) because of high electrostatic attractions. Upon LZM glycation with galactose and GOS, no significant change (less than 10%) in its solubility was observed at pH 5 and 7; however, a decrease in its solubility was obtained upon glycation with galactan. The substitution of LZM lysine residues upon the glycation with galactose and GOS did not make unfavorable contribution to its solubility at a more acidic pH; these results reveal that the hydration effect of the carbohydrates overcame the effect of the decrease in the p*Ka* value on LZM solubility (Quan et al., 2008). On the other hand, the low solubility of LZM:galactan conjugates at acidic and neutral pH values could be attributed to the linearity of galactan, which may have formed aggregates by intermolecular hydrogen bonding (Braudo, 1992).

The results also show that the conjugation of LZM with galactan and galactose increased its solubility at pH 9 from 49.6% to 82.5% and 79.3%, respectively. Similarly, Aminlari et al. (2005) have reported a significant improvement in the solubility of LZM at pH 9, when it was glycated with 2.99 moles of dextran. The increase in the solubility of glycated LZM at pH 9 could be attributed to the hydration capacity of the saccharides, to the decrease in the exposed hydrophobicity of the protein, and/or to the increase in the negative charge of LZM due to the substitution of its lysine residues (Nakamura et al., 1994). The solubility of LZM:GOS conjugates was similar to that of the unmodified LZM at pH 9. These results may be due to the binding of GOS to limited LZM glycation sites as demonstrated by the fractionation of LZM:GOS conjugates (Fig. 3.2B) and by the low percentage distribution of multiglycoforms (Fig. 3.3B). Li et al. (2009) have shown that the most significant improvement in the solubility of rice protein was obtained upon glycation with glucose and lactose than maltodextrin and dextrin, and attributed this effect to the high degree of glycation with the short carbohydrates. Using conjugates with similar glycation degree to each other, Niu et al. (2011) have demonstrated that the best improvement in protein solubility of wheat germ protein was obtained upon glycation with dextran than with glucose and lactose. Both the degree of glycation and the carbohydrate length determine the extent to which protein solubility is improved upon glycation.

Table 3.2 Effect of LZM glycation on its solubility at selected pH values.

Conjugates	Protein Solubility (%)[a]		
	pH 5	**pH 7**	**pH 9**
Native LZM	93.1 ± 2.0	91.1 ±3.5	49.6 ± 2.4
LZM:Galactose	91.4 ± 5.2	94.8 ± 0.7	79.3 ± 5.8
LZM:GOS	100.0 ± 2.5	94.5 ± 5.4	51.0 ± 4.1
LZM:Galactan	69.5± 2.4	80.5 ± 3.6	82.5 ± 4.2

[a] The percent solubility was calculated as the protein concentration of the supernatant recovered after centrifugation over the total protein.

3.4.4.2. Thermal Stability

The thermal stability of unmodified and conjugated LZM was assessed, over a wide range of temperatures (50 to 95°C) and at selected pH values of 7 and 9, by measuring the increase in turbidity at 500 nm (Fig. 3.4). As expected, the unmodified LZM exhibited a high thermal stability at pH 7 than at pH 9 with a denaturation temperature, at which a maximum loss of solubility was observed, of 85 and 75°C, respectively. At pH 7, the relative turbidity of the LZM:galactose and LZM:GOS conjugates at 70 to 85°C was higher (44.3–52.7%; 12.4–25.6%) as compared to the unmodified protein (1.0–6.7%). These results indicate the low thermal stability of LZM:galactose and LZM:GOS conjugates at pH 7 as compared to the unmodified LZM; such findings may be due to the conformational changes of LZM upon glycation with galactose and GOS that may have decreased the α-helix content and hence favored the protein aggregation at high temperatures (Shu et al., 1996; Takahashi et al., 2000). Above 85°C at pH 7, the relative turbidity of the LZM:galactose conjugates decreased to reach 9.4% at 95°C, whereas that of LZM:GOS conjugates increased in a similar manner to the unmodified LZM to achieve 65.6% turbidity at 95°C. In addition to the conformational changes, the shift of the isoelectric point of LZM towards the neutral region upon its glycation with GOS may have occurred and favored the protein aggregation at pH 7.0 and at high temperatures (>70°C). Although the LZM:GOS conjugates produced higher turbidity at pH 9 than at pH 7 over the investigated temperatures, the relative turbidity values (70-78.7%) obtained upon incubation above 80°C at pH 9.0 were slightly lower than those of the unmodified LZM (86.3–100%). These results may be due to the attached oligosaccharide moieties that may have sterically limited the aggregation of proteins at high temperatures and at pH 9 as compared to the unmodified LZM (Shu et al., 1996). Fig. 3.4 also shows that LZM:galactose conjugates started to form turbidity at the same temperature as the unmodified LZM (70°C) at pH 9; however, the relative turbidity of LZM:galactose conjugates at temperature higher than 85°C was lower (36.6%) as compared to that of the unmodified protein. These results indicate the high thermal stability of LZM:galactose conjugates at pH 9 and this could be due to the low occurrence of protein-protein interactions as a result of the decrease of the LZM hydrophobicity upon glycation (Broersen et al., 2004). Similarly, Broersen et al. (2004) have reported an increase in the heat stability of β-lactoglobulin after glycation with lactose, fructose, and glucose.

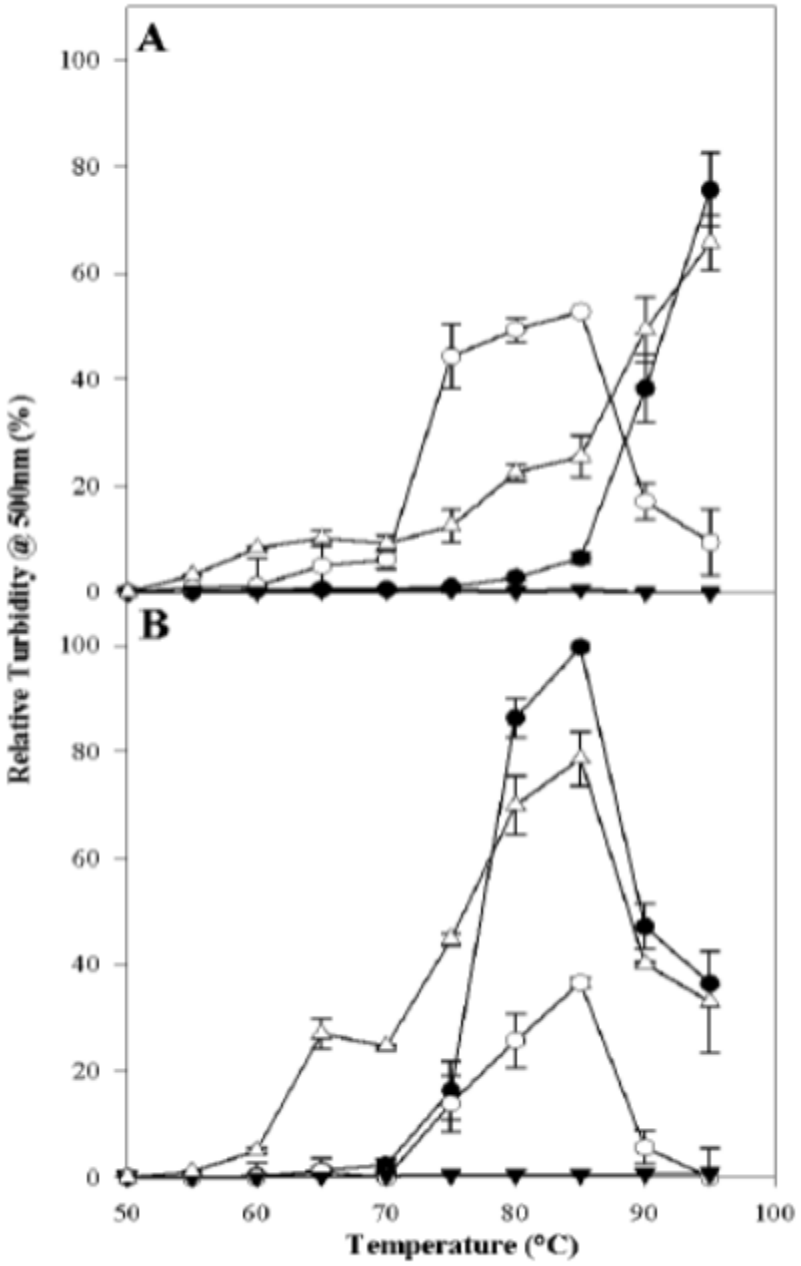

Figure 3.4 Effect of LZM glycation on its heat stability at pH 7 (A), and at pH 9 (B): unmodified LZM (●), and LZM:galactose (○), LZM:GOS (△) and LZM:galactan (▼) conjugates. Data are means ± standard deviation of triplicates.

Contrary to LZM and other conjugates, LZM:galactan conjugates did not produce any turbidity at both investigated pHs and over the wide investigated range of temperature. This lack of turbidity reveals the high thermal stability of LZM:galactan conjugates as compared to unmodified LZM and other conjugates. Similarly, the glycation of LZM with other polysaccharides, such as dextran, galactomannan and mannan, have led to an improvement of its heat stability (Aminlari et al., 2005; Li et al., 2009); such improvement was attributed to the ability of longer carbohydrate chains to protect sterically the unfolded LZM from aggregation during heating.

3.4.4.3. Emulsifying Property

Table 3.3 shows the effect of glycation on the emulsifying properties of LZM. The unmodified LZM was able to form an emulsion with a very small oil droplet size (346.3 nm) as compared to its conjugates (433.7 to 943.5 nm). Contrary to the conjugates, the unmodified globular LZM molecules associated rapidly around the oil droplets to form nanoparticles. The alteration of the ability of LZM to form nanoparticles upon glycation may be due to the modifications of its charges and of its hydrophobicity. Dickinson and Galazka (1991) have reported that the initial oil droplet size formed by the β-lactoglobulin:dextran conjugates was bigger than the one formed by the native protein and attributed these results to slower adsorption and rearrangement of the conjugates during emulsification.

The results also show that the stability of the emulsions was dependent on the type of glycoconjugates. The emulsion obtained with LZM:GOS conjugates showed the highest stability with only 5% loss of the emulsifying property after incubation at 65°C. As compared to the unmodified LZM (28.1%), LZM:galactan conjugates resulted in a relatively stable emulsion, with 15% loss of the emulsion property. LZM:galactose conjugates showed similar emulsifying stability (30.9%) as the unmodified LZM. Similarly, α_s-casein:glucose (Kato et al., 1992) and ovalbumin:glucose conjugates (Kato et al., 1990) did not demonstrate improvement in emulsifying properties. The high emulsifying stability of LZM:GOS and LZM:galactan conjugates may be attributed to the high hydration capacity of longer chain carbohydrate moieties as compared to the shorter ones (Shu et al., 1996). These hydrated carbohydrate moieties may have been oriented towards the aqueous layer of emulsion, leading to the formation of a thick steric stabilizing layer and limiting the coalescence of oil droplets (Kato & Kobayashi,

Table 3.3 Effect of LZM glycation on its emulsifying properties

Conjugates	Emulsifying properties[a]	
	Oil droplet size (nm)[b]	Loss of emulsion at 65°C (%)[c]
Native LZM	346.3	28.1
LZM:Galactose	943.5	30.9
LZM:GOS	433.7	5.0
LZM:Galactan	557.3	15.5

[a]Experimental results are averages of triplicates with a relative standard deviation less than 5% error

[b] Mean of a distribution of 70 measurements.

[c] Percent loss of emulsion was calculated as the percentage of the decrease in the absorbance at 500 nm after heat treatment.

1991). Similarly, Dickinson and Galazka (1991) have shown that the emulsion formed by the *β*-lactoglobulin:dextran conjugates was better protected against coalescence as compared to the unmodified protein. As compared to LZM:GOS conjugates (5% loss), the limited improvement of the emulsion stability with LZM:galactan conjugates (15%) may be explained by the molecular size of the long galactan polysaccharide chain (~100kDa), which may have reduced the mobility of the conjugates and hindered their saturation at the oil droplet surface (Dunlap & Côté, 2005). Both hydration level and mobility seem to be the major factors responsible for the improvement of the emulsion stability properties of conjugates.

3.4.4.4. ELISA Assessment of the Immunoreactivity of the Conjugates

The effect of glycation on LZM immunoreactivity was assessed by sandwich ELISA. Fig. 3.5 shows that LZM immunoreactivity was significantly reduced by glycation, especially for LZM:galactose conjugates (> 99 % reduction in immunoreactivity). This decrease occurred rapidly after day 1 of glycation. Longer period of LZM glycation with galactan further reduced its immunoreactivity to 99% compared to the unmodified LZM at day 4. However, LZM:galactose and LZM:GOS conjugates demonstrated increased immunoreactivity with incubation time. Alterations in protein structure may have occurred as a result of protein:carbohydrate interactions, leading to either epitope modification or steric hindrance thereby affecting the antigen-antibody recognition (Sathe et al., 2005). Contradictory results, however, have been reported so far regarding the effect of glycation on the immunobinding ability of food allergens, indicating that this effect might be allergen- and/or carbohydrate-dependent (Taheri-Kafrani et al., 2009). It is important to point out that protein allergenicity is dependent on the specificity of antibody-antigen interactions. Changes in the structure of the targeted protein will inevitably influence the overall immunogenic response and may, thus, affect its allergenic potential. An appreciation of the impact of glycation on protein immunoreactivity is an essential step in the development of knowledge-based food processing strategies for controlling and manipulating food allergenicity.

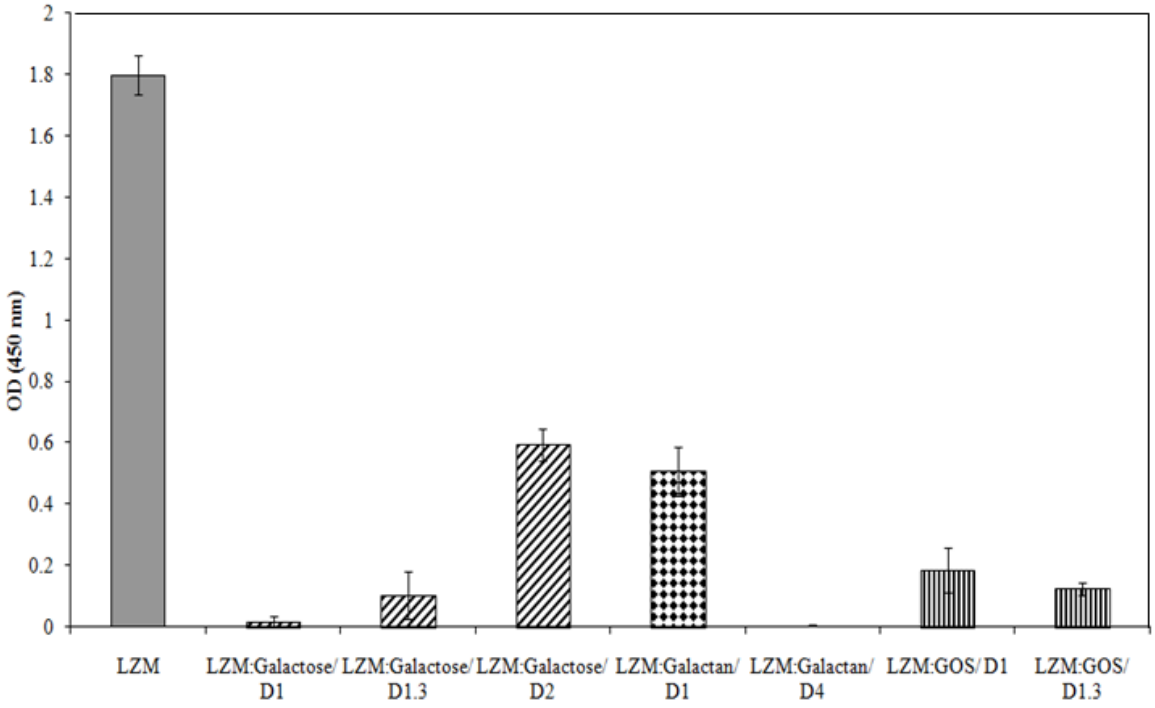

Figure 3.5 Effect of glycation on LZM immunoreactivity (IgG-binding). The results obtained were statistically significant ($p < 0.05$). Data are means ± standard deviation of duplicates.

3.5. Conclusion

Maillard reaction was successfully used to produce LZM:galactose/GOS/galactan conjugates. This study demonstrated that galactose reacts more readily with LZM through the Maillard reaction compared to its longer chain counterparts. The structural analyses of conjugates indicate the heterogeneous multiplicity of conjugated derivatives obtained upon the glycation of LZM with galactose and GOS. In overall, the glycation of LZM improved its functional properties and decreased its immunoreactivity. The improvement in protein solubility, heat stability and emulsion stability was dependent on the level of glycation and on the length of carbohydrate.

CONNECTING STATEMENT 2

The production of LZM:carbohydrate conjugates with improved functional properties was previously investigated (Chapter III). In Chapter IV, the effect of water activity (a_w) on the percent blocked lysine of LZM:carbohydrate conjugates was investigated, and the produced conjugate species were characterized structurally by ESI-MS. In addition, the conjugation of LZM with prebiotic GOS was optimized by response surface methodology (RSM) using a 5-level 3-factor central composite design (CCD). The effects of substrate ratio, temperature, and a_w were studied, and their interactions were highlighted. The percent blocked lysine and the protein aggregation index were selected as responses to monitor the progress of the Maillard reaction. The important parameters affecting the percent blocked lysine and the protein aggregation index were identified. The optimum conditions leading to the production of LZM:GOS conjugates with the highest level of percent blocked lysine and with the lowest level of protein aggregation were determined.

The results presented in this chapter were presented at the 79th ACFAS congress and published in *Process Biochemistry.*

Seo, S. & Karboune, S. (2011) *Glycation through the Maillard reaction and structural characterization of glycated lysozyme with galactose, galactooligosaccharides and galactan*. 79ième congrès de l'ACFAS, Sherbrooke, Canada.

Seo, S., Karboune, S., Yaylayan, V. A., & L'Hocine, L. (2012). Glycation of lysozyme with galactose, galactooligosaccharides and potato galactan through the Maillard reaction and optimization of the production of prebiotic glycoproteins. *Process Biochemistry, 47*(2), 297–304.

CHAPTER IV

OPTIMIZATION OF PROTEIN GLYCATION THROUGH THE MAILLARD REACTION AND STRUCTURAL CHARACTERIZATION OF GLYCATED LYSOZYME WITH GALACTOSE, GALACTOOLIGOSACCHARIDES AND GALACTAN

4.1. Abstract

The production of glycated lysozyme (LZM), with galactose, galactooligosaccharides (GOS), and galactan through the Maillard reaction was investigated. The percent blocked lysine, estimated from the furosine content, reached a maximum value of 11.2% for LZM:galactan conjugates after 1 day incubation at a a_w of 0.65. Maximum percent blocked lysine of 7.0 and 13.5% were obtained for LZM:galactose/GOS conjugates at a lower a_w of 0.45 after 3 and 7 days, respectively. However, the low percent blocked lysine and the high protein aggregation index of LZM:galactose/GOS conjugates at a_w 0.79 and 0.65 revealed the prevalence of the degradation of the Amadori compounds and the protein cross-linking. Mass spectrometry of LZM conjugates revealed the formation of different glycoforms. Glycated LZM containing up to seven galactose moieties were formed; while only mono- and diglycated LZM with GOS were detected. 2–3 moles of galactan were conjugated to one mole of LZM. Response surface methodology, based on a 5-level and 3-factor central composite design, revealed that molar ratio and temperature were the most significant variables for the glycation of LZM with GOS. The optimal conditions leading to a high percent blocked lysine (16.11%) with a low protein aggregation index (0.11) were identified: temperature of 49.5ºC, LZM:GOS molar ratio of 1: 9 and a_w of 0.65. To the best of our knowledge, this is the first study on the optimization of LZM glycation with GOS.

4.2. Introduction

In order to improve the functional properties of proteins and their technological applications, several methods, based on genetic (Nakamura et al., 1993), physical (Jegouic et al., 1997), chemical (Park et al., 2000), and enzymatic (Ali et al., 2010) modifications were reported. Among these modifications, the glycation of proteins via naturally occurring Maillard reaction, under controlled conditions, led to a significant improvement of protein functionalities, such as emulsifying properties, protein solubility and heat stability (Aminlari et al., 2005; Miralles et al., 2007). The protein glycation was also found to be a very efficient method to decrease, *in vivo,* the allergenicity of protein (Arita et al., 2001). Moreover, the conjugation of prebiotic oligosaccharides with a protein could potentially increase their colonic persistence, allowing them to reach the distal colonic region, where most of chronic gut disorders originate (Gibson et al., 2004). Maillard reaction is, therefore, a promising approach to generate glycoproteins having improved functional and biological properties.

In the early stage of the Maillard reaction, the carbonyl group of a reducing carbohydrate interacts with the nucleophilic amino group in peptides/proteins, resulting in the reversible formation of *N*-substituted glycosylamine (Schiff base), which is labile and may undergo irreversible rearrangements (Hodge, 1953). The intermediate stage begins with the degradation of the Amadori/Heyn's products, which can undergo numerous transformations under various divergent pathways (Mossine et al., 1994). Further reactions lead to the formation of advanced glycation end products (AGEs) that are assumed to be responsible for a number of pathophysiological syndromes *in vivo* (Brownlee et al., 1984). In order to produce protein:carbohydrate conjugates with improved functional and biological properties with minimal cross-linking and color or flavor development, the Maillard reaction should be well controlled and limited to its early stages (Kato et al., 1990). Different conditions, such as the molar ratio of substrates, temperature, pH, incubation time, and water activity (a_w), have been reported to affect the rate of several steps involved in the Maillard reaction (van Boekel, 2001).

Although many studies have been reported on the glycation of proteins with small carbohydrates (i.e. galactose, glucose, fructose) (Corzo-Martínez et al., 2010b; Yeboah et al., 1999), and polysaccharides (i.e dextran, galactomannan, chitosan) (Nakamura et al., 1992; Song et al., 2002), to our knowledge, only few studies on the glycation of proteins with oligosaccharides have been carried out to date (Sanz et al., 2005; Trofimova & de Jongh, 2004). Conflicting results have been reported regarding the effects of the carbohydrate length on the protein glycation (Groubet et al., 1999; Kato et al., 1998; Matsudomi et al., 1994). Moreover, no optimization of the Maillard reaction conditions leading to the maximum formation of protein-oligosaccharide conjugates has been carried out.

The present study was aimed at the investigation of the glycation of a selected protein with mono- (galactose), prebiotic oligo- (potato GOS) and polysaccharides (potato galactan) through the Maillard reaction. LZM, derived from hen egg white protein, was selected as the model protein because it is well characterized and has many desirable properties including antimicrobial activity (Hughey & Johnson, 1987) and heat stability (Tomizawa et al., 1994). The specific objectives of this study were to investigate the effect of a_w and glycation time on the degree of glycation of LZM with galactose, GOS, and galactan, and to characterize the structural properties of the glycoproteins. Finally, the conjugation of LZM with prebiotic GOS was optimized by

response surface methodology (RSM) using a 5-level 3-factor central composite design (CCD). These findings will bring more insight to the production of LZM conjugated with prebiotic oligosaccharides with higher glycation level compared to LZM conjugated with longer chain carbohydrates and with possible increase in functional properties compared to LZM conjugated with monosaccharides, all the while providing the added benefit of incorporating a prebiotic activity to the conjugates.

4.3. Materials and Methods

4.3.1. Materials

LZM from chicken egg white (>96% purity), triolein and D-(+)-galactose were purchased from Sigma Chemical Co. (St-Louis, MO). Potato galactan (~100 kDa) and endo-1-4-*β*-D-galactanase from *Aspergillus niger* were purchased from Megazyme (Wicklow, Ireland). TNBSA (2,4,6-trinitrobezene sulfonic acid) and salts were purchased from Sigma Chemical Co. Furosine standard was purchased from Neosystem Lab. (Strasbourg, France).

4.3.2. Preparation of Galactooligosaccharides

GOS were prepared via the enzymatic hydrolysis of potato galactan according to the method described in Paragraph 3.3.2. The average molar mass of the obtained GOS was 1990.9 g/mol from ESI-MS analysis (data not shown).

4.3.3. Preparation of Conjugates

LZM and each of galactose or GOS or galactan at the molar ratio of 1:7 were dissolved in 0.1% (w/v) of 0.05 M sodium phosphate buffer (pH 7.0). The protein:carbohydrate mixtures were lyophilized at -25°C. The powder mixtures were incubated in sealed glass dessicators at 60ºC. The samples were incubated for selected times (1 to 11 days) under controlled a_w values of 0.79 (potassium bromide), 0.65 (potassium iodide), and 0.45 (magnesium nitrate) and thereafter analyzed for their degree of glycation.

4.3.4. Determination of the Extent of Glycation of Lysozyme with Selected Carbohydrates

4.3.4.1. Measurement of Proportion of Free Amino Groups

The proportion of free amino groups of LZM was determined using TNBSA assay, according to the previously described method (Seo et al., 2013). The amount of free amino groups obtained

from LZM and galactose/GOS/galactan mixtures before incubation was used as references for the calculation of the total lysine (Equation 4.2). All assays were run in triplicates.

4.3.4.2. Furosine Analysis

To estimate the degree of glycation, ε-N-2-(furoylmethyl)-L-lysine (furosine) analysis was performed using the method as described previously by Seo et al. (2013).

4.3.4.3. Determination of Percentage of Blocked Lysine

The concentration of blocked lysine was indirectly estimated from the furosine content, considering that the Amadori compound tagatosyllysine formed during the Maillard reaction between lysine residues and galactose moieties, upon 8 N acid hydrolysis, generate about 42% furosine (Krause et al., 2003). The amount of total lysine before glycation was determined through the TNBSA assay and a conversion factor was used to account for one of the seven free amino groups that could not be detected from the reference LZM. The furosine content and the total lysine content allowed the calculation of the percentage of blocked lysine that was not caused by protein cross-linking according to the following equations.

$$Blocked\ lysine = (1/0.42 \times furosine) \times ((MW\ of\ furosine)/(MW\ of\ lysine)) \quad (4.1)$$

$$\%\ Blocked\ lysine = (blocked\ lysine \times 100)/(total\ lysine\ \times 1.167) \quad (4.2)$$

4.3.4.4. Measurement of the Protein Aggregation Index and of the Browning

To estimate the extent of protein cross-linking, favored during the advanced stages of Maillard reaction, the turbidity of LZM conjugates (10 mg/ml) was estimated spectrophotometrically at 500 nm. The browning of the LZM conjugates was measured in parallel at 420 nm. All assays were run in triplicates.

4.3.5. Structural Characterization of Lysozyme Conjugates

The mass spectra of LZM:galactose and LZM:GOS conjugates were analyzed according to the method that was previously described by Seo et al. (2013).

The molecular weight of the LZM:galactan conjugates was estimated using a 25 ml Superose 12 gel filtration column (GE Healthcare). 20 μl of the aqueous solution of purified LZM:galactan conjugates (5 mg/ml) was applied to the column using a FPLC system (GE Healthcare). The elution was carried out with a 0.05 M sodium phosphate buffer at pH 7.0, containing 0.15 M of

sodium chloride at a flow rate of 0.5 ml/min. The sample was detected at 280 nm with a UV-MII detector (Pharmacia). A protein mixture consisting of bovine serum albumin (67 kDa), ovalbumin (44 kDa) and ribonuclease A (13.7 kDa) was used as standard. The standard curve was constructed by plotting the log of the molecular weight of the standards versus the elution volume. The column void volume was determined using blue dextran 2000.

4.3.6. Optimization of the Production of LZM:GOS Conjugates

4.3.6.1. Experimental Design

A five–levels, three variable CCD design was employed using Design-Expert 8.0.2 (Stat-Ease Inc., Minneapolis, MN) for the optimization of the production of LZM:GOS conjugates. The fractional factorial design consisted of 26 points (12 factorial, 12 axial, 2 central). To avoid bias, the runs were performed in a totally random order. The coded variables and their levels selected for the study of LZM:GOS conjugate synthesis were: LZM to GOS molar ratio as X_1 (1:1–1:9), temperature as X_2 (30–70°C); and a_w as X_3 (0.45–0.96). The salts used for the approximate equilibration of a_w are magnesium nitrate (~ 0.4), sodium bromide (~ 0.53), potassium iodide (~ 0.66), potassium bromide (~ 0.79), and potassium sulfate (~ 0.92). The reaction time was set at 21 h.

4.3.6.2. Statistical Analysis

Regression analysis was performed, based on the experimental data, and was fitted into the following empirical quadratic polynomial equation using the response surface regression (RSREG) procedure of SAS System software 9.2 and the software Design-Expert 8.0.2.

$$Y = \beta_0 + \sum \beta_i X_i + \sum \beta_{ij} X_i X_j + \sum \beta_{ii} X_i^2 \qquad (4.3)$$

Where Y is the response variable, β_0 the constant, β_i the coefficient for the linear effect, β_{ij} the coefficient for the interaction effect, β_{ii} the coefficient for the quadratic effect, and X_i and X_j the coded level of variables. The contour plots were obtained using the fitted model, by keeping the least effective independent variable at a constant value while changing the other two independent variables.

4.4. Results and Discussion

4.4.1. Production and Characterization of GOS

GOS were produced by the enzymatic hydrolysis of potato galactan by endo-1,4-*β*-D-galactanase from *A. niger*. After 23 h of reaction, the degree of hydrolysis of potato galactan was estimated to be at 50%. The TLC analysis (Fig. 4.1) of different fractions, collected by gel filtration (Biogel P2) after the enzymatic hydrolysis, indicates the formation of a variety of GOS ranging from di- to decasaccharides. These results were confirmed by high-performance anion-exchange chromatography analysis (data not shown). The oligosaccharide fractions free from mono- and polysaccharides (fractions 13–20) were collected and used in glycation assays.

4.4.2. Determination of the Extent of Glycation of Lysozyme with Selected Carbohydrates

The extent of glycation of LZM with galactose, GOS and potato galactan was assessed by measuring the percentage of blocked lysine. The protein aggregation index, as a useful indicator of protein cross-linking favored during the intermediate and advanced stages of the Maillard reaction, was also determined. The browning of the LZM conjugates, which is another indicator of the advanced stages of the Maillard reaction, was measured in parallel and demonstrated the same kinetics as the protein aggregation (data not shown). Fig. 4.2 shows the time courses for the percent blocked lysine of LZM conjugates and their protein aggregation index over an incubation period of 1 to 11 days at 60°C and at selected a_w (0.45, 0.65, 0.79). When LZM was incubated in the presence of galactose/GOS/galactan, significant increases in the percent blocked lysine and in the protein aggregation index were obtained. However, the rate and the extent of glycation of LZM were found to be dependent on the type of carbohydrate and the a_w value.

The results (Fig. 4.2A–C) show that the percent blocked lysine of LZM:galactan conjugates reached a maximum value of 11.2% upon incubation at a_w value of 0.45, 0.65, 0.79, for 7, 1, 5 days, respectively, and decreased thereafter. The rate of the LZM glycation with galactan was faster at a a_w of 0.65. It has been reported that the Maillard reaction occurs more rapidly at intermediate a_w values (Ames, 1990). A decrease in the percent blocked lysine obtained after reaching a maximum glycation extent can be attributed to the advancement of the Maillard reaction leading to the degradation of the Amadori compounds. At all investigated a_w, the protein aggregation index of LZM:galactan conjugates was not significant (Fig. 4.2D–F), indicating that the formation of the Amadori products prevailed over the protein cross-linking.

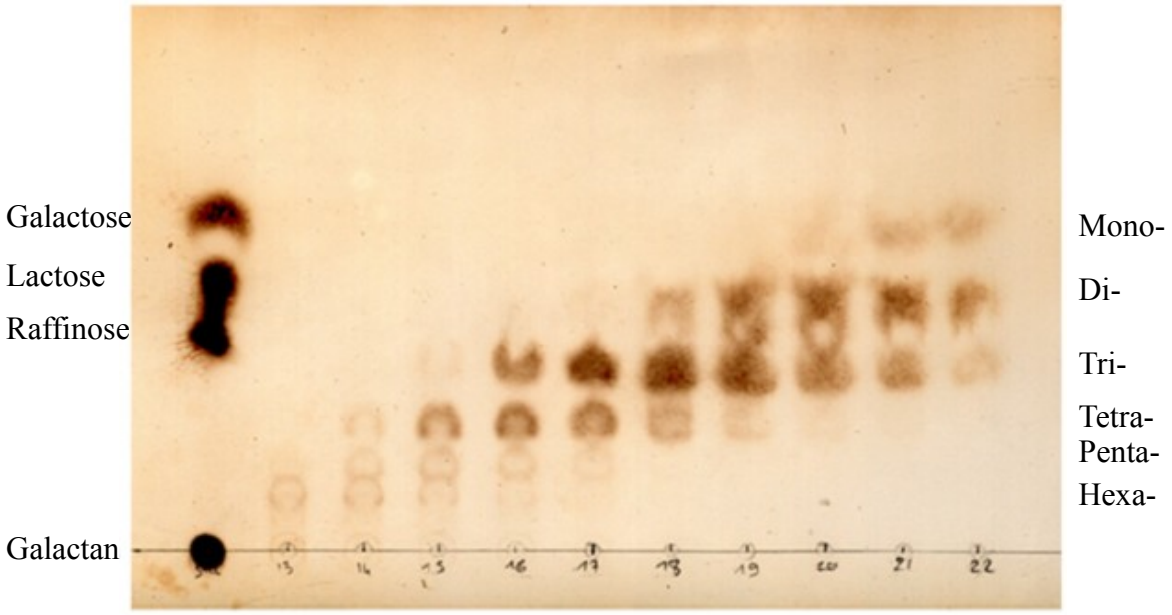

Figure 4.1. TLC analysis of fractions containing GOS obtained by gel filtration using Biogel P2 column.

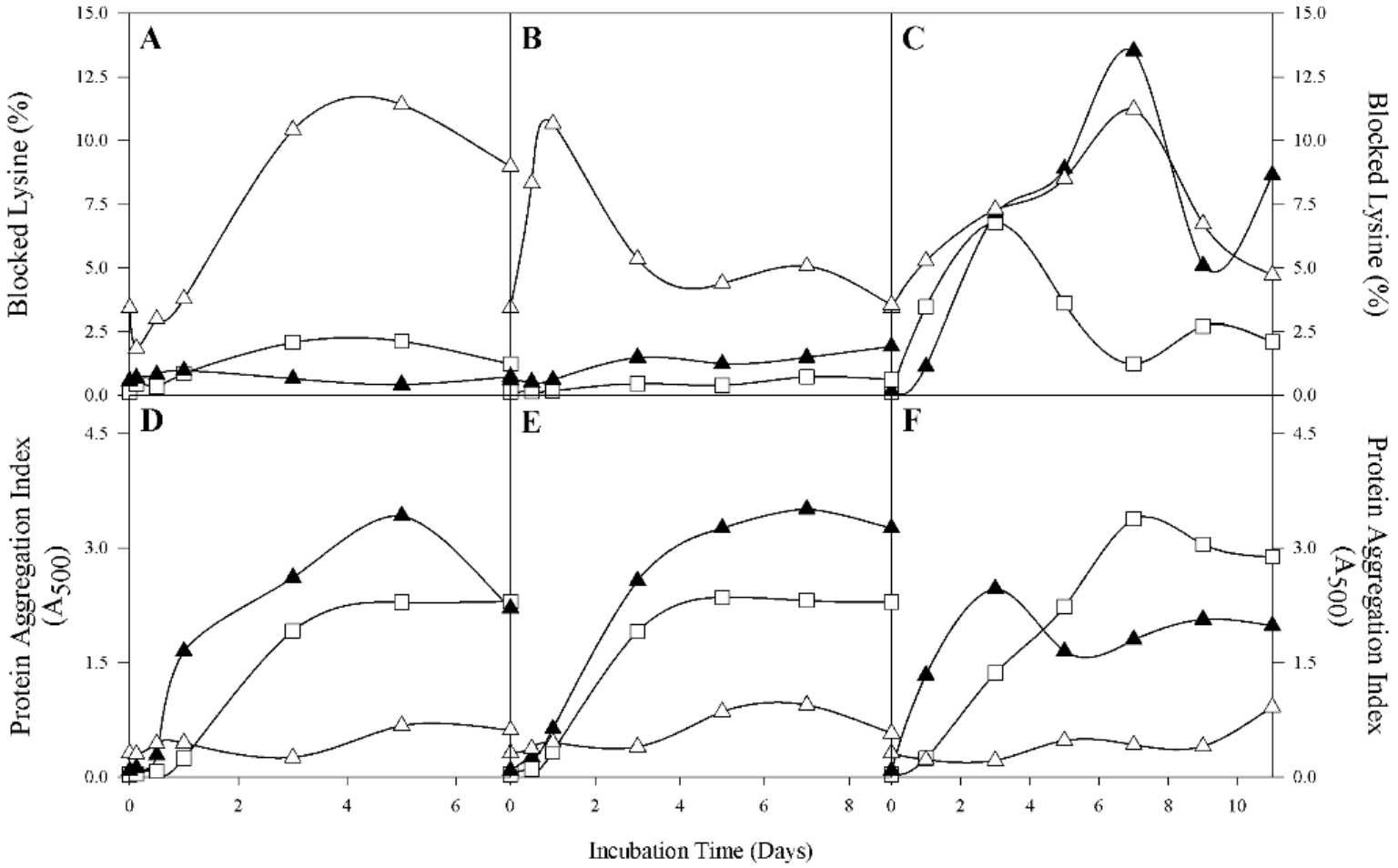

Figure 4.2 Percent blocked lysine (A–C) and protein aggregation index (D–F) of LZM:galactose (□), LZM:GOS (▲), LZM:galactan (△) after incubation at 60°C and at a_w of 0.79 (A, D), 0.65 (B, E) and 0.45 (C, F).

The results (Fig. 4.2) also indicate that the glycation of LZM with galactose and GOS at a lower a_w of 0.45 increased with the incubation time up to a maximum percent blocked lysine of 7.0 and 13.5% after 3 and 7 days of incubation, respectively. However, at a_w 0.79 and 0.65, the low percent blocked lysine of LZM:galactose/GOS conjugates and their high protein aggregation index values revealed the very rapid progress of the Maillard reaction at these conditions favoring the degradation of the Amadori products and the protein cross-linking (Miller et al., 2003). Similar results have been reported using β-lactoglobulin glycated with galactose and tagatose, where high degree of protein aggregation was observed only after 2 days of incubation at 50°C at a a_w of 0.44 (Corzo-Martínez et al., 2010c). At all investigated a_w, LZM:galactose/GOS conjugates showed higher protein aggregation index values, over the glycation time course, as compared to LZM:galactan conjugates. These results reveal the prevalence of the covalent polymerization of LZM, by reacting with dicarbonyls formed during the Maillard reaction, in the presence of galactose and GOS (Oliver et al., 2006b).

The different reactivity of galactose, GOS and galactan to glycate LZM may be explained by the differences in their length, their conformation and their ability to undergo glycoxidation (Scaman et al., 2006; Yeboah et al., 1999). Indeed, the dicarbonyl compounds generated through glycoxidation of saccharides can react with the guanidine groups of arginine residues and hence increase the rate of glycation (Yeboah et al., 2000). In addition to the guanidine group of arginine residues, LZM has different glycation sites, including the *N*-terminal α-amino group and ε-amino groups of lysine (Lys) residues (Tagami et al., 2000), three of which (Lys-1, Lys-33, Lys-97) have been identified as the most reactive ones (Yeboah et al., 2004); however, the affinity of these reactive LZM glycation binding sites vary depending on the type of carbohydrates (mono or polysaccharides) (Aoki et al., 2001). Moreover, the highest percent blocked lysine obtained with GOS (13.5%) and galactan (11.2%) at a a_w of 0.45 and 0.65, respectively, may be attributed to their ability to depress the protein polymerization and the browning associated with the advanced Maillard reaction at these conditions (Aoki et al., 2001). The optimal conditions, where a high degree of LZM glycation with low protein cross-linking (Ab_{500nm} <1.0) was obtained, were selected for further investigations.

4.4.3. Structural Characterization of Lysozyme Conjugates

Evidences of LZM glycation with galactose and GOS were obtained by ESI-MS analyses. Fig. 4.3 represents typical electrospray ionization mass spectra of glycated LZM, showing a heterogeneous distribution of different glycoforms at a similarly charged state. The molecular mass difference between glycoforms was determined to be 162 atomic mass units, which is equivalent to the mass of a covalently bound galactose moiety (Fig. 4.3A). The small peaks adjacent to each main peak were produced by a further loss of water to form dehydrated products. Fig. 4.3A indicates the formation of glycated LZM containing up to 7 galactose moieties, which exceeds the number of the reactive ε-amino groups of LZM (six groups). These high sugar loadings of LZM may be explained by the complete glycation of the primary amino groups of LZM and/or by the diglycation at some of the highly reactive ε-amino groups of LZM (Blakytny et al., 1997). Similarly, Yeboah et al (2000) reported a high level of glycation of LZM with glucose after 1 and 10 days of incubation at 50ºC and a wide distribution of glycoforms with up to 5 and 11 glucose moieties, respectively. The results (Fig. 4.3A) also show that the mono- and multiglycated LZM with di-, tri- and tetra- galactose moieties were preferentially formed over the higher glycoforms with hexa- and hepta- galactose moieties. These findings reveal some selectivity in the glycation of the amino groups of LZM.

The ESI-MS spectrum of LZM glycated with GOS shows a heterogeneous distribution of glycated forms with different chain length varying from 2 to 4 galactose residues (Fig. 4.3B). The percentage distributions of LZM:galactobiose and LZM:galactotriose conjugates were relatively higher as compared to that of LZM:galactotetraose. The results also indicate the formation of multiglycated LZM with up to only two GOS moieties; only the galactobiose and the galactotriose were able to form the highly glycated forms. The low sugar loading of LZM reveal that GOS reacted mainly with one or two most reactive ε-amino groups of Lys residues and had low affinity for LZM glycation binding sites as compared to galactose.

The molecular weight of LZM:galactan conjugates was found to be at around 300 kDa by SEC on Superose 12 (data not shown). These results indicate that 2–3 moles of galactan (average MW of 100 kDa) are covalently linked to one mole of LZM under the optimal glycation conditions. Similarly, Aminlari et al. (2005) have reported that one mole of LZM was conjugated with 2 to 3 moles of dextran with the amino terminal Lys-1 and Lys-98 being the highly reactive residues.

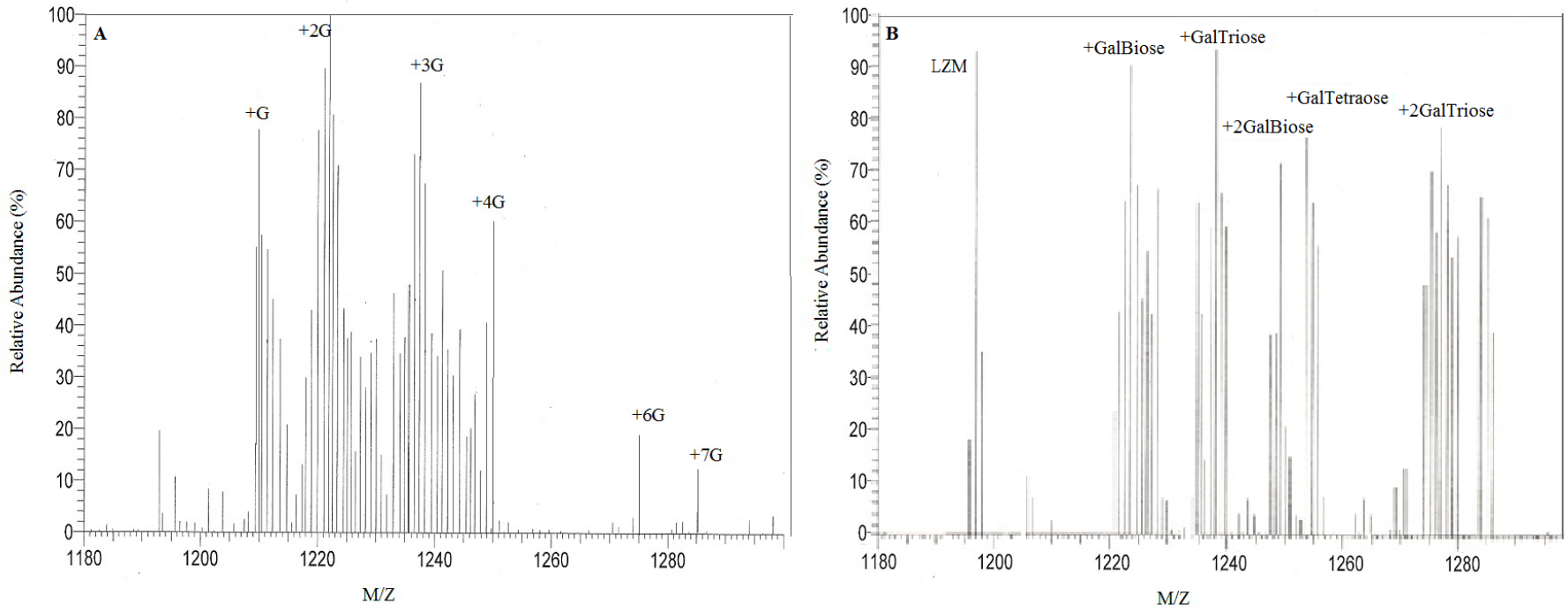

Figure 4.3. Mass Spectra of glycated LZM with galactose (A) and galactooligosaccharides (B) upon glycation at 60ºC and at a a_w of 0.45.

4.4.4. Optimization of the Production of LZM:GOS Conjugates Using RSM

In order to optimize the glycation of LZM with GOS and to better understand the relationships between the glycation parameters, RSM has been used. CCD was performed with three independent variables at five levels, including temperature, substrate molar ratio, and a_w. Table 4.1 shows the experimental conditions and the experimental data for percent blocked lysine and protein aggregation index along with their predicted values. Among the various conditions, the maximum percentage of blocked lysine of 14.27 % (run # 17) was obtained at LZM:GOS molar ratio of 1:9, 60ºC and a a_w of 0.66. The lowest percentage of blocked lysine (< 0.01 %) was obtained (run # 10 and 20) at LZM:GOS molar ratio of 1: 5, 60 ºC and a a_w of 0.92. The protein aggregation index was highest (8.55) at run # 7 (LZM:GOS molar ratio of 1:7, 70 ºC, a_w of 0.53) and lowest (0.06) at run # 9, 25, and 26 (LZM:GOS molar ratio of 1:5, a_w of 0.66, 30 and 40 ºC). By applying multiple regression analysis using the software Design-Expert version 8.2, the quadratic model was statistically more suitable for the description of the glycation of LZM with GOS. The results were transformed to square root for the percentage of blocked lysine and to inverse square root for the protein aggregation index according to the recommended transformation suggested by the Box-Cox plot ($\lambda = 0.5$ and -0.5 respectively).

The analysis of variance (ANOVA) and the adequacy of the models are summarized in Table 4.2. The quadratic polynomial model was statistically significant and adequate to represent the actual relationships between the percent blocked lysine or the protein aggregation index and the significant variables within the experimental range, with an *F*-value of 76.3 and 452.4, a *p* -value of < 0.01 and a coefficient R^2 of 0.977 and 0.994, respectively. The overall effect of the three variables on the percent blocked lysine is also shown in Table 4.2. The *F*- and *p*- values can be used to verify the significance of each variable and of their interactions. The results indicate that the independent variable molar ratio (X_1) was the most significant model linear term (*F*-value of 41.52; $p < 0.01$), affecting importantly the percentage of blocked lysine. The temperature (X_2, *F*-value of 3.67) and a_w (X_3, *F*-value of 2.37) had a less significant effect ($p > 0.05$) on the percent blocked lysine. In addition, all cross product coefficients (X_1X_2, X_1X_3, X_2X_3) and also all quadratic terms of variables (X_1^2, X_2^2, X_3^2) were significant, with very small *p* -values ($p < 0.05$). Among the variables, molar ratio (X_1) and incubation temperature (X_2) showed the most significant interaction effect *(F*-value of 24.9) and the a_w (X_3^2) was the most important quadratic term.

Table 4.1 Experimental design of 5-levels 3-variables central composite design

Run No.	Coded values [a]						Blocked lysine (%)		Protein aggregation index	
	X_1 Protein:Sugar Molar Ratio		X_2 Temperature (ºC)		X_3 a_w		Experimental	Predicted	Experimental	Predicted
1	-1	(1:3)	+2	(70)	+1	(0.79)	5.05	5.06	4.49	5.26
2	0	(1:5)	+1	(60)	-2	(0.4)	0.18	0.09	0.46	0.47
3	+1	(1:7)	0	(50)	+1	(0.79)	6.93	6.73	0.10	0.12
4	-2	(1:1)	+1	(60)	0	(0.66)	5.47	5.73	0.07	0.07
5	+1	(1:7)	0	(50)	-1	(0.53)	7.96	9.93	0.11	0.11
6	+1	(1:7)	0	(50)	-1	(0.53)	7.78	6.73	0.11	0.11
7	+1	(1:7)	+2	(70)	-1	(0.53)	2.82	2.92	8.55	13.55
8	+1	(1:7)	+2	(70)	+1	(0.79)	4.66	4.22	5.99	8.98
9	0	(1:5)	-1	(40)	0	(0.66)	5.54	4.07	0.06	0.05
10	0	(1:5)	+1	(60)	+2	(0.92)	0.00	0.02	1.60	1.26
11	0	(1:5)	-1	(40)	0	(0.66)	4.33	4.07	0.06	0.05
12	-1	(1:3)	+2	(70)	+1	(0.79)	5.81	5.06	4.72	5.26
13	-1	(1:3)	+2	(70)	-1	(0.53)	3.69	3.42	1.27	1.03
14	0	(1:5)	+1	(60)	-2	(0.4)	0.44	0.09	0.45	0.47
15	0	(1:5)	+1	(60)	0	(0.66)	12.32	11.60	0.16	0.15
16	+2	(1:9)	+1	(60)	0	(0.66)	13.99	12.71	0.23	0.20
17	+2	(1:9)	+1	(60)	0	(0.66)	14.27	12.71	0.23	0.20
18	+1	(1:7)	+2	(70)	+1	(0.79)	5.05	4.45	5.95	8.98
19	-1	(1:3)	+2	(70)	-1	(0.53)	3.50	3.42	1.26	1.03
20	0	(1:5)	+1	(60)	+2	(0.92)	0.00	0.02	1.59	1.26
21	+1	(1:7)	+2	(70)	-1	(0.53)	1.45	2.92	8.06	13.55
22	-2	(1:1)	+1	(60)	0	(0.66)	5.01	5.73	0.07	0.07
23	+1	(1:7)	0	(50)	+1	(0.79)	7.00	6.73	0.11	0.12
24	0	(1:5)	+1	(60)	0	(0.66)	11.24	11.60	0.16	0.15
25	0	(1:5)	-2	(30)	0	(0.66)	0.00	0.01	0.06	0.06
26	0	(1:5)	-2	(30)	0	(0.66)	0.00	0.01	0.06	0.06

[a] Numbers in parenthesis represent actual experimental values

Table 4.2 Analysis of variance for response surface quadratic model

Source	Blocked lysine (%)[a]					Protein aggregation index[d]			
	df[b]	Sum of squares	Mean square	*F*-value	*p*-value[c]	Sum of squares	Mean square	*F*-value	*p*-value[c]
Model	9	32.81	3.65	76.26	< 0.01	51.58	5.73	452.43	< 0.01
X_1 (Molar Ratio)	1	1.98	1.98	41.52	< 0.01	3.27	3.27	258.23	< 0.01
X_2 (Temp.)	1	0.18	0.18	3.67	0.07	27.58	27.58	2176.91	< 0.01
X_3 (a_w)	1	0.11	0.11	2.37	0.14	0.48	0.48	37.73	< 0.01
X_1X_2	1	1.19	1.19	24.95	< 0.01	0.27	0.27	21.17	< 0.01
X_1X_3	1	0.22	0.22	4.51	0.04	0.22	0.22	17.65	< 0.01
X_2X_3	1	0.86	0.86	17.98	< 0.01	0.00	0.00	0.29	0.60
X_1^2	1	0.29	0.29	6.16	0.02	0.27	0.27	21.25	< 0.01
X_2^2	1	6.64	6.64	138.91	< 0.01	4.01	4.01	316.93	< 0.01
X_3^2	1	16.37	16.37	342.43	< 0.01	3.12	3.12	246.19	< 0.01

[a] $R^2 = 0.9772$
[b] Degree of freedom
[c] p -value < 0.05 = statistically significant
[d] $R^2 = 0.9939$

(F-value of 342.4). In addition, the negative sign of the most significant cross product coefficient (X_1X_2) indicates the opposite effect of these variables. Neglecting the insignificant terms by backward elimination regression (α out = 0.1), the final predictive equation in terms of coded factors is given below:

$$\sqrt{(\%\ Blocked\ lysine)} = 3.41 + 0.29X_1 - 0.12X_2 - 0.039X_3 - 0.36X_1X_2 + 0.24X_2X_3 - 0.11X_1^2 - 0.41X_2^2 - 0.79X_3^2 \quad (4.4)$$

The overall effects of the three variables on the protein aggregation index (Table 4.2) indicate that the independent variable temperature (X_2) was the most significant parameter (F-value of 2176.9; $p < 0.01$), affecting importantly the protein aggregation index. The molar ratio (X_1, F-value of 258.2) and the a_w (X_3, F-value of 37.7) had a less important effect on the protein aggregation index, but they were still statistically significant ($p < 0.01$). Two cross product coefficients (X_1X_2, X_1X_3) and all quadratic term coefficients (X_1^2, X_2^2, X_3^2) were statistically significant, with very small p -values ($p < 0.05$). The most important interaction effect was between molar ratio and temperature (X_1X_2; F-value of 21.2) and the temperature (X_2^2; F-value of 316.9) was the most important quadratic term affecting the protein aggregation index. Neglecting the insignificant terms, the final predictive equation in terms of coded factors is as given below:

$$1/\sqrt{(Turbidity)} = 2.56 - 0.38X_1 - 1.49X_2 - 0.14X_3 + 0.17X_1X_2 + 0.14X_1X_3 + 0.10X_1^2 - 0.32X_2^2 - 0.35X_3. \quad (4.5)$$

4.4.4.1. Effect of Glycation Parameters

The contour graphs (Fig. 4.4) show the effect of glycation temperature and LZM:GOS molar ratio at three different a_w (0.53, 0.66, 0.79), and their mutual interactions on the percent blocked lysine (Fig. 4.4, 1A–C), and on the protein aggregation index (Fig. 4.4, 2A–C) after 21 h of incubation. All three contour plots at selected a_w (Fig. 4.4, 1A–C) display similar trends in that the predicted percent blocked lysine increased with an increase in the temperature until it reached a turning point between 50 to 60ºC; however, the highest percentage of blocked lysine was achieved at a_w of 0.66. Above the optimal temperature, the Maillard reaction did most likely pass to the stage of Amadori product degradation resulting in a lowering of percent blocked lysine.

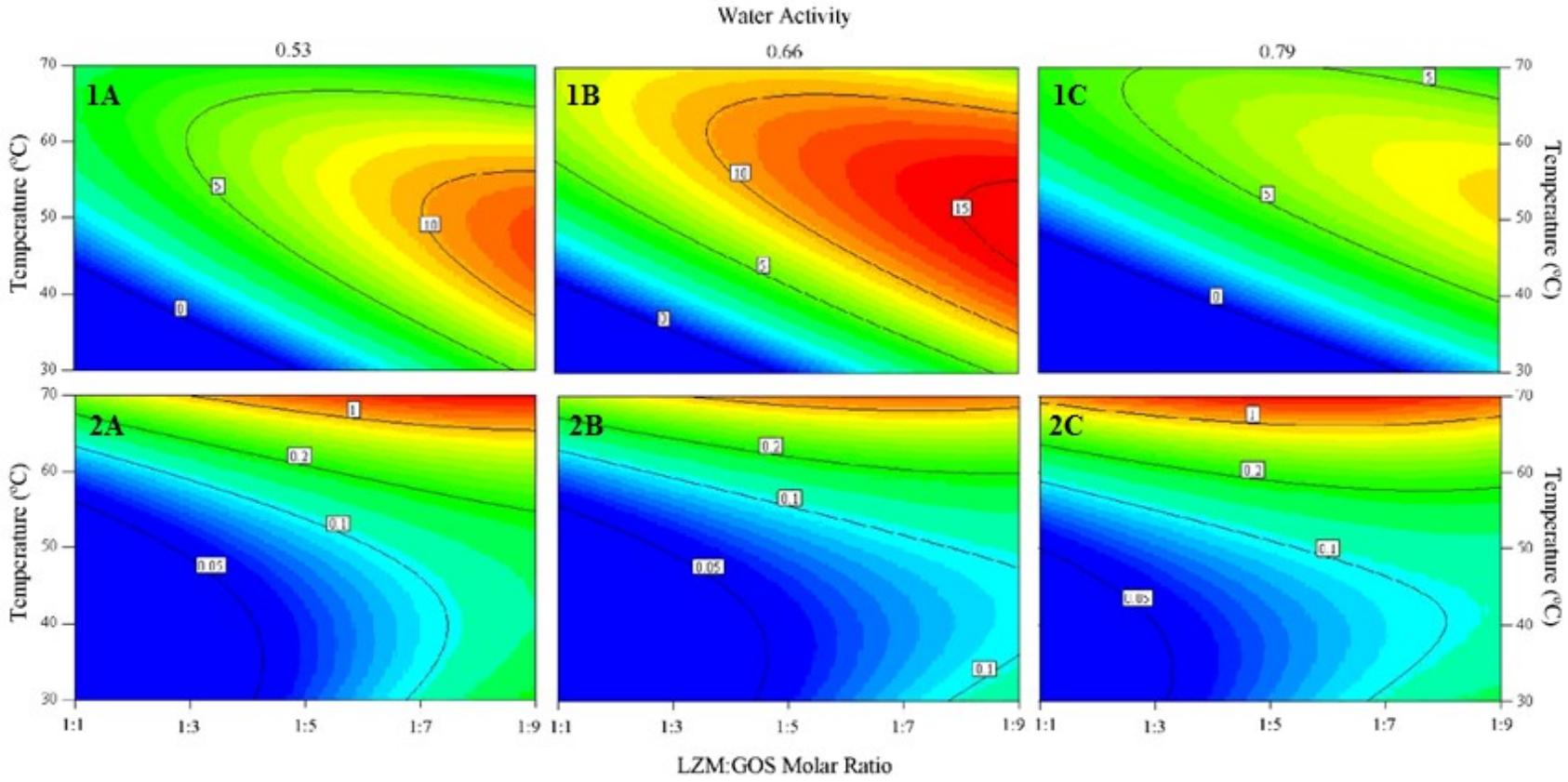

Figure 4.4 Contour plots of percent blocked lysine (1A–1C) and of protein aggregation index (2A–2C). The numbers inside the contour plots indicate the predicted values under given reaction conditions.

On the other hand, at a_w of 0.53 and of 0.79, the increase in the concentration of GOS did not significantly influence the change in the percent blocked lysine at high temperature (70ºC) (Fig.4.4, 1A–C). While at lower temperatures (below 60ºC), the percent blocked lysine increased, when the concentration of GOS was increased. The diagonal ellipses formed in the contour graphs (Fig. 4.4, 1A–C) confirm the opposite interactive effect between the temperature and the substrate molar ratio. Indeed, at lower substrate molar ratios, the percentage of blocked lysine formation was higher at higher temperatures, and at higher substrate molar ratios, the blocking of lysine residues was favored at lower temperatures. Similarly, Jiménez-Castaño et al. (2005) have reported an opposite relationship between the temperature and the ratios of dextran to β-lactoglobulin. The effects of temperature and substrate molar ratio on the protein aggregation index resulted in similar contour graphs at three selected a_w, where the index increased as the variables increased (Fig.4.4, 2A–C). The protein aggregation index was generally lower at a_w 0.66 as compared to the other a_w values.

4.4.4.2. Optimal Conditions and Model Verification

Canonical analysis was performed to confirm if the response surface has a true maximum, minimum or a saddle point within the limit of the investigated surface (Hoerl, 1985). The obtained eigenvalues (λ_i) had mixed signs, which demonstrate that the stationary point obtained was a saddle point, indicating that the response surface is shaped like a saddle (data not shown). Since a simple optimum was not found within the investigated range using the canonical analysis, the ridge analysis was computed to estimate the ridge of optimum response by increasing radii from the center of the original response surface design (Table 4.3). This allows the determination of the direction that should further be investigated in order to locate the simple optimum. The results from the ridge analysis demonstrated similar trends compared to the contour plots where the percent blocked lysine increased with an increase in substrate molar ratio. The a_w and temperature did not demonstrate important changes as the radius was increased.

The optimal conditions for the glycation of LZM with GOS through the Maillard reaction were predicted using the values obtained through the ridge analysis. The uncoded optimal conditions for the highest percent blocked lysine were: temperature of 49.52 ºC; LZM:GOS molar ratio of 1: 9; a_w of 0.65. Under the optimum conditions, the predicted percent blocked lysine and protein aggregation index were estimated to be 16.11% ± 0.73 and 0.11 ± 0.11, respectively. On the

Table 4.3 Ridge analysis of the response surface

Coded radius	Estimated response of % blocked lysine	Standard error	Uncoded factor values		
			Ratio LZM:GOS	Temperature (ºC)	a_w
0.0	9.72	0.44	1:5.00	50.00	0.66
0.1	10.87	0.43	1:5.28	51.30	0.65
0.2	11.83	0.41	1:5.63	52.34	0.65
0.3	12.63	0.39	1:6.03	52.94	0.65
0.4	13.29	0.36	1:6.47	53.05	0.65
0.5	13.87	0.35	1:6.92	52.79	0.65
0.6	14.38	0.35	1:7.35	52.30	0.65
0.7	14.85	0.40	1:7.78	51.69	0.65
0.8	15.30	0.48	1:8.19	51.01	0.65
0.9	15.71	0.59	1:8.60	50.28	0.65
1.0	16.11	0.73	1:9.00	49.52	0.65

other hand, the mean value of triplicate experiments of percent blocked lysine was 18.10 % ± 1.23, whereas the experimental protein aggregation index was determined to be 0.16 ± 0. These values are within the statically significant range of the optimum given by the ridge analysis. These results demonstrate the validation of the RSM model. The three-dimensional plot generated using the fitted model equation (Fig. 4.5) confirms the interactions between the independent variables, temperature and substrate molar ratio. Thus, the optimization of LZM:GOS conjugate synthesis was successfully achieved by RSM. However, as demonstrated by the ridge analysis, further studies are required using an increased concentration of GOS.

4.5. Conclusion

Maillard reaction was successfully used to produce LZM:galactose/GOS/galactan conjugates. The highest percentage of blocked lysine obtained with galactan and GOS demonstrated their ability to depress the protein polymerization and the browning associated with the advanced Maillard reaction. The structural analyses reveal the high reactivity of galactose in undergoing condensation reactions with amines under dry heating conditions, resulting in the formation of multiglycated LZM with a high distribution. The results also suggest the limited interaction of GOS and galactan to the most reactive ε-amino groups of LZM, resulting in a narrow distribution of glycoforms (mono and diglycated LZM). The optimization of the production of LZM:GOS conjugates was performed using RSM with CCD. The molar ratio was the most significant independent variable affecting importantly the percentage of blocked lysine, whereas the temperature was the most significant parameter for the protein aggregation index. Among the variables, molar ratio and incubation temperature showed the most significant interaction effect for both the percentage of blocked lysine and the protein aggregation index.

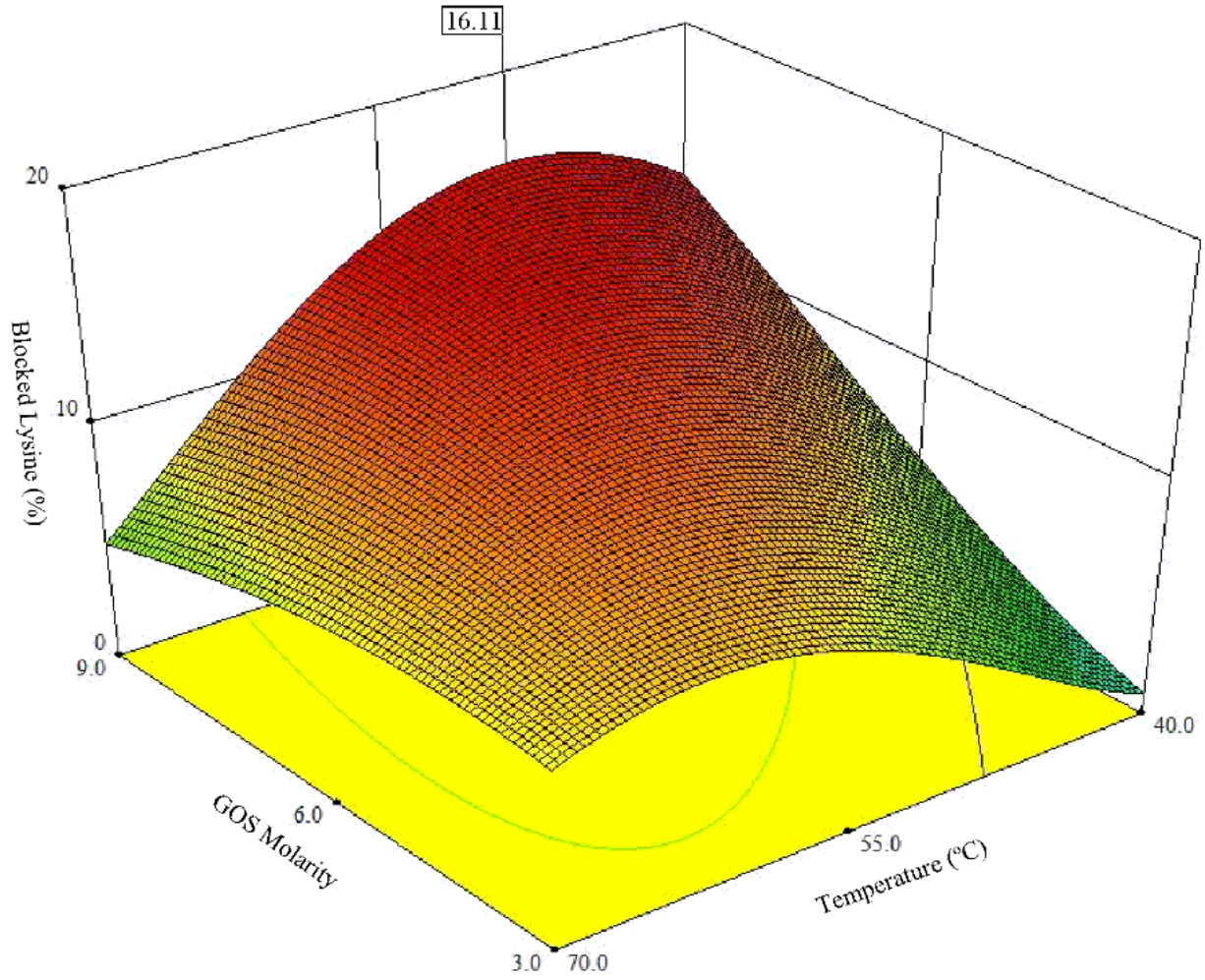

Figure 4.5 Response surface plot showing the effect of incubation temperature, GOS molarity (LZM molarity at 1), and their mutual interaction on percent blocked lysine. The a_w is constant at 0.66.

CONNECTING STATEMENT 3

The previous study provided a good understanding of the effects of protein:carbohydrate ratio, temperature, incubation time, and a_w as well as of their interactions on the glycation rate of LZM. The production of LZM:carbohydrate conjugates with improved functional properties was also successfully achieved (Chapter III and IV). The carbohydrate conjugation to potato proteins, which are undervalued by-products of the starch industry, through the Maillard reaction was investigated in Chapter V. The effect of carbohydrate conjugation on the secondary/tertiary structures of patatin (PTT) was investigated, and the changes in heat stability, protein solubility, antioxidant activity, and emulsifying properties are discussed in this Chapter.

The results from this chapter were presented at IFT12 Annual Meeting & Food Expo and published in *Food Chemistry* journal.

Seo, S., & Karboune, S. (2012) *Glycation of patatin with galactose, galactooligosaccharides and galactan: Structural and functional properties of conjugates*. IFT12 Annual meetings. Las Vegas. Nevada.

Seo, S., Karboune, S., & Archelas, A. (2014). Production and characterization of potato patatin-galactose, galatooligosaccharides, and galactan conjugates of great potential as functional ingredients. *Food Chemistry, 158*(1), 480-489.

CHAPTER V

PRODUCTION AND CHARACTERIZATION OF STRUCTURAL AND FUNCTIONAL PROPERTIES OF POTATO PATATIN:GALACTOSE, GALACTOOLIGOSACCHARIDES, AND GALACTAN CONJUGATES OF GREAT POTENTIAL AS FUNCTIONAL INGREDIENTS

5.1. Abstract

Potato proteins are of high interest because of their high nutritional quality and multiple health benefits, but they are currently undervalued due to their limited solubility and stability. Glycated patatin (PTT) with galactose, galactooligosaccharides (GOS) and galactan was produced through the Maillard reaction and characterized structurally and functionally. Fourier transform infrared and fluorescence spectroscopy data revealed important changes in total secondary structures through glycation with GOS (61.2%) and galactan (36.7%) and also significant tertiary structural changes leading to an exposure of tryptophan residues. These structural changes led to more heat stable forms of PTT with a higher unfolding temperature (70–90°C) than the unmodified protein (50–70°C) and with higher antioxidant activity. PTT:galactose conjugates exhibited similar thermal stability and pH-structural behavior as native PTT. However, the high level of galactose conjugation to PTT and increased exposure of hydrophobic residues led to a significant increase in its emulsifying stability at pH 3.

5.2. Introduction

There is an increasing demand for the use of plant proteins as an alternative to animal proteins. Compared to proteins from other vegetable and cereal sources, potato proteins are of great potential as food ingredients because of their higher nutritional quality (Ralet & Gueguen, 2001), and their ability to regulate serum cholesterol levels (Liyanage et al., 2008), and to reduce food intake by increasing the circulation of cholecystokinin levels (Komarnytsky et al., 2011). Potato proteins include three major classes: a) patatin (PTT, up to 40% w/w), b) protease inhibitors (~40–50% w/w) and c) other high molecular weight proteins (~10%) (Ralet & Gueguen, 2000). PTT is a glycoprotein with up to two carbohydrate chains and a molecular weight of approximately 40 kDa (Ralet & Gueguen, 2000). In addition to its antioxidant activity (Liu et al., 2003), PTT has excellent foaming (Ralet & Gueguen, 2001), gelling (Creusot et al., 2010), and emulsifying properties (Ralet & Gueguen, 2000). However, due to its very high exposed hydrophobicity (Creusot et al., 2010), PTT has lower solubility when the ionic strength of the solution is increased. Furthermore, the denaturation temperature of PTT has been shown to be around 59ºC (Creusot et al., 2010), which is lower than those of other animal proteins being used as food ingredients. To make better use of PTT as a functional ingredient and broaden its applications, the improvement of its solubility and its heat stability through structural modification is of great interest.

Among the various existing protein modification techniques, the glycation of proteins, via naturally occurring Maillard reaction, led to the improvement of various functional properties of food proteins (Seo et al., 2013). The formation of protein:carbohydrate conjugates occurs during the early stage of the Maillard reaction, where the free amino group of protein reacts with the carbonyl group of carbohydrates to form Amadori products. During the advanced stages of the reaction, the products resulting from the degradation of the Amadori products can undergo numerous transformations under various pathways giving rise to peptide-bound adducts, to protein cross-linking, and to the formation of brown and polymeric materials (Horvat & Jakas, 2004). To limit the Maillard reaction to its early stages, the Maillard reaction rate needs to be controlled. Our previous study (Seo et al., 2012) and other studies (Oliver et al., 2006a) provided a good understanding of the effects of protein:carbohydrate ratio, temperature, incubation time, and water activity (a_w) as well as of their interactions on the glycation rate.

The secondary and tertiary structural changes of proteins upon glycation through the Maillard reaction (Corzo-Martínez et al., 2008) and the improvements of their functional properties have been well investigated (Oliver et al., 2006a). However, the relationships between the structural and functional properties of the protein conjugates have been overlooked and there is a need for more studies looking into structure-function relationships. The understanding of the mechanisms behind the improvements in functional properties of glycated food proteins is expected to result in a more effective production of targeted glycated proteins with enhanced functional properties.

As part of ongoing research, the objective of the present study was the investigation of the glycation of potato proteins, consisting mostly of PTT (75%), with galactose, galactooligosaccharides (GOS) and galactan, through Maillard reaction under controlled conditions. The secondary/tertiary structural properties of purified PTT conjugates and their functional characteristics (heat stability, emulsifying activity, antioxidant activity) were studied and their relationships were discussed.

5.3. Materials and Methods

5.3.1. Materials

Solanic 206P (≈75% PTT, ≈25% protease inhibitors) was kindly provided by Solanic (Foxhol, Netherlands). Potato galactan (~280 kDa) was purchased from Megazyme (Wicklow, Ireland).

Furosine standard was purchased from Neosystem Lab. (Strasbourg, France). All other chemicals were purchased from Sigma Chemical Co. (St-Louis, MO).

5.3.2. Preparation of Galactooligosaccharides

GOS were prepared from potato galactan according to our previous method (Paragraph 3.3.2). The average molar mass of GOS was calculated to be 1990.9 g/mol.

5.3.3. Preparation of Conjugates

Potato proteins and carbohydrates (galactose or GOS or galactan) at the molar ratio of 1:9 were dissolved (10 mg of Solanic 206P per ml) in 0.05 M sodium phosphate buffer (pH 7). After freeze drying at -25°C, the mixtures were incubated in sealed glass desiccators at 48ºC for 1 to 7 days under controlled a_w value of 0.65 using a saturated solution of potassium iodide. Control experiments were performed with only potato proteins incubated under the same conditions.

5.3.4. Determination of the Extent of Glycation of PTT with Selected Carbohydrates

5.3.4.1. Furosine Analysis

To estimate the degree of glycation, *ε-N*-2-(furoylmethyl)-L-lysine (furosine) was determined using a modified method by Seo et al. (2013). Five milligrams of incubated protein and carbohydrate mixture was added to 2.5 ml of 8 N HCl in vials, capped under nitrogen, and incubated at 110°C for 23 h. The hydrolysates were centrifuged at 13,000 x *g* for 15 min and 0.5 ml of the supernatant was applied to an activated Sep-pak C18 cartridge (Waters Corp., Milford, MA). Furosine was eluted with 3 ml of 3 N HCl, and the eluate was evaporated until dryness under nitrogen and resolubilized in 1 ml of water: acetonitrile: formic acid mixture (95:4.5:0.5, v/v/v). Furosine concentration was quantified using a Beckman high-pressure-liquid chromatography (HPLC) system equipped with a programmable solvent module (model 126), a photodiode array detector and 32 Karat software for data collection. The separation was performed on a Waters Symmetry Shield RP8 3.5 μm (4.6 x 50 mm) column using an isocratic elution of 5 mM octanesulfonic acid in a mixture of water: acetonitrile: formic acid (79.8:20:0.2, v/v/v) for 30 min at a flow rate of 0.3 ml/min. Injected sample volume was 20 μl and the detection of furosine was performed at 280 nm. The calibration curve was constructed using a furosine standard. All assays were run in triplicates.

5.3.4.2. Measurement of Proportion of Free Amino Groups

The proportion of free amino groups of potato proteins and of their corresponding conjugates was assayed using trinitrobenzene sulfonic acid (TNBSA) method according to a method described previously (Seo et al., 2013). All assays were run in triplicates.

5.3.4.3. Determination of Percentage of Blocked Lysine

The percentage of blocked lysine due to glycation and not to protein cross-linking was indirectly estimated from the furosine content and the initial total lysines of potato protein. The Amadori compound tagatosyl-lysine formed during the Maillard reaction between lysine residues and galactose moieties was reported to generate about 42% furosine upon 8 N acid hydrolysis (Krause et al., 2003). The estimated concentations of furosine were, therefore, adjusted accordingly. There are 24 lysines on PTT and 10–14 lysines on the major protease inhibitors (accession number, Q2MY50, P58514, Q41448, P16348, UniProtKB). By considering the proportions of PTT (75%) and of protease inhibitors (25%) present in potato proteins (Solanic 206P), 21 free amino groups were calculated. By taking the above information into account, the percentage of blocked lysine was estimated according to the following equation.

$$\% \text{ Blocked lysine} = (1/0.42 \times \text{furosine}) \times 100/(\text{total lysine}) \quad (5.1)$$

5.3.4.4. Measurement of the Protein Aggregation Index

The extent of protein inter/intramolecular cross-linking was expressed as the protein aggregation index obtained spectrophotometrically by measuring the turbidity of protein:carbohydrate conjugates (10 mg/ml) at 600 nm according to a method by Wang and Ismail (2012). All assays were run in triplicates.

5.3.5. Purification of the Conjugates

Potato proteins and their respective galactose- and GOS-conjugates, recovered after 1 and 3 days of glycation, respectively, were purified through anionic exchange chromatography on MonoQ 5/50 GL (GE Healthcare, Piscataway, NJ) using an ÄKTApurifier system (GE Healthcare). PTT:galactan conjugates were first ultrafiltered using a stirred ultrafiltration unit (Amicon system, Millipore, Billerica, MA) fitted with a 300 kDa molecular mass cut-off membrane to remove unbound galactan, protease inhibitors, and unconjugated PTT; the retentate was further subjected to purification on MonoQ. Protein:carbohydrate conjugate mixtures (2–3 mg protein)

were loaded on the column equilibrated with 50 mM potassium phosphate buffer (pH 6). PTT conjugates were eluted using the same buffer containing 1 M of sodium chloride at a flow rate of 1 ml/min. The gradient system was 0–2 min, 0% B; 2–12 min, 0–25% B; 12–17 min, 25% B; 17–22 min, 25–40% B; 22–27 min, 40% B; 27–32 min, 40–100% B; 32–37 min, 100% B. The elution profile was monitored by UV-absorbance detection at 280 nm. Fractions of 1 ml were collected and subjected to total carbohydrate analysis using the phenol-sulfuric acid method. The fractions containing purified glycated PTT were collected and dialyzed against distilled water for 48 h at 4ºC. The purified conjugates were used for the assessment of the structural and functional properties.

5.3.6. Structural Characterization of the Conjugates

5.3.6.1. Fourier Transform Infrared Spectroscopy (FTIR)

The concentration of the purified PTT conjugates was determined through the Bradford assay (Bradford, 1976) and were subsequently dissolved in $^{2}H_2O$ to achieve a final concentration of 100 mg protein/ml. To investigate the thermal stability of the conjugate structures, they were heated from 30 to 90°C in 5°C increments using a cell regulated by an Omega temperature controller (Omega Engineering, Laval, Qc, Canada). At each temperature, the sample was equilibrated for 10 min before the spectrum was obtained. Infrared spectra were recorded using a Bomem MB FTIR spectrometer (4 cm^{-1}, ABB-Bomem, Quebec, QC, Canada) equipped with a deuterated triglycine sulfate (DTGS) detector. The spectrometer was continuously purged with dry air from Balston dryer (Balston, Haverhill, MA). The samples (9 μl) were placed between two CaF_2 windows separated by a 25 μm Teflon film spacer (Harrick Scientific, Pleasantville, NY). Each spectrum was obtained by co-adding 256 scans to maximize signal-to-noise ratio. Fourier self-deconvolution (FSD) in the amide I′ region was performed using Omnic 6.0 software (Thermo Electron Corporation, Madison, WI) applying a bandwidth of 20 cm^{-1} and a resolution enhancement parameter of 2. The curve fitting was performed by using Origin 8 (OriginLab, Northampton, MA). Gaussian function was chosen to fit the overlapped peaks.

5.3.6.2. Fluorescence Analysis

Hundred microliters of PTT conjugates (0.6 mg/ml) were placed into different wells in black FluoroNunc 96 wells plate (Nunc, Thermo Fisher, Rochester, NY). Their fluorescence spectra were recorded as averages of 25 spectra on a Tecan Infinite 200 (Tecan, Männedorf,

Switzerland) at 25°C. Excitation was set at 295 nm, and the emission was measured from 325 to 375 nm. The emission step size was 5 nm. To study the effect of temperature on the tertiary structure of the glycated proteins, purified PTT conjugates (1 mg/ml) were preincubated for 1 h at selected temperatures, ranging from 27 to 90°C, prior to measurements. To study the effect of pH, purified PTT conjugates (1 mg/ml) were dissolved in appropriate buffer solution: 50 mM sodium acetate buffer (pH 3, 5), 50 mM sodium phosphate buffer (pH 6, 7, 8), 50 mM sodium bicarbonate buffer (pH 10). The blank was substracted from all spectra.

5.3.6.3. Patatin Sequence and Homology Modeling

The FASTA format of amino acid sequence of PTT (accession number Q2MY50, UniProtKB) was submitted to Swissmodel (Kiefer et al., 2009). This server used template of SeMet Patatin (Protein Data Bank number: 1OXW) for the prediction. The predicted model had a Q-MEAN Z-score, a useful measure for the description of the absolute quality of theoretical models of -1.12, which indicates acceptable quality.

5.3.7. Emulsifying Properties

The emulsifying properties of PTT conjugates (1–10 mg/ml) were investigated using oil-in-water emulsions made of 30% triolein (v/v) in 10 mM sodium acetate buffer (pH 3) or in 10 mM sodium phosphate buffer pH 7. Pre-emulsions were formed by sonicating the oil-in-water mixtures for 3 min at 20% power (120 W) with an ultrasonic liquid processor (Misonix, Farmingdale, NY) equipped with a titanium horn (tip diameter of 12.7 mm). The pre-emulsions were then homogenized by three passes through an Emulsiflex C5 homogenizer (Avestin, Ottawa, Canada) at an operating pressure of 100 MPa. Dynamic light scattering (DLS) measurements were carried out using Delsa Nano C (Beckman Coulter, Fuellerton, CA) at 25ºC to estimate the droplet size of the emulsions as a mean of size distributions obtained from 70 measurements. The stability of the emulsions was assessed by heating the emulsified sample at 65ºC for 2 h and then measuring the turbidity of the sample at 500 nm after dilution with 0.1% (w/v) SDS.

5.3.8. 2,2-Diphenyl-1-picrylhydrazyl (DPPH·) Radical Scavenging Activity

The antioxidant activity of PTT conjugates was assessed through their ability to scavenge $DPPH^{\cdot}$ radicals. PTT conjugates solution (0.4 ml, 1–10 mg/ml) in 1M Tris-HCl buffer (pH 7.9) was mixed with 0.6 ml of 100 µM $DPPH^{\cdot}$ in methanol (final concentration of 60 µM, initial

absorbance, Abs_{intial} of 0.7) for 20 min at 25ºC. Ferulic acid (10–40 μM) was used as the positive control. The absorbance of the mixture at 517 nm was measured. The percent reduction (Q) of the $DPPH^{\cdot}$ was calculated as follows:

$$Q = 100(Abs_{initial} - Abs_{sample})/Abs_{initial} \quad (5.2)$$

IC_{50} value, defined as the concentration of half-reduction of the $DPPH^{\cdot}$, was estimated. All assays were run in triplicates.

5.4. Results and Discussion

5.4.1. Maillard Reaction Progress

The Maillard reaction was conducted at 48°C to prevent the denaturation of potato proteins during incubation. There are published studies demonstrating that protein:carbohydrate conjugates can be formed at similar or even at lower temperatures (Jindal & Naeem, 2013; Medrano et al., 2009).

Tagatosyl-lysine residues formed during the early stage of the Maillard reaction are converted to furosine upon their acid hydrolysis (Krause et al., 2003). Furosine is a direct marker of Amadori product and is currently the most specific and important indicator of early Maillard reactions (Erbersdobler & Somoza, 2007). To estimate the extent of cabohydrate conjugation to the protein, the percent blocked lysine was calculated by quantifying the furosine formed and comparing it to the initial amount of free amino groups on the proteins. On the other hand, the protein aggregation index provides an indirect estimation of inter/intramolecular cross-linking of proteins.

Table 5.1 summarizes the percent blocked lysine of potato protein conjugates and their protein aggregation index over an incubation period of 1 to 7 days at 48ºC and at a_w of 0.65. As expected, the percent blocked lysine of incubated control potato proteins was negligible (data not shown). As compared to GOS and galactan, the initial glycation rate of potato proteins with galactose was higher, leading to a maximum percent blocked lysine of 97.9% upon incubation for 3 days. As the incubation was extended to day-5, the percent blocked lysine of potato proteins:galactose conjugates significantly decreased to 18.2% and, in parallel, an increase in the

Table 5.1 Progress of PTT conjugation through Maillard reaction at 48°C at a_w of 0.65

PTT mixtures	Incubation time	Percent blocked lysine[a]	Protein aggregation index[b]
PTT:Galactose	1	7.66 ± 0.12	0.61 ± 0.12
	3	97.93 ± 0.24	0.21 ± 0.33
	5	18.18 ± 1.02	4.68 ± 0.16
	7	0.00 ± 0.00	3.23 ± 0.14
PTT: GOS	1	0.84 ± 0.11	0.51 ± 0.03
	3	1.25 ± 0.20	1.02 ± 0.06
	5	1.00 ± 0.00	0.86 ± 0.20
	7	6.13 ± 0.80	1.60 ± 0.05
PTT:Galactan	1	0.19 ± 0.10	0.00 ± 0.05
	3	1.2 ± 0.73	0.01 ± 0.02
	5	4.3 ± 0.01	0.01 ± 0.01
	7	2.20 ± 1.07	1.73 ± 0.11

[a]Percentage of blocked lysine was calculated from furosine content and total free amino groups.

[b]Turbidity measurement at 600 nm.

protein aggregation index was observed. These results reveal the rapid advancement of the Maillard reaction in the presence of galactose leading to the degradation of the Amadori compounds and to the protein cross-linking (Oliyai et al., 1994). The glycation of potato proteins with GOS and galactan only achieved a maximum level of blocked lysine of 6.1 and 4.3% at day 7 and 5 of incubation, respectively. The overall results confirm that the shorter carbohydrate, present in a high proportion in the open-ring form, had higher reactivity. The lower glycation extent obtained in the presence of galactan may be due to the limited accessibility of this more bulky carbohydrate to the available lysine residues on the potato proteins. ter Haar et al. (2011) have highlighted that saccharide reactivity and lysine accessibility are the most determining factors for the rate of the Maillard reaction. Contrary to shorter galactose and GOS carbohydrates, the glycation of potato proteins with galactan resulted in negligible protein aggregation index during the first 5 days of incubation and increased to 1.7 at day 7. These results indicate the ability of galactan to limit the protein polymerization and the browning associated with the advanced Maillard reaction. In potato proteins:GOS glycation reaction, the progress of the reaction did not follow the same pattern as the other carbohydrates; at the initial stage of the glycation reaction with GOS, high protein aggregation index and low percent blocked lysine were achieved. This trend can be interpreted as a result of the release of dicarbonyl compounds, generated through glycoxidation of GOS, promoting protein aggregation during the initial stage by reacting with guanidine or arginine residues on the protein (Hollnagel & Kroh, 2000). The glycoxidation/autoxidation reaction of GOS may also have slowed down the carbohydrate conjugation by competing with the glycation reaction (Yeboah et al., 2000). Similar results were obtained in our previous studies (Seo et al., 2013; Seo et al., 2012) upon the glycation of GOS with lysozyme. The control samples (protein and carbohydrate) were run separately and they did not lead to any furosine formation upon acid hydrolysis demonstrating that the furosine quantified was indeed from the acid hydrolysis of the conjugated Amadori products. The formation of the conjugates has also been confirmed through mass spectrometric analyses (data not shown).

5.4.2. Purification of PTT Conjugates

To assess their functional properties, PTT conjugates were purified by anionic exchange chromatography. In Fig. 5.1, the elution profiles of potato proteins and their conjugates on a Mono Q column are shown. Since most protease inhibitors (~25% of Solanic 206P) have high

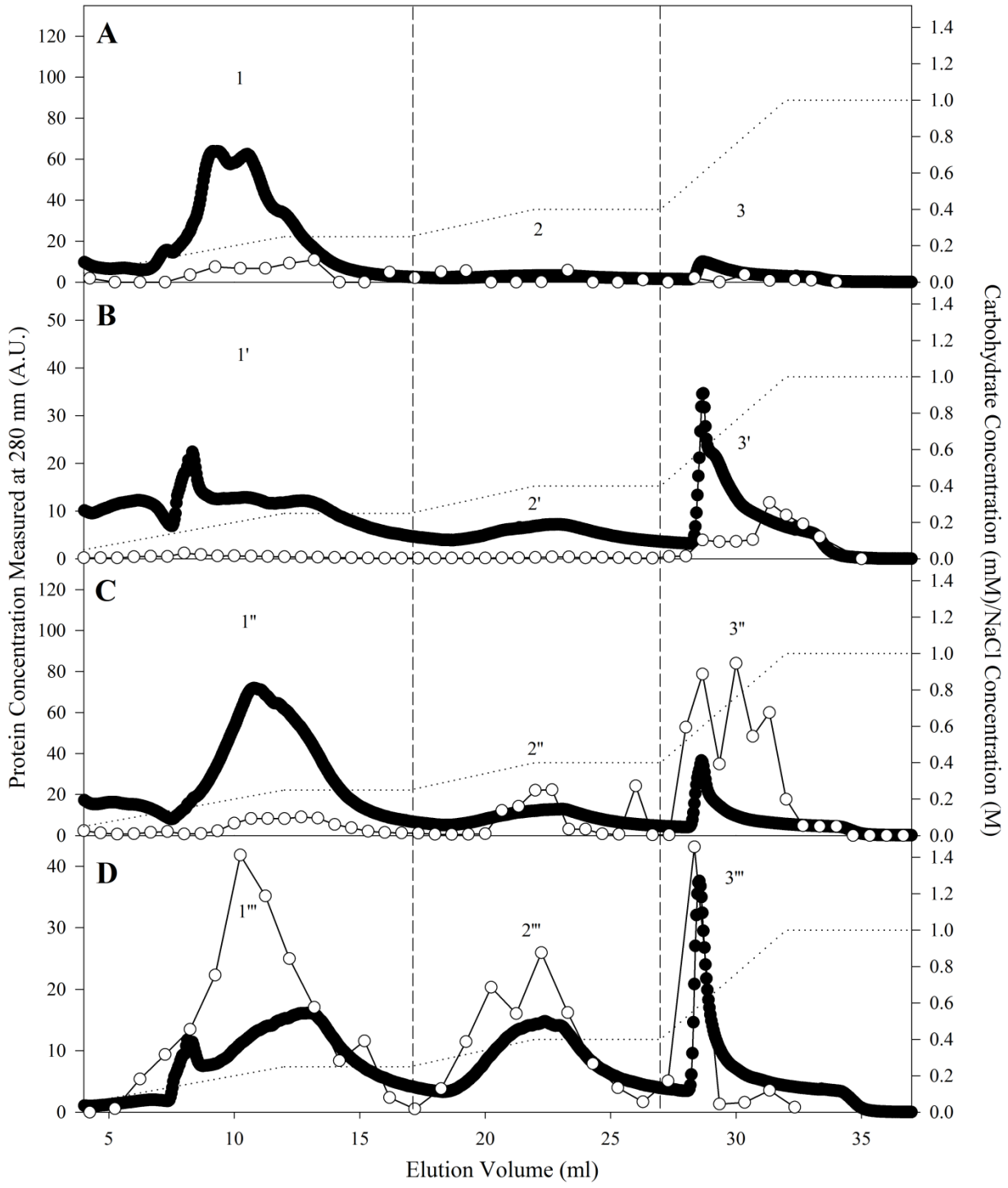

Figure 5.1 Purification of PTT conjugates through anionic exchange chromatography: PTT (A), PTT:galactose (B), PTT:GOS (C), PTT:galactan (D): protein concentration (●), carbohydrate concentration (○), sodium chloride concentration (·····).

isoelectric points of 6 to 9 (Pouvreau et al., 2001), they did not bind to the Mono Q column and were eluted at 0 M sodium chloride (data not shown). However, PTT with an isoelectric point of 4.0 was eluted as a broad peak between 0.05 and 0.25 M of sodium chloride (Fig. 5.1A, peak #1). The elution profiles of conjugates showed additional broad and sharp peaks eluting at higher concentrations of sodium chloride. Compared to unconjugated PTT, the high binding affinity of PTT conjugates to the anionic exchange column can be attributed to the decrease in positively charged free amino groups due to glycation (Fenaille et al., 2003). It can be hypothesized that peaks #2–2”’, eluted at 0.25–0.40 M sodium chloride, are composed of lower level of glycated conjugates, whereas peaks #3–3”’, eluted at 0.40–1.0 M, consist of highly glycated conjugates. Potato proteins:galactose conjugates (Fig. 5.1B) were fractionated into 21% of less glycated PTT conjugates (peak #2’) and 27% of highly glycated ones (peak #3’); these results confirm the high level of glycation in the presence of galactose observed (Table 5.1). The fractionation of potato proteins:GOS conjugates (Fig. 5.1C) resulted in low percentage of less (13%, peak #2”) and highly (6%, peak #3”) glycated conjugates, but most remained non-glycated (81%, peak #1”). The carbohydrate content profiles reveal the multiplicity of PTT conjugated derivatives obtained upon the glycation with GOS compared to galactose and galactan. The multiplicity of PTT:GOS glycoforms may be due to the different reactivity of heterogeneous GOS covering a wide range of degree of polymerization (DP of 2–12), leading to the difference in the glycation level. Similar multiplicity was reported in our previous study (Seo et al., 2013) upon glycation of lysozyme with a same pool of GOS. To overcome the decrease in the adsorption affinity of conjugates to the column due to the bulkiness and the excess of galactan, the potato proteins glycated with galactan were first ultrafiltered to remove the unconjugated PTT and galactan (Seo et al., 2012). The elution profile of PTT:galactan conjugates showed three main peaks: 52% peak #1”’, 34% peak #2”’, and 14% peak #3”’ (Fig. 5.1D). As compared to galactose and GOS, the elution profile of PTT:galactan conjugates cannot only be interpreted as a decrease in the number of Lys residues, but also as an alteration of the protein adsorption affinity to the column due to the steric hindrance of the bulky galactan chains conjugated to PTT. The conjugation level, estimated from the protein:carbohydrate ratio, revealed 1–10, 1–4, and 1–3 moles of galactose, GOS, galactan, conjugated to one mole of PTT, respectively. To assess the functional properties, peaks #2’–2”’ and 3’–3”’ were pooled for each conjugate.

5.4.3. Structural Characterization of Purified PTT Conjugates

5.4.3.1. Secondary Structure

Fig. 5.2A shows the percent change in the secondary structure of the conjugates compared to the control PTT (after incubation) estimated through FTIR. The amide I′ region of PTT solution in $^{2}H_2O$ revealed five components upon deconvolution and curve-fitting (data not shown). The band at 1618 cm^{-1} had been assigned to strongly bonded β-strands indicative of aggregated strands type structure (Pots et al., 1998). The remaining structures were assigned as follows: bands at 1637 ± 3.0 and 1675 ± 5.0 cm^{-1} as β-sheets, band at 1645 ± 4.0 cm^{-1} as random coils, bands at 1653 ± 4.0 cm^{-1} as α-helix, and bands at 1671 ± 3.0 and 1689 ± 2.0 cm^{-1} as β-turns (Kong & Yu, 2007). The FTIR spectrum of native PTT shows the presence of 15.2% aggregated strands, 40.8% β-sheet, 13.0% β-turns, and 31.0% α-helix (data not shown). Higher proportions of α-helix (45%) and β-sheet (33%) were reported for PTT (Pots et al., 1998). This discrepancy may be due to the fact that PTT examined by Pots et al. (1998) was freshly extracted from potatoes, which may have helped in preserving the secondary structure. The FTIR spectrum of the control PTT had a small increase in aggregated strands (≈5%) and a decrease in α-helix (≈5%), which are indicative of a minor change in the protein's secondary structure upon incubation at mild temperature of 48°C. The results also show that the glycation with galactose had minimal effects on the secondary structure of PTT with 1.7, 1.0, and 0.8% increases in aggregated strands, β-turn, and α-helix, respectively. A small decrease of 3.6% in β-sheet was also found. These results may reveal the high affinity of galactose for exposed glycation sites located at the termini of PTT secondary structures (Lys 159, 173, 269, 278, 352, 353, 357, 384), which may have prevented pronounced secondary structural changes of PTT upon glycation. The most significant changes in the secondary structure of PTT were observed upon glycation with GOS with 30.6% increase in aggregated strands, and with 6.1, 10.8, and 13.7% decreases of β-turn, α-helix, and β-sheet, respectively. Similar structural changes were exhibited by PTT:galactan conjugates, in which 18.3% increase in aggregated strands, and 3.2, 1.1 and 14.0% decreases in β-turn, α-helix, β-sheet, respectively, had taken place. The greater structural changes observed upon glycation with larger carbohydrates (GOS, galactan) is probably due to their bulkiness, leading to the disruption of intermolecular non-covalent interactions that stabilize the secondary structure of PTT (Povey et al., 2008). The high level of protein cross linking upon glycation with GOS may have also contributed to these changes (Table 5.1).

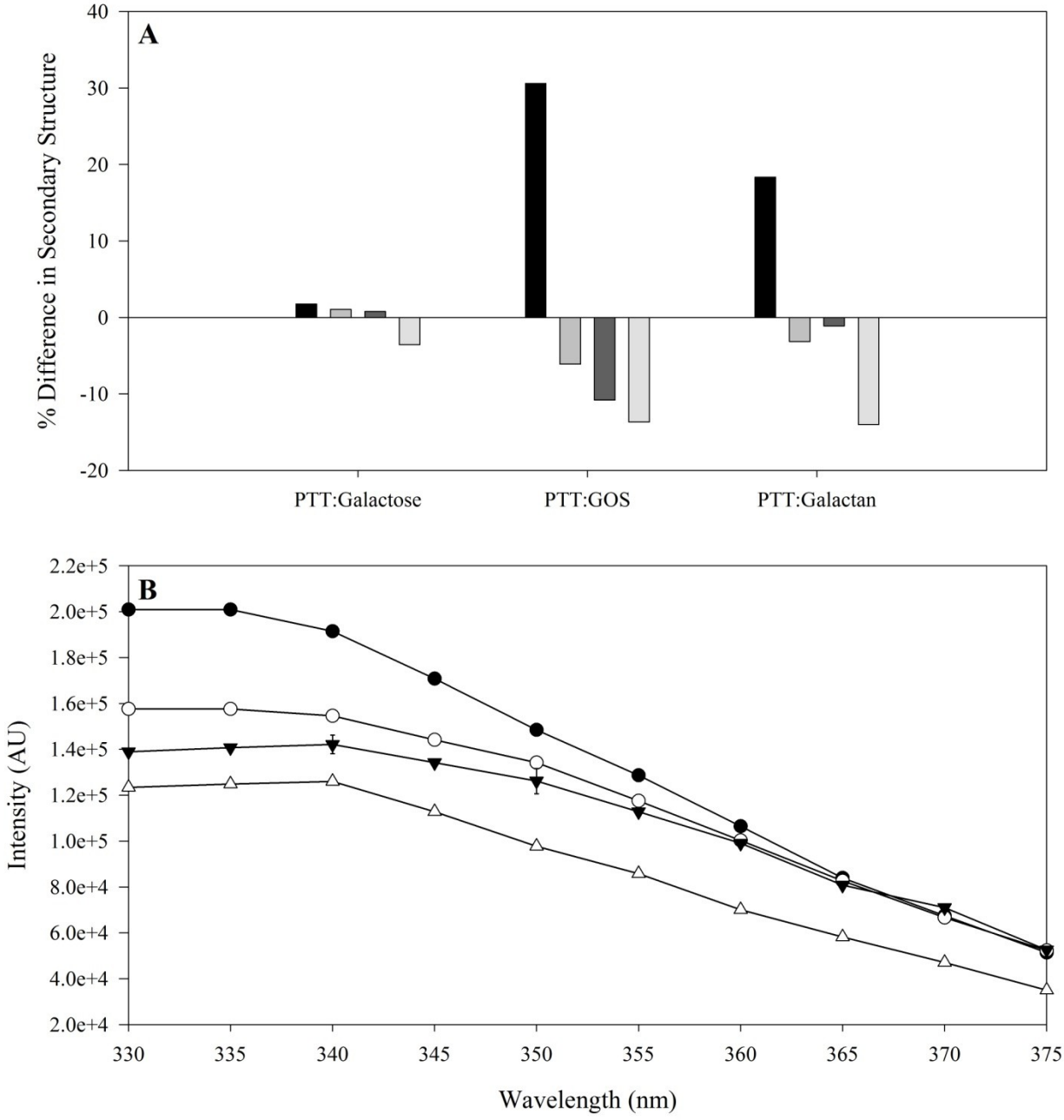

Figure 5.2 Effect of glycation on (A) PTT secondary structure obtained through FTIR analysis, intermolecular *β*-sheet (■), intramolecular *β*-sheet (▭), *α*-helix (▬), *β*-turn (▭) and (B) PTT tertiary structure obtained through fluorescence spectroscopy, PTT (●), PTT:galactose (○), PTT:GOS (▼), PTT:galactan (△).

5.4.3.2. Tryptophan Fluorescence

The tryptophan fluorescence emission spectra of control and glycated PTT (Fig. 5.2B) were investigated to assess the change in the tertiary structure due to glycation. PTT contains two tryptophan (Trp 279, Trp 284) residues in the primary sequence that can be used as intrinsic fluorophores for analyzing the protein tertiary structure. When excited at 295 nm, control PTT exhibited a fluorescence wavelength of maximum emission (λ_{max}) of 330 nm, while the native PTT demonstrated a λ_{max} of 335 nm. It has been reported that PTT exhibits two λ_{max} of 336 and 347 nm, as a result of the presence of buried and more exposed Trp residues, respectively (Koppelman et al., 2002). The detection of only fluorescence maximum wavelength in native and control PTT could be explained by the small level of aggregation, which might have led to a closer packing of the tertiary structure. Pots et al. (1998) have also reported one λ_{max} of 335 nm for PTT. The results show that similar λ_{max} (330 nm) as the control was exhibited by PTT:galactose conjugates, indicating that the local environment of the Trp residues was not affected by glycation with galactose and that the tertiary structure of PTT was conserved. However, PTT:GOS and PTT:galactan conjugates showed a red-shift of the Trp emission maximum to 340 nm, indicating an increased exposure of Trp toward a more hydrophilic surrounding. This suggests that a large conformational change of PTT may have occurred around the Trp residues as a result of the glycation of some of the nearby Lys residues (identified according to 3D model predicted by Swissmodel: Lys 253, 357) with GOS and galactan (data not shown). These results are in good agreement with the secondary structural changes (Fig. 5.2A), which reveal a more unfolded structure of PTT glycated with GOS and galactan.

5.4.4. Functional Properties of Purified PTT Conjugates

5.4.4.1. Thermal Stability

To assess the thermal stability of PTT conjugates, the changes in their secondary structure upon heat treatment (50, 70, 90°C) were evaluated by FTIR spectroscopy. The change in proportions of secondary structures of the conjugates upon heat treatment over that of the conjugates at 30°C is presented in Fig. 5.3. As overall, heating the control PTT resulted in pronounced changes in various amide I′ bands (Fig. 5.3A). Upon heat treatment at 50°C, PTT has 11.3% increase in aggregated strands and less than 10 % decrease in proportions of other secondary structures. The change in secondary structure became more pronounced for control PTT treated at 70°C with

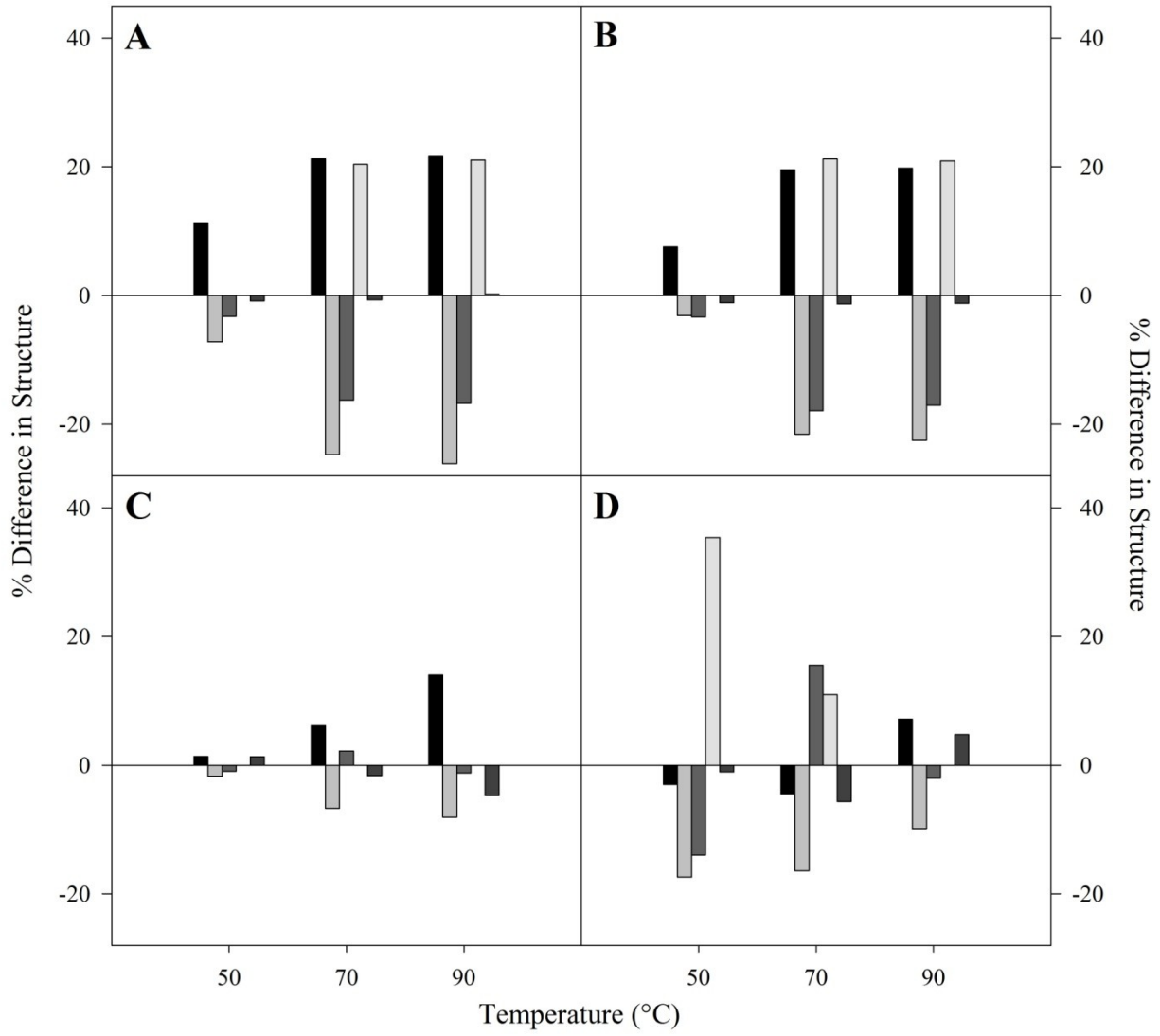

Figure 5.3 Heat stability of PTT (A), PTT:galactose (B), PTT:GOS (C), PTT:galactan (D) estimated by measuring changes in the secondary structures using FTIR as compared to the secondary structure of the conjugates at 30°C: intermolecular *β*-sheet ( ), intramolecular *β*-sheet ( ), *α*-helix( ), random coil ( ), and *β*-turn ( ).

21.2 and 20.4% increases in aggregated strands and random coils, respectively, with accompanying 24.7 and 16.3% decrease of β-sheets and α-helix. At 90°C, the changes in secondary structure did not significantly differ from the changes observed at 70°C. These results reveal the dependence of the secondary structure of PTT on the temperature and the occurrence of the unfolding between 50–70°C. Creusot et al. (2010) have reported an unfolding temperature of PTT of 59ºC, which is in agreement with the control PTT's loss in secondary structure between 50–70ºC. Upon heat treatment, PTT:galactose conjugates (Fig. 5.3B) exhibited similar secondary structure changes to control PTT. Unlike control PTT and PTT:galactose, the unfolding of PTT:GOS (Fig. 5.3C) conjugates occurred at temperatures higher than 70°C. Indeed, no significant changes (>10%) in the secondary structure of PTT:GOS conjugates were observed at 50 and 70ºC. The most important changes in PTT:GOS conjugates' secondary structure were observed at 90°C with 14% increase in aggregated strands, and with 8.1, 1.2, and 4.5% decreases in β-sheet, α-helix, and β-turn, respectively. Although the conjugation of PTT with GOS disrupted its local secondary structure, the interactions between the sugar moiety and the protein stabilized the remaining secondary structure. On the other hand, the changes in the secondary structure of PTT:galactan conjugates increased upon treatment at 50 and 70°C, but conversely decreased at higher temperature of 90°C. Indeed, at 50°C, the secondary structure of PTT:galactan conjugates (Fig. 5.3D), had a 35.4% increase in random coils and decreases of 3.0, 17.4, 14.0, and 1.1% in aggregated strands, β-sheet, α-helix, and β-turn, respectively. When the temperature was increased to 70°C, 15.5 and 11.0% increases in α-helix and random coils, respectively, were obtained in addition to decreases in aggregated strands (4.5%), β-sheet (16.4%), and β-turn (5.6%). Minor changes in the secondary structure of PTT:galactan were observed at 90°C with 7.1% increase in aggregated strands and 9.8% decrease in β-sheet being the most important ones. PTT:galactan conjugates seem to undergo the unfolding process at around 50°C, but at higher temperature of 90°C, they undergo refolding of the damaged structure as evidenced by the sudden increase in random coils and the subsequent decrease in the change of secondary structure. The refolding pattern of the PTT:galactan conjugates at higher temperature can be attributed to the high interaction of amino acids with large carbohydrate chain of polysaccharides. Similarly, Povey et al. (2008) have demonstrated that the interaction of nearby amino acids with the attached carbohydrate can lead to a preferred secondary structure of the glycated protein.

The effect of temperature on the tertiary structure of the conjugates was also estimated through Trp fluorescence (data not shown). Trp λ_{max} was maintained with control PTT and its conjugates until the temperature reached 60ºC. At 60ºC, control PTT and PTT glycated with galactose had a red-shift of λ_{max} from 330 nm to 340 nm, which reveals that the polarity of the local Trp environment changed to a more hydrophilic one. These results are in good agreement with the FTIR results (Fig. 5.3). For PTT:GOS and PTT:galactan conjugates, λ_{max} was not affected by heating, which demonstrates that the modified local environment of Trp on these glycated proteins was thermostable.

5.4.4.2. pH Stability

Fig. 5.4 shows the effect of glycation on the tertiary structure of PTT and its conjugates at selected pH values (3, 5, 6, 8, 10) measured by the change in Trp fluorescence intensity at λ_{max}. The tertiary structure of control PTT exhibited a high pH stability with small changes (-0.1 to 14.4%) in fluorescence intensity at different pHs and no change in λ_{max}. In contrast, PTT:GOS conjugates showed a significant increase in fluorescence intensity (8.7–57.0%) with the pH and a change in λ_{max} at pH 8 from 340 to 345 nm, which are indicative of the low pH stability of their tertiary structure. It seems likely that the change in secondary and tertiary structure caused by the glycation of PTT with GOS (Fig. 5.2A, B) led to a modified structure, in which the local environment of the Trp residues is more easily affected by the change in pH. No change in λ_{max} was observed for the PTT:galactose and PTT:galactan conjugates (data not shown). At pH 3, PTT:galactose and PTT:galactan conjugates demonstrated significant changes in their fluorescence intensity as compared to the control; these results may be due to the lower isoelectric point of the conjugates. At pH 6 and 8, the changes in fluorescence intensity of PTT:galactose (2.8, -0.4%) and PTT:galactan (0.5, 2.2%) conjugates were very comparable to the results obtained with the control (0.1, 1.2%). At pH 5 and 10, PTT:galactose (-3.3, 4.9%) and PTT:galactan (-0.5, 9.2%) conjugates demonstrated slightly better pH stability than the control PTT (8.0, 14.4%) with less change in florescence intensity. The change in fluorescence intensity of PTT:galactose conjugates are in good agreement with the structural data. As an overall, control PTT and PTT:galactose conjugates exhibited similar pH-structural behavior. On the other hand, PTT:galactan conjugates demonstrated small changes in fluorescence intensity with pH, revealing the high pH stability of the structure adopted from the interaction of nearby amino acids of PTT with the attached galactan moieties.

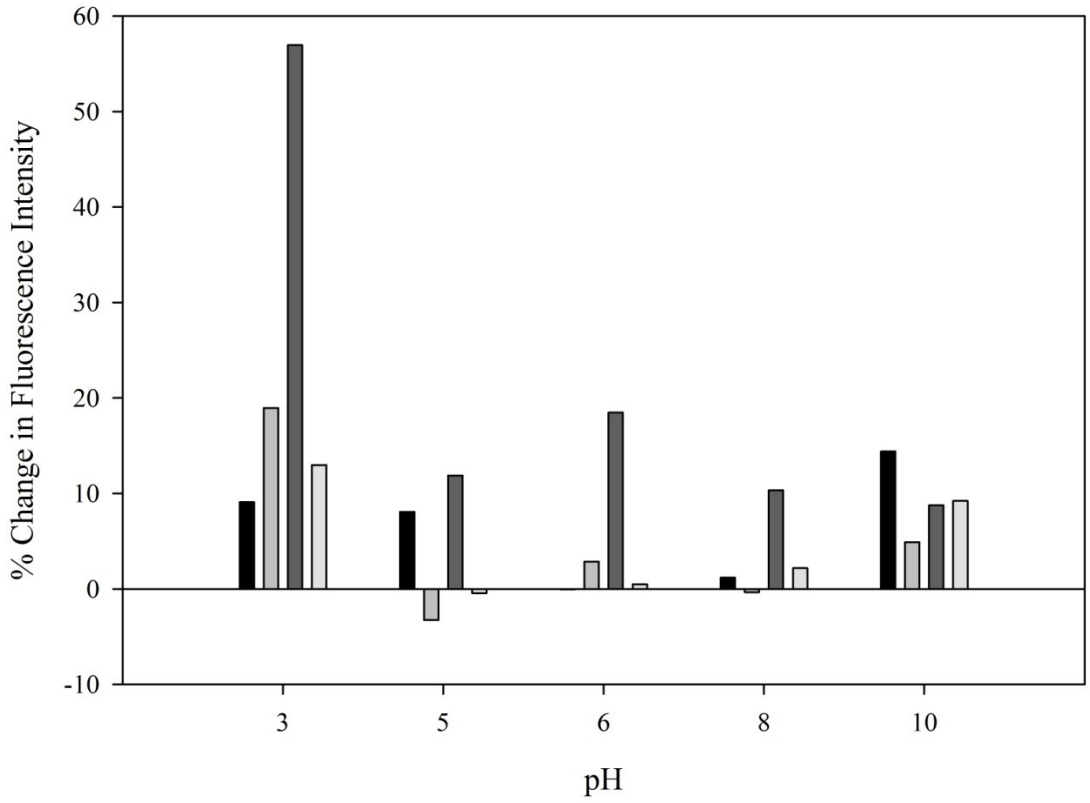

Figure 5.4 pH stability of PTT conjugates determined using fluorescence spectroscopy compared to pH 7: PTT ( ), PTT:galactose ( ), PTT:GOS ( ), and PTT:galactan ( ).Data are averages ± standard deviation of triplicates.

5.4.4.3. Emulsifying Properties

Effect of PTT glycation on its emulsifying properties at pH 3 and 7 is shown in Fig. 5.5A. The diameter of the oil droplets as well as the turbidity loss after heat treatment at 65ºC were used as an indicator of the emulsifying activity and stability, respectively. Using control PTT, the mean diameters of the droplets at pH 3 and 7, were 467.8 nm and 2007.2 nm, respectively. The larger oil droplets at pH 7 can be attributed to the rapid formation of gel-like protein layer around the oil, which may have increased the interfacial tension during emulsion/oil droplet formation (Beverung et al., 1999). Contrary to control PTT, PTT:galactose and PTT:galactan conjugates led to smaller droplets at pH 7 (1353.3 nm and 946.9 nm) than at pH 3 (1829.5 nm and 2490.7 nm); these results indicate that the hydrophobic interactions between the oil and PTT were more favored at pH 7 upon its glycation with galactose and galactan. On the other hand, PTT:GOS conjugates led to an emulsion with the largest oil droplets (6562.6 nm at pH 3, 10838.7 nm at pH 7). The high pH-dependence of mean oil droplet size can be attributed to the pronounced effect of pH on the diffusion of protein molecules onto the oil-water interface, affecting, the interfacial properties and/or to the significant alterations of electrostatic inter-molecular interactions (Israelachvili, 1991).

As indicated by the loss in turbidity, native PTT (53.2%) and PTT:galactan conjugates (61.0%) exhibited lower emulsion stability at pH 3 than at pH 7. In contrast, PTT:galactose conjugates resulted in a lower emulsion stability at pH 7 (59.8%). The emulsion stability at pH 3 was vastly improved upon glycation of PTT with galactose. PTT:GOS conjugates displayed lower emulsion stability as compared to native PTT at both pH 3 (48.6%) and 7 (61.7%). The stabilization of emulsion is, generally, attributed to the film forming ability of proteins at the oil-water interface, favoring electrostatic and steric repulsive forces between droplets (McClements, 2004). Khan et al. (1999) have suggested that protein and carbohydrate conjugates enhance synergistically the emulsifying properties by reinforcing the adsorption of the protein to the oil-water interface and by stabilizing the oil droplets through the viscoelastic layer of carbohydrates in the aqueous phase. The increased number of carbohydrate conjugation on PTT:galactose conjugates in addition to its more exposed tertiary structure at pH 3 (Fig. 5.4) seems to have contributed to its emulsion stability. However, PTT conjugated with GOS formed the least stable emulsions with the largest droplet diameter. Berthold et al. (2007) have previously suggested that a very flexible

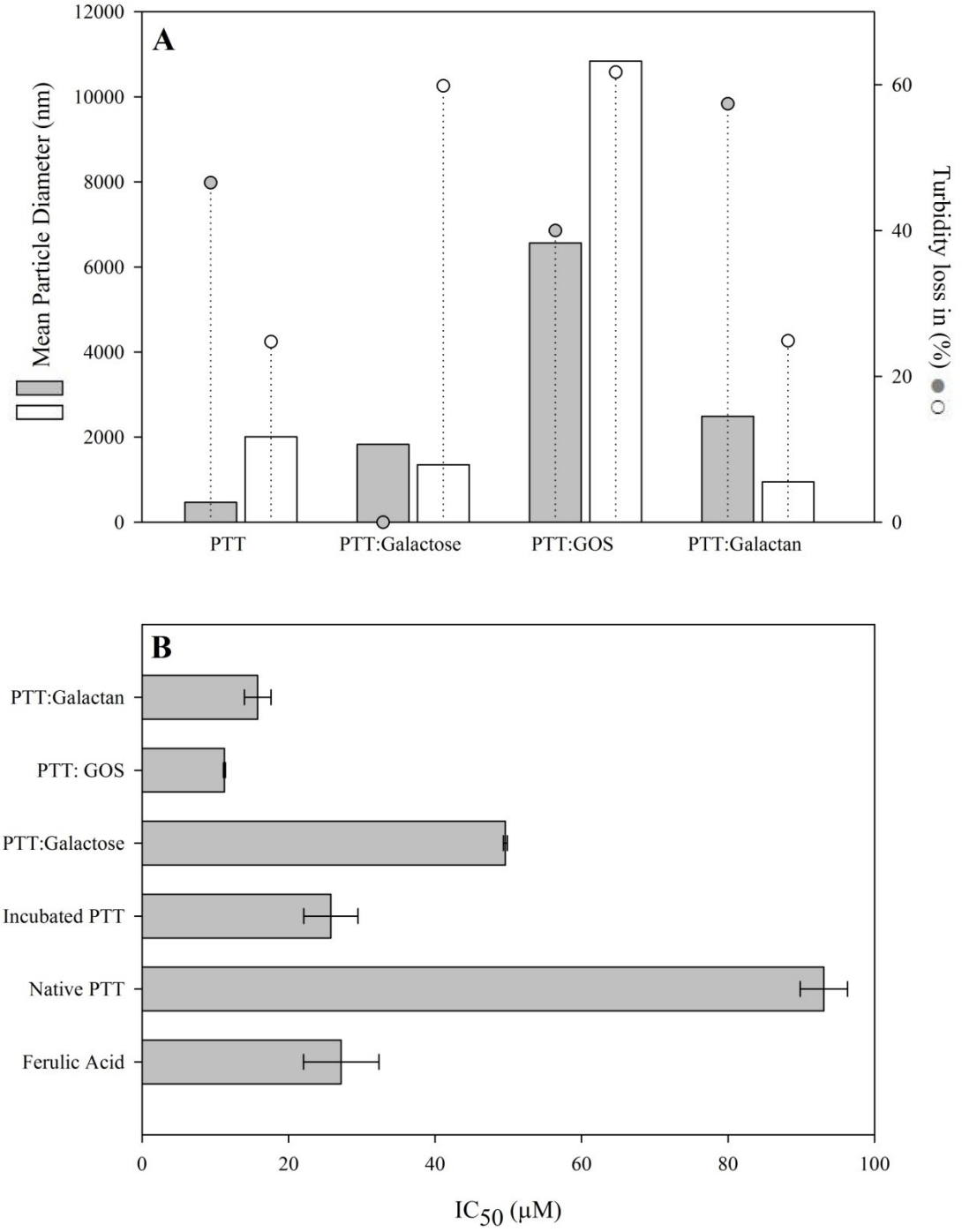

Figure 5.5 (A) Emulsifying properties of PTT conjugates: The droplet size at pH 3( ) and 7( ) is a mean of 70 measurements; the emulsifying stability is estimated at pH 3 (●) and 7 (○). (B) Effect of PTT glycation on $DPPH^{\cdot}$ radical scavenging activity. Data are averages of triplicates.

protein interface film will easily be broken during collisions between oil droplets, resulting in accelerating coalescence and droplet size increment. PTT:GOS conjugates, with the most unfolded conformation and the highest tertiary flexibility, may have most likely formed a very flexible film at the oil-water interface resulting in a larger oil droplet formation and lower emulsion stability.

5.4.4.4. 2,2-Diphenyl-1-picrylhydrazyl ($DPPH^{\cdot}$) Radical Scavenging Activity

$DPPH^{\cdot}$ scavenging activity was measured to assess the antioxidant activity of PTT conjugates (Fig. 5.5B). The main structural characteristics of protein, required for an efficient radical scavenging activity, were reported to be the number of free radical scavenging amino acids and their solvation (Elias et al., 2008). PTT has 12 solvent exposed free radical scavenging amino acids, such as methionine, tryptophan, tyrosine, phenylalanine, cysteine and histidine (Petersen et al., 2009). Among the investigated proteins, PTT:GOS and PTT:galactan conjugates were found to be the most potent scavengers, with a IC_{50} of 11.25 and 15.8 μM, respectively. On the other hand, PTT:galactose conjugates (IC_{50} of 49.6 μM) showed lower radical scavenging activity than that of control PTT (IC_{50} of 25.8 μM). As compared to the native PTT (IC_{50} of 93.1 μM), the control PTT exhibited a much higher radical scavenging activity, which was comparable to the potent antioxidant, ferulic acid (IC_{50} of 27.2 μM). These results demonstrate that the mild heat treatment alone can increase the antioxidant activity of PTT. However, the fluorescence results indicated closer packing of the control PTT around the Trp residues upon heat treatment. The high antiradical scavenging activity of control PTT may be due to the exposure of other oxidatively labile and hydrophobic amino acids than Trp. Similarly, Elias et al. (2007) have reported an increase in the protein's antioxidant activity of β-lactoglobulin upon heat treatment. The high scavenging potency of PTT:GOS and PTT:galactan conjugates can be attributed to the tertiary structure rearrangement of PTT upon glycation, resulting in a high solvation and accessibility of free radical scavenging amino acid residues. These results are in good agreement with the results obtained from the fluorescence measurements (Fig. 5.2B), where a more exposed Trp environment was observed for PTT:GOS and PTT:galactan conjugates

5.5. Conclusion

PTT:galactose/GOS/galactan conjugates were produced through the Maillard reaction. Galactose was more reactive, resulting in a higher proportion of highly glycated PTT, as compared to its longer chain counterparts. The most important secondary and tertiary structural changes were obtained upon glycation of PTT with GOS and galactan. These structural changes led to more heat stable forms of PTT with a higher unfolding temperature than the unmodified protein. In addition, the interaction of nearby amino acids of PTT with the attached galactan moieties resulted in high pH stability of its tertiary structure. The changes in structure also increased the antioxidant activity of PTT glycated with GOS or galactan. On the other hand, high level of galactose conjugation to PTT and increased exposure of hydrophobic residues led to a significant increase in the emulsifying stability at pH 3. Overall, this comprehensive structure-function study will help with the production of improved targeted protein:carbohydrate conjugates and contribute to the conversion of the unexploited potato proteins into high value functional ingredients.

CONNECTING STATEMENT 4

In Chapter V, the produced PTT:carbohydrate conjugates demonstrated improvements in selected functional properties, and the overall results led to a better understanding of structure-function relationships. The effect of carbohydrate conjugation on the allergenicity of PTT needed to be elucidated. Therefore, the effects of carbohydrate conjugation, heat treatment and simulated gastric digestion on the immunoreactivity of PTT and of its conjugates were investigated (Chapter VI).

The results reported in this chapter were presented at IFT13 Annual Meeting & Food Expo and published in the *Journal of Agricultural and Food Chemistry*.

Seo, S., & Karboune, S (2013) *The change in allergenicity of potato proteins upon glycation*. IFT13 Annual meetings. Chicago, Illinois, July 13–16

Seo. S., Karboune, S. & L'Hocine, L. (2014) Allergenicity of potato proteins and of their conjugates with galactose, galactooligosaccharides and galactan in native, heated and digested forms, *Journal of Agricultural and Food Chemistry*, *62*(16), 3591-3598.

CHAPTER VI

ALLERGENICITY OF POTATO PROTEINS AND OF THEIR CONJUGATES WITH GALACTOSE, GALACTOOLIGOSACCHARIDES AND GALACTAN IN NATIVE, HEATED AND DIGESTED FORMS

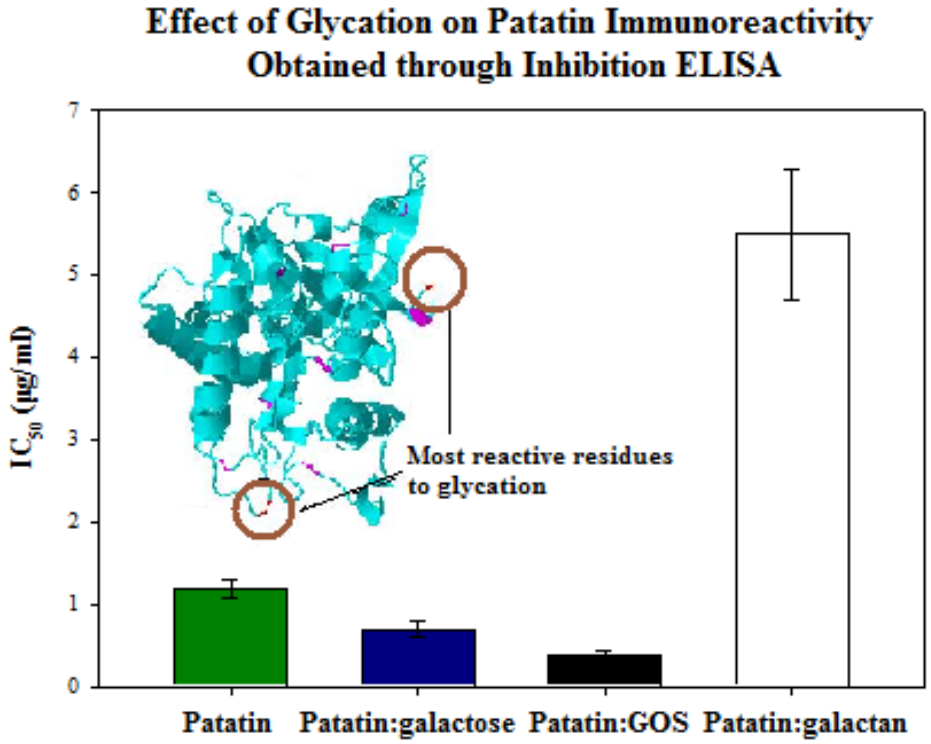

6.1. Abstract

The effect of glycation of potato proteins on their immunoreactivity was studied by using a pool of human sera with specific IgE to potato proteins. Patatin conjugates were more immunoreactive than protease inhibitors ones. To better understand this behavior, the changes in patatin structure upon glycation and heat treatment were investigated. Patatin demonstrated an increase in total immunoreactivity when glycated with galactose and galactooligosaccharides. However, galactan conjugation to patatin resulted in a decrease in immunoreactivity by restricting IgE's access to the epitopes. Although the heat treatment resulted in a decrease in patatin's immunoreactivity through aggregation, it was less effective when patatin conjugates were used, due to the decrease in aggregation and the secondary structural changes. Upon digestion, native patatin exhibited the largest decrease in immunoreactivity resulting from the disruption of both conformational and sequential epitopes. Patatin conjugates were less digested and had higher IgE-immunoreactivity as compared to the digested patatin.

6.2. Introduction

Food allergy occurs in 2–6% of the population (Hefle et al., 1996). The mechanism underlying an allergen response involves an exposure of the allergenic patient to the causative allergen leading to increased terminally differentiated B lymphocyte (plasma cell) immunoglobulin E (IgE) antibody production. The IgE binds to IgE receptors of mast cells. When the antigen interacts with the bound IgE, mast cells release various substances, such as histamine, to the surrounding environment, which are responsible for the clinical symptoms typical of immediate hypersensitivity (Church et al., 1997). Although food allergy to potato is rare, a number of IgE binding proteins have been identified in potato tubers (Wahl et al., 1990). It has been demonstrated that the sensitization to potato proteins occurs in conjunction with birch pollen allergy due to the structural similarities between the proteins (Ebner et al., 1995). Most documented allergic reactions involve contact with raw potatoes (Iliev & Wuthrich, 1998; Seppala et al., 1999), and to a lesser extent, boiled potatoes (Castells et al., 1986).

Compared to proteins from other sources, potato proteins are considered higher in nutritional quality as they contain a high proportion of lysine similar to egg proteins (Ralet & Gueguen, 1999). Potato proteins, being abundant in the potato by-products, are emerging as interesting replacements for many existing food proteins (Shieber et al., 2001). There are three major

fractions of potato proteins: 1) patatin (PTT, ~40%); 2) protease inhibitors (PIs, ~50%) and 3) other high molecular weight (MW) proteins (~10%) (Waglay et al., 2014). PTT, which is the major allergen found in potato (Seppala et al., 1999), is a dimer glycosylated protein with up to two carbohydrate chains, resulting in isoforms with MWs ranging from 40 to 45 kDa (Pots et al., 1999a). In addition to its anticarcinogenic (Sun et al., 2013) and antimicrobial effects (Sharma et al., 2004), PTT has demonstrated emulsifying and foaming properties, which make it suitable for diverse applications (Deveaux-Gobert, 2008); however, its low solubility and low denaturation temperature have limited its applications (Creusot et al., 2010). PIs have also been involved in allergic reactions to potato tuber (Seppala et al., 2001) and are composed of diverse proteins with a MW ranging from 5 to 25 kDa. PIs can promote satiety by increasing the cholecystokinin circulation (Komarnytsky et al., 2011).

The glycation of potato proteins through the Maillard reaction has been demonstrated as a promising method to improve their functional properties (Giuseppin et al., 2011). However, overall, the conjugation of food protein allergens with carbohydrates may decrease (Taheri-Kafrani et al., 2009) or enhance (de Jongh et al., 2013) their allergenicity (Sathe et al., 2005). Indeed, the decrease in the allergenicity of proteins upon conjugation with carbohydrates was attributed to the steric inhibition of some epitope bindings, as a result of protein conformational change and/or glycation of the amino acid residues located on the epitopes (Arita et al., 2001). However, the formation of new epitopes and/or the exposure of the buried epitopes upon glycation have contributed to the increase in the allergenicity of glycoproteins (Gruber et al., 2005; Nakamura et al., 2005). To the best of the authors' knowledge, the effect of glycation on the IgE-immunoreactivity of potato proteins has not yet been investigated.

The presented study was aimed at the investigation of the effect of glycation on the IgE-immunoreactivity of glycated potato proteins, PTT and PIs, with galactose, galactooligosaccharides (GOSs), and galactan, through the Maillard reaction. PTT being the major potato allergen, the IgE-binding properties of their conjugates were investigated in relation to their protein structures. Because heat treatment and gastric digestion can affect the allergenic character, the immunoreactivity of PTT conjugates was assessed after these two treatments.

6.3. Materials and Methods

6.3.1. Materials

Potato protein Solanic 206P (PTT ≈ 75%, PIs ≈ 25%) was kindly provided by Solanic (Foxhol, Netherlands). Potato galactan and endo-1-4-*β*-D-galactanase from *Aspergillus niger* were purchased from Megazyme (Wicklow, Ireland). Furosine standard was purchased from Neosystem Laboratories (Strasbourg, France). Biogel P2 extra fine, Bradford reagent and broad range SDS–PAGE standards were purchased from Bio–Rad (Philadelphia, PA). Four potato-sensitive human sera (Table 6.1) were acquired from PlasmaLab (Everett, WA) (8.75–22.40 kU_A/1 potato specific IgE, ImmunoCAP; Pharmacia, Uppsala, Sweden). Sera from non-allergic and dust-mite allergic (>100.00 kU_A/1 dust-mite specific IgE) individuals as controls were also obtained from PlasmaLab. All other chemicals were from Sigma Chemical Co. (St–Louis, MO).

6.3.2. Preparation of Conjugates

PTT and PIs present in Solanic 206P were separated by ultrafiltration using a stirred ultrafiltration unit (Amicon system, Millipore, Billerica, MA) fitted with a 30 kDa molecular mass cut–off membrane. The SDS-PAGE gels (Fig. 6.1) of the purified PTT and PIs were analyzed using AlphaView Software (Cell Biosciences, Santa Clara, CA). The retentate recovered upon ultrafiltration was composed of 90% PTT, while the filtrate consisted of 95% protease inhibitors. The retentate and the filtrate containing PTT and PIs-enriched extracts were freeze-dried separately. GOSs (MW of 1,990.9 g/mol) were prepared from potato galactan using endo-(1-4)-*β*-D-galactanase from *A. niger* as described previously (Paragraph 3.3.2). PTT or PIs and each of the galactose or GOSs or galactan at the molar ratio of 1:9 were dissolved in 0.1% (w/v) of 0.05 M sodium phosphate buffer (pH 7.0). Protein:carbohydrate mixtures were lyophilized and incubated in sealed glass desiccators at 48 ºC for 1 to 3 days under controlled a_w value of 0.65 equilibrated with a saturated solution of potassium iodide. Control experiments (control PTT and PIs) were performed with selected proteins incubated under the same conditions in the absence of carbohydrates.

6.3.3. Determination of Glycation Extent of Potato Proteins with Selected Carbohydrates

To determine the extent of glycation of PTT and PIs, the percent blocked lysine was estimated from the total free amino content and the acid-generated furosine content, according to a modified method that was previously described (Seo et al., 2014a). Briefly, 500 μl of 20 mg/ml

Table 6.1 Level of specific IgE found in the serum of donors characterized by ImmunoCAP

Origin of the allergen	Code*	Specific IgE from Donor A[a] ($kU_A/1$)	Specific IgE from Donor B[b] ($kU_A/1$)	Specific IgE from Donor C[c] ($kU_A/1$)	Specific IgE from Donor D[d] ($kU_A/1$)
Potato	F35	8.8	22.4	12.1	17.2
Carrot	F31	6.8	27.1	17.4	14.4
White bean	F15	8.3	–	–	–
Pea	F12	–	3.9	–	–
Peanut	F13	–	32.8	8.0	19.7
Soybean	F14	–	8.9	–	–
Hazelnut	F17	–	–	74.7	–
Almond	F20	–	–	–	10.0
Tomato	F25	–	–	13.5	–
Bermuda grass pollen	G2	–	98.5	25.7	47.1
Common ragweed pollen	W1	–	36.8	–	20.3
Wall pellitory pollen (*officinalis*)	W19	–	–	–	16.7
White ash tree pollen	T15	–	54.2	–	–
Common silver birch pollen	T3	–	45.0	>100.0	–
Olive tree pollen	T9	–	42.2	–	–
Maple leaf sycamore tree pollen	T11	–	–	–	19.7
Japanese cedar tree pollen	T17	–	–	–	11.8
Latex	K82	–	10.1	–	–

* ImmunoCAP allergen code
[a] Male, Caucasian, 28 years old
[b] Male, Caucasian, 24 years old
[c] Male, Caucasian, 24 years old
[d] Male, Native American, 47 years old

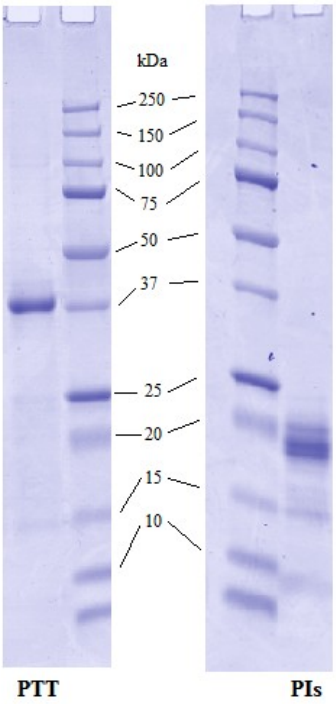

Figure 6.1 SDS-PAGE gel of isolated PTT and PIs through ultrafiltration

of protein sample in water was hydrolyzed with 200 μl of 8 M HCl for 23 h at 110 °C capped under nitrogen. The hydrolyzed sample was cooled to room temperature and centrifuged at 13,000 × g for 15 min. The supernatant (500 μl) was applied to previously activated Sep-Pak C18 cartridge (Waters Corp, Milford, MA). Furosine was eluted with 3 M HCl and evaporated until dryness under nitrogen. The sample was resolubilized in 200 μl of water: acetonitrile: formic acid mixture (95:4.5:0.5, v/v/v) and analyzed through high-pressure liquid chromatography (HPLC). A Waters Bioseparations module, a photodiode array detector equipped with Empower 2 software for data collection was used. A sample volume of 20 μl was separated using Waters Symmetry Shield RP8 3.5 μm (4.6×50 mm) column using an isocratic elution of 5 mM octanesulfonic acid in water: acetonitrile: formic acid mixture (79.8:20:0.2, v/v/v) for 20 min at a flow rate of 0.3 ml/min. The detection of furosine was performed at 280 nm. The calibration curve was constructed using a furosine standard. All assays were run in triplicates and injected with and without the internal standard. No furosine was detected in the control samples, non-incubated mixtures of protein and carbohydrate. The final percentage of blocked lysine was indirectly estimated according to the previously described method (Seo et al., 2014a).

6.3.4. Purification of Patatin Conjugates

Native PTT, incubated control PTT as well as PTT:galactose, PTT:GOS, and PTT:galactan conjugates were subjected to ultrafiltration using a stirred ultrafiltration unit (Amicon system, Millipore) fitted with 30 kDa or 300 kDa molecular mass cutoff membrane to remove the smaller Maillard reaction species and the unreacted saccharides present in the mixture. The retentates were collected for further analyses.

6.3.5. Simulated Gastric Digestion

Native PTT, incubated control PTT, and PTT conjugates were subjected to simulated gastric digestion according to the modified method of Moreno et al. (2008). Proteins and glycoproteins (1 mg/ml) were solubilized in simulated gastric fluid (0.75 M NaCl, pH 2.5). To initiate the enzymatic digestion, porcine pepsin (7 mg/ml, ≥ 2,500 units/mg protein) was then added at a ratio of 1:50 (v/v). After the digestion was performed at 37 °C for 2 h, the pH was raised to 7.5 with 0.125 M ammonium carbonate. To simulate the duodenal environment, the following solutions were added: 1) 10 μl of the following bile salt mixture (0.025 M sodium taurocholate,

0.025 M sodium glycodeoxycholic acid, 0.4 M $CaCl_2$, 0.5 M Bis–Tris), 2) 6 μl of porcine trypsin (3 mg/ml, ≥ 6,000 units/mg protein) and 10 μl of bovine α-chymotrypsin (4.77 mg/ml, ≥ 39 units/mg protein). The samples were then incubated at 37 °C for 1 h. The reaction was stopped by heating the samples in boiling water for 5 min. The control without the incubation steps was prepared as the unhydrolyzed control and the native PTT was used as the hydrolyzed control. All assays were done in triplicates.

The quantification of the digested species was performed with a Beckman HPLC (Beckman Coulter, Fuellerton, CA) system equipped with a programmable solvent module (model 126), a photodiode array detector and 32 Karat software for data collection. The separation was performed on a Zorbax SB–C8 (4.6 × 150 mm, 5 μm, Agilent Technologies, Mississauga, ON, Canada). The digested sample (20 µL) was injected in triplicates. The absorbance was measured at 214 nm. A linear gradient at a flow of 0.5 ml/min was used using water: acetonitrile: formic acid (90: 10: 0.1, ml: ml: ml) as solvent A and water: acetonitrile: formic acid (10: 90: 0.07, ml: ml: ml) as solvent B. The elution gradient was as follows: 1–45 min, 50 % B; 45–50 min, 100 % B; 50–55 min, 58 % B; 55–60 min: 0 % B, 60–80 min: 0 % B. The unhydrolyzed control was used as a standard to quantify the unhydrolyzed PTT in the samples.

Percent protein digestion = 100 – ((the peak area of unhydrolyzed PTT over the peak area of the PTT control) × 100). (6.1)

The samples were kept at -20 °C before the assessment of their immunoreactivity.

6.3.6. Determination of IgE-Immunoreactivity

Native PTT or PIs were diluted with PBS buffer containing 0.1% (v/v) Tween 20 (PBS–T) to reach a final concentration of 5.4 μg/ml, coated onto flat–bottom high binding polystyrene Costar 3590 microtiter plates with 96 wells (50 μl per well, Corning, Tewksbury, MA) and incubated overnight at 4 °C. Sera pool or control serum (diluted 1:3 with 1% w/v BSA in PBS–T) was mixed with conjugates as inhibitor (0.001–2000 μg/ml in 1% w/v BSA in PBS–T) at a ratio of 1:1 (v/v) and incubated overnight at 4 °C. As a positive control, a BSA solution (0.001–2000 μg/ml in 1% w/v BSA in PBS–T) was incubated with the anti-potato sera pool. The pool was composed of sera from 4 subjects with high levels of specific IgE antibody to potato proteins (PlasmaLab). Human serum with specific IgE antibody to dust–mite, but none to potato proteins was used as control. The microtiter plate coated with native proteins was washed 3 times with

300 μl of PBS-T using Biotek ELx405 microplate washer (Winooski, VT) and was blocked using 5% (w/v) BSA in PBS-T for 2 h at 25 °C. After washing 3 times with PBS–T, 50 μl of PTT conjugates and serum pool mixtures were added onto the PTT–coated microtiter plate. The plate was incubated at 25 °C for 2 h and washed with PBS-T three times. After incubation with 50 μl of anti–human IgE conjugated with horseradish peroxidase (1:2000 dilution with 1 % w/v BSA in PBS-T) for 1 h at 25 °C, the plate was washed 3 times and developed with 50 μl of substrate solution (3,3′,5,5′–tetramethylbenzidine, TMB, Bioshop, Burlington, ON, Canada) at 25 °C for 15 min. The reaction was stopped by adding 50 μl of 0.5 M sulfuric acid solution. The absorbance was measured at 450 nm. The loss of the specific IgE–binding ability of the patients' sera resulting from conjugation of PTT with galactose/GOSs/galactan was expressed as follows:

$$\textit{Percent inhibition} = 100 - ((\textit{absorbance of the glycated samples preincubated with sera pool/absorbance of positive control}) \times 100) \quad (6.2)$$

The experimental values were fitted to a four–parameter logistic equation using the SigmaPlot software from SPSS Inc. (Chicago, IL) and were subjected to normality (Shapiro-Wilk) and to constant variance test to validate assumptions of one-way analysis of variance (ANOVA). IC_{50} was defined as the concentration of inhibitor at the inflection of the fitted curve. All assays were done in triplicates. p values ≤ 0.05 were considered to be statistically significant. To assess the effect of heat treatment, PTT and its conjugates (20 mg/ml) were incubated at 80 °C for 15 min before assessing their immunoreactivity.

6.3.7. Protein Primary Sequence Analysis

The primary sequence of PTT and its conjugates were analyzed through protein mass mapping, which consists of the tryptic hydrolysis of proteins followed by mass spectrometric analysis of the released peptides.

6.3.7.1. Tryptic Digestion

The digestion of PTT and its conjugates were performed on a MassPrep liquid handling robot (Micromass, Manchester, U.K.) according to the protocol of Shevchenko et al. (1996) with modifications of Havlis et al. (2003) The native PTT, the incubated control PTT, and the PTT conjugates (10 µL each; 1 µg/ml) were resolved by electrophoresis (Mini–Protean Tetra system, Bio–Rad) on Mini–Protean TGX precast gels (Bio–Rad). Proteins bands taken from the SDS-

PAGE gel were reduced with 10 mM dithiothreitol and alkylated with 55 mM iodoacetamide. Trypsin digestion was performed using 105 mM of modified porcine trypsin (sequencing grade, Promega, Madison, WI) at 58 °C for 1 h. Digestion products were extracted using formic acid/ acetonitrile/water mixture (1:2:97, v/v/v) followed by a formic acid/acetonitrile/water mixture (1:50:49, v/v/v). Recovered extracts were pooled, dried by vacuum centrifugation, resuspended into 10 µL of 0.1% (v/v) formic acid, and analyzed by mass spectrometry.

6.3.7.2. Mass Spectrometry

Peptide samples were separated by online reversed-phase (RP) nanoscale capillary liquid chromatography (nanoLC) and analyzed by electrospray mass spectrometry (ES- MS/MS). Analyses were performed with a Thermo Surveyor MS pump connected to an LCQ Deca XP mass spectrometer (Thermo Electron, San Jose, CA) supplied with a nanoelectrospray ion source (Thermo Electron, San Jose, CA). Peptides were bound on a cap trap (Michrom Bioresources, Auburn, CA) at 10 µL/min after which chromatographic separation took place using a PicoFrit column BioBasic C18 (10 cm × 0.075 mm) (New Objective, Woburn, MA) set with a linear gradient from 2 to 50% of solvent B (acetonitrile, 0.1% v/v formic acid) for 30 min, at 200 nL/min (obtained by flow-splitting). Mass spectra were acquired using a data-dependent acquisition mode using Xcalibur software version 1.2. Each full scan mass spectrum (400–2000 *m/z*) was followed by collision-induced dissociation of the three most intense ions. The dynamic exclusion (30s exclusion duration) function was enabled, and the relative collisional fragmentation energy was set to 35%.

6.3.7.3. Database Searching

All MS/MS samples were analyzed using Mascot (Matrix Science, London, UK; version 2.4.1) and X! Tandem (The GPM, thegpm.org; version CYCLONE (2010.12.01.1)). X! Tandem was set up to search the UR12_5_SolanumTub_20120718 database (2615 entries) also assuming trypsin. Mascot was set up to search the UR12_5_SolanumTub_20120718 database assuming the digestion enzyme trypsin. Mascot and X! Tandem were searched with a fragment ion mass tolerance of 0.100 Da and a parent ion tolerance of 0.100 Da. Carbamidomethyl of cysteine was specified in Mascot and X! Tandem as a fixed modification. Dehydrated of the *N*-terminus, Glu→pyro-Glu of the N-terminus, ammonia-loss of the *N*-terminus, Gln→pyro-Glu of the *N*-terminus, deamidated of asparagine and glutamine, oxidation of methionine and hex of lysine

and arginine were specified in X! Tandem as variable modifications. Glu→pyro-Glu of the *N*-terminus, Gln→pyro-Glu of the *N*-terminus, deamidated of asparagine and glutamine, oxidation of methionine, hex of lysine and arginine, galactosyl of lysine and galactosyl (R) of arginine were specified in Mascot as variable modifications.

6.3.7.4. Criteria for Protein Identification

Scaffold (version Scaffold 3.6.2, Proteome Software Inc., Portland, OR) was used to validate MS/MS based peptide and protein identifications. Peptide identifications were accepted if they could be established at greater than 95.0% probability as specified by the Peptide Prophet algorithm (Keller et al., 2002). Protein identifications were accepted if they could be established at greater than 95.0% probability and contained at least 2 identified peptides. Protein probabilities were assigned by the Protein Prophet algorithm (Nesvizhskii et al., 2003). Proteins that contained similar peptides and could not be differentiated based on MS/MS analysis alone were grouped to satisfy the principles of parsimony.

6.3.8. Secondary Structure Analysis

The secondary structure analysis of PTT and its conjugates was analyzed by Fourier transform infrared spectroscopy (FTIR). The samples were dissolved in ^2H_2O to achieve a final concentration of 100 mg protein/ml. Infrared spectra were recorded using a 8210 Nicolet FTIR spectrometer (Thermo Electron Corporation, Madison, WI) equipped with a deuterated triglycine sulfate (DTGS) detector. The spectrometer was continuously purged with dry air from Balston dryer (Balston, Haverhill, MA). The samples (9 μl) were placed between two CaF_2 windows separated by a 25 μm Teflon film spacer (Harrick Scientific, Pleasantville, NY). Each spectrum was obtained by co-adding 256 scans to minimize the signal-to-noise ratio. Fourier self-deconvolution (FSD) in the amide I′ region was performed using Omnic 6.0 software (Thermo Electron Corporation, Madison, WI) applying a bandwidth of 40 cm^{-1} and a resolution enhancement parameter of 3. The curve fitting was performed by using Origin 8 (OriginLab, Northampton, MA). The Gaussian function was chosen to fit the overlapped peaks. The amide I′ region of PTT solution in ^2H_2O revealed five components upon deconvolution and curve-fitting. The band at 1618 cm^{-1} had been assigned to strongly bonded intermolecular β-sheetss indicative of an aggregated strands type structure (Pots et al., 1998). The remaining structures were assigned as follows: bands at 1637 ± 3.0 and 1675 ± 5.0 cm^{-1} as β-sheets, band at 1645 ± 4.0 cm^{-}

^{1} as random coils, bands at 1653 ± 4.0 cm^{-1} as α-helices, and bands at 1671 ± 3.0 and 1689 ± 2.0 cm^{-1} as β-turns (Kong & Yu, 2007).

6.3.9. Three-dimensional Mapping

The FASTA format of amino acid sequence of PTT (accession number Q2MY50, UniProtKB) was submitted to Swissmodel (Kiefer et al., 2009). This server used the template of SeMet Patatin (Protein Data Bank ID: 1OXW) for the prediction. The predicted model had a Q-MEAN Z-score, a useful measure for the description of the absolute quality of theoretical models, of -1.12, which indicates acceptable quality. The predicted model was viewed by Jmol.

6.4. Results and Discussion

6.4.1. Glycation Extent of Potato Proteins

Table 6.2 shows the percent blocked lysine of conjugates of PTT and PIs. As compared to GOS and galactan, higher levels of glycation of PTT and PIs with galactose were obtained with percent blocked lysine of 33.3 and 25.2%, respectively. These results are in agreement with other studies (Oliver et al., 2006b), in which the higher reactivity of monosaccharides was attributed to their higher proportion in the open-ring form and/or to their high affinity to the glycation sites of PTT (ter Haar et al., 2011). The difference in the number of glycated residues between PTT and PIs can be explained by the different accessibilities of Lys ε-amino groups (Jiménez-Castaño et al., 2007). Indeed, there are 24 and 10–14 reactive amino groups on PTT and on major PIs, respectively (accession numbers, Q2MY50, P58514, Q41448, P16348, UniProtKB). The higher percent blocked lysine of PTT is attributed to the high number of its more exposed Lys residues as compared to the PIs. However, the lower level of conjugation of potato proteins with GOS can be attributed to the high rate of the glycoxidation reaction of GOS competing with the glycation rate through Maillard reaction progress (Hollnagel & Kroh, 2000; Yeboah et al., 2000). The results also show that the percent level of blocked lysine of PTT (4%) upon glycation with GOS was lower as compared to that of PIs (10.3%). These results reveal the higher susceptibility of PTT to form protein aggregates upon the generation of protein cross-linking dicarbonyls through the glycoxidation/autoxidation of GOS (Hollnagel & Kroh, 2000), therefore leading to the lower accessibility of the glycation sites as compared to PIs.

Table 6.2 Extent of glycation of PTT and PIs with selected carbohydrates

Conjugates	Incubation time (days)	Blocked lysine (%)[a]
PTT:Galactose	1	33.3 (± 0.5)
PTT:Galactose	3	77.0 (± 1.7)
PTT:GOS	3	4.0 (± 0.0)
PTT:galactan	3	9.1 (± 0.0)
PIs:galactose	1	25.2 (± 0.0)
PIs:GOS	3	10.3 (± 0.0)

[a] Experimental results are averages of triplicates and the standard deviations are given.

6.4.2. Effect of Glycation on the Immunoreactivity of PTT and PI Conjugates

To determine the allergenic potential of native and conjugated potato proteins, IgE binding activity of the native protein was investigated by an inhibition ELISA assay using a serum pool of four subjects with specific IgE to potato proteins. The sera from different donors were first tested individually against native PTT and protease inhibitors to verify that the immunoreactivity profile was similar between each other (data not shown). Once this was confirmed, the sera were pooled to obtain a more general immunoreactivity profile. The IgE's in the serum pool showed immunoreactivity to patatin band (Sol t 1 allergen), but also to some protease inhibitors (Sol t 2–4 allergen) (Fig. 6.2). An anti-dust-mite serum sample was used as a negative control. Fig. 6.3 demonstrates a typical inhibition curve for the native PTT and the PTT conjugates. Control experiments performed with incubated PTT without carbohydrates demonstrated a decrease in the concentration required for half-maximal inhibition of IgE binding (IC_{50} of 0.82 μg/ml, $p < 0.01$) as compared to the native PTT (IC_{50} of 1.19 μg/ml, $p < 0.01$). This increase in IgE binding affinity of PTT upon incubation may be due to a change in PTT structure, leading to a higher exposure of its epitopes. The IC_{50} of PTT:galactose and PTT:GOS conjugates were estimated to be 0.70–0.90 μg/ml (1–3 days incubation; $p < 0.01$) and 0.38 μg/ml ($p < 0.01$), respectively. These experimental findings reveal an increase in the level of IgE binding extent upon the glycation of PTT with galactose and GOS as compared to the native PTT. These results are attributed to an increased exposure of the epitopes and/or the formation of novel IgE-binding sites upon covalent modifications of PTT during glycation with small carbohydrates (Aoki et al., 2010; Jiménez-Saiz et al., 2011). As compared to PTT:galactose conjugates formed upon 1 day of incubation, the slighly lower immunoreactivity obtained with PTT:galactose conjugates obtained upon 3 days of incubation indicates further structural changes, due to extensive glycation leading to lower exposure of the epitopes. In contrast, lower immunoreactivity of ovalbumin after glycation with glucose was reported by Ma et al. (2013). On the other hand, the results show that the glycation of PTT with galactan (IC_{50} of 5.49 μg/ml; $p < 0.01$) resulted in a significant decrease in the affinity for the specific IgE as compared to the native PTT (IC_{50} of 1.19 μg/ml, $p < 0.01$). Similarly, Aoki et al. (2010) have reported a decrease in IgE-binding activity of major allergen of Japanese cedar, Cry j 1, conjugated with galactomannan and attributed this decrease in immunoreactivity to the effectiveness of polysaccharide chains at masking the molecular surface epitopes of an allergen.

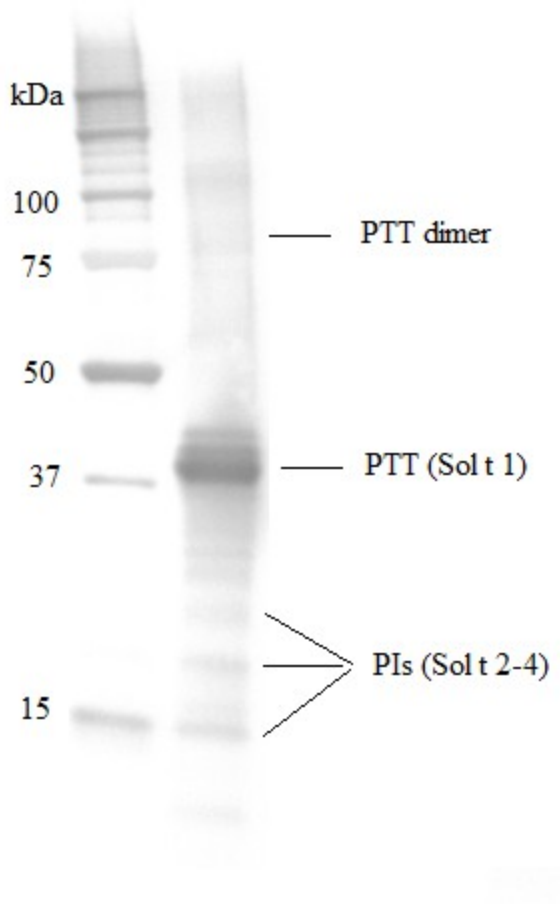

Figure 6.2 Western blot of potato proteins using the serum pool taken from four donors with specific IgE towards potato proteins

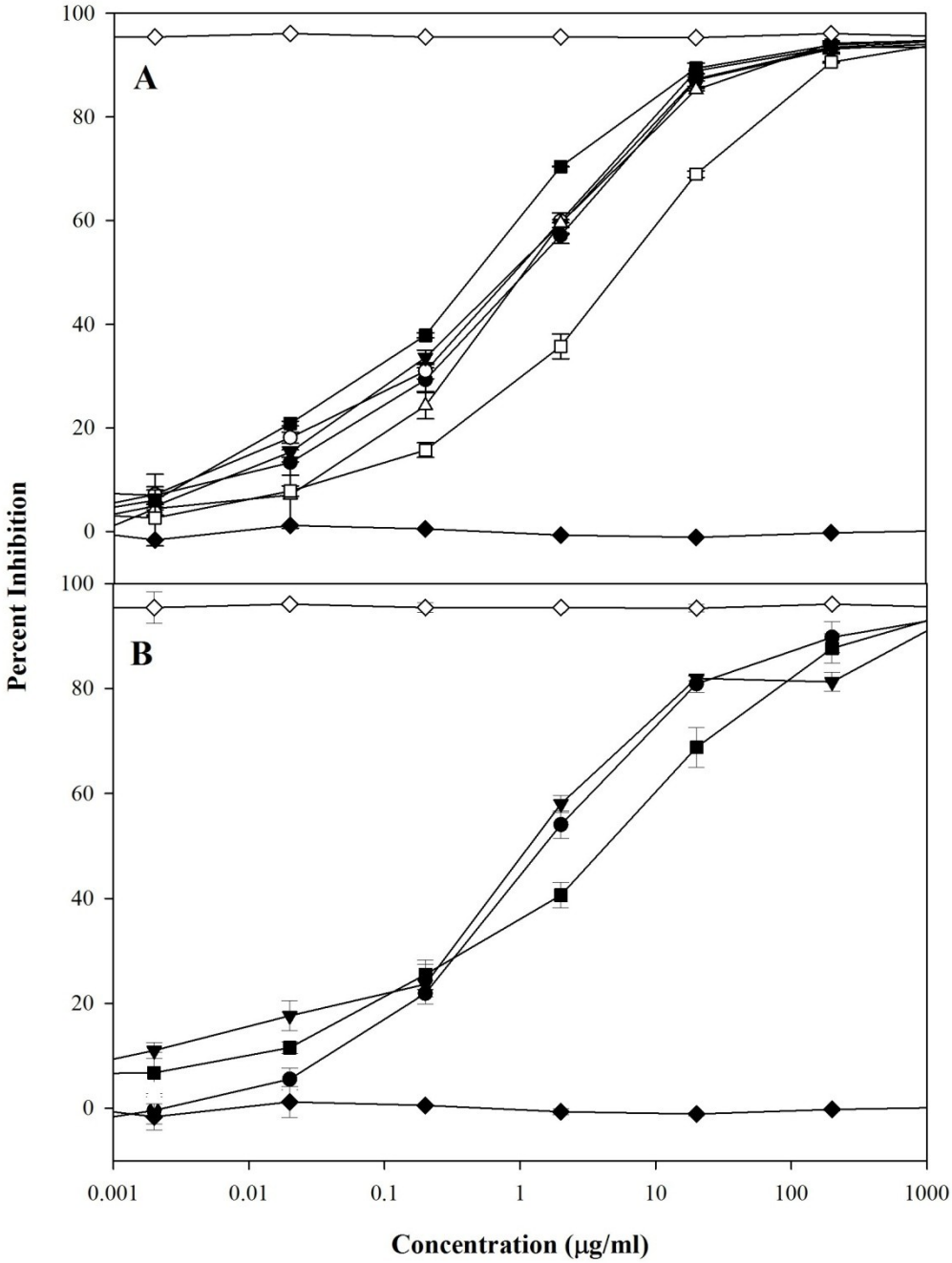

Figure 6.3 Effect of glycation on PTT and PIs immunoreactivity obtained through inhibition ELISA: (A) PTT (●),incubated PTT (○), PTT:galactose conjugates (1-day) (▼), PTT:galactose conjugates (3-day) (△), PTT:GOS conjugates(■), PTT:galactan conjugates (□), positive control (◆), negative control (◇). (B): PIs (●), PIs:galactose conjugates (▼), PIs:GOS conjugates (■), positive control (◆), negative control (◇).

Control experiments performed with control incubated PIs without carbohydrates did not show any difference in IgE binding level compared to that of the native proteins (data not shown). Contrary to the results obtained with PTT (Fig. 6.3A), the conjugation of PIs to carbohydrates resulted in lower immunoreactivity as compared to the native (IC_{50} of 1.11 μg/ml, $p < 0.01$), where the conjugation with GOS (IC_{50} of 5.17 μg/ml, $p < 0.01$) resulted in a higher decrease in the immunoreactivity than that with galactose (IC_{50} of 1.21 μg/ml, $p < 0.01$) (Fig. 6.3B). It is likely that the conjugation of PIs to galactose or GOS resulted in epitope modification and/or to epitope shielding, thereby affecting the antigen-antibody recognition (Ma et al., 2013). A decrease in the immunoreactivity of lysozyme was also obtained, in our previous study, upon its conjugation with galactose and GOS (Seo et al., 2013).

The overall results emphasize that the immunoreactivity effect is allergen and carbohydrate dependent (Taheri-Kafrani et al., 2009). For further studies, PTT, being a heat-labile allergen, was selected to study the effects of the primary and secondary molecular modifications upon glycation and thermal treatment on immunoreactivity.

6.4.3. Location of Conjugated PTT Residues

To determine the conjugated residues on PTT, the skipped trypsin cleavage sites due to glycation of lysine residues and the increase in molecular weight of the digested peptides were identified by peptide mapping of conjugated PTT (Fig. 6.4). Table 6.3 summarizes the peptide masses identified through MS analysis. As expected, the highest number of glycated residues was found in PTT glycated with galactose, after one day of incubation (Lys 129, 159, 162, 168, 173, 253, 269, 331, 353, and 357, in red), as compared to PTT glycated with GOS, after three days of incubation (Lys 159, 162, 173, 353, and 357, underlined in red) confirming the higher reactivity of the smaller carbohydrate compared to that of the larger one. The most reactive residues were Lys 159 and 357, which were found in the highest proportion in their conjugated state. The glycated residues did not overlap with the amino acid sequence of the epitopes previously identified in PTT (in bold, Fig. 6.4) (Alibhai et al., 2005), which demonstrates that the direct blocking of these epitopes did not occur. This supports our inhibition ELISA findings where no decrease in the immunoreactivity of PTT was observed upon its conjugation with galactose (Fig. 6.3A). On the contrary, the minor increase observed in the immunoreactivity might be explained by the conjugation of the carbohydrate to the residues that are found in close

A

10 20 30 40 50 60
MATTKSFLIL SVMILATTSS TFASLEEMVT VLSIDGGGIK GIIPGTILEF LEGQLQKMDN

70 80 90 100 110 120
NADARLADYF DVIGGTSTGG LLTAMITTPN ENNRPFAAAN EIV**PFYFEHG PHI**FNSSTGQ

130 140 150 160 170 180
FFGPKYDGKY LMQVLQEK**LG ETRVHQAL**TE VAISSFDIKT NKPVIFTKSN LAKSPELDAK

190 200 210 220 230 240
MYDI**CYSTAA APTYFPPH**YF ATNTINGDKY EFNLVDGAVA TVADPALLSV SVATRRAQED

250 260 270 280 290 300
PAFASIRSLN YKKMLLLSLG TGTTSEFDK**T HTAEETAK**WG ALQWMLVIQQ MTEAASSYMT

310 320 330 340 350 360
DYYLSTVFQD LHSQNN**YLRV QENALT**GTTT KADDASEANM ELLAQVGENL LKKPVSKDNP

370 380
ETYEEALKRF AKLLSDRKKL RANKASY

B

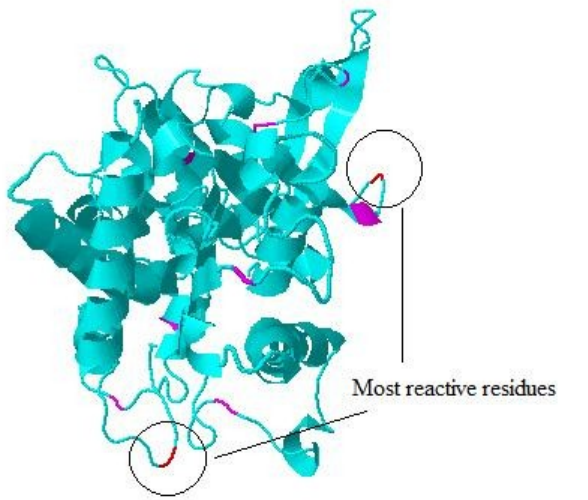

Figure 6.4 Amino acid sequence of PTT: glycated with galactose (red), glycated with GOS (red, underlined), documented epitopes (bold) (A). Three-dimensional mapping of PTT with glycated residues (magenta) and most reactive glycated residues (red) (B)

Table 6.3 Peptide composition of the tryptic hydrolysates of PTT and its PTT:galactose conjugates

Residues	Sequence	Number of peptides	Actual Mass (amu)
332–352	(K)ADDASEANMELLAQVGENLLK(K)	4	2,230.09
332–357	(K)ADDASEANMELLAQVGENLLKKPVSK(D)	2	2,785.43
237–247	(R)AQEDPAFASIR(S)	24	1,203.58
358–369	(K)DNPETYEEALKR(F)	20	1,463.70
243–252	(A)FASIRSLNYK(K)	1	1,197.63
41–57	(K)GIIPGTILEFLEGQLQK(M)	2	1,855.04
41–65	(K)GIIPGTILEFLEGQLQKMDNNADAR(L)	2	2,758.40
312–319	(L)HSQNNYLR(V)	2	1,030.50
253–269+G	(K)K*MLLLSLGTGTTSEFDK(T)	2	2,002.02
253–278	(K)KMLLLSLGTGTTSEFDKTHTAEETAK(W)	4	2,808.44
253–278+G+H_2O	(K)K*MLLLSLGTGTTSEFDKTHTAEETAK(W)	1	2,986.47
253–278+G	(K)K*MLLLSLGTGTTSEFDKTHTAEETAK(W)	2	2,970.48
353–369	(K)KPVSKDNPETYEEALK(R)	9	1,846.94
353–369+G	(K)K*PVSKDNPETYEEALK(R)	4	2,165.09
353–369+G	(K)KPVSK*DNPETYEEALK(R)	5	2,165.05
353–369+2G	(K)K*PVSK*DNPETYEEALK(R)	2	2,327.15
25–40	(S)LEEMVTVLSIDGGGIK(G)	2	1,659.84
139–159	(K)LGETRVHQALTEVAISSFDIK(T)	5	2,313.25
139–169	(K)LGETRVHQALTEVAISSFDIKTNKPVIFTK(S)	2	3,341.85
139–169+G	(K)LGETRVHQALTEVAISSFDIK*TNKPVIFTK(S)	1	3,503.90
254–269	(K)MLLLSLGTGTTSEFDK(T)	9	1,711.86
254–278	(K)MLLLSLGTGTTSEFDKTHTAEETAK(W)	17	2,680.35
236–247	(R)RAQEDPAFASIR(S)	15	1,359.69
169–180+G	(K)SNLAK*SPELDAK(M)	2	1,433.73
169–180	(K)SNLAKSPELDAK(M)	4	1,271.67
160–168	(K)TNKPVIFTK(S)	37	1,046.61
160–168+G	(K)TNK*PVIFTK(S)	2	1,208.67
160–173	(K)TNKPVIFTKSNLAK(S)	2	1,559.91
144–159	(R)VHQALTEVAISSFDIK(T)	66	1,756.93
144–168	(R)VHQALTEVAISSFDIKTNKPVIFTK(S)	9	2,785.54
144–168+G	(R)VHQALTEVAISSFDIK*TNKPVIFTK(S)	8	2,947.60
144–173+2G	(R)VHQALTEVAISSFDIKTNKPVIFTK*SNLAK*(S)	1	3,622.96
320–331	(R)VQENALTGTTTK(A)	24	1,261.64
320–352	(R)VQENALTGTTTKADDASEANMELLAQVGENLLK(K)	6	3,473.74
320–352+G+ H_2O	(R)VQENALTGTTTK*ADDASEANMELLAQVGENLLK(K)	2	3,651.77
126–138	(K)YDGKYLMQVLQEK(L)	9	1,613.82
126–138+G	(K)YDGK*YLMQVLQEK(L)	1	1,775.87
130–138	(K)YLMQVLQEK(L)	18	1,150.60
130–143	(K)YLMQVLQEKLGETR(V)	2	1,706.90

* Glycated residue

proximity to the documented epitopes, such as Lys 269 and 357, which could have resulted in an increased exposure of these epitopes. The three-dimensional mapping of the PTT (Fig. 6.4B) demonstrated that the glycation sites (in magenta) were mostly found toward the termini of individual PTT secondary structures, such as α-helix and β-sheet, which indicates a minimal change in the secondary structure due to glycation. The most reactive residues (in red) are very easily accessible according to the three-dimensional mapping of the native PTT.

6.4.4. Investigation of the Secondary Structure of PTT Conjugates

Table 6.4 shows the percent change in the secondary structure of the conjugates compared to that of the native PTT estimated through FTIR. The FTIR spectrum of native PTT shows the presence of 6.1% intermolecualr β-sheets, 51.0% β-sheet, 9.2% β-turns, and 33.7% α-helix. The FTIR spectrum of the control incubated PTT showed negligible change (<5%) in protein's secondary structure upon incubation at mild temperature of 48 °C. The results also show that the glycation with galactose had minimal effects on the secondary structure of PTT with 9.2, 43.1, 8.6, and 39.1% of aggregated strands, β-sheet, β-turn, and α-helix, respectively. These results confirm the high affinity of galactose to exposed glycation sites located at the termini of PTT secondary structures (Fig. 6.4B), leading to minimal secondary structural changes of PTT upon glycation. Similar low structural changes were exhibited by PTT:GOS conjugates with 12.7, 43.3, 9.4, and 34.6% of aggregated strands, β-sheet, β-turn, α-helix, respectively. The most significant changes in the secondary structure of PTT were observed upon glycation with galactan with 24.0, 38.0, 6.9, and 31.1% of aggregated strands, β-sheet, β-turn, and α-helix, respectively; these results are due to the disruption of intermolecular non-covalent interactions that stabilize the secondary structure of PTT (Povey et al., 2008). The significant structural changes observed in the PTT:galactan conjugates resulted in the burying of IgE specific epitopes between the protein molecules and to the subsequent decrease in IgE-binding affinity (Koppelman et al., 2002). Although relatively small, the changes in PTT secondary structure upon conjugation with the smaller carbohydrates seems to have induced an exposure of inner epitopes, leading to an increase in the immunoreactivity as observed in Fig. 6.3A. Ma et al. (2013) have reported that the increase in the immunoreactivity of the ovalbumin conjugated with glucose was due to the exposure of hydrophobic epitopes upon glycation.

Table 6.4 Effect of glycation on the secondary structures of PTT and its conjugates obtained through FTIR[a]

PTT sample	*α*-Helix (%)	*β*-Sheets (%)	*β*-Turns (%)	Intermolecular *β*-sheets (%)
PTT	33.75	51.02	9.16	6.07
Incubated PTT	34.19	46.21	9.07	10.53
PTT:Galactose	39.02	43.14	8.62	9.22
PTT:GOS	34.54	43.29	9.43	12.74
PTT:Galactan	31.10	37.99	6.94	23.96

[a] Each spectrum was obtained by co-adding 256 scans.

Table 6.5 Effect of heat treatment on PTT conjugates' immunoreactivity obtained through competition ELISA[a]

Conjugates	Incubation time (days)	IC_{50} (μg/ml)[a]	
		Non Heated	Heated
PTT	–	1.19 (± 0.11)	2.77 (± 0.66)
Incubated PTT	3	0.82 (±0.16)	2.64 (± 0.28)
PTT:Galactose	1	0.70 (± 0.10)	0.98 (± 0.65)
PTT:GOS	3	0.38 (± 0.05)	0.03 (± 0.01)
PTT:Galactan	3	5.49 (± 0.79)	0.81 (± 0.05)

[a] IC_{50} is the concentration of PTT conjugates that produced 50% inhibition of antibody binding to the native PTT. All assays were done in triplicates. p values ≤ 0.05 were considered to be statistically significant..

6.4.5. Effect of Heat Treatment on the Immunoreactivity and the Secondary Structure of PTT Conjugates

The effect of heat treatment (80 °C for 15 min) on the immunoreactivity of native PTT and PTT conjugates was assessed (Table 6.5). The heat-treated native PTT demonstrated a significant decrease in the IgE-binding affinity with an IC_{50} value of 2.77 μg/ml ($p < 0.01$) as compared to the non-heat treated PTT (IC_{50} value of 1.19 μg/ml ($p < 0.01$). Koppelman et al. (2002) have obtained similar results to native PTT after heat treatment, and attributed the decrease in the immunoreactivity to the hiding of the epitopes through their aggregation, caused by the exposure of hydrophobic regions of PTT during heat induced denaturation. On the other hand, the heat treatment did not affect the IgE-binding affinity of PTT:galactose conjugates (IC_{50} of 0.98 μg/ml, $p < 0.01$). Contrary to PTT:galactose conjugates, an increase in the IgE-binding affinity of PTT:GOS conjugates (IC_{50} of 0.03 μg/ml, $p < 0.01$), and of PTT:galactan conjugates (IC_{50} of 0.81 μg/ml, $p < 0.01$) were obtained after heat treatment. These results can be explained by an increase in the exposure of the epitopes after a partial protein unfolding and/or by the efficiency of longer carbohydrate chains (GOS, galactan) in preventing thermal protein aggregation upon glycation, leading to a better accessibility of the epitopes by IgE (Koppelman et al., 2002). The increase in the immunoreactivity observed with the PTT conjugates are in direct contrast to the results obtained by Vissers et al. (2011) where carbohydrate conjugated 2S albumins had lower IgE-binding capacity after heat treatment.

To better understand the effect of the conformational changes on the immunoreactivity of PTT conjugates, the changes in secondary structures after heat treatment (Fig. 6.5) were assessed. The results demonstrate that the partial unfolding of PTT and its conjugates upon heat treatment supports previous findings (Pots et al., 1998). Indeed, an increase in the intermolecular β-sheets (> 23.03%) after heat treatment was observed for PTT and its conjugates, except for PTT:galactan conjugates. These results confirm the strong tendency of native PTT and its conjugates with galactose and GOS to aggregate upon partial denaturation. Although the largest increase in the aggregated sheets was observed with PTT:galactose (32.67%) and PTT:GOS (32.45%) conjugates upon heat treatment, these changes did not lead to a decrease in the immunoreactivity of the conjugates, as observed with the native and the control PTT (Table 6.5). The major secondary structural changes observed with PTT:galactose and PTT:GOS conjugates were the complete loss of α-helices and β-turns, respectively; such structural modifications

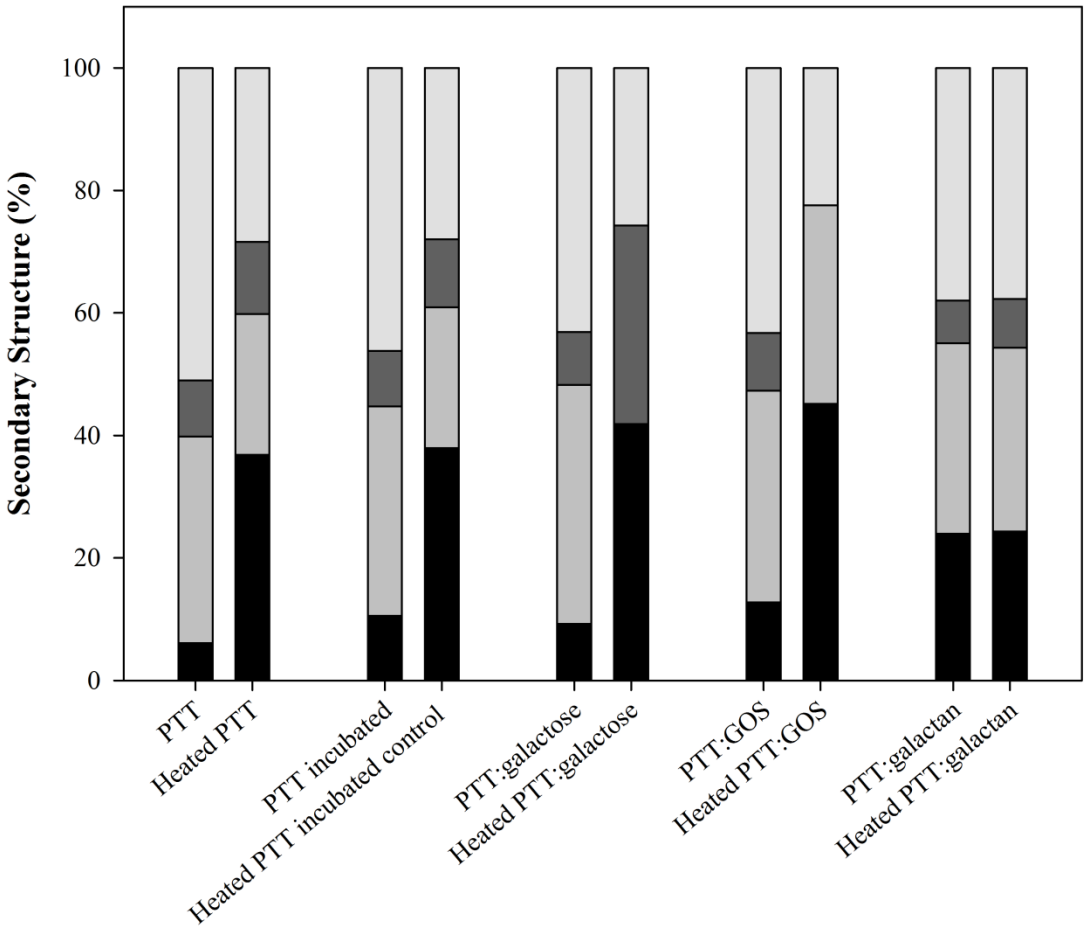

Figure 6.5 Effect of heat treatment on PTT and its conjugates' secondary structure obtained through FTIR: intermolecular (aggregated) *β*-sheet ( ), *α*-helix ( ), *β*-turn ( ), intramolecular *β*-sheet ( ).

resulted in an increased exposure of the PTT epitopes, leading to an increase in the immunoreactivity of these conjugates even after aggregation (Table 6.5). On the contrary, galactan seems to have stabilized PTT against heat denaturation with only 2.71% total change in the secondary structure. However, the relatively small change in the secondary structure resulted in an exposure of the hydrophobic epitopes. In addition, the lack of subsequent protein aggregation after exposure of the hydrophobic groups due to galactan conjugation seems to have resulted in a significant increase in the immunoreactivity (Table 6.5).

6.4.6. Effect of Digestion on the Immunoreactivity of PTT Conjugates

The effect of *in vitro* simulated gastric digestion on the allergenic potential of native PTT and its conjugates was assessed by subjecting the samples to simulated gastric digestion before measuring their immunoreactivity by inhibition ELISA (Fig. 6.6). The highest percent digestion was obtained with the native PTT (59.6%) as compared to PTT conjugates. The low percent digestion of PTT conjugates is explained by the fact that the cleavage site of one of the digestive enzymes, trypsin, is specific toward the Lys residues, which are involved in the conjugation reaction with carbohydrates. These results are in accordance with those reported by Jiménez-Saiz et al. (2011) showing a decrease in ovalbumin conjugates' digestibility as a result of glycation. Nevertheless, as compared to PTT:galactose conjugates (29.5% degree of digestion), the higher resistance of PTT:GOS (15.7%) and PTT:galactan (14.2%) conjugates to digestion could be due to the large size of their carbohydrates moieties, shielding PTT proteolytic sites. The results (Fig. 6.6) also show that the digestion resulted in a 6.51-fold decrease in the IgE-binding affinity of native PTT as compared to the non-digested one; these experimental findings can be explained by the disruption of both conformational and sequential epitopes. Similarly, a decrease in the IgE-binding affinity of PTT:galactose and PTT:GOS conjugates by 3.94 and 7.66-fold, respectively, was obtained upon digestion. In contrast, the IgE-binding affinity of digested PTT:galactan conjugates remained unchanged compared to the undigested conjugates; this can be due to the large polysaccharide chains that have sterically blocked the disruption of the epitopes (Aoki et al., 2010). However, compared to the digested native PTT (IC_{50} of 7.75 μg/ml, $p < 0.01$), a higher retention in the IgE-binding was exhibited by digested PTT:galactose (IC_{50} of 2.76 μg/ml), PTT:GOS (IC_{50} of 2.91 μg/ml), and PTT:galactan conjugates (IC_{50} of 4.90 μg/ml). These high immunoreactivities of digested conjugates is due to their lower susceptibility to digestion, thereby preserving the integrity of IgE binding sites on conjugated PTT.

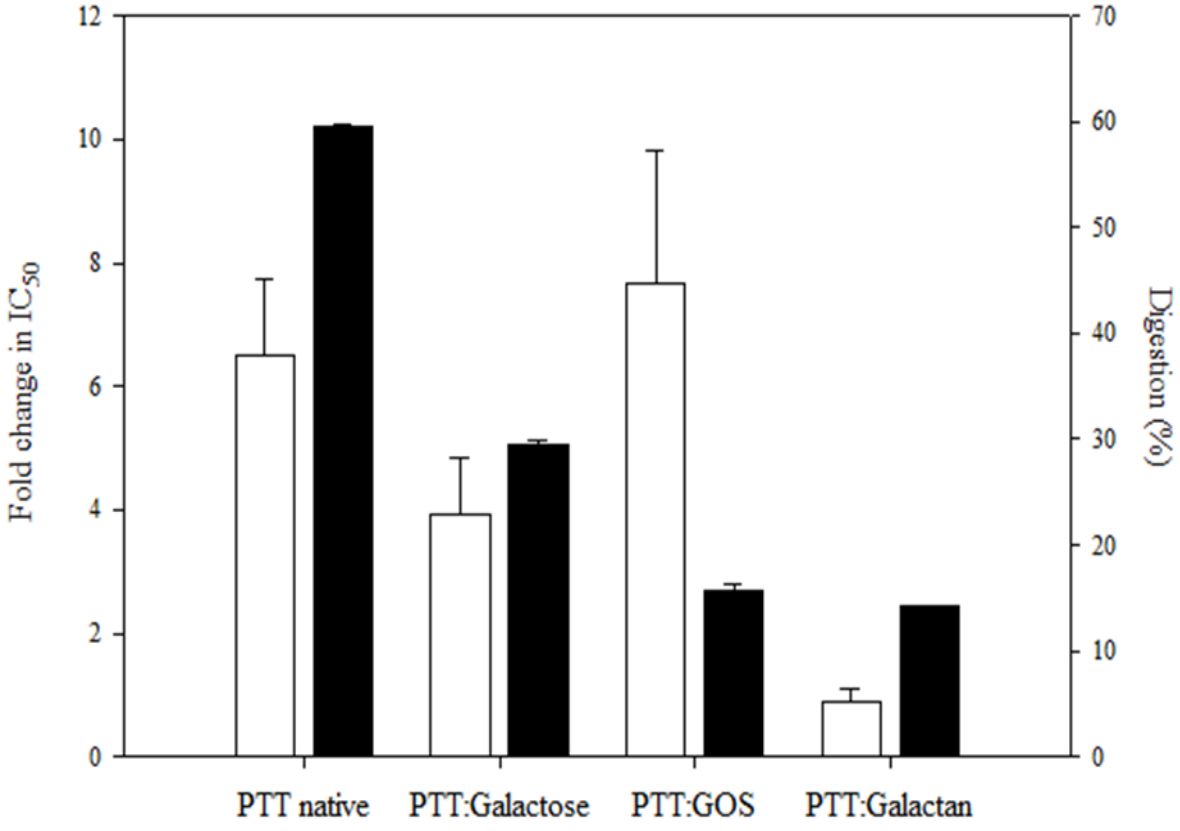

Figure 6.6 Effect of simulated gastric digestion on PTT conjugates' immunoreactivity: Fold change in IC_{50} (□) and percent digestion (■).

6.5. Conclusion

The immunoreactivity of the conjugates after carbohydrate conjugation increased slightly for PTT:galactose and PTT:GOS conjugates indicating an increased exposure of the epitopes after conjugation. Galactan conjugation to PTT led to the largest decrease in immunoreactivity following glycation by restricting the access of IgE to the epitopes through steric hinderance. Although the heat treatment of the native PTT led to a decrease in immunoreactivity through protein aggregation, it remained less effective when conjugated PTT was used due to the decrease in protein aggregation, and also due to the difference in the change in protein secondary structure after heat treatment leading to more exposure of buried epitopes. After simulated gastric digestion, native PTT exhibited the largest decrease in immunoreactivity as a result of protein hydrolysis and disruption of both conformational and sequential epitopes. PTT glycation, however, increased PTT resistance to digestion and resulted in less important decrease in IgE-immunoreactivity. This was particularly true for PTT:galactan, which exhibited no change in immunoreactivity.

CONNECTING STATEMENT 5

The production of PTT:carbohydrate conjugates with improved functional properties was achieved (Chapter V) and the changes in immunoreactivity of these conjugates were also investigated (Chapter VI). In order to minimize the protein cross-linking that occurs during the advanced stages of Maillard reaction and improve the quality of produced PTT:carbohydrate conjugates, the effect of Maillard reaction inhibitors on the production of PTT:galactose/xylose/GOS/XOS/galactan/xylan conjugates was investigated in Chapter VII. The effectiveness of selected inhibitors, aminoguanidine, cysteine, pyridoxamine, sodium bisulfite, to control the glycation of PTT was assessed by monitoring the glycation extent and the protein cross-linking along with the formation of dicarbonyl compounds as well as by determining the digestibility of the PTT conjugates.

The results from this chapter was presented at IFT14 Annual Meeting & Food Expo.

Seo, S., & Karboune, S. (2014) *Production of Potato Patatin:Carbohydrate Conjugates through the Use of Maillard Reaction Inhibitors*, IFT14 Annual Meeting & Food Expo, New Orleans, Louisiana, June 21-24 .

Seo, S., & Karboune, S. (2014). Investigation of the use of Maillard reaction inhibitors for the production of patatin:carbohydrate conjugates (To be Submitted).

CHAPTER VII

INVESTIGATION OF THE USE OF MAILLARD REACTION INHIBITORS FOR THE PRODUCTION OF PATATIN:CARBOHYDRATE CONJUGATES

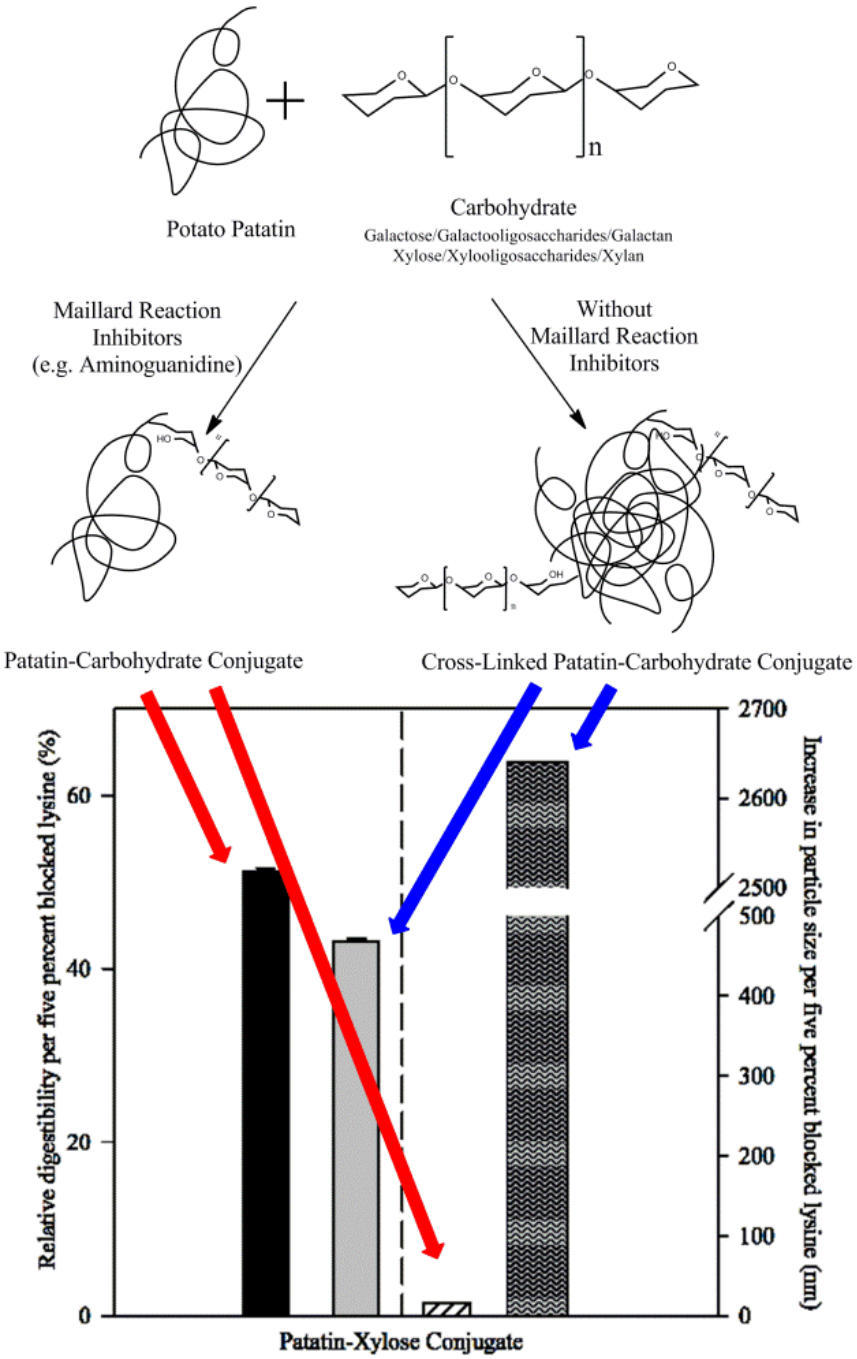

7.1. Abstract

Selected Maillard reaction inhibitors, including aminoguanidine, cysteine, pyridoxamine, and sodium bisulfite, were evaluated for the production of carbohydrate conjugated proteins with less cross-linking/browning. Patatin, one of the major potato proteins, was glycated with galactose, xylose, galactooligosaccharides, xylooligosaccharides, galactan, and xylan under controlled conditions. The effectiveness of the inhibitors to control the glycation reaction was assessed by monitoring the glycation extent and the protein cross-linking along with the formation of dicarbonyl compounds. Sodium bisulfite was the most effective inhibitor for PTT:galactose and PTT:xylan reaction systems (reaction control ratios of 210.0 and 12.8). On the other hand, aminoguanidine and cysteine led to the highest reaction control ratios for the PTT:xylose/xylooligosaccharide (160.0 and 143.0) and PTT: galactooligosaccharides/galactan (663.0 and 71.0) reaction systems, respectively. Using the identified inhibitors, lower proportions of extensively polymerized species (3.5–37.3%) and lower amounts of total unreacted dicarbonyls (0.0–2.8 μg/ml) were obtained as compared to the reaction without inhibitor (5.1–94.2%, 0.0–6.3 μg/ml). The use of cysteine and aminoguanidine as inhibitors led to 1.7–99.4% decreases in the particle size distribution of the PTT conjugates and to 0.4–9.3% increases in their relative digestibility, per 5% blocked lysine.

7.2. Introduction

The Maillard reaction has been demonstrated to be an effective method to produce protein:carbohydrate conjugates as biomacromolecules with improved functional properties. However, the control of the Maillard reaction rate to limit the protein cross-linking/polymerization, associated with the intermediate and advanced stages of the reaction, is very challenging. It has been reported that such control may lead to the preservation of functional properties, gained by the conjugation of protein with carbohydrates at the early stage, and to the limited formation of advanced glycation end-products (Corzo-Martínez et al., 2010a; Huang et al., 2011). In addition, the decrease in the protein digestibility and the amino acid bioavailability, that can result from protein cross-linking, can be reduced (Mauron, 1990). Dicarbonyl compounds generated during the Maillard reaction, such as methylglyoxal, glyoxal, and deoxyosones, have been identified as active cross-linkers (Meade et al., 2003; Nagaraj et al., 1996), and the arginine and lysine have been identified as the main amino acid residues involved in cross-linking (Degenhardt et al., 1998; Miller et al., 2003).

Our previous studies (Seo et al., 2013; Seo et al., 2012) and others (Jiménez-Castaño et al., 2005; ter Haar et al., 2011; Yeboah et al., 1999) have provided good understanding of the effects of selected key Maillard reaction parameters, including protein:carbohydrate ratio, temperature, incubation time, and water activity (a_w), on the control of the glycation rate. Because of the complexity of the Maillard reaction, the use of inhibitors may be required to better control its progress and to limit the protein cross-linking. Aminoguanidine is a known α-dicarbonyl scavenging agent that can prevent the formation of advanced glycation end-products (Thornalley et al., 2000). Indeed, the nucleophilic hydrazine ($–NHNH_2$) and the dicarbonyl-directing guanidino ($–NH\text{-}C(=NH)NH_2$) groups of aminoguanidine contribute to the bifunctional scavenging of α-dicarbonyls. Aminoguanidine has effectively inhibited advanced stages of the glycation reaction of RNAse A with glucose with no effect on the conjugate formation (Edelstein & Brownlee, 1992). On the other hand, cysteine's thiol group, being a scavenger of reactive dicarbonyls, has been efficient in the inhibition of the color formation that occurs during the advanced stage of the Maillard reaction of soybean peptide with xylose (Huang et al., 2012). Furthermore, the use of pyridoxamine, a natural derivative of vitamin B_6, delayed the formation of Amadori compounds and inhibited the protein cross-linking during the Maillard reaction between β-lactoglobulin and galactose/tagatose; such effect was attributed to the ability of pyridoxamine to chelate the metal ions that are involved in the generation of reactive dicarbonyls and also to scavenge the reactive dicarbonyls (Adrover et al., 2008). In addition, pyridoxamine has effectively delayed the formation of N^{ε}-(carboxymethyl)lysine, which has an inhibition effect on the post-Amadori pathway (Booth et al., 1997). Sulfites and sulfate-containing compounds have been reported to inhibit the cross-linking and the browning occurring during the advanced stages of the Maillard reaction by scavenging the free-radicals and the reactive dicarbonyls through its bisulfite ion (Friedman & Molnar-Perl, 1990). Scaman et al. (2006) have reported that both sodium bisulfite and cysteine decreased the rate of conjugation of lysozyme with dextran.

Although the control of the progress of the Maillard reaction through the use of inhibitors can be beneficial in modulating the functional properties of glycoproteins, only limited studies (Corzo-Martínez et al., 2010a; Huang et al., 2011; Scaman et al., 2006) have assessed the effectiveness of these inhibitors to produce functional protein:carbohydrate conjugates for food and biological applications. To our knowledge, to date, no literature has systematically compared the efficiency of aminoguanidine, cysteine, pyridoxamine, and sodium bisulfite as inhibitors for the purpose of

producing functional protein:carbohydrate conjugates. In addition, the effects of the carbohydrate structure (chain length; pentose/hexose) on the efficiency of these inhibitors have not been studied.

The aim of the present study was to investigate the effects of selected Maillard reaction inhibitors, including aminoguanidine, cysteine, pyridoxamine, and sodium bisulfite, on the production of potato patatin (PTT):galactose/xylose/galactooligosaccharides (GOS)/xylooligosaccharides (XOS)/galactan/xylan conjugates with specific functionalities. PTT has previously demonstrated numerous biological and functional properties including lipid acyl hydrolase activity (Anderson et al., 2002), antiproliferative activity on mouse melanoma cells, and antioxidant activity (Sun et al., 2013), which makes it an interesting candidate for carbohydrate conjugation. The effectiveness of the investigated inhibitors to control the glycation of PTT was assessed by monitoring the glycation extent and the protein cross-linking along with the formation of dicarbonyl compounds. The PTT:carbohydrate conjugates were produced using the effective inhibitors and their digestibility was assessed.

7.3. Materials and Methods

7.3.1. Materials

Solanic 206P (≈75% PTT, ≈25% protease inhibitors) was kindly provided by Solanic (Foxhol, Netherlands). Potato galactan (~280 kDa) and endo-1-4-*β*-D-galactanase from *Aspergillus niger* were purchased from Megazyme (Wicklow, Ireland). Furosine standard was purchased from Neosystem Lab. (Strasbourg, France). Biogel P2 extra fine, Bradford reagent and broad range SDS-PAGE standards were purchased from Bio-Rad (Philadelphia, PA, USA). XOS were obtained from Shandong Longlive Bio-tech (Yucheng, China). Xylan from beechwood (≥90%) and all other chemicals were purchased from Sigma Chemical Co. (St-Louis, MO, USA).

7.3.2. Production of Conjugates

Potato proteins (Solanic 206P) in sodium phosphate buffer (50 mM, pH 7) were ultrafiltered using a stirred ultrafiltration unit (Amicon system, Millipore, Billerica, MA, USA) fitted with a 30 kDa molecular mass cut-off membrane to remove the protease inhibitors. Galactose, xylose, GOS, XOS, potato galactan and soluble xylan were investigated as selected carbohydrates for the preparation of conjugates. GOS, with an average molar mass of 1,990.9 g/mol, were produced according to Paragraph 3.3.2. Mixtures of enriched PTT and selected carbohydrates at a molar

ratio of 1:7 were prepared. The appropriate Maillard reaction inhibitor (aminoguanidine/ cysteine/ pyridoxamine or sodium bisulfite) was added to the mixtures at a protein to inhibitor ratio of 1:0.2 (w/w). The mixtures were freeze dried and incubated at 48°C for 1, 3, 5, and 7 days at a_w of 0.65 (saturated potassium iodide). The collected mixtures were kept at −20°C.

7.3.3. Determination of Glycation Extent

Previously described methods were used for the quantification of furosine (Seo et al., 2014b) and for the measurement of free amino groups (Seo et al., 2013). All assays were run in triplicates. No furosine was detected from control unincubated mixtures of protein, carbohydrate, and inhibitors.

The final percentage of blocked lysine was indirectly estimated from the furosine content, considering that the Amadori compound tagatosyl-lysine formed during the Maillard reaction between lysine residues and galactose moieties generate about 42% furosine upon 8 N acid hydrolysis (Krause et al., 2003). Since the percent conversion of xylulosyl-lysine into furosine upon acid hydrolysis is unknown, the same conversion factor of tagtosyl-lysine to furosine was used for the estimation of xylulosyl-lysine. The furosine content and the total available lysine content before glycation were used for the estimation of the percentage of blocked lysine that was due to the glycation and not to the protein cross-linking according to the Equation 5.1.

7.3.4. Determination of the Level of Protein Cross-Linking

7.3.4.1. Advanced Reaction Index of PTT Glycoforms

Advanced glycation reaction index was estimated by measuring spectrophotometrically the turbidity/browning of protein:carbohydrate mixtures (10 mg/ml) at 600 nm. All assays were run in triplicates.

7.3.4.2. Molecular Weight Distribution of PTT Glycoforms

The glycated sample mixtures were subjected to size exclusion chromatography on Superdex 200 5/150 (GE Healthcare, Piscatawa, NJ, USA) column on ÄKTA purifier system (GE Healthcare). The isocratic elution was run with potassium phosphate buffer (50 mM, pH 7) containing 0.15 M sodium chloride (3CV) at a flow rate of 0.3 ml/min. The fractions were detected at 280 nm. Selected proteins, including β-amylase, albumin, chymotrypsinogen A, and lysozyme, were used as standards for calibration.

7.3.4.3. Particle Size Distribution of PTT Glycoforms

To estimate the distribution of the protein aggregates, the particle size was estimated through dynamic light scattering (DLS) measurements by Delsa Nano C system (Beckman Coulter) at 25 ºC. The means of intensity distributions were obtained from 70 measurements.

7.3.5. Quantification of α-Dicarbonyls

The quantification of α-dicarbonyls was carried out according to the method of Marceau and Yaylayan (2009). Glycated samples (20 mg/ml) were suspended in 0.5% (w/v) solution of *o*-phenylenediamine solution and incubated overnight in darkness at 25°C. After centrifugation (5,000 x *g*, 5 min), the quantification of α-dicarbonyls was performed with a Beckman HPLC system equipped with a programmable solvent module (model 126), a photodiode array detector and 32 Karat software for data collection. The separation was performed on a Zorbax SB-C18 (4.6 x 150 mm, 5 μm, Agilent Technologies, Palo Alto, CA, USA) at 25°C. The elution of the derivatized samples (20 μL) was carried out with an isocratic mobile phase of methanol:water:formic acid (55: 45: 0.1, v/v/v) at 0.7 ml/min. The detection was done at 312 nm and the spectrum was recorded from 200 to 400 nm. The unglycated proteins/carbohydrate mixtures with and without inhibitor were run as controls. To assess the presence of any side derivatization reactions due to the presence of protein, carbohydrate, and/or inhibitors, control reactions were run with each of these glycation components separately. Glyoxal, methylglyoxal, and 2,3-butanedione were used as standards for the identification of the formed dicarbonyls. The derivatization of these standards at selected concentration varying from 8.33 to 300 μg/ml was carried out as discussed here above. The identification of deoxyosone was done based on the characteristic two absorption maxima of the quinoxaline derivatives (~250 nm, ~330nm) and on the RP-HPLC elution order characterized by Marceau and Yaylayan (2009).

7.3.6. Simulated Gastric Digestion of PTT and its Glycoforms

The simulated gastric digestion of PTT and its corresponding glycoforms was performed according to the modified method of Moreno et al. (2008). The glycated and non-glycated PTT samples (1 mg/ml) were suspended in 20% (v/v) simulated gastric fluid (0.75 M sodium chloride, pH 2.2). To initiate the enzymatic digestion, porcine pepsin (7 mg/ml, ≥ 2,500 units/mg protein) at a ratio of 1:50 (v/v) was added. After 2 h incubation at 37 °C, the pH of the mixture was raised to 7.5 with ammonium carbonate (0.125 M). Following solutions were added to

slightly lower the pH and to simulate a duodenal environment: 1) 10 μl bile salt mixture consisting of 0.025 M sodium taurocholate, 0.25 M sodium glycodeoxycholic acid, 0.4 M calcium chloride and 0.5 M Bis-Tris, 2) 6 μl of porcine trypsin (3 mg/ml, ≥ 6,000 units/mg protein) and 10 μl of bovine α-chymotrypsin (4.77 mg/ml, ≥ 39 units/mg protein). The sample was then incubated at 37 °C for 1h. The reaction was stopped by heating the samples in boiling water for 5 min. The control without the incubation steps was prepared as the unhydrolyzed control and the native PTT was used as hydrolyzed control. All assays were done in triplicates.

The analysis of hydrolysates was performed by HPLC using a Beckman HPLC system equipped with a programmable solvent module (model 126), a photodiode array detector and 32 Karat software for data collection. The separation was performed on a Zorbax SB-C8 (4.6 x 150 mm, 5 μm) at 25°C. The hydrolyzed sample (20 μl) was injected in triplicates. The absorbance was measured at 214 nm. A linear gradient at a flow of 0.5 ml/min was used using water: acetonitrile: formic acid (90: 10: 0.1, v/v/v) as solvent A and water: acetonitrile: formic acid (10: 90: 0.07, v/v/v) as solvent B. The elution gradient was as follows: 1–45 min. 50 % B; 45–50 min, 100 % B; 50–55 min, 58 % B; 55–60 min: 0 % B, 60–80 min: 0 % B. The unhydrolyzed control was used as a standard to quantify the unhydrolyzed PTT in the samples. Percent hydrolysis was calculated as follows:

$$\textit{Percent protein digestion} = 100 - (\textit{the peak area of unhydrolyzed PTT over the peak area of the PTT control}) \times 100 \quad (7.2)$$

7.4. Results and Discussion

7.4.1. Effect of the Inhibitors on the Progress of the Maillard Reaction

7.4.1.1. Changes in the Glycation Level of PTT with Galactose/Xylose in the Presence of Inhibitors

To investigate the effects of inhibitors on the level of PTT glycation and protein cross-linking, the percent blocked lysine, the advanced reaction index and their ratio (reaction control index) were estimated (Table 7.1). The results show a faster glycation reaction rate of PTT with galactose (3 to 5 days) than with xylose (3 to 7 days). Similar findings were reported by Hofmann (1999) where the low glycation rate of L-alanine with pentoses was attributed to the higher degradation of pentoses as compared to hexoses, limiting their availability. In addition, higher advanced reaction index values of PTT:xylose conjugates (0.1–9.8) were obtained as

Table 7.1 Progress of the Maillard reaction at 48°C at a_w of 0.65

PTT mixtures	Incubation time	Percent blocked lysine[a*+]					Advanced reaction index[b*+]					Reaction control ratio[c*]				
		N	A	C	P	S	N	A	C	P	S	N	A	C	P	S
PTT:Galactose	1	7.7	3.5	0.0	3.8	0.0	0.6	0.1	0.8	0.4	0.1	12.8	35.0	0.0	9.5	0.0
	3	97.9	4.0	18.0	2.9	4.3	1.2	0.2	1.7	0.8	0.1	81.6	20.0	10.6	3.6	43.0
	5	18.2	0.0	15.4	1.8	21.0	4.7	0.7	0.1	0.1	0.1	3.9	0.0	154.0	18.0	210.0
	7	1.0	0.8	12.4	2.8	2.9	3.2	0.6	1.4	0.1	0.1	0.3	1.3	8.9	28.0	29.0
PTT:Xylose	1	0.0	0.0	3.6	0.0	0.8	3.9	0.1	0.4	0.1	0.1	0.0	0.0	9.0	0.0	8.0
	3	2.4	3.5	13.7	1.7	0.0	3.6	0.1	1.0	2.4	0.1	0.7	35.0	13.7	0.7	0.0
	5	13.0	6.4	0.4	0.0	1.7	3.3	3.7	6.1	9.8	1.7	3.9	1.7	0.1	0.0	1.0
	7	0.0	16.0	0.0	0.0	0.0	4.5	0.1	4.3	4.5	2.1	0.0	160.0	0.0	0.0	0.0
PTT:GOS	1	0.8	0.0	0.0	0.0	0.0	0.5	3.0	0.1	0.1	0.1	1.6	0.0	0.0	0.0	0.0
	3	1.3	0.0	66.3	0.0	0.0	1.0	6.0	0.1	0.1	0.1	1.3	0.0	663.0	0.0	0.0
	5	0.0	0.0	0.0	0.0	0.0	0.9	2.5	1.8	0.1	0.4	0.0	0.0	0.0	0.0	0.0
	7	6.1	0.0	0.0	1.2	0.0	1.6	3.1	0.1	0.1	0.1	3.8	0.0	0.0	12.0	0.0
PTT:XOS	1	0.0	0.0	3.2	0.0	0.0	1.5	0.2	0.4	3.1	0.1	0.0	0.0	8.0	0.0	0.0
	3	0.4	14.3	6.9	2.3	0.0	1.1	0.1	0.1	11.6	0.1	0.4	143.0	69.0	0.2	0.0
	5	11.7	7.8	1.2	0.5	2.7	0.6	0.1	0.1	12.0	0.1	19.5	78.0	12.0	0.0	27.0
	7	3.0	2.9	3.6	7.3	0.9	1.0	0.1	0.8	14.5	1.0	3.0	29.0	4.5	0.5	0.9
PTT:Galactan	1	0.2	1.7	0.0	0.0	2.0	0.1	3.8	0.1	9.3	0.1	2.0	0.4	0.0	0.0	20.0
	3	1.2	2.5	2.7	0.7	2.2	0.1	4.0	0.1	14.5	0.1	12.0	0.7	27.0	0.0	22.0
	5	4.3	2.0	7.1	4.6	2.2	0.1	4.1	0.1	16.9	0.1	43.0	0.5	71.0	0.3	22.0
	7	2.2	0.9	5.7	1.5	0.3	1.7	10.8	0.1	17.0	0.1	1.2	0.1	57.0	0.1	3.0
PTT:Xylan	1	3.1	1.5	16.6	2.2	0.7	2.0	0.9	4.6	9.0	0.4	1.0	1.7	3.6	0.2	1.8
	3	3.9	2.4	1.6	7.0	3.8	2.9	0.7	2.4	11.7	1.0	1.3	3.4	0.7	0.6	3.8
	5	8.2	15.0	2.9	8.4	16.7	3.6	2.1	3.1	16.3	1.3	2.3	7.1	0.9	0.5	12.8
	7	16.5	3.0	2.5	3.4	5.4	6.5	6.6	4.6	18.5	5.7	2.5	0.5	0.5	0.2	0.9

[a] Percentage of blocked lysine was calculated from furosine content and total free amino groups.
[b] Turbidity/browning measurement at 600 nm.
[c] Reaction control ratio = Percent blocked lysine/advanced reaction index
[*] Mixture containing different Maillard reaction inhibitiors: no inhibitor (N), aminoguanidine (A), cysteine (C), pyridoxamine (P), sodium bisulfites (S)
[+] Experimental results are averages of triplicates and the standard deviations are less than 5%.

compared to those of PTT:galactose conjugates (0.1–4.7). These results may be due to the formation of more reactive dicarbonyls with xylose, than with galactose (Hofmann, 1999). As compared to other inhibitors, the highest percent blocked lysine of PTT:galactose conjugates (21.0%) and the lowest advanced reaction index (0.1) was achieved in the presence of sodium bisulfite; while aminoguanidine inhibitor resulted in the highest percent blocked lysine of PTT:xylose conjugates (16.0%) with the lowest advanced reaction index (0.1). As compared to the reaction without inhibitor (maximum blocked lysine of 97.9%, day 3), the presence of sodium bisulfite limited both the glycation rate and the conjugation level of PTT with galactose achieving maximum percent blocked lysine of 21.0% upon 5 days. On the other hand, the aminoguanidine lowered the glycation rate of PTT with xylose, without affecting the maximum conjugation level, which was slightly higher as compared to the reaction without inhibitor (maximum blocked lysine of 13.0%, day 5). The results also indicate that sodium bisulfite and aminoguanidine were efficient in limiting the browning and the protein cross-linking occurring during the advanced stages of the Maillard reaction of PTT with galactose and xylose, respectively, leading to the highest reaction control ratio of 210.0, and 160.0. Such effect of sodium bisulfite may be attributed to its ability to trap the free-radicals and the reactive dicarbonyls formed during the reaction through its sulfite ion (Friedman & Molnar-Perl, 1990). Contrary to galactose, the inhibitory effect of sodium bisulfite on the glycation rate of PTT with xylose was more pronounced than that on the protein cross-linking, resulting in low reaction control ratio (0.0–8.0). These results may be due to the initial xylose degradation, which may have led to lower glycation level and to the scavenging of the reactive species by sodium bisulfite. Aminoguanidine was less efficient in improving the reaction control ratio of PTT:galactose (0.0–35.0) conjugates as compared to that of PTT:xylose conjugates. These results may be attributed to the high inhibitory effect of the aminoguanidine on the early-stage glycation rate of PTT with galactose, resulting in maximum percent blocked lysine of only 4.0%. Conflicting results have been reported in the literature regarding the inhibitory effect of aminoguanidine at the early stage of the reaction. Edelstein and Brownlee (1992) have shown that in the presence of excess of carbohydrates, aminoguanidine had no effect on the conjugate formation and inhibited the Maillard reaction at the advanced stage. On the other hand, Requena et al. (1993) have reported that at concentrations of aminoguanidine similar to the concentration used in this study, the early glycation reaction of albumin with glucose was inhibited. For both

PTT:galactose and PTT:xylose conjugates, pyridoxamine did not lead to any improvement in their reaction control ratio (0. 0–28.0); these results may be due to the fact that the primary amino group of pyridoxamine competes with protein lysine residues for the carbonyl group of the carbohydrate during the early stage of the reaction, leading to the delay of Schiff base formation and hence to lower glycation rate. In our controls containing only pyridoxamine and xylose, important browning/aggregates formation was found (0.3–2.2, data not shown). Similarly, Corzo-Martínez et al. (2010a) have obtained a high level of browning of the control samples containing only pyridoxamine and galactose or tagatose as high as the reaction samples containing *β*-lactoglobulin. However, contrary to our results, higher levels of glycation of *β*-lactoglobulin with galactose/tagatose (18.8–100.0%) were reported in the presence of pyridoxamine. These results may be attributed to the higher concentration of galactose/tagatose used in their study leaving more carbohydrates available to react with the lysine residues on *β*-lactoglobulin. Table 7.1 also shows that in the presence of cysteine, the maximum level of glycation of PTT was achieved at similar (galactose) or shorter (xylose) reaction time (3 days) as without inhibitor. In addition, cysteine did not affect the maximum level of blocked lysine of PTT:xylose conjugates (13.7%), while it decreased that of PTT:galactose conjugates (18.0%). In contrast, Scaman et al. (2006) have reported that cysteine inhibited the glycation of lysozyme at acidic (3.5) and at basic (8.5) pHs. The discrepancy may be due to the neutral pH used in our study at which the reactivity of the thiol group on the cysteine is lower than at basic pH of 8.5. The results also show that the inhibitory effects of cysteine on the cross-linking of PTT:galactose and PTT:xylose conjugates or on the formation of browning compounds were lower as compared to those of sodium bisulfite. The highest reaction control ratio obtained in the presence of cysteine was 154.0 and 13.7 for PTT:galactose and PTT:xylose conjugates, respectively.

7.4.1.2. Changes in the Glycation Level of PTT with XOS/GOS in the Presence of Inhibitors

XOS (maximum blocked lysine of 11.7%, day 5) exhibited more or less the same reactivity towards the glycation of PTT as its corresponding monosaccharide, xylose (Table 7.1). However, GOS showed a much slower rate of glycation with the *ε*-amino groups of PTT lysine residues, reaching a maximum percent blocked lysine of 6.1% after 7 days. The lower reactivity of longer chain carbohydrates has been previously reported (Corzo-Martínez et al., 2010b; ter Haar et al., 2011). Furthermore, at the early stage of the reaction (1–3 days), the low percentage of blocked

lysine of PTT:GOS (0.8–1.3%) and PTT:XOS (0.0–0.4%) conjugates was accompanied by high advanced reaction index (0.5–1.5); these results reveal that the high advanced reaction index values were not significantly due to the degradation of the Amadori products, but to the initial degradation of the oligosaccharides through autoxidation/glycoxidation leading to the formation of reactive dicarbonyls that favor protein cross-linking (Hollnagel & Kroh, 2000). As compared to GOS, the higher maximum glycation level of XOS is probably due to the high release of the degradation products that may have promoted the glycation. Yeboah et al. (2000) have demonstrated that the accumulation of reactive oxidative species during the early stages can increase the formation of protein:carbohydrate conjugates. As compared to other inhibitors, the highest percent blocked lysine of PTT:GOS conjugates and the lowest advanced reaction index (0.1) were achieved in the presence of cysteine (66.3%, 3 days), resulting in the highest reaction control ratio (663.0). These results may be due to the reaction of cysteine with GOS leading to the accumulation of reactive species that increased the affinity of GOS towards PTT glycation binding sites. As compared to PTT:GOS conjugates, cysteine was less effective in improving the reaction control ratio of PTT:XOS (69.0) due to the low percent blocked lysine of PTT:XOS conjugates (6.9% at 3 days). This demonstrates the lower reactivity of cysteine towards XOS and its high scavenging of the reactive species generated upon XOS degradation. Aminoguanidine was the most efficient in improving the reaction control ratio of PTT:XOS conjugates (143.0), with a maximum percent blocked lysine of 14.3% at 3 days and an advanced reaction index of 0.1. However, no glycation of PTT with GOS was detected in the presence of aminoguanidine. The results reveal the inhibitory effect of aminoguanidine in excess on the formation of Amadori compounds with GOS. However, the concentration of aminoguanidine used in this study was adequate to scavenge the higher amount of reactive dicarbonyls generated with XOS, leading to low advanced reaction index and higher level of glycation. Similarly to their monosaccharide counterparts, the use of pyridoxamine led to low percent blocked lysine with GOS and XOS (0.0–7.3%). Such results may be due to the reaction between pyridoxamine and XOS/GOS, which may have decreased their availability for reacting with free amino groups of PTT. The advanced reaction index of PTT:XOS conjugates in the presence of pyridoxamine was higher (3.1–14.5) as compared to that of PTT:xylose conjugates (0.1–9.8). Indeed, in the control containing only pyridoxamine and XOS, high advanced reaction index was found (1.4–4.8), which demonstrates important browning/aggregates formation during the reaction between

pyridoxamine and XOS (data not shown). The results also reveal no to lower reactivity of GOS and XOS to glycate PTT in the presence of sodium bisulfite (0.0–2.7%), which may have inhibited the early and the intermediate stages of the Maillard reaction through its scavenging ability of free-radicals and reactive dicarbonyls (Friedman & Molnar-Perl, 1990). The accumulation of reactive species produced as precursors at the early stage seems to be important for the initiation of Schiff base formation and hence favoring the glycation of PTT with GOS/XOS.

7.4.1.3. Changes in the Glycation Level of PTT with Xylan/Galactan in the Presence of Inhibitors

Similarly to their mono- and oligosaccharides counterparts, xylan (maximum blocked lysine of 16.5%, day 7) resulted in higher percent blocked lysine of PTT as compared to galactan (4.3%, day 5). However, the effect of chain length on the glycation extent of PTT seems to be less significant in the case of pentose, xylose, than the hexose, galactose. As compared to PTT:galactan conjugates (0.1–1.7), the higher advanced reaction index values of PTT:xylan conjugates (2.0–6.5) demonstrates the high extent of side autoxidation/glycoxidation reactions of xylan (Hofmann, 1999). These results may be due to the presence of arabinose on the disaccharide side chains of the soluble xylan (Teleman et al., 2002). Indeed, arabinose has been identified as an intermediate during the autoxidation/glycoxidation of monosaccharides, leading to the formation of reactive dicarbonyls (Usui et al., 2007; Wells-Knecht et al., 1995). Contrary to the reaction with its oligosaccharide counterpart (XOS), the use of Maillard reaction inhibitors with xylan was less effective at inhibiting the formation of protein aggregates and the browning compounds at the intermediate and advanced stages. In addition, the maximum level of glycation of PTT with xylan obtained using the inhibitors (16.7%) was more or less similar to that achieved without inhibitor (16.5%). In contrast, all investigated inhibitors, with the exception of aminoguanidine, limited the glycation of PTT with XOS. This may be explained by the higher degradability of xylan into reactive dicarbonyl compounds compared to XOS. Nevertheless, the highest reaction control ratio (12.8) of PTT:xylan conjugates was obtained in the presence of sodium bisulfite with a percent blocked lysine of 16.7% (5 days) and moderate level of advanced reaction index of 1.3. These results reveal that the use of sodium bisulfite did not inhibit the conjugation of PTT with xylan at the early stages, but slightly prevented the protein cross-linking from occurring. Similarly, Scaman et al. (2006) have reported that the use of sodium bisulfite did

not inhibit the percent glycation of lysozyme with dextran at pH 8.5 at 40°C, but prevented protein cross-linking. Similarly to PTT:GOS conjugates, the highest reaction control ratio (71.0) of PTT:galactan conjugates was achieved in the presence of cysteine after 5 days, where the highest percent blocked lysine of 7.1% and the lowest advanced reaction index of 0.1 were obtained. As compared to the reaction with GOS, sodium bisulfite, aminoguanidine, and pyridoxamine had less inhibitory effect on the glycation of PTT with galactan leading to maximum level of glycation of 2.2, 2.5, and 4.6%, respectively. As compared to PTT:GOS conjugates, the higher advanced reaction index of PTT:galactan conjugates in the presence of aminoguanidine (3.8–10.8) and of pyridoxamine (9.3–17.0) may be due to the higher reactivity of galactan towards these inhibitors as demonstrated by the high level of advanced reaction index of the incubated controls containing only pyridoxamine (0.3–4.6) or aminoguanidine (0.4–1.7) with galactan (data not shown). The reaction between aminoguanidine (Requena et al., 1993) or pyridoxamine (Corzo-Martínez et al., 2010a) and carbohydrates has previously been reported by others and these conjugates can further be degraded to cause ultimately the browning/protein cross-linking.

7.4.2. Protein Cross-Linking and Formation of Reactive Carbonyl Species in the Presence of Selected Inhibitors

Selected reactive carbonyl species, including methylglyoxal, glyoxal, 2,3-butanedione, and deoxyosone, can lead to protein cross-linking at different rates and, as a result, to the formation of aggregates (Thornalley et al., 1999). The reactive dicarbonyl compounds can be formed during the autoxidation/glycoxidation of carbohydrates and/or from the Schiff base, the initial condensation product of a reducing carbohydrate and an amino compound, via the so-called Namiki pathway under oxidative conditions (Hayashi & Namiki, 1980). In addition, the Amadori products, although fairly stable in foods with low water activity, may undergo several degradation reactions leading to the formation of dicarbonyls (Henle, 2005). Some authors have identified the methylglyoxal as the important intermediate in the formation of protein cross-linking products (Meade et al., 2003; Miller et al., 2003). Others have identified glyoxal, deoxyosone, and methylglyoxal as the key intermediates (Usui et al., 2007). To elucidate the protein cross-linking inhibition mechanism for PTT cross-linking in the presence of aminoguanidine, cysteine, pyridoxamine or sodium bisulfite, the molecular distribution of

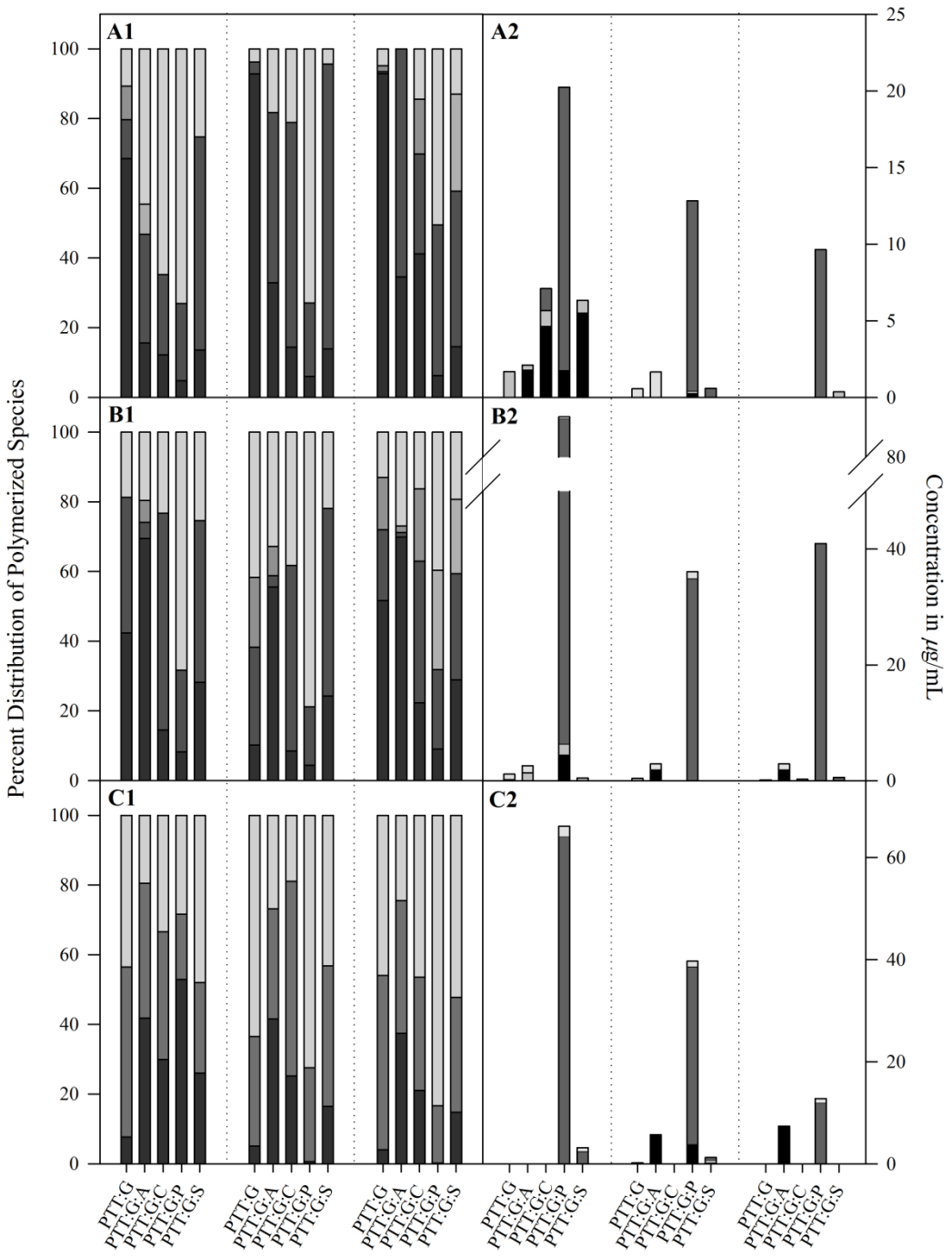

Figure 7.1 Effect of inhibitors on the degree of polymerization of proteins during the reaction between PTT and galactose (A1), GOS (B1), galactan (C1) at day 3, 5, and 7: extensive polymerization ( ), degree of polymerization >10 ( ),8–10 ( ),5–7 ( ),3–4 ( ),<3 ( ). Quantification of *α*-dicarbonyls present in the incubated mixtures of PTT:galactose (A2), PTT:GOS (B2), PTT:galactan (C2) estimated by measuring quinoxalines derivatized with *o*-phenylenediamine: deoxyosone ( ), glyoxal ( ), methylglyoxal ( ), 2,3-butanedione ( ).

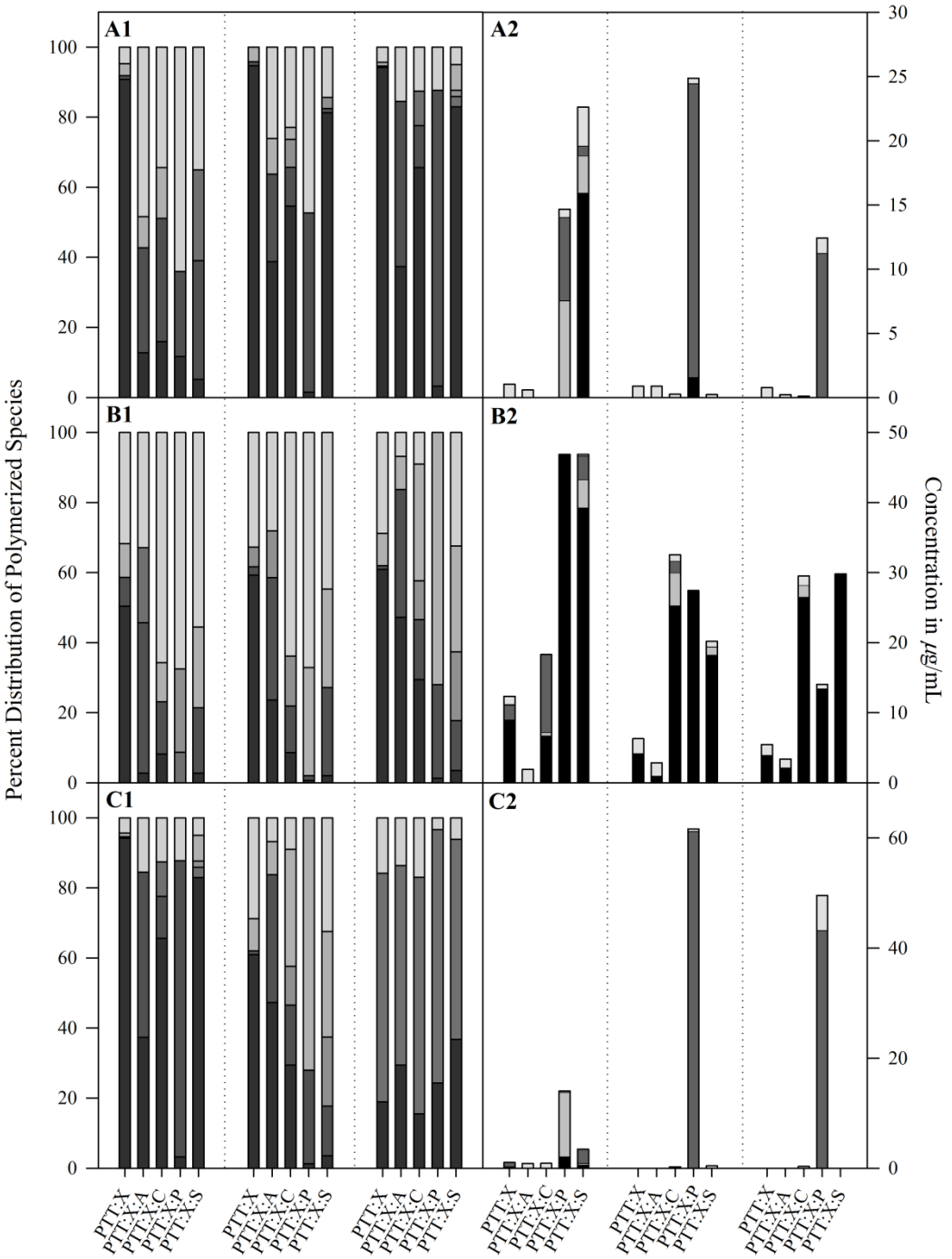

Figure 7.2 Effect of inhibitors on the degree of polymerization of proteins during the reaction between PTT and xylose (A1), XOS (B1), xylan (C1) at day 3, 5, and 7: extensive polymerization ( ), degree of polymerization >10 ( ),8–10 ( ),5–7 ( ),3–4 ( ),<3 ( ). Quantification of *α*-dicarbonyls present in the incubated mixtures of PTT:xylose (A2), PTT:XOS (B2), PTT:xylan (C2) estimated by measuring quinoxalines derivatized with *o*-phenylenediamine: deoxyosone ( ), glyoxal ( ), methylglyoxal ( ), 2,3-butanedione ( ).

polymerized species of PTT conjugates and the formation of dicarbonyls' *o*-phenylenediamine derivatives were investigated. The comparison of protein polymerization degree and the quantity of dicarbonyls' *o*-phenylenediamine derivatives can reveal the effectiveness of inhibitors to scavenge the reactive dicarbonyls. Mild protein aggregation of PTT occurred upon incubation at 48°C forming dimers (59.9%) with some oligomerized species (27.2%) (data not shown). The Maillard reaction between PTT and galactose (Fig. 7.1A1) and xylose (Fig. 7.2A1) led to the formation of a high proportion of extensively polymerized species of 68.5 and 90.8 %, respectively, at day 3; as the incubation increased, the proportion of extensively polymerized species increased to reach more than 92.9% by day 7. At day 3, the presence of inhibitors led to a lower proportion of extensively polymerized species of PTT:galactose/xylose conjugates (4.7–16.0%) and to a higher proportion of its mono/dimer (34.4–73.1%); as the reaction proceeded, there was a shift toward high molecular weight species (27.1–100.0%; >10, extensively polymerized species) at different rates. These results support the higher advanced reaction index obtained with PTT:xylose conjugates (Table 7.1) that was attributed to the high autoxidation of pentoses than hexoses. As compared to other inhibitors, the cross-linking of PTT:galactose/xylose conjugates in the presence of pyridoxamine exhibited the lowest rate, which can be attributed to the low amount of percent blocked lysine. The effectiveness of pyridoxamine as an inhibitor of protein cross-linking occurring during the Maillard reaction has already been demonstrated by Corzo-Martinez et al. (2010a), where they have observed lower poly-oligomer formation within the reaction between *β*-lactoglobulin and galactose/tagatose in the presence of pyridoxamine.

The only *α*-dicarbonyls formed in the reaction with galactose (Fig. 7.1A2) or xylose (Fig. 7.2A2) without inhibitor was glyoxal (1.7 *μ*g/ml) and butanedione (1.1 *μ*g/ml), respectively. Glyoxal was found to be formed during the degradation of monosaccharide by retroaldol condensation reactions activated by deprotonation of the 2- or 3-hydroxy groups (Thornalley et al., 1999), which supports the higher amount of glyoxal found in galactose reactions. Butanedione is a well-known sugar fragmentation product, which could arise from xylose fragmentation (Ames & Apriyantono, 1993). The results also show that the concentration of unreacted *α*-dicarbonyls produced at day 3 upon the Maillard reaction of PTT with galactose was lower without inhibitor, revealing their high reactivity as intermediates in the formation of large proportion of extensively polymerized species (Nasiri et al., 2011). Higher total amount of *α*-dicarbonyls of 2.1, 7.1, 20.2,

and 6.3 μg/ml was detected in the PTT:galactose mixture at day 3 in the presence of aminoguadinine, cysteine, pyridoxamine, and sodium bisulfites, respectively. For the reaction between PTT and xylose at day 3, total amount of α-dicarbonyls of 0.6, 0.0, 14.7, and 22.6 μg/ml was detected in the presence of aminoguadinine, cysteine, pyridoxamine, and sodium bisulfites, respectively. The decrease in α-dicarbonyls upon longer incubation time corresponded to the increase in polymerized species observed in Fig. 7.1A1 and in Fig. 7.2A1. The major dicarbonyl formed in the presence of aminoguanidine, cysteine, and sodium bisulfites was deoxyosone for the reactions with galactose, and butanedione and deoxyosone for the reactions with xylose. As compared to methylglyoxal and glyoxal, the lower reactivity of deoxyosone and butanedione (Meade et al., 2003; Miller et al., 2003; Tessier et al., 2003) towards Maillard reaction inhibitors and towards the lysine/arginine residues of the protein may explain the accumulation of these dicarbonyls. The reaction between PTT and galactose/xylose in the presence of pyridoxamine led to more methyglyoxal formation. Scheme 1, adapted from Miller et al. (2003), offers a possible explanation for the high amount of methyglyoxal, and the low proportion of extensively polymerized species formed in the presence of pyridoxamine. From our results, it seems possible that pyridoxamine only reacted with one of the two carbonyl groups of methylglyoxal leaving the other carbonyl group available to react with the lysine residues found on the protein preventing its cross-linking. The decrease in lysine residues and pyridoxamine led to the accumulation of unreacted methylglyoxal in the system. Similar mechanism was proposed by Miller et al. (2003) when describing the inhibitory effect of 3, 5-dimethylpyrazole-1-carboxamidine on the protein cross-linking caused by dicarbonyls. The inhibitors identified previously (Table 7.1), sodium bisulfite for galactose (day 5) and aminoguanidine for xylose (day 7), that led to the highest reaction control ratios resulted in the release of low amounts of total unreacted dicarbonyls (0.6 and 0.2 μg/ml, respectively) and to lower proportions of extensive polymerized species (13.9 and 37.3%, respectively) as compared to the reaction without inhibitor, demonstrating the efficiency of these inhibitors to modulate the reaction progress.

The reaction between PTT and GOS or XOS (Fig. 7.1B1, 7.2B1) without inhibitor led to higher formation of oligomerized species (18.7 and 41.3%; < 3, 3–4, 5–7) at day 3 as compared to their monosaccharide counterparts (galactose and xylose). Contrary to monosaccharides, the increase in the proportion of extensively polymerized species within the reaction time course was not noticeable with GOS and XOS. These results are in good agreement with the estimated low

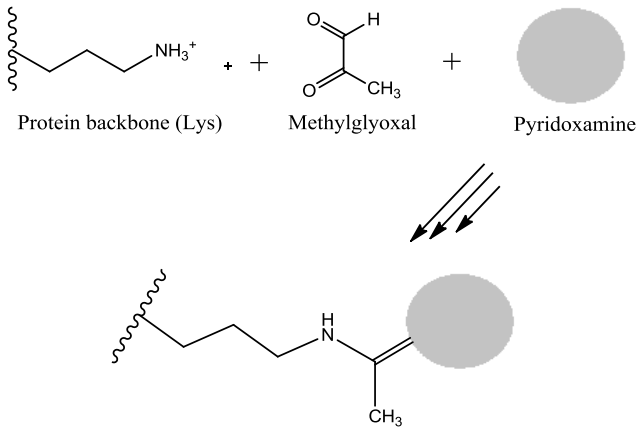

Scheme 7.1 Possible reaction pathway for methylglyoxal's reaction with lysine residues on PTT in the presence of pyridoxamine adapted from Miller et al. (2003).

percent blocked lysine (Table 7.1), confirming the lower reactivity of oligosaccharides as compared to the shorter carbohydrates. In the PTT:GOS/XOS reaction systems, all investigated inhibitors limited the rate of protein cross-linking over 7 days of reaction time, with the exception of aminoguanidine. However, the inhibitory effect on cross-linking rates was more significant in the PTT:XOS reaction system than in the PTT:GOS one. These results are in good agreement with the quantified amounts of unreacted dicarbonyl species, which were higher in the PTT:XOS system containing inhibitors (Fig. 7.1B2, 7.2B2). Similarly to the reaction of PTT with galactose/xylose, the most effective inhibitor for the prevention of protein cross-linking during the reaction of PTT with GOS and XOS was pyridoxamine, leading to only 9.0 and 1.3% of extensively cross-linked polymers, respectively, after 7 days of incubation. As their monosaccharide counterparts, the methylglyoxal (34.9–83.4 μg/ml) was identified as the main unreacted dicarbonyl with GOS in the presence of pyridoxamine, whereas, deoxyosone (13.5–46.9 μg/ml) was the major dicarbonyl with XOS. The difference in the distribution of dicarbonyls between the reaction with XOS and that with GOS may be due to the higher degradation ability of pentose-type oligosaccharides compared to the hexose-type ones, leading to the higher production of deoxyosones (Hollnagel & Kroh, 2000). The accumulation of methylgloxal in the reaction between PTT and GOS with pyridoxamine may also be due to the partial reaction between pyridoxamine, methylgloxal, and the lysine residues on the protein leading to the depletion of available reactant for the highly reactive dicarbonyl and to its accumulation. The best identified inhibitors, leading to the highest reaction control ratio for

PTT:GOS (cysteine, day 3) and PTT:XOS (aminoguanidine, day 5) (Table 7.1) systems resulted in low amounts of total unreacted dicarbonyls (0.0–2.8 μg/ml) and in lower proportions of extensive polymerized species (14.4–23.6%) as compared to the reaction without inhibitor (1.1–6.3 μg/ml; 42.4–59.3%).

PTT:xylan reaction system without inhibitor (Fig. 7.2C1) exhibited a higher proportion of extensively polymerized species (94.2%) than in the presence of inhibitors (3.2–82.9%) after 3 days of incubation. In contrast, PTT:galactan reaction system (Fig. 7.1C1) showed lower proportion of extensively polymerized species (7.7%) than in the presence of inhibitors (26.0–52.9%). However, the decrease in the proportion of extensively polymerized species of PTT:xylan with an increase in incubation time reveals the non-covalent interactions of these species. Indeed, the decrease in the hydrophobicity of PTT upon glycation may have decreased its affinity to interact with xylan and to form large non-covalent complexes (Fig. 7.2C1). The low energy interactions, such as hydrogen bonding and hydrophobic bonding, between proteins and large polysaccharides have been previously documented (Turgeon et al., 2007). The lower protein cross-linking observed with galactan may be attributed to its ability to depress the protein polymerization associated with the advanced Maillard reaction. Similar results were reported previously for the conjugates formed between lysozyme and galactan (Seo et al., 2013). However, as compared to the system without inhibitor, the higher proportion of extensively polymerized species observed at day 3 in the PTT:galactan reaction system containing aminoguanidine (41.8%) or pyridoxamine (52.9%) could be due to the higher reactivity of galactan towards these inhibitors, leading to the formation of reactive dicarbonyl species. These results support the high advanced reaction index (Table 7.1) in the PTT:galactan reaction system containing aminoguanidine or pyridoxamine. The results also show that the effect of Maillard reaction inhibitors on the protein polymerization in the PTT:xylan reaction system was not significant. Methylglyoxal (34.9–41.0 μg/ml) was identified as the main unreacted dicarbonyl with galactan/xylan (Fig. 7.1C2, 7.2C2) in the presence of pyridoxamine as with their monosaccharide counterparts (Fig. 7.1A2, 7.2A2), except for the reaction with xylan at day 3 of incubation. Butanedione, one of the dicarbonyls produced from carbohydrate degradation, was the main unreacted dicarbonyl with xylan in the presence of aminoguanidine, cysteine, or pyridoxamine at day 3 of incubation demonstrating that there was an accumulation of the dicarbonyl with the lowest reactivity during the earlier stage of the reaction. The best identified

inhibitors, leading to the highest reaction control ratio for PTT:galactan (cysteine, day 5) and PTT:xylan (sodium bisulfite, day 5) (Table 7.1) systems resulted in lower amounts of total unreacted dicarbonyls (0.0 μg/ml) for the galactan reaction system and in lower proportions of extensive polymerized species (3.5%) for the xylan reaction system as compared to the reaction without inhibitor (0.0–0.2 μg/ml; 5.1–60.9%).

7.4.3. Particle Size and Digestibility of the Conjugates Produced Using Selected Inhibitors

Cysteine and aminoguanidine were identified as the best inhibitors for each galactose-type or xylose-type PTT conjugates, favoring high glycation level and limiting the protein cross-linking to a certain extent during the advanced stage of Maillard reaction. Although pyridoxamine was the most efficient in inhibiting protein cross-linking, it exhibited an inhibition effect on the PTT conjugation by limiting or delaying the formation of Amadori product (Table 7.1). PTT conjugates were produced using the identified inhibitors and their particle size distribution and digestibility were investigated (Fig. 7.3). These conjugates produced with or without inhibitor were compared to the native PTT on the basis of their relative percent digestibility and their increase in average particle size per 5.0% blocked lysine to normalize the effect of the different levels of glycation on these parameters. The average particle size and the total digestibility of the PTT controls was 321.3–347.2 nm and 59.6%–60.2%, respectively (data not shown). PTT:galactose conjugates showed more or less similar increase in the particle size of their aggregates, per 5.0% blocked lysine, in the presence (44.0 nm) or in the absence (45.9 nm) of cysteine inhibitor. In contrast, a significantly smaller increase in the particle size distribution of PTT:xylose conjugates, per 5.0% blocked lysine, was obtained in the presence of aminoguanidine (16.3 nm) as compared to without inhibitor (2,640.6 nm). These results demonstrate the effectiveness of aminoguanidine to prevent important protein cross-linking of PTT:xylose conjugates caused by the dicarbonyls generated from the reaction. The decrease in digestibility of Maillard reaction conjugates due to glycation has been previously reported (Corzo-Martínez et al., 2012; Yeboah et al., 2004). Because of the higher cross-linking level of PTT:xylose conjugates produced without inhibitor, their relative digestibility (43.1%) was lower than that of PTT:galactose (94.8%). However, the use of cysteine and aminoguanidine as inhibitors resulted in an increase in the relative digestibility of PTT:galactose and PTT:xylose conjugates by 0.4 and 8.2%, respectively, as compared to without inhibitor. It is important to mention that the relative digestibility of PTT:xylose conjugates was non-concomitantly increased

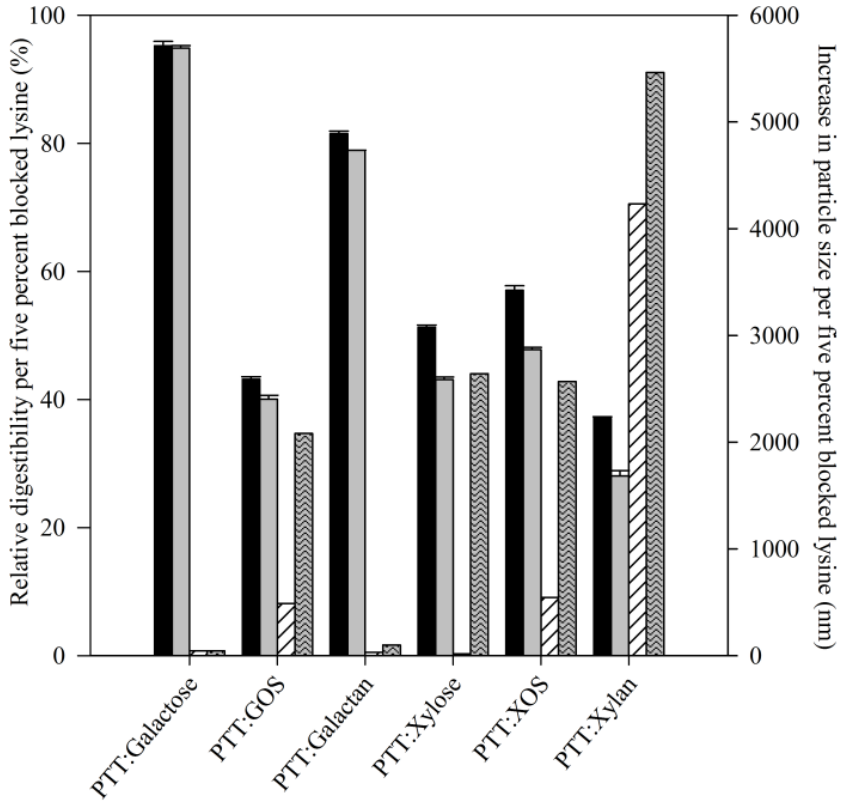

Figure 7.3 The relative digestibility and the increase in particle size, per 5% blocked lysine, of the PTT:galactose/GOS/galactan:cysteine incubated mixtures and of the PTT:xylose/XOS/xylan:aminoguanidine incubated mixtures compared to the reaction mixture without inhibitors: digestibility with (■) and without inhibitors (▭), and the particle size with (▨) and without inhibitors (▩). The particle size is an average of 70 measurements and the polydispersity index of each sample was ≤ 0.5.

to the same extent, upon the use of aminoguanidine, as compared to the large decrease of their particle size. These results may reveal that the large particle size of PTT:xylose conjugates produced without inhibitor was only apparent and was largely due to their non-covalent aggregation. The results also show the high increase of the average particle size, per 5.0% blocked lysine, of PTT:GOS conjugates (2080.8 nm) produced without inhibitor, revealing the very high level of protein cross-linking. As expected, the use of cysteine dropped the increase in the average particle size of PTT:GOS conjugates to 487.3 nm. The increase in average particle size of PTT: XOS conjugates, per 5.0% blocked lysine, produced with and without aminoguanidine was 544.0 and 2,567.3 nm, respectively. Similar levels of relative digestibility were obtained for PTT:GOS and PTT:XOS conjugates (40.1 and 47.8%) produced without inhibitor; this may be due to the similar level of protein cross-linking observed in these conjugates. On the other hand, the larger average particle size of PTT:GOS conjugates produced without inhibitor (2,080.8 nm) led to lower relative digestibility (40.1%) as compared to its monosaccharide counterpart (45.9 nm, 94.8%), whereas the comparable particle sizes obtained for PTT:XOS and PTT:xylose conjugates (2,567.3 and 2,640.6 nm, respectively) led to similar relative digestibility (47.8 and 43.1%, respectively). As a result of the lower level of protein cross-linking, PTT:GOS and PTT:XOS conjugates produced in the presence of the inhibitors showed 3.1 and 9.3% increases in their percent digestion, respectively. However, the higher increase in the relative digestibility and the higher decrease in the particle size obtained with PTT:XOS:aminoguanidine system reveal the effective inhibition of protein cross-linking in this reaction system as compared to the PTT:GOS:cysteine reaction system. The experimental findings also show that PTT:galactan conjugates produced in the presence of cysteine (29.9 nm) had a smaller increase in the average particle size of its aggregates, per 5.0% blocked lysine, than without cysteine (100.2 nm). Contrary to PTT:galactan conjugates, the average particle size of PTT:xylan conjugate aggregates increased significantly (5,463.4 nm) per 5.0% blocked lysine, and the use of aminoguanidine as inhibitor slightly limited this increase to 4,231.6 nm. As expected, without inhibitor, the relative digestibility of PTT:xylan conjugates (37.1%) was lower than that of PTT:galactan conjugates (81.5%). The extensive cross-linking/aggregation of PTT:xylan conjugates may have limited the accessibility of the digestive enzymes to PTT cleavage sites. The digestibility of lowly cross-linked PTT:galactan conjugates produced in the presence of cysteine (81.5%) was lower as compared to its monosaccharide counterpart

conjugates (PTT:galactose, 95.3%) despite their small relative increase in the particle size (29.9 and 44.0 nm, respectively). This can be attributed to the large size of galactan, leading to steric hindrance and limiting the digestion of PTT:galactan conjugates. As with the oligosaccharides, the use of cysteine or aminoguanidine as inhibitors for the production of PTT:xylan or PTT:galactan conjugates led to 2.6 and 9.0 % increase in the percent digestion. These increases are in good agreement with the decrease in the particle size of the conjugate aggregates. To the best of our knowledge, this is the first study where the effect of Maillard reaction inhibitors on the improvement of digestibility of protein:carbohydrate conjugates has been investigated.

7.5. Conclusion

The effect of selected Maillard reaction inhibitors on the production of PTT:carbohydrate conjugates was investigated. Sodium bisulfite (galactose, xylan), aminoguanidine (xylose, xylooligosaccharides), and cysteine (galactooligosaccharides, galactan) were the inhibitors that led to the highest glycation level of the conjugates. These glycation levels were mostly similar or even higher than those of the conjugates produced without inhibitors. The use of these inhibitors led to lower proportions of extensive polymerized species or to lower amounts of total unreacted dicarbonyls. By using cysteine for the production of PTT:galactose/GOS/galactan conjugates, and by using aminoguanidine for the production of PTT:xylose/XOS/xylan conjugates, the particle size distribution of the conjugates was lowered and the digestibility of the produced conjugates was improved. The use of the Maillard reaction inhibitors to limit the protein cross-linking/polymerization, associated with the intermediate and advanced stages of the reaction, will allow the production of protein:carbohydrate conjugates with improved properties as potential functional food ingredients.

CONNECTING STATEMENT 6

The Maillard reaction inhibitors were proven to be efficient in modulating the Maillard reaction progress and minimizing the protein cross-linking of PTT conjugates (Chapter VII). The optimization of the production of PTT:carbohydrate conjugates by the combined use of two selected inhibitors, cysteine and sodium bisulfite, was investigated in Chapter VIII. The effects of incubation time, total quantity of inhibitors, the ratio of cysteine to sodium bisulfite, and the type of monosaccharide on percent blocked lysine and on particle size distribution of PTT conjugates were discussed in this chapter.

Seo, S., & Karboune, S. (2014). Optimization of the production of patatin-galatose/xylose conjugates, by the combined use of L-cysteine and sodium bisulfite inhibitors, through response surface methodology (To be Submitted).

CHAPTER VIII

OPTIMIZATION OF THE PRODUCTION OF PATATIN-GALATOSE/XYLOSE CONJUGATES, BY THE COMBINED USE OF L-CYSTEINE AND SODIUM BISULFITE INHIBITORS, THROUGH RESPONSE SURFACE METHODOLOGY

8.1. Abstract

The optimization of the production of potato patatin:galactose/xylose conjugates through the Maillard reaction was investigated using a combination of cysteine and sodium bisulfite as inhibitors to minimise the protein cross-linking. Using response surface methodology, models were developed to relate independent variables (incubation time, ratio of cysteine to total inhibitors, total quantity of inhibitors, monosaccharide used) to responses (percent blocked lysine, particle size). The most important variable affecting the percent blocked lysine and the particle size was the incubation time and the ratio of cysteine to total inhibitors, respectively. The interaction between the monosaccharide type and the cysteine/total inhibitors ratio and between cysteine/total inhibitors ratio and total quantity of inhibitors exhibited significant effect on the percent blocked lysine and the particle size of the conjugates, respectively. The identified optimal glycation conditions for the production of patatin:galactose/xylose conjugates demonstrated the synergistic effect of cysteine and sodium bisulfite as inhibitors.

8.2. Introduction

Patatin (PTT) is one of the major proteins found in potato tuber (*Solanum tuberosum*). PTT is a glycoprotein with up to two *N*-linked glycans, Man_2-Man(Xyl)-GlcNAc-GlcNAc(Fuc)- (Welinder & Jørgensen, 2009) and a molecular weight of 40-45 kDa (Pots et al., 1999a). The use of PTT as potential food ingredient is of great interest due to its high nutritional quality that is similar to egg proteins (Camire et al., 2009), its antioxidant activity, and its anti-proliferative activity against cancer cells (Sun et al., 2013). In addition, PTT offers many functional properties such as foam forming, gelling, and emulsifying properties (Creusot et al., 2010; Ralet & Gueguen, 2000, 2001). However, the application of PTT as food ingredient has been limited by its very high exposed hydrophobicity (Creusot et al., 2010), leading to limited solubility at increased ionic strength. As compared to many other proteins being used as food ingredients, PTT exhibits a very low thermal stability with a denaturation temperature at around 59ºC (Creusot et al., 2010).

The improvement of the solubility of PTT and the decrease of its astringency, through conjugation with different carbohydrates by the Maillard reaction, have already been reported by Giuseppin et al. (2011). In addition, our previous study (Seo et al., 2014a) demonstrated improvements in the thermal stability and the antioxidant activity of PTT upon its conjugation

with galactooligosaccharides (GOS) and galactan through the Maillard reaction. However, the difficulty in controlling the Maillard reaction rate makes it challenging to limit the intermediate and advanced stages of the reaction, leading to protein cross-linking/polymerization and to the loss of functional properties gained by the conjugation of the carbohydrate (Oliver et al., 2006a; Seo et al., 2012). Our previous results (Seo & Karboune, 2014) demonstrated that the use of Maillard reaction inhibitors can result in a decrease in the protein cross-linking of PTT:galactose /GOS/xylose/xylooligosaccharide/xylan conjugates. This decrease in the protein cross-linking ultimately led to an increase in the digestibility of these conjugates, while improving or preserving the glycation level of most of these conjugates as compared to the conjugates produced without inhibitors. Cysteine and sodium bisulfite were among the most promising inhibitors for modulating the Maillard reaction rate to produce well defined PTT:carbohydrate conjugates (Seo & Karboune, 2014). In addition, the easier availability of these inhibitors in the food industry validates them as the Maillard reaction inhibitors that need to be focused on. Sulfites inhibit protein cross-linking and browning occurring during the intermediate and advanced stages of the Maillard reaction by scavenging through the sulfite anion free-radicals and the reactive carbonyl species formed and by forming bisulfite adducts with the degradation products of the Amadori compound (Farmar et al., 1988; Friedman & Molnar-Perl, 1990). Cysteine's modulation of the Maillard reaction occurs through its thiol group, which also scavenges the reactive species formed during the reaction (Huang et al., 2012). In addition, cysteine also competes with the protein for the carbonyl groups of the carbohydrates to slow down the overall reaction. The separate effect of each of these two inhibitors, cysteine and sodium bisulfite, on the Maillard reaction rate to produce protein:carbohydrate conjugates has already been investigated (Scaman et al., 2006; Seo & Karboune, 2014). However, so far, no study has looked at the synergistic and interactive effects of these two inhibitors. Understanding their synergistic effects of cysteine and sodium bisulfite may help better modulate the progress of the Maillard reaction.

Response surface methodology (RSM) is a combination of mathematical and statistical techniques used to optimize a response (an output), which is influenced by different independent variables (parameters) (Montgomery, 2008). RSM offers the advantage of reducing the number of experiments needed by developing mathematical models to assess the relevance and the statistical significance of the variables being studied as well as the interaction effects between the

variables (Ferreira et al., 2007). These advantages make RSM a useful tool for the optimal production of PTT:carbohydrate conjugates with high level of carbohydrate conjugation and with minimal protein cross-linking.

As part of our ongoing research, the overall objective of this study was the optimization of the production of PTT conjugates by the combined use of two Maillard reaction inhibitors, cysteine and sodium bisulfite, through RSM. The effects of selected glycation parameters, including cysteine to total inhibitors weight ratio, total inhibitor quantity, incubation time, and the use of galactose or xylose, on the glycation extent and the protein cross-linking of PTT conjugates were investigated. These findings will bring more insight into the interactions between the glycation parameters and the possible synergistic effects of these two inhibitors, cysteine and sodium bisulfite, for the production of low-cross linked PTT:galactose/xylose conjugates.

8.3. Materials and Methods

8.3.1. Materials

Solanic 206P (PTT ≈ 75%, protease inhibitors ≈ 25%) was kindly provided by Solanic (Foxhol, Netherlands). Furosine standard was purchased from Neosystem Laboratories (Strasbourg, France). All other chemicals were purchased from Sigma Chemical Co. (St–Louis, MO, USA).

8.3.2. Preparation of the Conjugates

PTT was purified from the Solanic 206P by ultrafiltration using a stirred ultrafiltration unit (Amicon system, Millipore, Billerica, MA, USA) fitted with a 30 kDa molecular mass cut–off membrane. Mixtures of PTT:galactose or xylose at the molar ratio of 1:9 in 0.1% (w/v) of 0.05 M sodium phosphate buffer (pH 7.0) were prepared. A specific quantity of cysteine and sodium bisulfite was added to the mixtures before freeze drying at –25°C (Table 8.1). The recovered powders were incubated in sealed glass desiccators at 48ºC for 2 to 6 days under controlled a_w value of 0.65 (a saturated solution of potassium iodide). Control experiments were performed with PTT incubated under the same conditions in the absence of galactose/xylose or in the absence of cysteine/sodium bisulfite.

8.3.3. Determination of Percent Blocked Lysine

The furosine assay and the measurement of free amino groups for the calculation of blocked lysine were made from a previously described method by Seo et al. (2014a).

Considering that the Amadori compound tagatosyl-lysine, formed during the Maillard reaction between lysine residues and galactose moieties, generates about 42 % furosine upon 8 N acid hydrolysis (Krause et al., 2003), the final percentage of blocked lysine was estimated from the furosine content using a conversion factor of 2.4. Although the conversion factors from xylulosyl-lysine to furosine is unknown, the difference between the conversion factors for different carbohydrates has been demonstrated to be smaller at conditions used in this study (stronger acid hydrolysis, 8N HCl) (Krause et al., 2003). Therefore, the same correction factor for the conversion of tagtosyl-lysine to furosine was used for the estimation of xylulosyl-lysine. The percentage of blocked lysine that was not due to the protein cross-linking was estimated from the furosine content and the total initial available lysine content according to the Equation 5.1.

8.3.4. Particle Size Analysis

The average particle size of the polymerized conjugates was estimated by dynamic light scattering measurements using Delsa Nano C system (Beckman Coulter) at 25 ºC. The mean of size distributions was obtained from 70 measurements. The polydispersity index (PI) as a measure of the width of particle size distributions was also measured. To validate the use of the particle size as an indicator of the cross-linking level of conjugates, the molecular weight distribution of PTT:galactose conjugates, determined according to the previous size exclusion chromatography method (Seo & Karboune, 2014), was correlated to the particle size distribution of the aggregates of the same conjugates.

8.3.5. Experimental Design and Data Analysis

The production of PTT:galactose/xylose conjugates using both cysteine and sodium bisulfite as inhibitors was optimized using RSM and a central composite rotatable design (CCRD). Central composite design consists of a 2^k full factorial design, $2k$ axial designs at a distance α from the origin, and m center points, where k is the number of variables and m is more than 1. Incubation time in days (X_1), cysteine to total inhibitors weight ratio (X_2), quantity of total inhibitors (X_3) in mg/mg of PTT were chosen as independent numerical variables. The type of monosaccharide (galactose or xylose) was chosen as the categorical variable (X_4). The range and center point values of independent variable incubation time (X_1) and quantity of total inhibitors (X_3) presented in Table 8.1 were based on our previous results (data not shown). The experimental design consists of eight factorial points, six axial points at α distance of ± 1.682 from the center and six

replicates of the central point for each categorical variable. The central values (zero level) of the experimental design were: 4 days of incubation, 0.5 weight ratio of cysteine to total inhibitors, and 0.18 mg of total quantity of inhibitors /mg of PTT. Percent blocked lysine and particle size were the quantified responses. Each observed response for an experimental design point is an average of triplicate experiments. The runs were randomized. The variables were coded according to the following Equation 8.1:

$$\chi = (X_i - X_o) / \Delta X \quad (8.1)$$

Where χ is the coded value, X_i is the corresponding actual value, X_o is the actual value in the centre point, and ΔX is the value of the step change.

The relationship between variables and responses was expressed by a second order polynomial Equation 8.2:

$$Y = \beta_0 + \sum_i \beta_i x_i + \sum_i \sum_j \beta_{ij} x_{ij} + \sum \beta_{ii} x_i^2 \quad (8.2)$$

Where Y is the measured response (percent blocked lysine, particle size), β_o is the model constant, and β_i, β_{ij} and β_{ii} are the measures of the linear, interaction, and quadratic effects of variables X_i, X_iX_j, and X^2_i, respectively. Analysis of the experimental design data and calculation of predicted responses were carried out using Design Expert software (Version 8.0, Stat-Ease, Inc. Minneapolis, MN, USA). Statistical analysis of the model was performed to evaluate the analysis of variance (ANOVA) including lack of fit, Fisher's *F*-test (overall model significance), its associated probability *P*(*F*) and correlation coefficient *R*, and determination coefficient R^2 to measure the goodness of fit of quadratic model. The predicted optimum conditions by the generated quadratic model were validated by conducting quadruplicate experiments.

8.4. Results and Discussion

8.4.1. Effects of Incubation Time, Inhibitor Parameters, and Monosaccharide Type

RSM approach was applied in order to investigate the effects of incubation time (X_1), the ratio of cysteine to total inhibiors (X_2), the total inhibitor concentration (X_3), as well as the monosaccharide type (X_4) on the glycation of PTT through Maillard reaction. The experimental design was performed based on the CCRD. The levels of the selected parameters were set based on preliminary trials, where one factor at a time was varied (data not shown). The percent blocked lysine and the particle size of the reaction species were chosen as selected responses to

monitor the progress of the Maillard reaction. Indeed, the percent blocked lysine, calculated from the furosine formed upon the acid hydrolysis of the Amadori products, provides a good estimation of the extent of early Maillard reaction (Krause et al., 2003), whereas the particle size of the reaction species allows the assessment of the level of protein cross-linking occurring during the intermediate and the advanced stages (Gerrard, 2002).

To validate the use of particle size distribution as an estimation of the level of protein cross-linking occurring during the Maillard reaction, the molecular weight distribution of PTT:galactose conjugates produced with (Fig. 8.1A) or without cysteine (Fig. 8.1B) were characterized by size exclusion chromatography (right) and correlated to the particle size distribution of their aggregates measured by dynamic light scattering measurement (left). The PTT:galactose conjugates produced in the presence of cysteine exhibited a smaller average particle size distribution (433.1 nm, PI of 0.19), which reflected the lower estimated level of highly polymerized species (35.3%; >10 degree of polymerization) obtained through size exclusion chromatography. Similarly, the higher average particle size distribution (527.3 nm, PI of 0.25) obtained for PTT:galactose conjugates produced without cysteine are in accordance with the higher proportion (79.7%) of species with high degree of polymerization (>10). These results validate the use of average particle size distribution as an indicator of the level of protein cross-linking within our conjugates.

Table 8.1 shows the experimental conditions and their corresponding observed responses as well as the predicted values for percent blocked lysine and particle size. Comparing runs #2 and 21, where only sodium bisulfite (0.18 mg/mg PTT) was used, and runs #4 and 16, where only cysteine (0.18 mg/mg PTT) was added, reveals the higher percent blocked lysine (7.3–10.4%) and the higher average value of particle size distribution (663.9–768.0 nm) in the presence of cysteine as inhibitor. Fig. 8.2 also shows the larger particle size distribution of the PTT:galatose and PTT:xylose conjugate species in the presence of cysteine (PI of 0.29–0.33) as compared to the reaction containing only sodium bisulfite as inhibitor (PI of 0.25–0.18). The PTT conjugates with higher percent blocked lysine (8.3–18.0%) and smaller particle size (306.9–371.5 nm) were obtained after 4-day incubation when both inhibitors were used at a ratio of 0.5 (runs #5, 7, 17, 26, 28, 30, 32, 37). The highest percent blocked lysine of 25.0 and 38.0 % for PTT:xylose and PTT:galactose conjugates, respectively, were achieved at runs #6 and 15 (6 days of incubation,

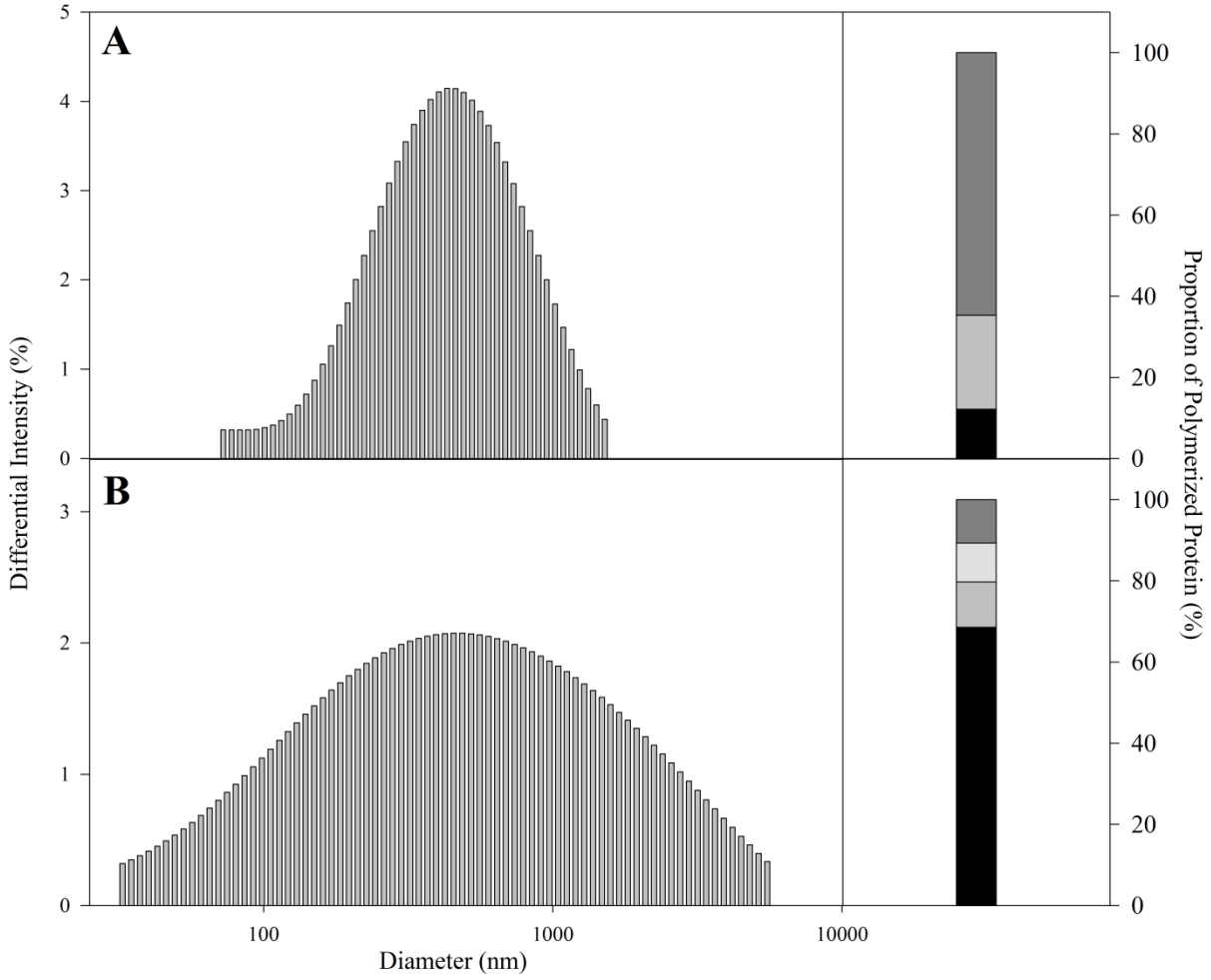

Figure 8.1 Intensity weighted particle size distribution (left) and the proportions of polymerized species (right) of PTT:galactose conjugates produced with (A) or without cysteine (B): extensive polymerization ( ), degree of polymerization >10 ( ), degree of polymerization 3–10 ( ), degree of polymerization <3 ( ).

Table 8.1 Design and experimental results of RSM

Run	Time (days) (X_1)		Inhibitor weight ratio (cys/total) (X_2)		Total inhibitor quantity (mg/mg PTT) (X_3)		Monosaccharide used (X_4)		% Blocked lysine[a]		Particle Size (nm)[b]		
	Actual	(Coded)	Actual	(Coded)	Actual	(Coded)	Actual	(Coded)	Observed	Predicted	Observed	Predicted	PI[c]
1	4.00	(0)	0.50	(0)	0.03	(-1.68)	Galactose	(-1)	20.00	17.83	350.00	288.05	0.20
2	4.00	(0)	0.00	(-1.68)	0.18	(0)	Galactose	(-1)	8.08	7.40	300.00	273.91	0.25
3	4.00	(0)	0.50	(0)	0.18	(0)	Xylose	(1)	3.27	5.71	460.90	390.29	0.25
4	4.00	(0)	1.00	(+1.68)	0.18	(0)	Xylose	(1)	7.27	7.97	768.00	757.37	0.33
5	4.00	(0)	0.50	(0)	0.18	(0)	Galactose	(-1)	17.59	13.01	306.90	340.24	0.27
6	6.00	(+1.68)	0.50	(0)	0.18	(0)	Xylose	(1)	25.00	22.65	947.50	972.00	0.40
7	4.00	(0)	0.50	(0)	0.18	(0)	Xylose	(1)	10.00	5.71	309.60	390.29	0.29
8	5.19	(+1)	0.20	(-1)	0.09	(-1)	Galactose	(-1)	20.00	23.39	348.00	419.31	0.18
9	2.81	(-1)	0.80	(+1)	0.09	(-1)	Xylose	(1)	2.62	2.73	331.30	391.01	0.26
10	4.00	(0)	0.50	(0)	0.33	(+1.68)	Galactose	(-1)	9.22	8.95	391.60	401.89	0.20
11	5.19	(+1)	0.20	(-1)	0.27	(+1)	Xylose	(1)	3.10	3.57	326.60	345.95	0.22
12	4.00	(0)	0.50	(0)	0.18	(0)	Xylose	(1)	3.08	5.71	447.20	390.29	0.25
13	2.81	(-1)	0.20	(-1)	0.09	(-1)	Galactose	(-1)	12.46	15.41	327.10	347.94	0.22
14	2.81	(-1)	0.20	(-1)	0.27	(+1)	Galactose	(-1)	5.12	6.05	277.00	315.12	0.25
15	6.00	(+1.68)	0.50	(0)	0.18	(0)	Galactose	(-1)	38.00	35.72	650.00	561.60	0.45
16	4.00	(0)	1.00	(+1.68)	0.18	(0)	Galactose	(-1)	10.38	8.15	663.90	660.25	0.29
17	4.00	(0)	0.50	(0)	0.18	(0)	Galactose	(-1)	13.95	13.01	310.30	340.24	0.23
18	4.00	(0)	0.50	(0)	0.33	(+1.68)	Xylose	(1)	5.55	6.36	361.60	354.09	0.18
19	5.19	(+1)	0.20	(-1)	0.09	(-1)	Xylose	(1)	5.18	6.10	715.90	718.92	0.34
20	2.81	(-1)	0.80	(+1)	0.09	(-1)	Galactose	(-1)	6.00	6.80	394.80	372.14	0.18
21	4.00	(0)	0.00	(-1.68)	0.18	(0)	Xylose	(1)	0.36	0.10	348.20	314.20	0.18
22	5.19	(+1)	0.80	(+1)	0.27	(+1)	Xylose	(1)	25.00	22.86	836.20	921.91	0.33
23	5.19	(+1)	0.80	(+1)	0.09	(-1)	Galactose	(-1)	20.00	23.49	400.00	448.48	0.22
24	2.81	(-1)	0.80	(+1)	0.27	(+1)	Galactose	(-1)	4.49	6.81	920.90	839.74	0.35
25	2.81	(-1)	0.20	(-1)	0.09	(-1)	Xylose	(1)	3.28	2.43	343.00	365.58	0.18
26	4.00	(0)	0.50	(0)	0.18	(0)	Galactose	(-1)	18.03	13.01	333.70	340.24	0.20
27	4.00	(0)	0.50	(0)	0.18	(0)	Xylose	(1)	3.27	5.71	500.00	390.29	0.26
28	4.00	(0)	0.50	(0)	0.18	(0)	Galactose	(-1)	18.00	13.01	319.50	340.24	0.22
29	2.81	(-1)	0.20	(-1)	0.27	(+1)	Xylose	(1)	0.74	0.96	259.30	241.84	0.29
30	4.00	(0)	0.50	(0)	0.18	(0)	Galactose	(-1)	10.00	13.01	371.50	340.24	0.18
31	2.00	(-1.68)	0.50	(0)	0.18	(0)	Xylose	(1)	5.97	4.47	423.40	407.71	0.20
32	4.00	(0)	0.50	(0)	0.18	(0)	Galactose	(-1)	11.63	13.01	332.00	340.24	0.21
33	2.81	(-1)	0.80	(+1)	0.27	(+1)	Xylose	(1)	8.44	6.46	608.30	644.47	0.28
34	5.19	(+1)	0.20	(-1)	0.27	(+1)	Galactose	(-1)	11.58	11.35	272.70	276.25	0.25
35	2.00	(-1.68)	0.50	(0)	0.18	(0)	Galactose	(-1)	10.38	11.09	565.70	536.28	0.25
36	5.19	(+1)	0.80	(+1)	0.27	(+1)	Galactose	(-1)	20.67	23.51	828.90	736.15	0.33
37	4.00	(0)	0.50	(0)	0.18	(0)	Xylose	(1)	8.28	5.71	307.40	390.29	0.29
38	5.19	(+1)	0.80	(+1)	0.09	(-1)	Xylose	(1)	15.15	15.14	809.30	768.94	0.35
39	4.00	(0)	0.50	(0)	0.18	(0)	Xylose	(1)	3.82	5.71	417.50	390.29	0.24
40	4.00	(0)	0.50	(0)	0.03	(-1.68)	Xylose	(1)	5.17	5.10	450.00	430.19	0.36

[a] Observed values are averages of triplicate measurements
[b] Mean of size distributions obtained from 70 measurements [c] Polydispersity index

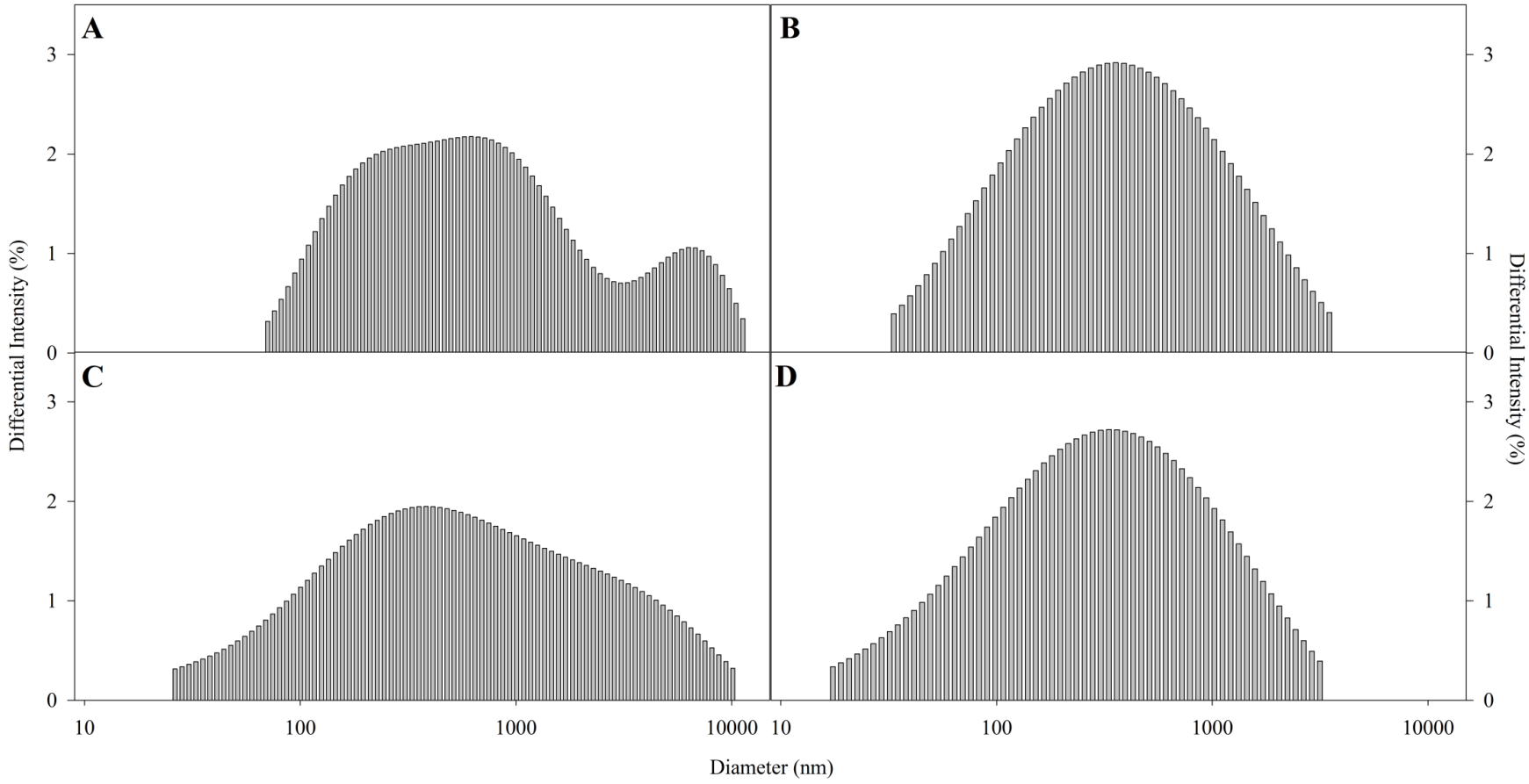

Figure 8.2 Effect of each of cysteine (A, C) and sodium bisulfite (B, D) inhibitors on the particle size distribution of PTT:galactose (A, B) and PTT:xylose (C, D) conjugates.

0.50 ratio of cysteine to total inhibitors, inhibitor quantity of 0.18 mg/mg PTT); at these conditions, the average value of particle size of PTT:galactose conjugates (650.0 nm, PI of 0.45) was lower than that of PTT:xylose conjugates (947.5 nm, PI of 0.40). Increasing the cysteine to total inhibitors ratio to 0.80 and their total quantity to 0.27 mg (run #22) resulted in the highest percent blocked lysine of PTT:xylose conjugates (25.0%) at day 5.19 with an average particle size of 836.2 nm and a PI of 0.33; however, at these conditions (run #36), the percent blocked lysine of PTT:galactose conjugates decreased to 20.7%, whereas the particle size distribution increased to an average of 828.9 nm with a PI of 0.33. The largest particle size of PTT:galactose conjugate species (920.9 nm, PI of 0.35) was obtained at run #24 (cysteine to total inhibitors weight ratio of 0.80; quantity of inhibitors of 0.27 mg/mg PTT; 2.81 days of incubation) with a low percent blocked lysine of 4.5%. The excess of cysteine promoted the cross-linking of PTT:galactose conjugates by generating reactive species upon short incubation time. Decreasing the cysteine to total inhibitors ratio to 0.20 with the same quantity of inhibitors of 0.27 mg/mg PTT (runs #34 and 29) led to the lowest mean particle sizes of PTT conjugate species (272.7 and 259.3 nm). At these conditions, lower percent blocked lysine of PTT:galactose and PTT:xylose conjugates of 11.6 and 0.7%, respectively, were obtained. These last results demonstrate the higher inhibitory effect of sodium bisulfite, which is concentration dependent.

8.4.2. Analysis of Variance and Model Fitting

To find the best percent blocked lysine and the particle size models, Box-Cox plot was used to determine the appropriate power transformation needed to normalize the response data (Sakia, 1992). The Lambda value indicates the power to which all data should be raised in order to transform the data into a normal distribution. Fig. 8.3A and B show the Box-Cox plots for the percent blocked lysine and the average value of particle size. The lower and upper confidence levels show that the best results for normality is reached with Lambda values between 0.17 and 0.61 for the percent blocked lysine and between -0.77 and 0.76 for the particle size. The best Lambda values calculated are 0.40 and 0.06 for the percent blocked lysine and the particle size, respectively. To make the transformation process easier, the best Lambda values were rounded. The recommended Lambda values by the Design Expert software for the transformation of the data were 0.50 (square root transformation) and 0.00 (log transformation) for percent blocked lysine and particle size, respectively.

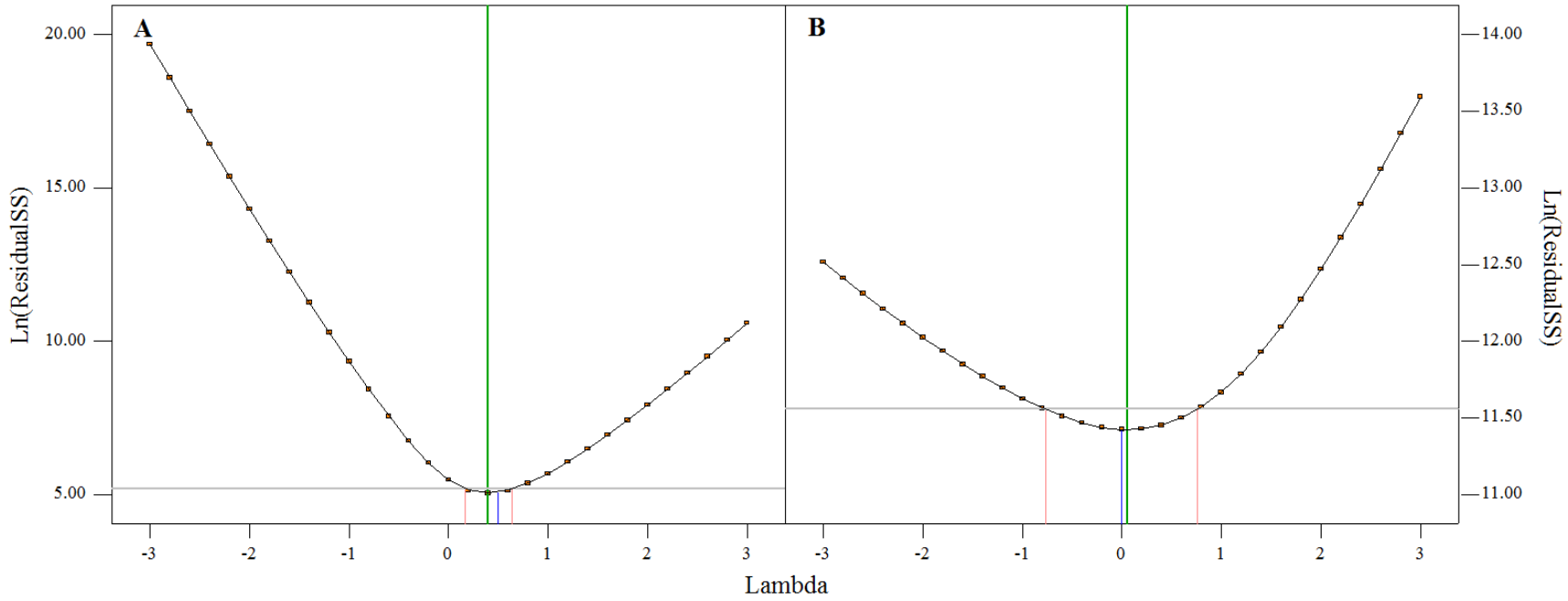

Figure 8.3 Box-Cox plot demonstrating the optimized Lambda for the transformation of the values obtained for percent blocked lysine (A) and particle size (B); confidence intervals (red), best Lambda value (green), recommended Lambda value (blue).

After applying these transformations to the observed data, quadratic model fitting was performed (Table 8.2). Neglecting the insignificant terms by backward elimination regression (α out = 0.05), the results of analysis of variance (ANOVA) indicate that the quadratic model was statistically significant for the description of the variations of the percent blocked lysine (F-value of 29.40 and p-value of < 0.0001) and the average value of particle size of the PTT conjugates (F-value of 30.11 and p-value of < 0.0001). The lack of fit was not significant relative to pure error with F value of 0.37-0.53 and p-value of 0.88–0.97; these results indicate a good quality of the fit and its ability to predict within a range of variables employed. In addition, the closer the coefficient of determination (R^2) value is to 1.00, the better is the model to predict the response (Kaushik et al., 2006). The R^2 of the fitted models was 0.91, which attributes the percent blocked lysine and the particle size to the given independent variables; the R^2 also indicates that only 9 % of the total variations were not explained by the model. The fitted quadratic model for percent blocked lysine and the average value of particle size in terms of coded factors is given in Equations 8.3 and 8.4.

$$\sqrt{Percent\ blocked\ lysine} = 3.00 + 0.79X_1 + 0.40X_2 - 0.14X_3 - 0.61X_4 + 0.33X_1X_2 + 0.37X_2X_3 + 0.35X_2X_4 + 0.22X_3X_4 + 0.37X_1^2 - 0.29X_2^2 \quad (8.3)$$

$$Log_{10}\ (Particle\ size) = 2.56 + 0.06X_1 + 0.11X_2 + 0.009X_3 - 0.03X_4 - 0.03X_1X_3 + 0.05X_1X_4 + 0.10X_2X_3 - 0.03X_3X_4 + 0.07X_1^2 - 0.03X_2^2 \quad (8.4)$$

The significance of each coefficient was determined using the F-test and p-value. The variables are deemed more significant if the F-value is bigger and the p-value is smaller (Atkinson & Doney, 1992). As expected, the linear term with the largest effect on the percent blocked lysine was the incubation time (X_1, F-value of 94.96, p-value of < 0.0001); more carbohydrate conjugation is expected to occur with an increase in the incubation time. The variable with the largest effect on the particle size of conjugates was the linear term of inhibitor ratio (X_2, F-value of 111.90, p-value of < 0.0001). This demonstrates the significance of the interaction occurring between both selected Maillard reaction inhibitors to modulate the protein cross-linking. On the other hand, the effect of incubation time on the level of protein cross-linking (particle size distribution) is expected to be significant due to the progress of the Maillard reaction towards the intermediate and the advanced stages. However, the presence of Maillard reaction inhibitors

Table 8.2 Analysis of variance of blocked lysine and of particle size

Source	Blocked Lysine[a]					Particle Size[b]				
	Sum of Squares	df[c]	Mean Square	*F* Value	*p*-value[d]	Sum of Squares	df[c]	Mean Square	*F* Value	*p*-value[d]
Model	52.47	10	5.24	29.40	< 0.0001	0.96	10	0.10	30.11	< 0.0001
X_1 (Time)	16.95	1	16.95	94.96	< 0.0001	0.10	1	0.10	29.96	< 0.0001
X_2 (Inhibitor ratio)	4.27	1	4.27	23.90	< 0.0001	0.36	1	0.36	111.90	< 0.0001
X_3 (Total inhibitors)	0.57	1	0.57	3.18	0.0848	0.002	1	0.002	0.69	0.4142
X_4 (Carbohydrate)	14.82	1	14.82	83.02	< 0.0001	0.04	1	0.04	11.13	0.0023
X_1X_2	1.80	1	1.80	10.10	0.0035	–	–	–	–	–
X_1X_3	–	–	–	–	–	0.02	1	0.02	6.02	0.0204
X_1X_4	–	–	–	–	–	0.08	1	0.08	24.22	< 0.0001
X_2X_3	2.21	1	2.21	12.36	0.0015	0.16	1	0.16	50.33	< 0.0001
X_2X_4	3.43	1	3.43	19.25	0.0001	–	–	–	–	–
X_3X_4	1.35	1	1.35	7.57	0.0101	0.03	1	0.03	9.98	0.0037
X_1^2	4.01	1	4.01	22.44	< 0.0001	0.16	1	0.16	49.43	< 0.0001
X_2^2	2.47	1	2.47	13.85	0.0008	0.03	1	0.03	10.83	0.0026
Residual	5.18	29	0.18			0.09	29	0.003		
Lack of Fit	2.12	19	0.11	0.37	0.9715	0.05	19	0.002	0.53	0.8845
Pure Error	3.05	10	0.31			0.05	10	0.005		
Cor Total	57.64	39				1.05	39			

[a] $R^2 = 0.910216$.
[b] $R^2 = 0.912094$.
[c] Degree of freedom.
[d] *p*-value < 0.05 = statistically significant.

diminished the extent of the effect of incubation time on the level of particle size (X_1, F-value of 29.96, p-value of < 0.0001) as compared to its effect on the percent blocked lysine. The linear term of the inhibitor ratio exhibited the third largest effect on the percent blocked lysine (X_2, F-value of 23.90, p-value of < 0.0001). The fact that cysteine can participate directly in the Maillard reaction must have affected the percent blocked lysine differently depending on the ratio of cysteine to total inhibitors.

For the percent blocked lysine model, the effect of the linear term of the type of the carbohydrate (X_4, F-value of 83.02, p-value of < 0.0001) was the second largest one. The difference in the glycation rate between aldopentoses and aldohexoses has already been reported (Seo & Karboune, 2014). The variable with the second largest effect on the particle size was the interactive parameter between the inhibitor ratio and the total quantity of inhibitors (X_2X_3, F-value of 50.30, p-value of < 0.0001); this confirms the effect of inhibitors on the level of protein cross-linking occurring during the Maillard reaction. Among all interactive effects, the most important one for the percent blocked lysine model was the one between the inhibitor ratio and the type of monosaccharide (X_2X_4, F-value of 19.25, p-value of < 0.0001), demonstrating that the two selected inhibitors have different effects on the glycation extent depending on the type of monosaccharide used. The interactive effect between the inhibitor ratio and the type of monosaccharide was non-significant for the particle size model. The second most important interactive parameter for the percent blocked lysine was the one between the inhibitor ratio and the total quantity of inhibitors (X_2X_3, F-value of 12.36, p-value of 0.0015); these results indicate that the effect of inhibitor ratio on the glycation extent is significantly affected by the total quantity of inhibitors used. Although the individual effect of incubation time on the particle size was less important as compared to its effect on the percent blocked lysine, it had statistically significant interactive effects with total quantity of inhibitors (X_1X_3, F-value of 6.02, p-value of < 0.0204) and with the type of monosaccharide used (X_1X_4, F-value of 24.22, p-value of < 0.0001). This demonstrates that depending on the quantity of inhibitors and the carbohydrate present within the reaction system, incubation time had different effects on the particle size distribution of the conjugates. These interactive effects were not observed in the percent blocked lysine model. In terms of quadratic effects, the incubation time (X_1^2, F-value of 22.44-49.43, p-value of

< 0.0001) and the inhibitor ratio (X_2^2, F-value of 10.83-13.85, p-value of 0.0008) had significant effects on both percent blocked lysine and the particle size.

To verify the accuracy of the predictive models, the observed values for the percent blocked lysine and the average value of particle size were plotted against the predicted ones (Fig. 8.4A, B). There was no significant deviation from the models, and the predicted data of the responses were in agreement with the observed ones in the investigated range of the variables. The values of residuals for the response factors were plotted in a normal probability plot (Fig. 8.4C, D). A residual is the difference between the observed value and the predicted value. The normal probability plot is often used to verify the normality assumption. Almost all data points formed a straight line and were placed within the 95% confidence interval indicating that the calculated residuals follow a normal distribution. To test for the assumption of constant variance, a plot of residuals versus the predicted response was verified (Fig. 8.4E, F). The residual scatters were randomly displayed (constant range of residuals across the graph), demonstrating that the variance of the original observation was constant for all values of the responses.

8.4.3. Effects of Glycation Parameters on the Percent Blocked Lysine of Conjugates

The 2D contour plots generated from the predicted model of the percent blocked lysine show the interactive effect of incubation time/ inhibitor ratio at constant quantity of total inhibitors of 0.18 mg/mg PTT and that of inhibitor quantity/ inhibitor ratio at an incubation time of 5.19 days (Fig. 8.5). Higher percent blocked lysine could be obtained with galactose (Fig. 8.5A, C) as compared to xylose (Fig. 8.5B, D). These results may be due to higher degradation of xylose decreasing its availability and leading to advanced cross-linking of its conjugates (Hofmann, 1999). The effect of the inhibitor ratio on the blocked lysine of conjugates was not as significant as that of the incubation time. The interaction between the incubation time and the inhibitor ratio (ellipsoidal lines) was mostly observed at higher cysteine to total inhibitors ratio and upon longer incubation time (Fig. 8.5A, B). Increasing the incubation time resulted in an increase of the percentage of blocked lysine of conjugates. On the other hand, the highest percent blocked lysine was achieved upon the use of a high ratio of cysteine to total inhibitors; however, higher quantities of cysteine had more effect on the percent blocked lysine of PTT:xylose conjugates than on that of PTT:galactose conjugates. This difference between xylose and galactose can be explained by the cysteine's participation in the Maillard reaction leading to the production of reactive dicarbonyls,

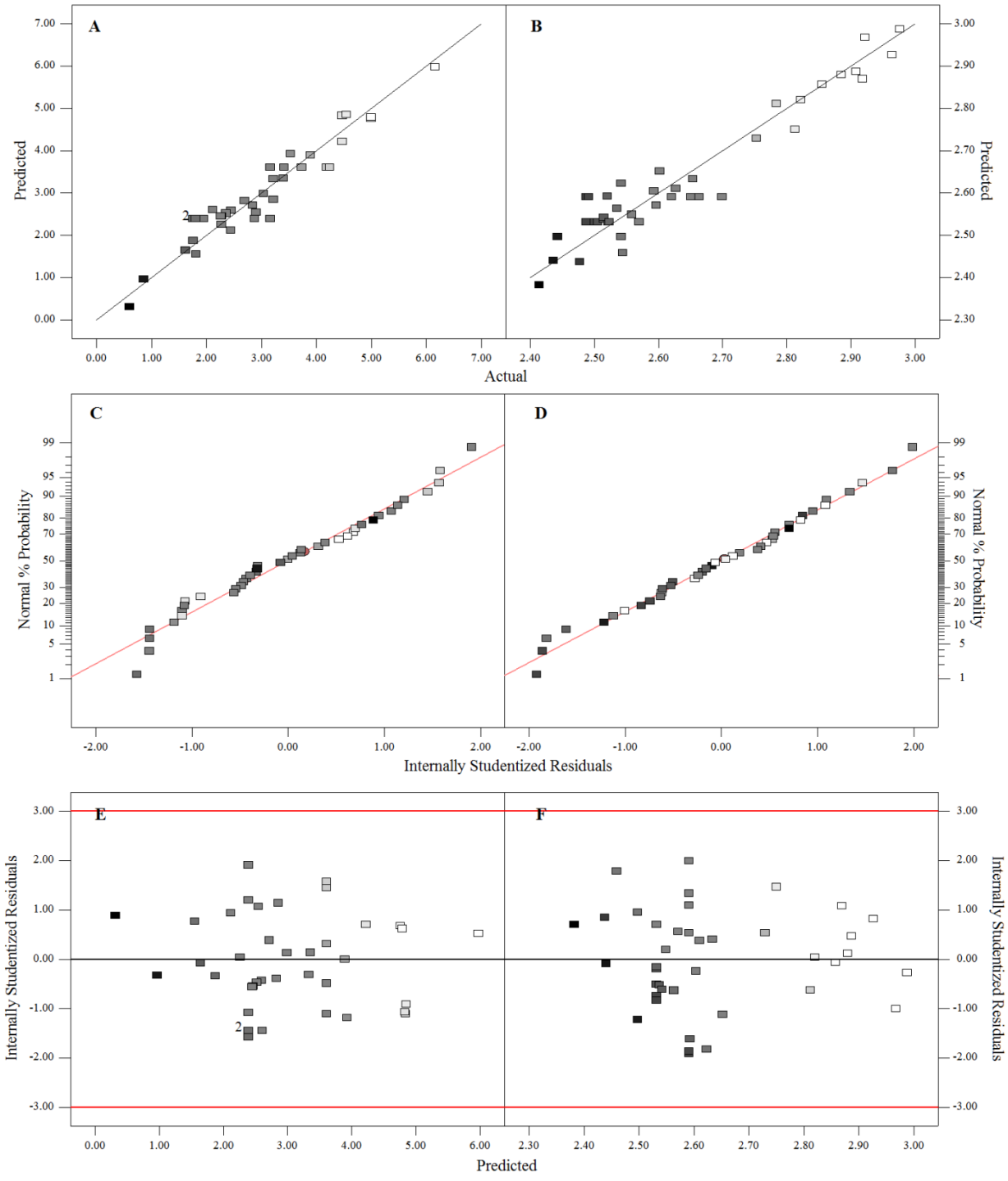

Figure 8.4 Actual vs predicted values (A, B), normal plots of residuals (C, D), plot of internally studentized residuals vs predicted values (E, F) for percent blocked lysine (A, C, E) and for particle size (B, D, F).

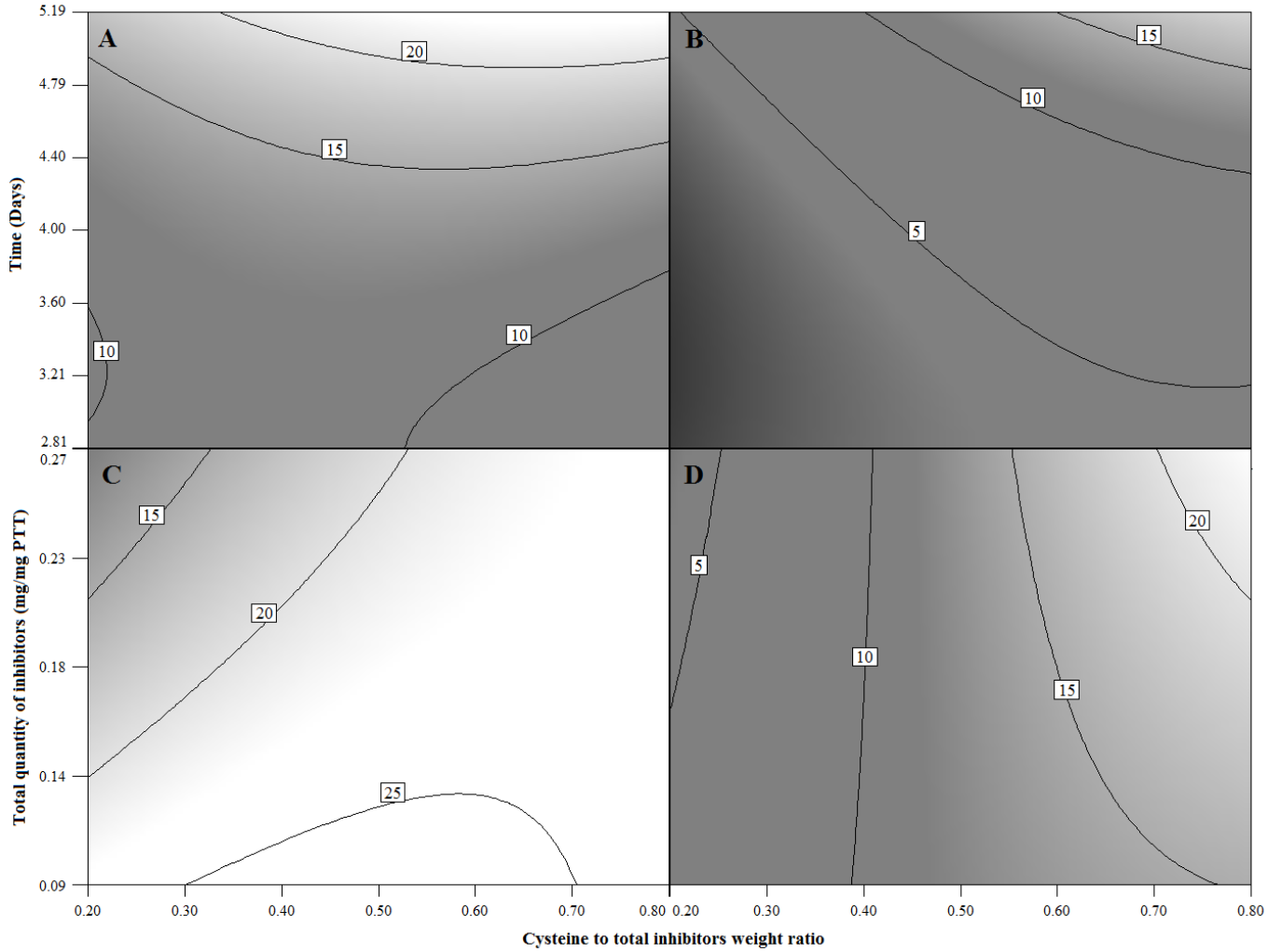

Figure 8.5 Contour plots of percent blocked lysine as a function of incubation time and cysteine/total inhibitors ratio at a constant total inhibitor quantity of 0.18 mg/mg of PTT (A, B) and as a function of cysteine/total inhibitors ratio and total inhibitor quantity at 5.19 days of incubation (C, D) of PTT conjugated with galactose (A, C) or with xylose (B, D). The numbers inside the contour plots indicate the predicted values under given reaction conditions. Percent blocked lysine: 0.36 38.00.

which may have increased the reactivity of xylose to undergo glycation with PTT (Yeboah et al., 2000).

Fig. 8.5C and D show that the interaction between the total quantity of inhibitors and their ratio occurred mainly in the PTT:galactose glycation reaction system in the presence of larger quantities of inhibitors. This interaction was not significant in the PTT:xylose glycation reaction system. Indeed, at a constant inhibitor ratio, the percent blocked lysine of PTT:xylose conjugates remained constant as the total quantity of inhibitors increased; however, increasing the cysteine to total inhibitors ratio resulted in an increase of the percent blocked lysine of PTT:xylose conjugates. Higher quantities of cysteine was needed in the PTT:xylose glycation reaction system to improve the glycation level, confirming the inducing effect of cysteine on the glycation level of PTT:xylose conjugates as previously mentioned. On the other hand, PTT:galactose conjugates achieved the highest percent blocked lysine when lower quantities of inhibitors were used at a ratio of 0.5. Indeed, in the PTT:galatose glycation reaction system, the increase in the quantity of total inhibitors had a negative effect on the percent blocked lysine in the presence of an excess of sodium bisulfite as compared to cysteine. These results can be attributed to the higher inhibitory effect of sodium bisulfite at higher concentrations at the initial stage of the Maillard reaction as reported by Scaman et al. (2006). The lower inhibitory effect of cysteine as compared to sodium bisulfite was demonstrated by Friedman and Molnar-Perl (1990), who have investigated the browning extent occurring during the incubation of different amino acids with glucose. Indeed, the reaction of the amino group of cysteine with the carbonyl group of the carbohydrate can lead to the formation of reactive species that favor the carbohydrate conjugation (Yeboah et al., 2000).

8.4.4. Effects of Glycation Parameters on the Particle Size Distribution of Conjugates

The 2D contour plots presented in Fig. 8.6 illustrate the interactive effects of incubation time/inhibitor quantity (at inhibitor ratio of 0.8) and inhibitor ratio/inhibitor quantity (at 5.19 days of incubation) on the predicted average value of particle size. Generally, higher average particle size of aggregates was obtained in the PTT:xylose glycation reaction system (Fig. 8.6B, D) as compared to the PTT:galactose one (Fig. 8.6A, C). These experimental findings confirm the higher formation of polymerized species in the presence of xylose. This accumulation of polymerized species may have been accelerated upon the autoxidation/glycoxidation of xylose.

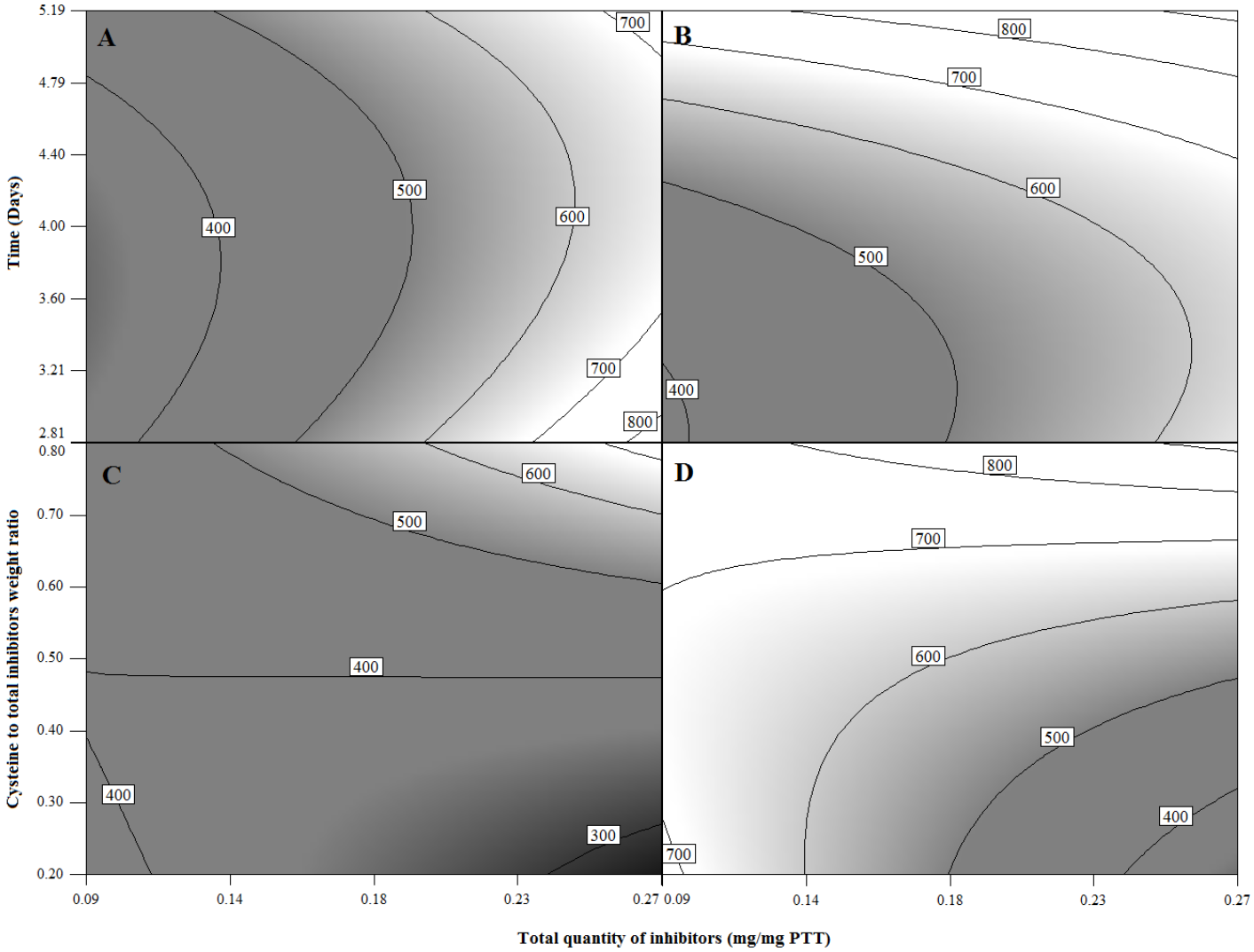

Figure 8.6 Contour plots of particle size as a function of incubation time and total inhibitor quantity at cysteine/total inhibitors ratio of 0.80 (A, B) and as a function of cysteine/total inhibitors ratio and total inhibitor quantity at 5.19 days of incubation (C, D) of PTT conjugated with galactose (A, C) or with xylose (B, D). The numbers inside the contour plots indicate the predicted values under given reaction conditions. Particle size (nm): 259.30 947.50.

Hofmann (1999) has reported that more reactive dicarbonyls were formed upon the autoxidation/glycoxidation of pentoses than hexoses. The incubation time/inhibitor quantity contour plots display different trends for both PTT:galactose (Fig. 6A) and PTT:xylose (Fig. 8.6B) conjugates. An hyperbolic interactive effect was obtained in the PTT:xylose glycation reaction system, in which an increase in the incubation time had more effect on the particle size compared to the total inhibitor quantity. The variations of the predicted particle size of PTT:xylose conjugates with the incubation time and the total inhibitor quantity showed similar trends as the predicted percent blocked lysine. On the other hand, the incubation time/inhibitor quantity interaction exhibited a polynomial effect on the predicted particle size of PTT:galactose conjugates with the total inhibitor quantity being more significant in increasing the particle size. The progression of the Maillard reaction with the incubation time is expected to lead to more protein cross-linking and hence to high particle size distribution of the conjugates. Contrary to the percent blocked lysine of PTT:galactose conjugates, the increase in the incubation time as the independent variable did not increase significantly their particle size distribution. These results may be due to the low generation of the reactive carbonyl over the investigated incubation time in the presence of galactose.

Fig. 8.6C and D indicate that the interactive effect of the inhibitor ratio and their total quantity on the particle size of conjugates was more significant in the presence of an excess of cysteine (> ratio of 0.6) for the PTT:galactose conjugates and of sodium bisulfite (< ratio of 0.5) for the PTT:xylose conjugates. Below and above these values of the inhibitor ratio, the particle size of the conjugates remained constant as the total quantity of the inhibitor increased. At a constant total quantity of inhibitors, the particle size of PTT:galactose and PTT:xylose conjugates increased with the increase of the ratio of cysteine to total inhibitor ratio. The contour plots of predictive percent blocked lysine (Fig. 8.5) showed similar trends in that higher levels of glycation were obtained when the proportion of cysteine was greater than the proportion of sodium bisulfite (> ratio of 0.50). The side reaction of cysteine with the carbohydrate may have led to the formation of reactive dicarbonyl species that favor the conjugation of PTT (Fig. 8.5), but also participate in protein cross-linking (Fig. 8.6).

8.4.5. Model Validation and Optimization

Using the predictive models (Equations 8.3 and 8.4), the optimum glycation parameters for the production of conjugates with the highest conjugation level and the lowest particle size were determined. The desirability being an objective function that ranges from zero outside of the limits to one at the goal was looked at as an indication to obtain the optimal PTT conjugates (Myers & Montgomery, 1995). The optimization process finds a point (or reaction condition) that maximizes the desirability function. The lowest observed blocked lysine (0.4 %, run #21) and the highest observed blocked lysine (38.0 %, run #15) values during the experimental runs (Table 8.1) were assigned as desirability of 0 and 1, respectively. In addition, the highest observed particle size (947.5 nm, run #6) and the lowest observed particle size (259.3 nm, run #29) values were assigned as desirability of 0 and 1, respectively. This assignment of desirability allows for the identification of the level of predicted variables producing the most desirable predicted responses. The 2D plot of the desirability indicates that the optimum reaction conditions were 5.19 days of incubation, 0.42 and 0.54 cysteine to total inhibitors ratio, and 0.09 and 0.27 mg of total inhibitors to obtain 26.3 and 14.0 % of blocked lysine and 400.2 and 544.3 nm of particle size for PTT:galactose conjugates (Fig. 8.7A) and PTT: xylose ones (Fig. 8.7B), respectively. The higher desirability of PTT:galactose glycation reaction system (0.71) as compared to the PTT:xylose one (0.45) demonstrates that the percent blocked lysine and the average particle size distribution of PTT:galactose conjugates were closer to the desired values obtained during the experimental runs. The approximately equal quantity of cysteine and sodium sulfite needed for the optimum production of these conjugates demonstrates that both inhibitors act synergistically at close to equal concentrations while exerting an adverse effect when the presence of one inhibitor is greater than the other. The validation of the model was done by carrying out quadruplicate experiments under the predicted optimum conditions. Under the optimum conditions, the experimental percent blocked lysine of 25.1 ± 1.5 % and 13.7 ± 0.5 % as well as the particle size of 404.0 nm and 506.3 nm obtained for the glycation reaction system with galactose and xylose, respectively, were in good agreement with the predicted values. The slight difference in the particle size between the experimental and the predicted values are due to the protein polymerization not occurring uniformly, as reflected by the PI of 0.25 for both PTT:galactose and PTT:xylose conjugates, which is indicative of a polydisperse system. Using the identified optimal combination of cysteine and sodium bisulfite, higher percents blocked

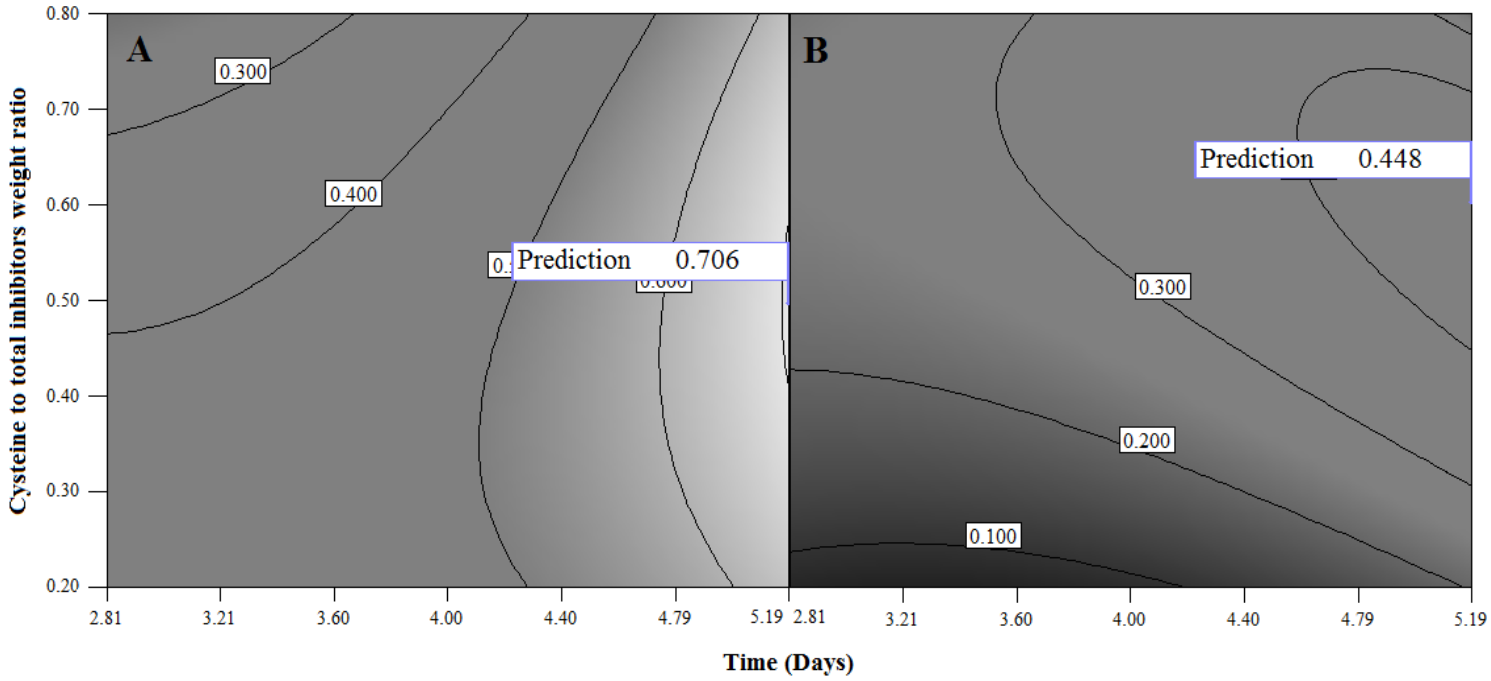

Figure 8.7 Desirability graph of PTT conjugation with galactose (A) or with xylose (B) to obtain the highest level of blocked lysine and the smallest particle size. Desirability: 0 1.

lysine values (13.7–25.1%) were obtained than using each of cysteine (7.3–10.4%) or sodium bisulfite (0.4–8.1%) inhibitor alone. The average particle sizes of conjugates produced in the presence of both inhibitors were higher than those obtained using only sodium bisulfite (300.0–348.2 nm), but lower than the sizes achieved using only cysteine (663.9–768.0 nm). Without inhibitors, higher particle sizes of PTT conjugates (645.7–2987.8 nm, ≤1 day of incubation) were previously obtained (Seo & Karboune, 2014). These results confirm the effectiveness of the identified optimal combination of cysteine and sodium bisulfite in inhibiting the protein cross-linking, occurring at the intermediate/advanced stages of the Maillard reaction, without limiting the glycation of PTT that takes place at the early stage.

8.5. Conclusion

The CCRD and RSM were successfully applied for the investigation of the effects of incubation time, cysteine to total inhibitorsratio, and total quantity of inhibitors on the production of PTT conjugated with galactose or with xylose through Maillard reaction. The optimal conditions for conjugates production that maximize the conjugation level of PTT and minimize the protein cross-linking were also identified. The incubation time and the inhibitor ratio were the most significant independent variables affecting the percent blocked lysine and the particle size, respectively. The most important interactive effects were between the monosaccharide used and the inhibitor ratio and between the inhibitor ratio and the total quantity of inhibitors for percent blocked lysine and particle size, respectively. The presence of larger quantities of cysteine led to higher percent blocked lysine, but also to bigger particle size due to the production of dicarbonyls during the early stage of the reaction; while the use of an excess of sodium bisulfite generally led to an overall inhibition of the Maillard reaction. Therefore, the combination of sodium bisulfite and cysteine was essential in improving the glycation extent of the PTT conjugates and in minimizing their protein cross-linking.

CONNECTING STATEMENT 7

In Chapter IX, a glycosidase-catalyzed transglycosylation reaction was investigated as a new approach for the production of amino acid/peptides/proteins:carbohydrate conjugates. The synthesis of galactosylated serine/threonine derivatives by *β*-galactosidase from *Escherichia coli* were investigated in buffer and biphasic organic solvent mixture and using lactose or ONPG as donors. Molecular docking simulations were explored as a structure-based computational tool to provide the structural basis of the enzyme's selectivity and to compare the relative binding affinities of enzyme towards different serine/threonine derivatives.

The results of this study will be presented at IUFoST2014 and published in the *Journal of Molecular Catalysis B:Enzymatic.*

Seo, S., Rebehmed, J., de Brevern, A. G., & Karboune, S. (2014) *Investigation of Transglycosylation by β-Galactosidase Using Serine/Threonine Derivatives as Acceptor Models*, IUFoST2014, Montreal, Quebec, August 17-21 .

Seo, S., Rebehmed, J., de Brevern, A. G., & Karboune, S. (2014) Enzymatic synthesis of galactosylated serine/threonine derivatives using *β*-galactosidase from *Escherichia coli*. (To be submitted)

CHAPTER IX

ENZYMATIC SYNTHESIS OF GALACTOSYLATED SERINE/THREONINE DERIVATIVES USING *β*-GALACTOSIDASE FROM *ESCHERICHIA COLI*

9.1. Abstract

The potential applications of structurally defined glycoproteins and glycopeptides have led to the investigation of different strategies for their production. In this study , experimental assays and docking simulations were used to study the second step of the mechanism of transgalactosylation of β-galactosidase from Escherichia coli for the synthesis of galactosylated serine/threonine derivatives. Using lactose or ONPG as donor substrates, the yields of galactosylated serine/threonine derivatives were dependent on the C/N-protecting groups of the acceptors. The highest yields were achieved in the heptane:buffer biphasic media (70:30). The structures of most abundant galactosylated serine products were characterised by MS/MS. The binding of serine/threonine derivatives to the enzyme's active site were found to be stronger (-4.6 - -7.9 kcal/mol) than the natural acceptor, glucose, and mainly occurred through interactions with aromatic residues. For N-tert-butoxycarbonyl serine methyl ester (6.8%) and N-carboxybenzyl serine benzyl ester (3.4%), their binding affinities and the distances between their hydroxyl side chain and the 1'-OH group of galactose moiety were in good accordance with the quantified transgalactosylation yields. Despite its lower predicted bioconversion yield. However, the high bioconversion experimental yield obtained with N-carboxybenzyl serine methyl ester (23.2%) despite its unfavorable theoretical predictions by the docking simulations demonstrated the importance of the thermodynamically driven nature of the transgalactosylation reaction.

9.2. Introduction

There is a growing interest in new approaches to synthesize glycoproteins and glycopeptides, consisting of amino acids/peptides/proteins moieties with carbohydrate substituents. These glycoproteins and glycopeptides play important roles in many biological systems (Schwarz & Datema, 1982), such as protection against proteolytic enzymes, cell-cell recognition, cell growth, oncogenesis (Feizi, 1985; Olden et al., 1982). In addition, the improvements in the functional properties of carbohydrate conjugated food proteins, such as emulsifying activity, protein solubility, and thermal stability, have been previously demonstrated (Oliver et al., 2006b). These advantages emphasize the need for a highly specific method for the formation of glycosidic bonds between carbohydrates and amino acids/peptides/proteins. Because of the presence of various functional hydroxyl groups in saccharides, sequential selective protection-deprotection steps of these functional groups are needed in order to control the stereochemical and

regiochemical specificity of the glycosidic bond formed through chemical synthesis. Contrary to the chemical synthesis, enzymatic synthesis often offers regio- and stereospecificity to the glycosidic linkages.

Glycosidases (EC 3.2.1.) catalyze the hydrolysis of glycosidic linkages but can also catalyze their formation. The applications of glycosidases for the synthesis of glycoproteins and glycopeptides rely on the thermodynamic equilibrium of the reaction and/or on the affinity of the enzyme to transfer the glycosyl moiety of a substrate to other acceptors than water. The synthetic reaction-catalyzed by glycosidases may be thermodynamically favored over the hydrolytic one by using high substrate concentration, elevated temperatures and organic co-solvents (Dordick, 1989). The use of an appropriate glycoside donor may also kinetically favor the transglycosylation activity of glycosidase.

β-Galactosidase (EC 3.2.1.23, Fig. 9.1A) hydrolyzes the *β*-D-1-4 linkage of lactose releasing glucose and galactose as end-products or converting them into allolactose (*β*-D-1-6 linkage). This enzyme is a retaining glycosidase because it maintains the initial conformation on the anomeric carbon of the substrate (Brás et al., 2010). The active site of *β*-galactosidase has two subsites with only one being highly specific for the galactose moiety. This lack of specificity of one subsite allows the binding of a wide variety of substrates, other than lactose, that can act as acceptors (Brás et al., 2010). The first step of the mechanistic action of *β*-galactosidase-catalyzed reaction involves a cleavage of the glycosidic bond of the lactose or galactose-substituted molecules, and the formation of the covalent galactosyl-enzyme intermediate (Sinnott, 1990). The initial shallow binding of donor is achieved through their stacking on Trp568 by a network of specific interactions made by the galactosyl hydroxyls with the galactose-specific subsite and by few interactions made by the leaving group with the second subsite. Subsequently, the donor substrate moves deeper into the active site pocket, improving the interactions made between the enzyme and the 2- and 3-OH. The deeper binding mode is associated with a conformational change in which the 794–804 loop moves closer to the active site (Juers et al., 2001). As the substrate moves into the deeper binding mode (Fig. 9.1B), the first catalytic carboxylic acid, Glu461, contacts the glycosidic oxygen and donates a proton to the glycosidic oxygen in concert with formation of the covalent intermediate with Glu537. The second mechanistic step of *β*-galactosidase-catalyzed reaction involves the galactosyl transfer from nucleophile Glu537 to an

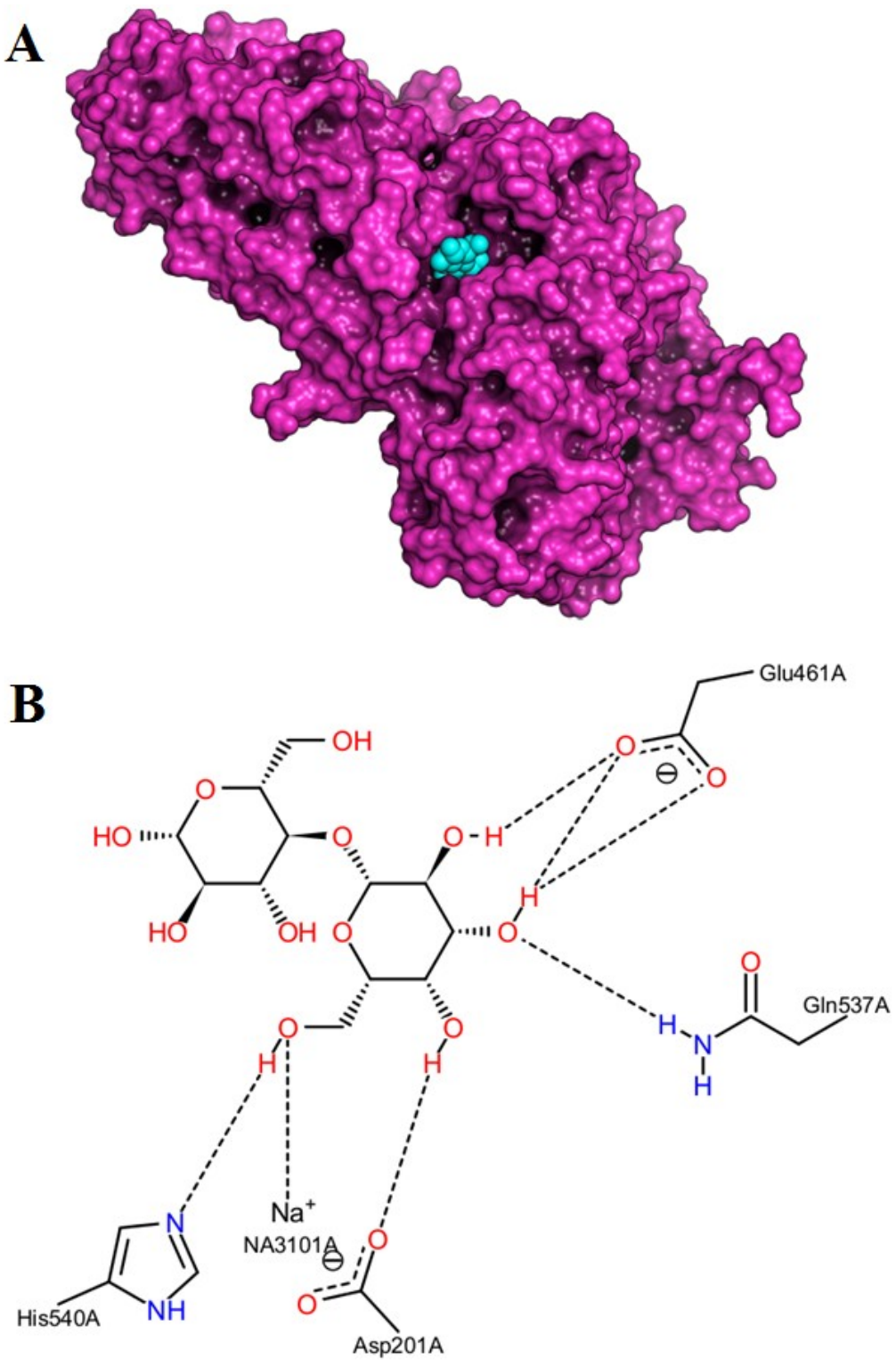

Figure 9.1 Experimental crystallography structure of the *β*-galactosidase lacZ of *E. coli* (PDB code: 1JYN, chain A, surface, purple) in complex with a lactose moiety (spheres, cyan) in the active site using PyMOL (A). Visualization of the interactions between the lactose moiety and the *β*-galactosidase enzyme with PoseView (B).

acceptor. During this degalactosylation step, a trigonal oxocarbenium ion as a transition state is formed and stabilized by interactions between Glu537, Try503, and the galactosyl ring oxygen. This transition state only forms in the presence of both incoming and leaving groups. The leaving group (glucose or *o*-nitrophenyl) can be replaced by a water molecule (hydrolysis) or by another acceptor substrate (transgalactosylation) (Matthews, 2005).

The elucidation of binding affinity, interactions and orientations of selected substrates in the *β*-galactosidase's active site can contribute to the understanding of its transgalactosylation efficiency and to the identification of a more suitable substrate for the effective production of galactosylated amino acid/peptide/protein derivatives. Only limited studies (Attal et al., 1992; Bay et al., 1993; Becker & Kuhl, 1999; Cantacuzene & Attal, 1991; Holla et al., 1992; Johansson et al., 1991; Layer & Fischer, 2006) have investigated the galactosylation of amino acid/peptide/protein by *β*-galactosidase. Structure-based computational methods, such as molecular docking, have been demonstrated to be useful in calculating the position and the orientation of a potential substrate in a binding site of an enzyme (Honarparvar et al., 2014). Most of the docking programs use empirical potential energy functions to calculate the binding energies of enzyme-substrate complexes, which involve Van-der-Waals, Coulomb electrostatic interactions, and hydrogen bonds.

In the present study, a commercially available *β*-galactosidase from *Escherichia coli* was used as biocatalyst for the transgalactosylation of a protected serine in the presence and in the absence of organic solvents, such as heptanone and heptane. The synthesis of galactosylated serine/threonine derivatives through *β*-galactosidase-catalyzed transgalactosylation reaction were investigated using the most suitable solvent. Molecular docking simulations were explored as a structure-based computational tool to provide the structural basis of the enzyme's selectivity and to compare the relative binding affinities of enzyme towards different serine/threonine derivatives.

9.3. Materials and Methods

9.3.1. Materials

The enzyme, E .coli *β*-galactosidase, lactose, *ortho*-nitrophenyl-*β*-galactoside (ONPG), the serine and threonine derivatives and other chemicals were purchased from Sigma Chemical Co. (St–Louis, MO, USA).

9.3.2. Enzymatic Transgalactosylation

Prior to each enzymatic reaction, stock solutions of lactose or ONPG and *N*-carboxy-benzyl-serine methyl ester (*N*-Z-Ser-OMe) were prepared in 50 mM sodium phosphate buffer pH 7.8 with 2 mM magnesium chloride. These stocks solutions were mixed with the appropriate amount of heptane and heptanone to achieve substrate molar ratios of 1:3, 1:3, 3:1, 9:1 (1 = 50 μmol) in heptane:buffer and heptanone:buffer (70:30) reaction mixture media. To initiate the reaction, β-galactosidase (80 U/ml) was added to the reaction mixture. All reactions were performed in an incubator at 40°C and with continuous shaking at 200 rpm. Trangalactosylation reactions were run in duplicate alongside controls containing no enzyme, and were monitored at specific time intervals over the course of 24 h of reaction. Aliquots of reaction mixtures were dried off under vacuum, using an Automatic Environmental Speed Vac system (Savant Instruments Inc., Holbrook, NY).

9.3.3. Acceptors Specificity

The acceptor specificity of *E .coli* β-galactosidase was investigated using serine and threonine derivatives as acceptors including *N*-*tert*-butoxy-carbonyl L-serine methyl ester (*N*-Boc-Ser-OMe), *N*-*tert*-butoxy-carbonyl L-serine (*N*-Boc-Ser-OH), Fluorenyl-methyloxy-carbonyl L-serine (*N*-Fmoc-Ser-OH), *N*-carboxy-benzyl L-threonine methyl ester *(N*-Z-Thr-OMe), *N*-carboxy-benzyloxy L-threonine (*N*-Z-Thr-OH), *N*-*tert*-butoxy-carbonyl L-serine benzyl ester (*N*-Boc-Ser-OBzl), *N*-carboxy-benzyl L-serine benzyl ester (*N*-*Z*-Ser-OBzl), and serine-glutamic acid (Ser-Glu). The transgalactosylation reactions were run as described previously using a substrate molar ratio of 1:3 in heptane: sodium phosphate buffer reaction mixture (70:30).

9.3.4. Analytical Methods

The quantification of galactosylated serine/threonine derivatives was performed using a Waters HPLC system (Milford, MA, USA) equipped with TSK Gel-Amide 80 column (4.6 mm × 250 mm, 5 μm particle size, TOSOH Bioscience LLC, Montgomeryville, PA, USA) equipped with UV diode-array detector (Model 2998) and refractive index detector (Model 410). The elution of the reaction mixture was conducted with acetonitrile:water mobile phase (82:18) at a flow rate of 0.7 ml/min. Amount of galactosylated serine/threonine derivatives was estimated using Breeze software. Yield (%) was calculated as the amount of galactosylated serine/threonine derivatives over the initial amount of acceptors, multiplied by 100.

Accurate mass measurements and MS/MS analyses for the identification of produced transgalactosylated serine/threonine derivatives were performed using a Synapt G2-S instrument (Waters) in positive and in negative electrospray and resolution mode. MS/MS spectra were acquired on defined masses with a 30V collision energy.

9.3.5. Computational Analysis

The experimental structure of *β*-galactosidase from *E. coli* in complex with a lactose moiety (PBD ID: 1JYN) or a galactose moiety (PDB ID: 1JZ7, resolution 1.5 Å) (Juers et al., 2001) were used as model for Fig. 9.1 and for the docking simulations, respectively. Autodock Vina search method, which consists of a genetic algorithm combined with local gradient optimization (Trott & Olson, 2010), was used to generate 20 different binding modes (docked poses) for each ligand with a grid box of 25 × 25 ×25 $Å^3$ positioned at the active site of the enzyme. A geometric criterion was used, i.e., the OH group of amino acid close to 1′-OH of the galactose moiety to form the linkage during the transgalactosylation. Then the most favorable binding modes according to predicted binding affinities were selected and analyzed. Visualization of the 3D enzyme/substrates complexes were made using PyMOL (The PyMOL Molecular Visualization System, Version 1.6, Shrödinger, LLC, Portland, OR). The 2D complex diagram was produced by PoseView webserver (Stierand et al., 2006).

9.4. Results and Discussion

9.4.1. Effect of Selected Reaction Media on the Transgalactosylation of Serine Derivative

The transgalactosylation of *N-Z*-Ser-OMe by *E.coli β*-galactosidase using lactose or ONPG as donor substrate was carried out in buffer and in selected two biphasic reaction systems (Table 9.1). Heptane (Log P of 4.27) and heptanone (Log P of 1.98) with different hydrophobicity were used as co-solvent to form the biphasic reaction systems. In order to reduce the water activity, 70% of organic solvent was used. Higher yields of transgalactosylated *N*-Z-Ser-OMe were obtained when using ONPG as donor compared to lactose. These results may reveal the high substrate affinity of *E.coli β*-galactosidase towards the ONPG, which may have released more energy upon its cleavage, leading to a more efficient transfer of the galactose to the acceptor. Using ONPG as donor, the highest yield of transgalactosylated *N-Z*-Ser-OMe (23.2%) was achieved in heptane:buffer reaction system, whereas with the lactose, the highest yield (3.94%)

Table 9.1 Transgalactosylation of *N*-Z-Ser-OMe in aqueous and in aqueous-organic solvent reaction systems using different substrate ratios

Ratio of sugar to serine	Sugar	Reaction time (h)	Bioconversion yield (%) Reaction media		
			Buffer	Heptane:buffer (70:30)	Heptanone:buffer (70:30)
1:1	ONPG	5	< 0.01	2.01 (± 0.47)	0.13 (± 0.12)
		12	0.26 (± 0.07)	0.42 (± 0.11)	< 0.01
		24	< 0.01	< 0.01	< 0.01
	Lactose	5	3.94 (± 0.80)	0.04 (± 0.02)	0.16 (± 0.05)
		12	0.47 (± 0.16)	< 0.01	0.07 (± 0.00)
		24	0.02 (± 0.01)	< 0.01	< 0.01
1:3	ONPG	5	< 0.01	3.86 (± 0.00)	< 0.01
		12	< 0.01	23.19 (± 2.53)	< 0.01
		24	< 0.01	19.24 (± 0.79)	< 0.01
	Lactose	5	< 0.01	0.08 (± 0.00)	< 0.01
		12	< 0.01	0.56 (± 0.20)	< 0.01
		24	0.05 (± 0.03)	< 0.01	< 0.01
3:1	ONPG	5	< 0.01	3.75 (± 0.50)	0.24 (± 0.04)
		12	< 0.01	2.90 (± 0.10)	0.01 (± 0.00)
		24	< 0.01	< 0.01	< 0.01
	Lactose	5	< 0.01	0.03 (± 0.00)	0.01 (± 0.00)
		12	< 0.01	< 0.01	< 0.01
		24	< 0.01	< 0.01	< 0.01
9:1	ONPG	5	< 0.01	0.92 (± 0.05)	0.02 (± 0.00)
		12	< 0.01	< 0.01	< 0.01
		24	< 0.01	0.83 (± 0.04)	< 0.01
	Lactose	5	0.17 (± 0.10)	0.29 (± 0.05)	< 0.01
		12	0.12 (± 0.08)	< 0.01	< 0.01
		24	0.01 (± 0.01)	< 0.01	< 0.01

was obtained in the buffer reaction system. These results may be attributed to the higher solubility of ONPG in the biphasic reaction system as compared to the aqueous reaction media. The lower yields of transgalactosylated serine derivative obtained using lactose as donor in biphasic reaction system (< 0.01–0.56%) are likely due to the limited solubility of lactose in these reaction media. The higher yields of transgalactosylated *N*-Z-Ser-OMe obtained with ONPG were also reported by other authors (Becker & Kuhl, 1999). Table 9.1 also shows that the yield of the transgalactosylated products was dependent on the type of organic solvent. As compared to heptane, the use of heptanone, denoted by its lower Log P value as a co-solvent, resulted in very low yields (< 0.01–0.24%) indicating its detrimental effect on the enzyme's transgalactosylating activity. These results are attributed to the fact that the hydrophilic solvents have higher tendency to strip off the water from the surface of the enzyme, which is essential for its catalytic activity (Klibanov, 1989; Yang et al., 2004). The effect of substrate-solvent interactions on the availability of substrate to the enzyme may also explain the results of the transgalactosylation yields.

The use of an excess of carbohydrate donor (ONPG or lactose) at molar ratios of 3:1 and 9:1 resulted in a decrease in the yield of transgalactosylated *N*-Z-Ser-OMe and in the formation of galactooligosaccharides (data not shown). Such results may be due to the high competition of galactose in excess to bind to both subsites of *E. coli β*-galactosidase, affecting the binding of the *N-Z*-Ser-OMe acceptor. The molar ratio of carbohydrate to serine derivative of 1:3 led to higher yields. The excess of serine derivative seems to favor kinetically the transgalactosylation reaction over the hydrolytic one. Similarly, Holla et al. (1992) have reported relatively high yields (4.00–39.00%) of transgalactosylated products when using 2 to 3.5 fold higher concentration of serine derivatives than ONPG. In contrast, Becker and Kuhl (1999) have obtained higher yields in the presence of higher concentration of carbohydrates and attributed these results to their protective effect on the enzyme in the presence of organic solvents.

9.4.2. Transgalactosylation of Selected Serine/Threonine Derivatives

It has been demonstrated that the selection of the amino blocking group is important for the improvement of the yield of transgalactosylated amino acid derivatives (Holla et al., 1992). Selected serine/threonine derivatives with different protecting groups were investigated as acceptors and their effects on the transgalactosylating efficiency of *E. coli β*-galactosidase were

assessed using ONPG (Fig. 9.2A) or lactose (Fig. 9.2B) as substrate donor. The identified optimal reaction conditions, including heptane:buffer mixture (70:30) and 1:3 sugar to serine derivative molar ratio, were used. Compared to *N*-Z-Ser-OMe (23.2%, Table 9.1), the transgalactosylation of the investigated serine/threonine derivatives exhibited lower yields. The use of *N*-Boc-Ser-OMe as acceptor resulted in the highest yields with both ONPG (6.77%) and lactose (6.51%) donors. Contrary to our results, Cantacuzene & Attal (1991) have reported lower yield for the transgalactosylation of *N*-*Z*-Ser-OMe (9.00%) by *β*-galactosidase, but higher one with *N*-Boc-Ser-OMe (15.00%). These differences are probably due to the low solubility of *N*-*Z*-Ser-OMe in the aqueous reaction system used by Cantacuzene & Attal (1991). The results also show that *N*-Fmoc-Ser-OH led to the second highest yield of transgalactosylated serine derivatives, but only using ONPG as donor (5.62%, Fig. 9.2A). Both threonine derivatives with the same carboxy-benzyl (Z) amino blocking group, *N*-Z-Thr-OMe, and *N*-Z-Thr-OH, gave comparable yields of 3.70% and of 3.38%, respectively; however, the high transgalactosylation yields could only be obtained when using ONPG as donor for *N*-Z-Thr-OMe and only using lactose as donor for *N*-Z-Thr-OH. These results may be due to the differences in the hydrophobicity between the two threonine derivatives. *N*-Z-Thr-OMe being more soluble in the organic phase, its transgalactosylation was more favored in the presence of hydrophobic ONPG and the opposite for *N*-Z-Thr-OH. The results also indicate the low reactivity of threonine derivatives as compared to the serine ones. The produced transgalactosylated products, *β*-D-galactopyranosyl-L-serine/threonine derivatives, can also be hydrolysed by *E. coli β*-galactosidase. Therefore, the yields obtained reflect a balance between the formation and the hydrolysis of these products. This is demonstrated in our results by the decrease in the bioconversion yields within the investigated time course.

No transgalactosylated products were obtained in the reaction containing a dipeptide Ser-Glu with no protection groups. This result indicates the importance of protecting groups in the transgalactosylation reaction-catalyzed by *E. coli β*-galactosidase as emphasized by others (Cantacuzene & Attal, 1991; Cantacuzene et al., 1991; Holla et al., 1992). In addition, the significant difference between the yields obtained using acceptors with the same *N*-protecting groups suggests that the *C*-protecting groups may play an important role in the transgalactosylation of the acceptor. Indeed, the acceptors with the same *N*-Boc protecting groups had significantly different yields depending on the *C*-protecting group: 1.07% (-OH,

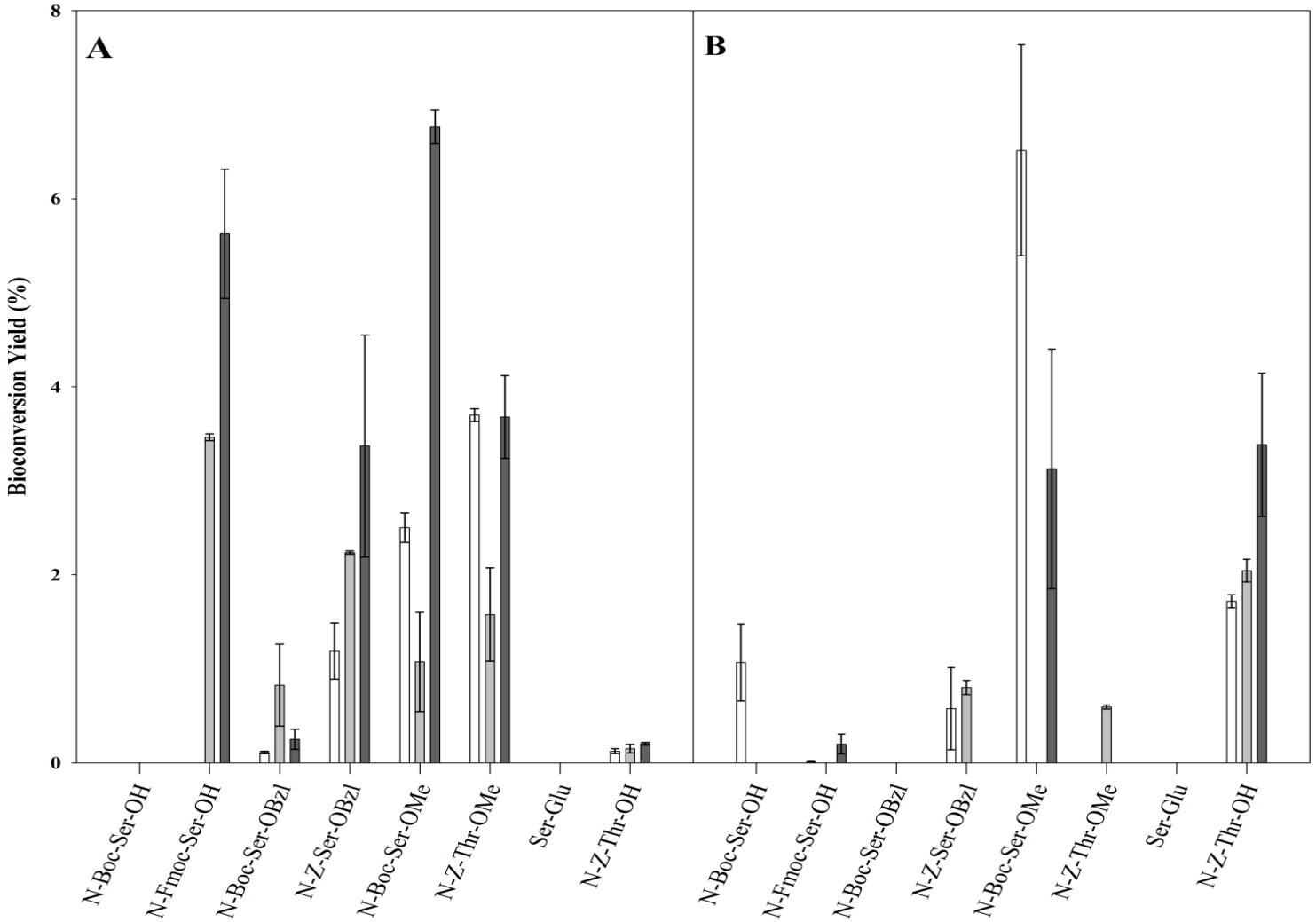

Figure 9.2 Transgalactosylation of serine/threonine derivatives by *E. coli* β-galactosidase in heptane:buffer (70:30) using ONPG (A), or lactose (B) as donors at 5h (□), 12h (▒), and 24h (■) of reaction.

lactose), 0.82% (-OBzl, ONPG), and 6.77% (-OMe, ONPG). The acceptors with the same *N*-Z protecting groups also had significantly different yields depending on the *C*-protecting group: 3.37% (-OBzl, ONPG), and 23.19% (-OMe, ONPG). This difference in bioconversion yields might be due to the relatively bigger size of the -OBzl protecting group of the serine derivative that limits the access to the active site, as compared to the derivative with -OMe group. The maximum yields also differed depending on the donor substrates, ONPG or lactose, suggesting the significant effects of acceptor/donor interactions and of the substrate availability in the enzyme's microenvironment.

The reactions in which the acceptors gave higher bioconversion yields of transgalactosylated products were analyzed by ESI/MS to confirm the product formation. Only stronger signals of galactosylated product ions, galactosylated *N*-Fmoc-Ser-OH (Fig. 9.3A) and galactosylated *N*-Boc-Ser-OMe (Fig. 9.3B), were fragmented in MS/MS-mode. The numerous fragmentation reactions on the sugar moiety producing many ions at relatively low intensities can lead to difficulty in the identification of the fragments (Mann & Jensen, 2003). The fragmentation pattern mostly constituted of the ions with a complete loss of the sugar moiety from the serine derivative. The galactosylated *N*-Fmoc-Ser-OH at *m/z* of 490.5 underwent fragmentation, leading to abundant molecular acceptor ions $[M-H]^-$ (324.1 m/z), galactose (179.1 *m/z*), and other fragments. The galactosylated *N*-Boc-Ser-OMe at *m/z* 400.4 underwent fragmentation leading to abundant molecular acceptor ions $[M-H]^-$ (218.1 *m/z*), galactose (180.1 *m/z*), and unfragmented product ions $[M+C_6H_{10}O_5-H_2O]^-$ (362.1 *m/z*) and other fragments.

9.4.3. Docking Simulations

In order to elucidate the possible orientation and the molecular binding of the acceptor substrates to the second subsite of *β*-galactosidase from *E. coli* during the second mechanistic step of the transgalactosylation reaction, molecular docking simulations were performed. The currently available crystallographic complex of the covalent enzyme-substrate complex was not built with galactose (2-*F*-α-D-glycosyl enzyme intermediate, 1JZ2, Juers et al., 2001). Therefore, the available crystallographic structure of galactose-enzyme non-covalent complex (1JZ7, Juers et al., 2001) was used as the enzyme model for the docking analysis. It has been reported that the non-existence of covalent linkage between the donor sugar and *β*-galactosidase will not

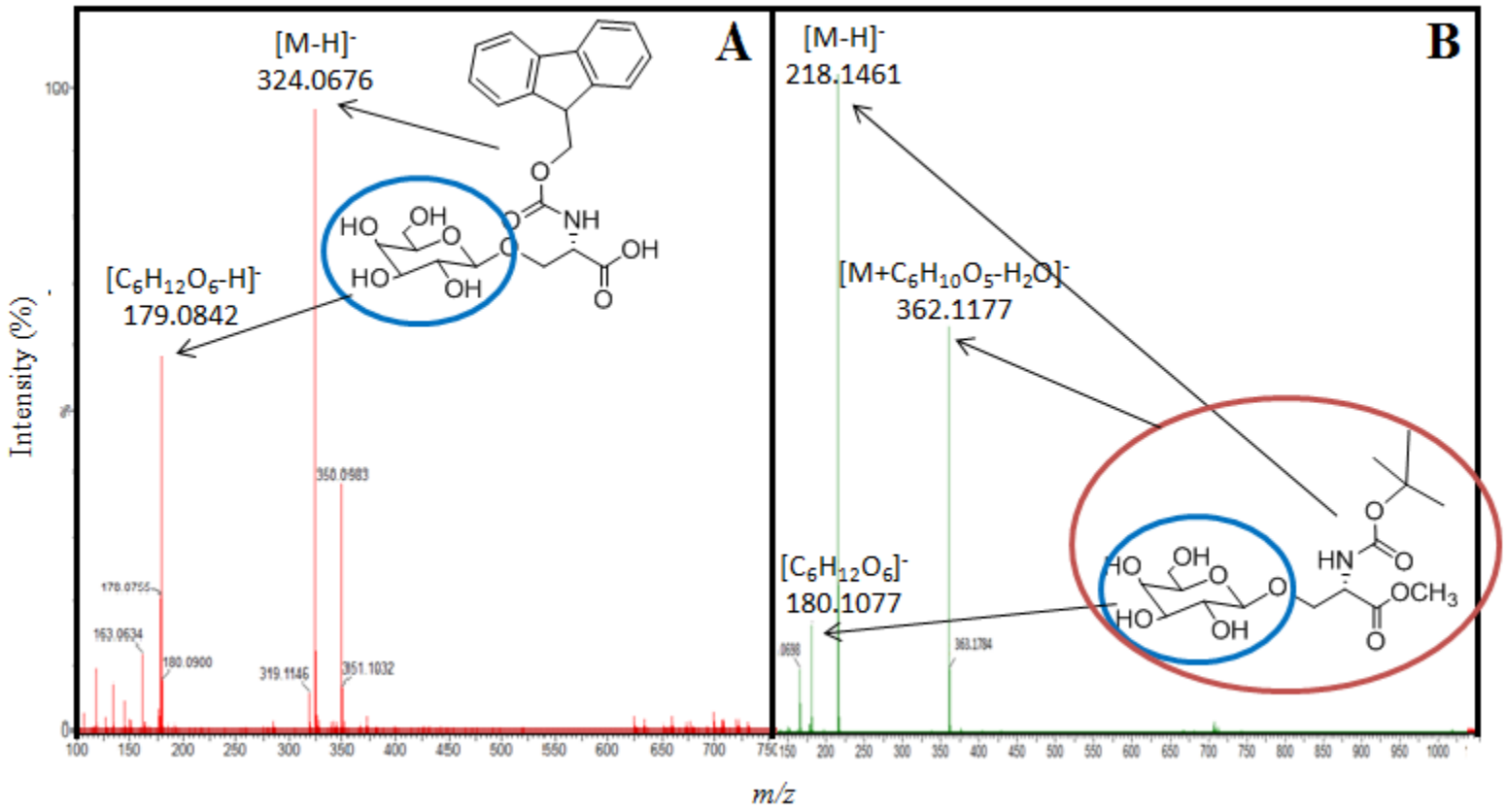

Figure 9.3 MS/MS spectra of fragmented transgalactosylated *N*-Fmoc-Ser-OH (A) and of fragmented transgalactosylated *N*-Boc-Ser-OMe (B).

significantly change the position and the orientation of the sugar as compared to the covalent enzyme-galactose intermediate (Brás et al., 2009). In addition, in the selected non-covalent complex model, galactose binds to the enzyme in the deeper binding mode, which is required for the hydrolysis and the transgalactosylation to occur subsequently.

As seen in Fig. 9.4, the interaction between the enzyme and the galactose moiety occurs mainly via hydrogen bonds, with the equatorial OH groups of galactose. During the docking simulations, each acceptor was positioned at the active site of the enzyme using twenty different orientations, and special attention was given to the binding modes that led to the strongest affinities and to the closest distances between the hydroxyl group of the acceptor and the 1′-OH of the galactose moiety (Table 9.2). For instance, Fig. 9.5 depicts two of the three possible docking solutions of *N*-Boc-Ser-OMe. Similarly to the leaving group of the natural substrate (Juers et al., 2001), glucose moiety of lactose, it was observed that most acceptor substrates formed π-π stacking interactions with Trp999 (Fig. 9.6). Other possible identified interactions include hydrogen bonding with the surrounding residues such as the carboxylic acids of Glu487, and the amino group of Lys517, and His418 (Fig. 9.6A).

The best identified docking solutions that can favor the synthesis of transgalactosylated product were reported (Table 9.2) and correlated with the experimental transgalactosylation yields (Fig. 9.2). The overall results show that the binding affinities of the serine/threonine derivatives (-4.5 – -7.1 kcal/mol) in the second subsite of *β*-galactosidase were similar or stronger than those reported for glucose (- 4.4 – - 5.1 kcal/mol) and galactose (-4.1 – 5.1 kcal/mol) as acceptors (data not shown). This may be due to the larger size of serine/threonine derivatives leading to better interactions with the amino acid residues found in the large acceptor binding site of the enzyme as compared to the smaller monosaccharides. However, these binding affinities were weaker than the experimental binding affinities of ONPG (-8.1 – -8.2 kcal/mol) at the degalactosylation step (Huber et al., 1984; Huber et al., 2003; Martinez-Bilbao & Huber, 1994). This slightly weaker binding affinity of *E. coli β*-galactosidase towards its acceptors may also reflect the importance of the thermodynamic equilibrium between the transgalactosylation and hydrolysis reaction. If the binding of the substrate at the subsite was both specific and tight, then the transgalactosylation reaction would be kinetically predominant. Conversely, if the binding were very weak, then the hydrolysis reaction would dominate (Matthews, 2005).

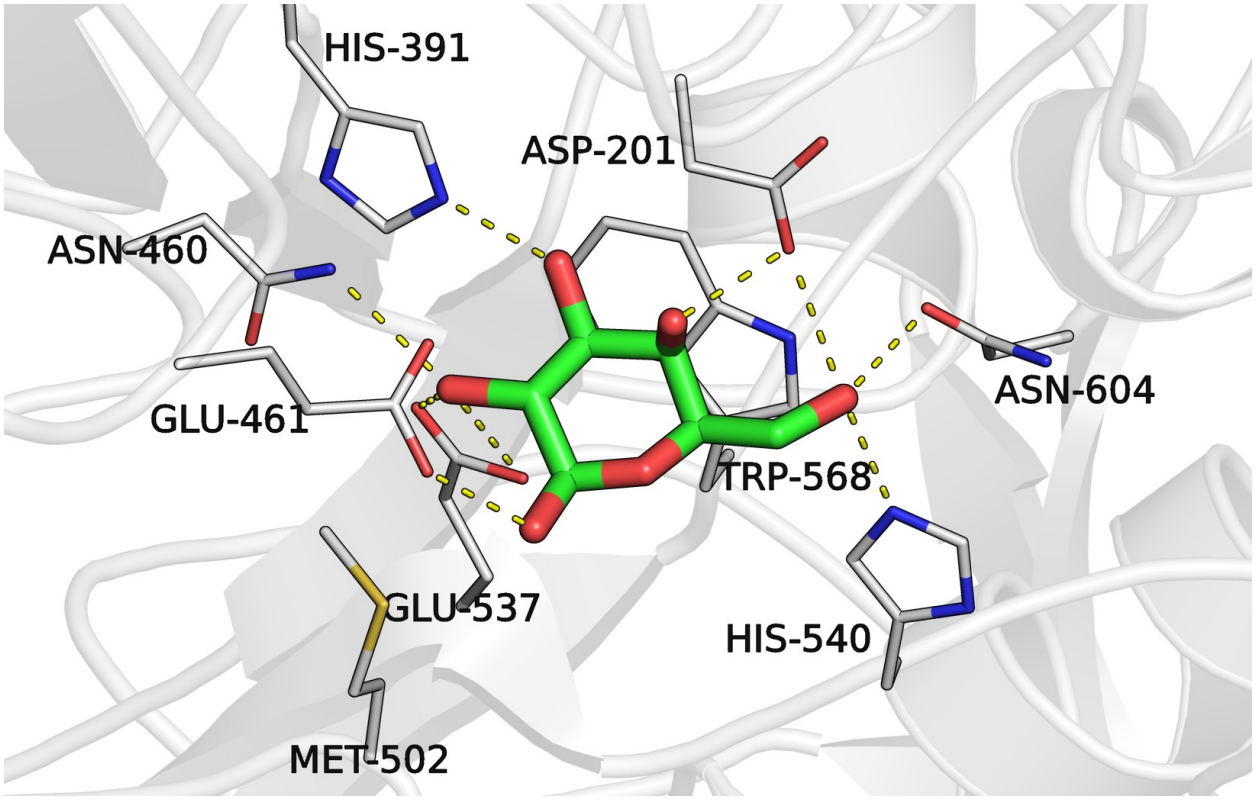

Figure 9.4 3D presentation of a galactose moiety and its interactions with the residues at enzyme's active site in deep binding mode

Table 9.2 Predicted binding affinities of the acceptors and the distance between the hydroxyl group of the serine/threonine derivatives and the 1'-OH of galactose moiety predicted by docking calculations at a specific binding mode of the acceptor

Substrates (acceptors)	Binding Modes	Binding Affinity (kcal/mol)	Distance (Å)
N-Fmoc-Ser-OH	1	-7.1	3.7
	2	-6.3	2.8
N-Boc-Ser-OBzl	1	-6.2	3.1
	2	-6.0	3.0
	3	-5.9	2.9
	4	-5.7	3.1
	5	-5.5	3.0
N-*Z*-Ser-OBzl	1	-7.0	3.0
	2	-6.6	2.7
	3	-6.6	2.8
N-*Z*-Ser-OMe	1	-4.9	3.1
N-Boc-Ser-OMe	1	-4.7	2.8
	2	-4.6	3.2
	3	-4.5	3.0
N-*Z*-Thr-OMe	1	-5.7	2.7
	2	-5.5	2.9
N-*Z*-Thr-OH	1	-5.7	3.6

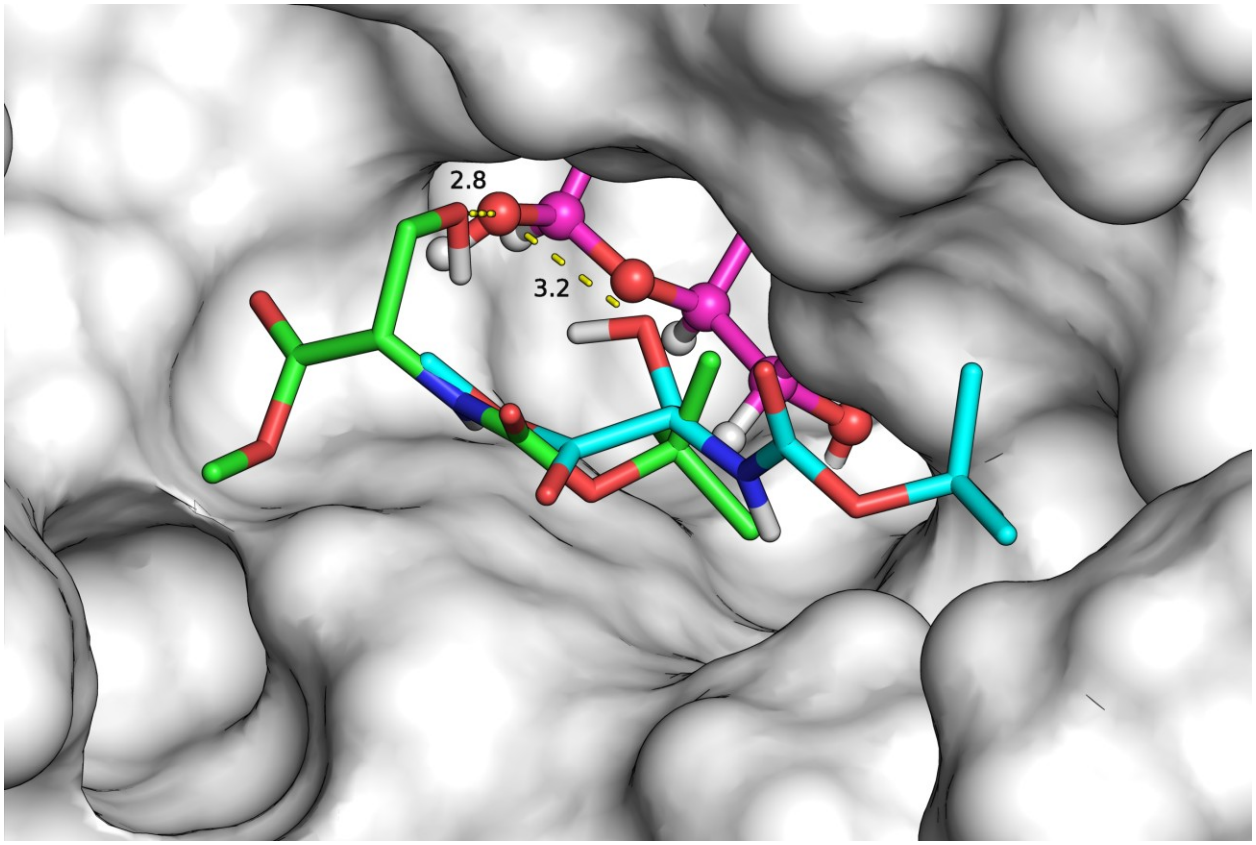

Figure 9.5 *N*-Boc-Ser-OMe acceptor substrate bound to *β*-galactosidase according to two of the three possible binding modes where carbon atoms are colored in green and cyan; galactose moiety (purple) and enzyme (surface, white).

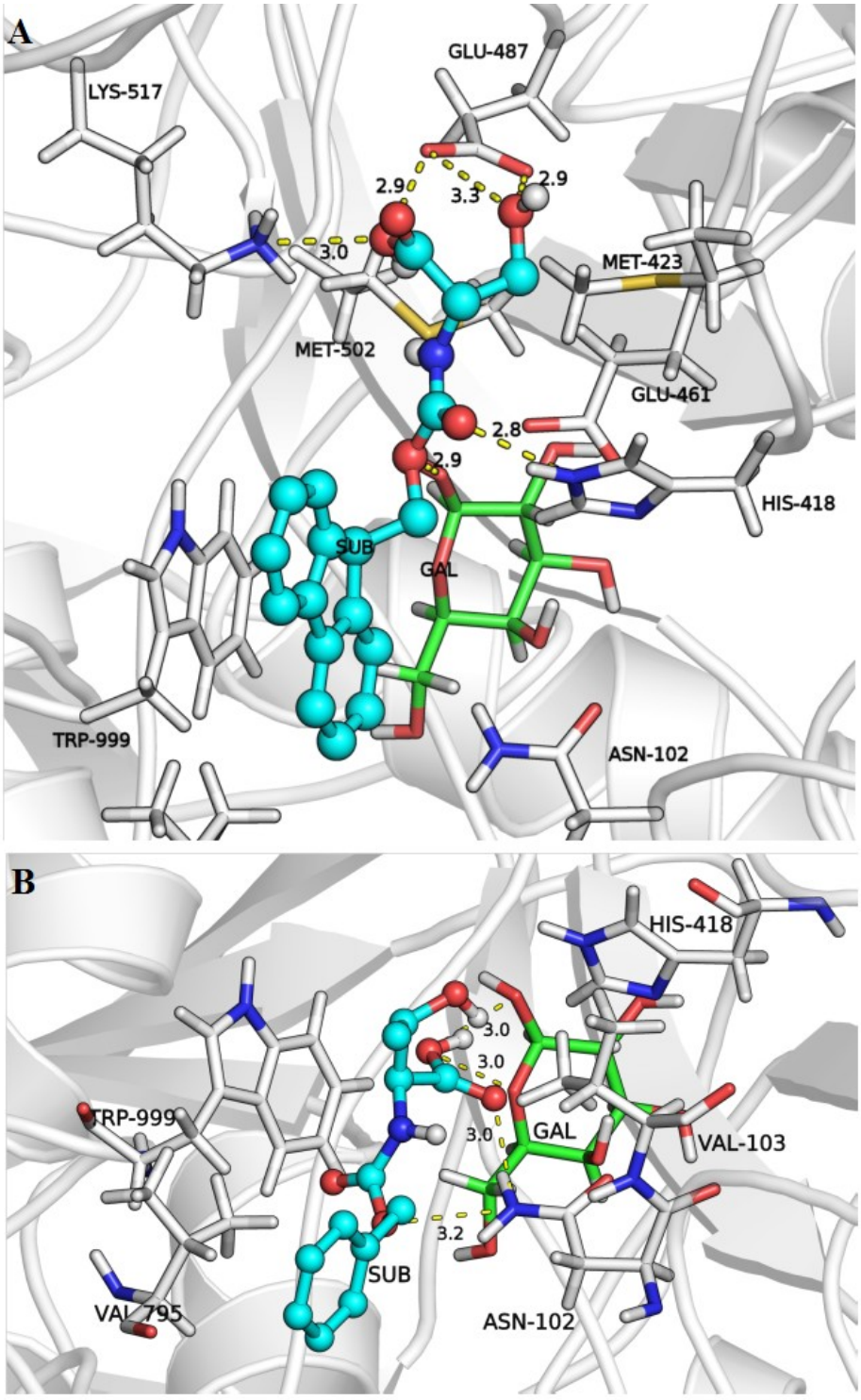

Figure 9.6 *β*-galactosidase enzyme in complex with galactose moiety and *N*-Fmoc-Ser-OH (A) or *N*-*Z*-Thr-OH (B). Enzyme is shown in cartoon presentation with the residues at the active site in sticks; galactose (sticks, green), *N*-Fmoc-Ser-OH/*N*-*Z*-Thr-OH (ball and sticks, cyan) and hydrogen bonds (dashed lines, yellow).

The results (Table 9.2) show that the binding mode (#1) identified for *N*-Fmoc-Ser-OH leading to the highest binding affinity (-7.1 kcal/mol) did not allow its hydroxyl group to be closer (3.7 Å) to the 1′-OH of the galactose moiety positioned in the first subsite. As compared to *N*-Fmoc-Ser-OH, the binding mode (#1) of *N*-Boc-Ser-OMe exhibited low affinity (-4.7 kcal/mol), but it favored the interaction between the hydroxyl group and the 1′-OH of the galactose, which were closer (2.87 Å). Indeed, closer distance values (<3.5 Å) are expected to favor the formation of the glycosidic linkage between the galactose moiety and the serine/threonine derivatives (Brás et al., 2009). The docked solutions can explain the slightly lower experimental bioconversion yield obtained with *N*-Fmoc-Ser-OH (5.63%) acceptor as compared to *N*-Boc-Ser-OMe (6.77%) (Fig. 9.2). However, *N*-*Z*-Ser-OBzl acceptor exhibited relatively higher binding affinities (-6.6 – -7.0 kcal/mol) and closer distances (2.7–3.0 Å) at the best identified binding modes, but only moderate transgalactosylation yield (3.37%) was obtained; these results can be explained by the larger size of its *C*-protecting group, which may have sterically prevented its displacement into the deeper part of the enzyme's active site. Similarly, *N*-Boc-Ser-OBzl with the same *C*-protecting group led to the lowest bioconversion yields (0.01–0.82%, Fig. 9.2), despite its high binding affinities (-5.5 – -6.2 kcal/mol) and the closer distances between its hydroxyl group and the 1'-OH of galactose moiety (2.9 – 3.1 Å). As compared to *N*-Boc-Ser-OBzl, the maximum transgalactosylation yields (6.51 and 6.77%) of the acceptor substrate *N*-Boc-Ser-OMe, with the same *N*-protecting group but with a smaller *C*-protecting group, were higher although it exhibited lower binding affinities (-4.5 – -4.7 kcal/mol). For the substrate *N*-*Z*-Thr-OH, the lack of a protecting group at its carboxylic end led the latter to interact with the 1′-OH group of the galactosyl moiety instead of the hydroxyl group of the threonine as shown in Fig. 9.6B. However, the transgalactosylation yield of *N*-Z-Thr-OH using lactose as donor (3.38%) was comparable to that of *N*-*Z*-Thr-OMe with the same *N*-protecting group, using ONPG (3.70%) (Fig. 9.2). Only one binding mode (Table 9.2) was found for *N*-*Z*-Ser-OMe where its side chain hydroxyl group was favorably placed in relation to the 1'-OH of the galactose moiety. As compared to other serine/threonine derivatives, the lower binding affinity (-4.9 kcal/mol) and the relatively higher estimated distance (3.1 Å) for *N*-*Z*-Ser-OMe were not in accordance with its higher transgalactosylation yield in heptane:buffer media (23.2%); however, no product formation could be detected in aqueous media. These results demonstrate the importance of the acceptors/solvent interactions and reveal the thermodynamically driven nature of the investigated

transgalactosylation reaction. To better understand the effect of substrate/solvent interactions, molecular dynamic simulations can be used. However, Bràs et al. (2009) have demonstrated that due to the lower selectivity of the second subsite of *E. coli* β-galactosidase and the lower binding affinity of the acceptors in this subsite, the initial configurations of the acceptor molecules found through docking are maintained during their molecular dynamics simulations. In contrast, using molecular dynamic simulations, Pérez-Sánchez et al. (2011) have found a better orientation of the substrate, *N*-acetylglucosamine, in the active site upon a favorable substrate-solvent interaction although no differences in the protein flexibility and in the positioning of the active site residues of *E. coli* β-galactosidase were found in glycerol-derived solvents as compared to water.

9.5. Conclusion

The transgalactosylation of serine/threonine derivatives by β-galactosidase was dependent on the stereochemical properties of acceptor/donor substrates and on the substrate/solvent interactions. The molecular docking analyses have generated detailed structural information on the binding modes of acceptor substrates. The correlations found between the docking solutions and the experimental transgalactosylation yields revealed the important role of *C*/*N*-protecting groups of serine/threonine derivatives in their transgalactosylations. The binding affinities of the acceptors and the estimation of the distances between their hydroxyl group and the 1′-OH of the galactose moiety also helped to identify the transgalactosylation reactions that were more thermodynamically driven than kinetically. The overall findings can contribute to the understanding of the mechanisms behind the selectivity of the transgalactosylating activity of β-galactosidase for its better application for the enzymatic synthesis of peptide/protein:carbohydrate conjugates.

CHAPTER X

GENERAL SUMMARY AND CONCLUSIONS

The focus of this research was the investigation of selected approaches for the production of protein:carbohydrate conjugates with improved functional properties as potential multi-functional food ingredients. Lysozyme (LZM) and patatin (PTT) were selected as protein models. Despite the desirable bioactivities and functionalities of LZM (e.g. antimicrobial activity, heat stability) and PTT (e.g. antioxidant, foaming, emulsifying, gelling, antiproliferative activities), and their high nutritional quality, their applications as food protein ingredients are limited by the low emulsifying properties of LZM, by the low solubility and stability of PTT, and by the allergenicity of both proteins. The development of strategies, based on the Maillard reaction and on the glycosidase-catalyzed reaction, for the carbohydrate conjugation of these selected proteins to improve their functional properties is therefore of great interest.

The production of LZM:carbohydrate conjugates through Maillard reaction was successfully achieved. As compared to galactose, limited conjugations of galactooligosaccharides (GOS) and galactan to LZM, were obtained resulting in a narrow distribution of PTT:GOS/galactan glycoforms (mono and diglycated LZM). The conjugation of LZM to galactose/GOS/galactan improved its functional properties and decreased its immunoreactivity. These improvements are of great importance for the technological use of LZM as functional food ingredient. The optimization of the production of LZM:GOS conjugates was performed using RSM with CCD. The protein: carbohydrate molar ratio was identified as the most significant independent variable affecting importantly the percentage of blocked lysine, whereas the temperature was the most significant parameter for the protein aggregation index. Among the variables, molar ratio and incubation temperature showed the most significant interaction effect for both the percentage of blocked lysine and the protein aggregation index. The produced LZM:GOS conjugates may conceivably possess prebiotic activity and added functional properties as compared to other LZM conjugates.

In regards to the conjugation of carbohydrates to PTT, important secondary and tertiary structural changes were demonstrated upon the conjugation with GOS and with galactan. These structural changes led to more heat stable forms of PTT than the unmodified protein. The interaction of nearby amino acids of PTT with the attached galactan moieties resulted in high pH stability of its tertiary structure. The changes in structures also increased the antioxidant activity of PTT glycated with GOS or galactan. On the other hand, the high level of galactose

conjugation to PTT and the increased exposure of hydrophobic residues led to a significant increase in the emulsifying stability at pH 3. Contrary to galactose and GOS, the conjugation of galactan to PTT resulted in a decrease in its immunoreactivity, and this lower level of immunoreactivity was maintained after simulated gastric digestion, demonstrating the potential of carbohydrate conjugation to lower the allergenicity of PTT. As an overall, the conjugation of PTT with pentose-type carbohydrates led to more protein cross-linking, whereas the conjugation of PTT with hexose-type carbohydrates led to higher levels of carbohydrate conjugation.

PTT:carbohydrate conjugates were effectively produced using selected Maillard reaction inhibitors. In particular, sodium bisulfite (galactose, xylan), aminoguanidine (xylose, xylooligosaccharides), and cysteine (galactooligosaccharides, galactan) were the inhibitors that led to the highest glycation level of the conjugates, to lower proportions of extensive polymerized species and to lower amounts of total unreacted dicarbonyls. The digestibilities of PTT conjugates produced in the presence of inhibitors were also improved. The combined use of cysteine and sodium bisulfite Maillard reaction inhibitors was investigated to maximize the carbohydrate conjugation level of PTT:galactose/xylose conjugates and to minimize their protein cross-linking. Understanding and exploring the synergistic interaction of cysteine and sodium bisulfite helped to modulate the progress of the Maillard reaction. Indeed, both cysteine and sodium sulfite acted synergistically at close to equal concentrations while exerting an adverse effect when the presence of one inhibitor was greater than the other.

The production of galactosylated serine/threonine derivatives by *Escherichia coli* β-galactosidase was investigated, and the computational docking simulations provided detailed structural information on the binding of the acceptor substrates. The transgalactosylation yield was dependent on the substrates/solvent interactions, the acceptors' accessibility to the active site, the binding affinities of the acceptors, and on their positioning in relation to the 1'-OH of the galactose moiety. The correlations between the docking solutions and the experimental transgalactosylation yields also helped to identify the transgalactosylation reactions that were more thermodynamically driven than kinetically.

Taken together, the overall experimental findings will contribute to lay the scientific ground for the production of protein:carbohydrate conjugates of potential applications as functional ingredients and nutraceuticals.

CHAPTER XI

CONTRIBUTION TO KNOWLEDGE AND RECOMMENDATION FOR FUTURE STUDIES

11.1. Contributions to Knowledge

The major contributions to knowledge of this study are:

1. This is the first study that investigated the production of LZM:GOS/galactan conjugates and characterized their structural and functional properties. The produced conjugated species were identified. The effect of carbohydrate length on the reaction rate and the functional properties was discussed.

2. For the first time, the production of LZM:GOS conjugates was optimized through response surface methodology. The most important variables affecting the glycation rate and the protein cross-linking were identified. The optimum conditions were predicted through a quadratic model and verified experimentally.

3. This is the first study that investigated the production of PTT:galactose/GOS/galactan conjugates and characterized their structural and functional properties.

4. For the first time, the effectiveness of aminoguanidine, cysteine, sodium bisulfite, and pyridoxamine was compared systematically for the production of Maillard reaction conjugates. The effect of Maillard reaction inhibitors on the digestibility of the conjugates was investigated. For the first time, the effect of carbohydrate type (pentose/hexose) and length of carbohydrate (mono-, oligo-, polysaccharides) on the progress of the Maillard reaction was investigated systematically.

5. The optimization of the production of Maillard reaction conjugates through RSM using Maillard reaction inhibitors was performed. The important variables affecting the level of conjugation and the level of protein cross-linking were identified. The optimum conditions were predicted through a quadratic model and verified experimentally.

6. The effect of glycation and simulated gastric digestion on the immunoreactivity of PTT was investigated for the first time.

7. This is the first study to have used molecular docking simulations to give a theoretical explanation of the trangalactosylating selectivity of *E. coli* β-galactosidase towards serine/threonine derivatives.

This research work will contribute to the understandings of the complex mechanisms involved in the production of protein:carbohydrate conjugates through the Maillard reaction and through enzymatic glycosylation. The presented study is expected to serve as a model for a better application of these two strategies for the effective production of protein:carbohydrate conjugates with improved functional properties.

11.2. Recommendations for Future Research

The biological properties of these produced conjugates should be investigated. In particular, it has been suggested that these conjugates might have the increased resistance to digestion to reach the distal region of the colon (colonic persistence) and therefore could deliver the prebiotic oligosaccharides more effectively. This colonic persistence and the prebiotic activity of these conjugates should be investigated.

The production of protein:carbohydrate conjugates at the industrial level should also be investigated, and optimized.

REFERENCES

Abtahi, S., & Aminlari, M. (1997). Effect of sodium sulfite, sodium bisulfite, cysteine, and pH on protein solubility and sodium dodecyl sulfate-polyacrylamide gel electrophoresis of soybean milk base. *Journal of Agricultural and Food Chemistry, 45*(12), 4768-4772.

Adrover, M., Vilanova, B., Frau, J., Muñoz, F., & Donoso, J. (2008). The pyridoxamine action on Amadori compounds: A reexamination of its scavenging capacity and chelating effect. *Bioorganic & Medicinal Chemistry, 16*, 5557-5569.

Akhtar, M., & Dickinson, E. (2003). Emulsifying properties of whey protein-dextran conjugates at low pH and different salt concentrations. *Colloids and Surfaces B: Biointerfaces, 31*, 125-132.

Al-Hakkak, J., & Al-Hakkak, F. (2010). Functional egg white-pectin conjugates prepared by controlled Maillard reaction. *Journal of Food Engineering, 100*(1), 152-159.

Alahdad, Z., Ramezani, R., Aminlari, M., & Majzoobi, M. (2009). Preparation and properties of dextran sulfate-lysozyme conjugate. *Journal of Agricultural and Food Chemistry, 57*, 6449-6454.

Ali, N. A., Ahmed, S. H., Mohammed, E. A., Ahmed, I. S. M., & Babiker, E. E. (2010). Effect of transglutaminase cross-linking on the functional properties as a function of NaCl concentration of legumes protein isolate. *International Journal of Biological and Life Sciences, 6*, 8-13.

Alibhai, M. F., Astwood, J. D., McWherter, C. A., & Sampson, H. A. (2005). Preparation of deallergenized proteins and permuteins. (WO 01/49834 A2). United States: Monsanto Technology LLC.

Amarnath, V., Amarnath, K., Amarnath, K., Davies, S., & Roberts, L. J. I. (2004). Pyridoxamine: An extremely potent scavenger of 1,4-dicarbonyls. *Chemical Reseach in Toxicology, 17*, 410-415.

Ames, J. M. (1990). Control of the Maillard reaction in food systems. *Trends in Food Science & Technology, 1*, 150-154.

Ames, J. M. (1992). The Maillard Reaction. In B. J. F. Hudson (Ed.), *Biochemistry of Food Proteins*, (pp. 99-153). London: Elsevier Applied Science Publishers.

Ames, J. M., & Apriyantono, A. (1993). Volatile reaction products from a heated xylose-lysine model system. *Food Chemistry, 48*, 271-277.

Amid, B. T., & Mirhosseini, H. (2014). Stabilization of water in oil in water (W/O/W) emulsion using whey protein isolate-conjugated durian seed gum: Enhancement of interfacial activity through conjugation process. *Colloids and Surfaces B: Biointerfaces, 113*, 107-114.

Aminlari, M., Ramezani, R., & Jadidi, F. (2005). Effect of Maillard-based conjugation with dextran on the functional properties of lysozyme and casein. *Journal of the Science of Food and Agriculture, 85*(15), 2617-2624.

Anderson, C., Pinsirodom, P., & Parkin, K. L. (2002). Hydrolytic selectivity of patatin (lipid acyl hydrolase) from potato (*Solanum tuberosum* L.) tubers toward various lipids. *Journal of Food Biochemistry, 26*(1), 63-74.

Aoki, R., Saito, A., Azakami, H., & Kato, A. (2010). Effects of various saccharides on the masking of epitope sites and uptake in the gut of cedar allergen Cry j 1-saccharide conjugates by a naturally occurring Maillard reaction. *Journal of Agricultural and Food Chemistry, 58*, 7986-7990.

Aoki, T., Hiidome, Y., Kitahata, K., Sugimoto, Y., Ibrahim, H. R., & Kato, Y. (1999). Improvement of heat stability and emulsifying activity of ovalbumin by conjugation with glucuronic acid through the Maillard reaction. *Food Research International, 32*, 129-133.

Aoki, T., Hiidome, Y., Sugimoto, Y., Ibrahim, H. R., & Kato, Y. (2001). Modification of ovalbumin with oligogalacturonic acids through the Maillard reaction. *Food Research International, 34*, 127-132.

Arita, K., Babiker, E. E., Azakami, H., & Kato, A. (2001). Effect of chemical and genetic attachment of polysaccharides to proteins on the production of IgG and IgE. *Journal of Agricultural and Food Chemistry, 49*(4), 2030-2036.

Atkinson, A. C., & Doney, A. N. (1992). *Optimum Experimental Designs*. Oxford: Oxford University Press.

Attal, S., Bay, S., & Cantacuzene, D. (1992). Enzymatic synthesis of *β*-galactosyldipeptides and of *β*-1,3-digalactosylserine derivatives using *β*-galactosidase. *Tetrahedron, 48*(42), 9251-9260.

Babiker, E. E., & Kato, A. (1998). Improvement of the functional properties of sorghum protein by protein-polysaccharide and protein-protein complexes. *Nahrung-Food, 42*(5), 286-289.

Bay, S., Namane, A., & Cantacuzene, D. (1993). Enzymatic synthesis of some *O-β*-D-digalactosyl glycopeptides, using b-D-galactosidase. *Carbohydrate Research, 248*, 317-325.

Baynes, J. W., Watkins, N. G., Fisher, C. I., Hull, C. J., Patric, J. S., Ahmed, M. U., Dunn, J. A., & Thorpe, S. R. (1989). The Amadori product on protein: structure and reactions. In J. W. Baynes & V. M. Monnier (Eds.), *The Maillard Reaction in Aging, Diabetes, and Nutrition*, (pp. 43-67).

Becker, K.-C., & Kuhl, P. (1999). Synthesis of *O-β*-galactopyranosyl-L-serine derivatives using *β*-galactosidase in aqueous-organic reaction systems. *Journal of Carbohydrate Chemistry, 18*(2), 121-129.

Beechem, J. M., & Brand, L. (1985). Time-resolved fluorescence of proteins. *Annual Review of Biochemistry, 54*, 43-71.

Berthold, A., Schubert, H., Brandes, N., Kroh, L., & Miller, R. (2007). Behaviour of BSA and of BSA-derivatives at the air/water interface. *Colloids and Surfaces A, 301*, 16-22.

Beverung, C. J., Radke, C. J., & Blanch, H. W. (1999). Protein adsorption at the oil/water interface: characterization of adsorption kinetics by dynamic interface tension measurements. *Biophysical Chemistry, 81*(1), 59-80.

Biemel, K. M., Buhler, H. P., Reihl, O., & Lederer, M. O. (2001). Identification and quantitative evaluation of the lysine-argininge crosslinks GODIC, MODIC, DODIC and glucosepan in foods. *Nahrung, 45*, 210-214.

Biemel, K. M., Reihl, O., Conrad, J., & Lederer, M. O. (2002). Formation pathways for lysine-arginine cross-links derived from hexoses and pentoses by Maillard processes. *International Congress Series, 1245*, 255-261.

Blakytny, R., Carver, J. A., Harding, J. J., Kilby, G. W., & Sheil, M. M. (1997). A spectroscopic study of glycated bovine α-crystallin: investigation of flexibility of the *C*-terminal extension, chaperone activity and evidence for diglycation. *Biochimica and Biophysica Acta, 1343*, 299-315.

Booth, A. A., Khalifah, R. G., Todd, P., & Hudson, B. G. (1996). Thiamine pyrophosphate and pyridoxamine inhibit the formation of antigenic advanced glycation end-products: Comparison with aminoguanidine. *Biochemical and Biophysical Research Communications, 220*, 113-119.

Booth, A. A., Khalifah, R. G., Todd, P., & Hudson, B. G. (1997). In vitro kinetic studies of formation of antigenic advanced glycation end products (AGEs). Novel inhibition of post-Amadori glycation pathways. *Journal of Biological Chemistry, 272*(9), 5430-5437.

Borrelli, R. C., Visconti, A., Mennella, C., Anese, M., & Fogliano, V. (2002). Chemical characterization and antioxidant properties of coffee melanoidins. *Journal of Agricultural and Food Chemistry, 50*(22), 6527-6533.

Bradford, M. M. (1976). A rapid and sensitive method for the quantitation of microgram quantities of protein utilizing the principle of protein-dye binding. *Analytical Biochemistry, 72*(1-2), 248-254.

Brandsdal, B. O., Österberg, F., Almlöf, M., Feierberg, I., Luzhkov, V. B., & Åqvist, J. (2003). Free energy calculations and ligand binding. *Advances in Protein Chemistry, 66*, 123-158.

Brás, N. F., Fernandes, P. A., & Ramos, M. J. (2009). Docking and molecular dynamics studies on the stereoselectivity in the enzymatic synthesis of carbohydrates. *Theoretical Chemistry Accounts, 122*, 283-296.

Brás, N. F., Fernandes, P. A., & Ramos, M. J. (2010). QM/MM studies on the *β*-galactosidase catalytic mechanism:hydrolysis and transglycosylation reactions. *Journal of Chemical Theory and Computation, 6*, 421-433.

Braudo, E. E. (1992). Mechanism of galactan gelation. *Food Hydrocolloids, 6*(1), 25-43.

Broersen, K., Voragen, A. G. J., Hamer, R. J., & de Jongh, H. H. J. (2004). Glycoforms of beta-lactoglobulin with improved thermostability and preserved structural packing. *Biotechnology and Bioengineering, 86*(1), 78-87.

Brownlee, M., Vlassara, H., & Cerami, A. (1984). Nonenzymatic Glycosylation and the Pathogenesis of Diabetic Complications. *Annals of Internal Medicine, 101*(4), 527-537.

Brownlee, M., Vlassara, H., Kooney, A., Ulrich, P. C., & Cerami, A. (1986). Aminoguanidine prevents diabetes-induced arterial wall protein cross-linking. *Science, 232*, 1629-1632.

Bubnis, W. A., & Ofner III, C. M. (1992). The determination of ε-amino groups in soluble and poorly soluble proteinaceous materials by a spectrophotometric method using trinitrobenzenesulfonic acid. *Analytical Biochemistry, 207*(1), 129-133.

Bunn, H. F., & Higgins, P. J. (1981). Reactions of monosaccharides with proteins: possible evolutionary significance. *Science, 213*, 222-224.

Byler, D. M., & Susi, H. (1986). Examination of the secondary structure of proteins by deconvoluted FTIR spectra. *Biopolymers, 25*, 469-487.

Camire, M. E. (1991). Protein functionality modification by extrusion cooking. *Journal of American Oil Chemists Society, 68*(2), 200-205.

Camire, M. E., Kubow, S., & Donnelly, D. J. (2009). Potatoes and human health. *Critical Reviews in Food Science and Nutrition, 49*, 823-840.

Cantacuzene, D., & Attal, S. (1991). Enzymic synthesis of galactopyranosyl-L-serine derivatives using galactosidases. *Carbohydrate Research, 211*, 327-331.

Cantacuzene, D., Attal, S., & Bay, S. (1991). Stereospecific chemoenzymatic synthesis of galactopyranosyl-L-serine. *Bioorganic & Medicinal Chemistry Letters, 1*(4), 197-200.

Castells, M. C., Pascual, C., Esteban, M. M., & Ojeda, J. A. (1986). Allergy to white potato. *Journal of Allergy and Clinical Immunology, 78*, 1110-1114.

Cayot, P., & Tainturier, G. (1997). The quantification of protein amino groups by the trinitrobenzenesulfonic acid method: A reexamination. *Analytical Biochemistry, 249*(2), 184-200.

Chellan, P., & Nagaraj, R. H. (1999). Protein crosslinking by the Maillard reaction: Dicarbonyl-derived imidazolium crosslinks in againg and diabetes. *Archives of Biochemistry and Biophysics, 368*, 98-104.

Chen, R., & Weng, Z. (2002). Docking unbound proteins using shape complementarity, desolvation, and electrostatics. *Proteins, 47*(3), 281-294.

Chetyrkin, S. V., Zhang, W., Hudson, B. G., Serianni, A. S., & Voziyan, P. A. (2008). Pyridoxamine protects proteins from functional damage by 3-deoxyglucosone: Mechanism of action of pyridoxamine. *Biochemistry, 47*, 997-1006.

Chevalier, F., Chobert, J.-M., Popineau, Y., Nicolas, M. G., & Haertlé, T. (2001a). Improvement of functional properties of *β*-lactoglobulin glycated through the Maillard reaction is related to the nature of the sugar. *International Dairy Journal, 11*(3), 145-152.

Chevalier, F., Chobert, J. M., Molle, D., & Haertle, T. (2001b). Maillard glycation of *β*-lactoglobulin with several sugars: Comparative study of the properties of the obtained polymers and of the substituted sites. *Lait, 81*(5), 651-666.

Choi, S. J., Kim, H. J., Park, K. H., & Moon, T. W. (2005). Molecular characteristics of ovalbumin-dextran conjugates formed through the Maillard reaction. *Food Chemistry, 92*, 93-99.

Church, M. K., Bradding, P., Walls, A. F., & Okayama, Y. (1997). Mast cells and basophils. In A. B. Kay (Ed.), *Allergy and Allergic Diseases*, (pp. 149-170). Oxford: Blackwell.

Corzo-Martínez, M., Ávila, M., Moreno, F. J., Requena, T., & Villamiel, M. (2012). Effect of milk protein glycation and gastrointestinal digestion on the growth of bifidobacteria and lactic acid bacteria. *International Journal of Food Microbiology, 153*(3), 420-427.

Corzo-Martínez, M., Moreno, F. J., Olano, A., & Villamiel, M. (2008). Structural characterization of bovine *β*-lactoglobulin-galactose/tagatose Maillard complexes by electrophoretic, chromatographic, and spectroscopic methods. *Journal of Agricultural and Food Chemistry, 41*, 1811-1815.

Corzo-Martínez, M., Moreno, F. J., Olano, A., & Villamiel, M. (2010a). Role of Pyridoxamine in the formation of the Amadori/Heyns compounds and aggregates during the glycation of *β*-lactoglobulin with galactose and tagatose. *Journal of Agricultural and Food Chemistry, 58*(1), 500-506.

Corzo-Martínez, M., Moreno, F. J., Villamiel, M., & Harte, F. M. (2010b). Characterization and improvement of rheological properties of sodium caseinate glycated with galactose, lactose and dextran. *Food Hydrocolloids, 24*(1), 88-97.

Corzo-Martínez, M., Soria, A. C., Belloque, J., Villamiel, M., & Moreno, F. J. (2010c). Effect of glycation on the gastrointestinal digestibility and immunoreactivity of bovine *β*-lactoglobulin. *International Dairy Journal, 20*, 742-752.

Creighton, T. E., & Freeman, W. H. (1983). *Proteins: Structures and Molecular Principles*. New York.

Creusot, N., Wierenga, P. A., Laus, M. C., Giuseppin, M. L. F., & Gruppen, H. (2010). Rheological properties of patatin gels compared with *β*-lactoglobulin, ovalbumin, and glycinin. *Journal of the Science of Food and Agriculture, 91*, 253-261.

Crout, D. H. G., & Vic, G. (1998). Glycosidases and glycosyl transferases in glycoside and oligosaccharide synthesis. *Current Opinion in Chemical Biology, 2*(1), 98-111.

Darewicz, M., & Dziuba, J. (2001). The effect of glycosylation on emulsifying and structural properties of *β*-casein. *Nahrung, 45*, 15-20.

Davidek, T., Clety, N., Aubin, S., & Blank, I. (2002). Degradation of the Amadori compound *N*-(1-deoxy-D-fructos-1-yl) glycine in aqueous model systems. *Journal of Agricultural and Food Chemistry, 50*(19), 5472-5479.

Davies, C. G. A., Netto, F. M., Glassenap, N., Gallaher, C. M., Labuza, T. P., & Gallaher, D. D. (1998). Indication of the Maillard reaction during storage of protein isolates. *Journal of Agricultural and Food Chemistry, 46*, 2485-2489.

Davis, P. J., & Williams, S. C. (1998). Protein modification by thermal processing. *Allergy, 53*, 102-105.

de Jongh, H. H. J., Robles, C. L., Timmerman, E., Nordlee, J. A., Lee, P.-W., Baumert, J. L., Hamilton, R. G., Taylor, S. L., & Koppelman, S. J. (2013). Digestibility and IgE-binding of glycosylated codfish parvalbumin. *BioMed Research International, 2013*.

Degenhardt, T. P., Thorpe, S. R., & Baynes, J. W. (1998). Chemical modification of proteins by methylglyoxal. *Cellular and Molecular Biology, 44*(7), 1139-1145.

Deveaux-Gobert, V. (2008). Protéines de pommes de terre: vers de nouveaux axes de valorisation? *Cahiers Agricultures, 17*, 407-411.

Dickinson, E., & Galazka, V. B. (1991). Emulsion stabilization by ionic and covalent complexes of *β*-lactoglobulin with polysaccharides. *Food Hydrocolloids, 5*(3), 281-296.

Dong, A., Huang, P., & Caughey, W. S. (1992). Redox-dependent changes in *β*-extended chain and turn structures of cytochrome c in water solution determined by second derivative amide I infrared spectra. *Biochemistry, 31*, 182-189.

Dong, S. Y., Panya, A., Zeng, M. Y., Chen, B. C., McClements, D. J., & Decker, E. A. (2012). Characteristics and antioxidant activity of hydrolyzed beta-lactoglobulin-glucose Maillard reaction products. *Food Research International, 46*(1), 55-61.

Dordick, J. S. (1989). Enzymatic catalysis in monophasic organic solvents. *Enzyme and Microbial Technology, 11*, 194-211.

Dubois, M., Gilles, K. A., Hamilton, J. K., Rebers, P. A., & Smith, F. (1956). Colorimetric method for determination of sugars and related substances. *Analytical Chemistry, 28*(3), 350-356.

Dunlap, C. A., & Côté, G. L. (2005). *β*-lactoglobulin-dextran conjugates: Effect of polysaccharide size on emulsion stability. *Journal of Agricultural and Food Chemistry, 53*(2), 419-423.

Ebner, C., Hirschwehr, R., Bauer, L., Breiteneder, H., Valenta, R., Ebner, H., Kraft, D., & Scheiner, O. (1995). Identification of allergens in fruits and vegetables: IgE cross-reactivities with the important birch pollen allergens Bet v 1 and Bet v 2 (birch profilin). *Journal of Allergy and Clinical Immunology, 95*, 962-969.

Edelstein, D., & Brownlee, M. (1992). Mechanistic studies of advanced glycosylation end product inhibition by aminoguanidine. *Diabetes, 41*(1), 26-29.

Einhorn-Stoll, U., Ulbrich, M., Sever, S., & Kunzek, H. (2005). Formation of milk protein-pectin conjugates with improved emulsifying properties by controlled dry heating. *Food Hydrocolloids, 19*, 329-340.

Elias, R. J., Kellerby, S. S., & Decker, E. A. (2008). Antioxidant activity of proteins and peptides. *Critical Reviews in Food Science and Nutrition, 48*, 430-441.

Elias, R. J., McClements, D. J., & Decker, E. A. (2007). Impact of thermal processing on the antioxidant mechanisms of continuous phase *β*-lactoglobulin in oil-in-water emulsions. *Food Chemistry, 104*(4), 1402-1409.

Erbersdobler, H. F., & Somoza, V. (2007). Forty years of furosine - Forty years of using Maiilard reaction products as indicators of the nutritional quality of foods. *Molecular Nutrition & Food Research, 51*(4), 423-430.

FAO. (2008). *Potato World*. <http://www.fao.org/potato-2008/en/world/imp/index.html>

Farmar, J. G., Ulrich, P. C., & Cerami, A. (1988). Novel pyrroles from sulfite-inhibited Maillard reactions: Insight into the mechanism of inhibition. *Journal of Organic Chemistry, 53*(10), 2346-2349.

Fechner, A., Knoth, A., Scherze, I., & Muschiolik, G. (2007). Stability and release properties of double-emulsions stabilised by caseinate-dextran conjugates. *Food Hydrocolloids, 21*(56), 943-952.

Feeney, R. E., & Whitaker, J. R. (1988). Importance of cross-linking reactions in proteins. In Y. Pomeranz (Ed.), *Advances in Cereal Science and Technology* vol. 4 (pp. 21-46). St Paul, USA: American Association of Cereal Chemists.

Feizi, T. (1985). Demonstration by monoclonal antibodies that carbohydrate structures of glycoproteins and glycolipids are onco-developmental antigens. *Nature, 314*, 53-57.

Fenaille, F., Morgan, F., Parisod, V., Tabet, J.-C., & Guy, P. A. (2003). Solid-state glycation of *β*-lactoglobulin monitored by electrospray ionisation mass spectrometry and gel electrophoresis techniques. *Rapid Communications in Mass Spectrometry, 17*(13), 1483-1492.

Ferreira, S. L. C., Bruns, R. E., Ferreira, H. S., Matos, G. D., David, J. M., Brandão, G. C., da Silva, E. G., Portugal, L. A., dos Reis, P. S., Souza, A. S., & dos Santos, W. N. (2007). Box-Behnken design: an alternative for the optimization of analytical methods. *Analytica Chimica Acta, 597*(2), 179-186.

Finot, P. A. (2005). The absorption and metabolism of modified amino acids in processed foods. *Journal of Aoac International, 88*(3), 894-903.

Frémont, S., Kanny, G., Nicolas, J. P., & Moneret-Vautrin, D. A. (1997). Prevalence of lysozyme sensitization in an egg-allergic population. *Allergy, 52*(2), 224-228.

Friedman, M. (1996). Food browning and its prevention: An overview. *Journal of Agricultural and Food Chemistry, 44*(3), 631-653.

Friedman, M., & Molnar-Perl, I. (1990). Inhibition of browning by sulfur amino acids. 1. Heated amino acid-glucose systems. *Journal of Agricultural and Food Chemistry, 38*, 1642-1647.

Frolov, A., & Hoffmann, R. (2010). Identification and relative quantification of specific glycation sites in human serum albumin. *Analytical and Bioanalytical Chemistry, 397*, 2349-2356.

Fu, M. X., Wells-Knecht, K. J., Blackledge, J. A., Lyons, T. J., Thorpe, S. R., & Baynes, J. W. (1994). Glycation, glycoxidation, and cross-linking of collagen by glucose. Kinetics, mechanisms, and inhibition of late stages of Maillard reaction. *Diabetes, 43*(5), 676-683.

Gerrard, J. A. (2002). Protein-protein crosslinking in food: Methods, consequences, applications. *Trends in Food Science & Technology, 13*, 391-399.

Gerrard, J. A., Brown, P. K., & Fayle, S. E. (2003). Maillard crosslinking of food proteins II: The reaction of glutaraldehyde, formaldehyde and glyceraldehyde with wheat proteins in vitro and in situ. *Food Chemistry, 80*, 35-43.

Gibson, G. R., Probert, H. M., Loo, J. V., Rastall, R. A., & Roberfroid, M. B. (2004). Dietary modulation of the human colonic microbiota: updating the concept of prebiotics. *Nutrition Research Reviews, 17*(2), 259-275.

Giuseppin, M. L. F., Nieuwenhuijzen, N. H., Lambers, R. R., & Spelbrink, R. E. J. (2011). Non-astringent protein products. (WO 2011/059330 A1). United States of America.

Glomb, M. A., & Tschirnich, R. (2001). Detection of alpha-dicarbonyl compounds in Maillard reaction systems and in vivo. *Journal of Agricultural and Food Chemistry, 49*(11), 5543-5550.

Goodsell, D. S., & Olson, A. J. (1990). Automated docking of substrates to proteins by simulated annealing. *Proteins, 8*(3), 195-202.

Goodwin, J. F., & Choi, S.-Y. (1970). Quantification of protein solutions with trinitrobenzenesulfonic acid *Clinical Chemistry, 16*, 24-31.

Groubet, R., Chobert, J. M., & Haertle, T. (1999). Functional properties of milk proteins glycated in mild conditions. *Sciences des Aliments, 19*, 423-438.

Gruber, P., Becker, W.-M., & Hofmann, T. (2005). Influence of the Maillard reaction on the allergenicity of rAra h 2, a recombinant major allergen from peanut (*Arachis hypogaea*), its major epitopes, and peanut agglutinin. *Journal of Agricultural and Food Chemistry, 53*, 2289-2296.

Gu, F.-L., Kim, J. M., Abbas, S., Zhang, X.-M., Xia, S.-Q., & Chen, Z.-X. (2010a). Structure and antioxidant activity of high molecular weight Maillard reaction products fomr casein-gluose. *Food Chemistry, 120*(2), 505-511.

Gu, F. L., Kim, J. M., Abbas, S., Zhang, X. M., Xia, S. Q., & Chen, Z. X. (2010b). Structure and antioxidant activity of high molecular weight Maillard reaction products from casein-glucose. *Food Chemistry, 120*(2), 505-511.

Havlis, J., Thomas, H., Sebela, M., & Shevchenko, A. (2003). Fast-response proteomics by accelerated in-gel digestion of proteins. *Analytical Chemistry, 75*, 1300-1306.

Hayase, F., Hirashima, S., Okamoto, G., & Kato, H. (1990). Scavenging of active oxygen by melanoidin. In P. A. Finot, H. U. Aeschbacher, R. F. Hurrel & R. Liardon (Eds.), *The Maillard Reaction in Food Processing, Human Nutrition and Physiology*, (pp. 361-366). Basel: Birkhauser Verlag.

Hayashi, T., & Namiki, M. (1980). Formation of two-carbon sugar fragment at an early stage of the browning reaction of sugar with amine. *Agricultural and Biological Chemistry, 44*(11), 2575-2580.

Hefle, S. L., Nordlee, J. A., & Taylor, S. L. (1996). Allergenic foods. *Critical Reviews in Food Science and Nutrition, 36*, S69-S89.

Henle, T. (2005). Protein-bound advanced glycation endproducts (AGEs) as bioactive amino acid derivatives in foods. *Amino Acids, 29*, 313-322.

Hill, S., & Easa, A. M. (1998). Linking proteins using the Maillard reaction and the implications for food processors. In J. O'Brien, H. E. Nursten, M. J. C. Crabbe & J. M. Ames (Eds.), *The Maillard Reaction in Foods and Medicine*, (pp. 133-138). Cambridge, UK: Royal Society of Chemistry.

Hirsch, J., Petrakova, E., Feather, M. S., & Barnes, C. L. (1995). The reaction of $_{D}$-glucose with aminoguanidine. *Carbohydrate Research, 267*, 17-25.

Hodge, J. E. (1953). Chemistry of browning reactions in model systems. *Journal of Agricultural and Food Chemistry, 1*, 928-943.

Hoerl, R. W. (1985). Ridge analysis 25 years later. *American Statistician, 39*, 186-192.

Hofmann, T. (1999). Quantitative studies on the role of browning precursors in the Maillard reaction of pentoses and hexoses with L-alanine. *European Food Research and Technology, 209*(2), 113-121.

Holla, E. W., Schudok, M., Weber, A., & Zulauf, M. (1992). Enzyme-catalyzed synthesis of o-glycopeptide building blocks. *Journal of Carbohydrate Chemistry, 11*(5), 659-663.

Hollnagel, A., & Kroh, L. W. (2000). Degradation of oligosaccharides in nonenzymatic browning by formation of α-dicarbonyl compounds via a "Peeling off" mechanism. *Journal of Agricultural and Food Chemistry, 48*(12), 6219-6226.

Honarparvar, B., Govender, T., Maguire, G. E. M., Soliman, M. E. S., & Kruger, H. G. (2014). Integrated approach to structure-based enzymatic drug design: molecular modeling, spectroscopy, and experimental bioactivity. *Chemical Reviews, 114*, 493-537.

Horie, K., Miyata, T., Maeda, K., Sakai, H., deStrihou, C. V., Monnier, V. M., & Kurokawa, K. (1997). Implication of glycoxidative stress in the pathogenesis of diabetic nephropathy: Co-localization of glycoxidation products and lipid peroxidation products in diabetic renal glomerular lesions. *Journal of the American Society of Nephrology, 8*, A2975-A2975.

Horvat, S., & Jakas, A. (2004). Peptide and amino acid glycation: New insights into the Maillard reaction. *Journal of Peptide Science, 10*, 119-137.

Huang, D., Ou, B., & Prior, R. L. (2005). The chemistry behind antioxidant capacity assays. *Journal of Agricultural and Food Chemistry, 53*(6), 1841-1856.

Huang, M., Liu, P., Song, S., Zhang, X., Hayat, K., Xia, S., Jia, C., & Gu, F. (2011). Contribution of sulfur-containing compounds to the colour-inhibiting effect and improved antioxidant activity of Maillard reaction products of soybean protein hydrolysates. *Journal of the Science of Food and Agriculture, 91*, 710-720.

Huang, M. G., Zhang, X. M., Eric, K., Abbas, S., Hayat, K., Liu, P., Xia, S. Q., & Jia, C. S. (2012). Inhibiting the color formation by gradient temperature-elevating Maillard reaction of soybean peptide-xylose system based on interaction of L-cysteine and Amadori compounds. *Journal of Peptide Science, 18*(5), 342-349.

Huber, R. E., Gaunt, M. T., & Hurlburt, K. L. (1984). Binding and reactivity at the "glucose" site of galactosyl-*b*-galactosidase (*Escherichia coli*). *Archives of Biochemistry and Biophysics, 234*(1), 151-160.

Huber, R. E., Hakda, S., Cheng, C., Cupples, C. G., & Edwards, R. A. (2003). Trp-999 of *β*-galactosidase (*Escherichia coli*) is a key residue for binding, catalysis, and synthesis of allolactose, the natural *Lac* operon inducer. *Biochemistry, 42*, 1796-1803.

Hughey, V. L., & Johnson, E. A. (1987). Antimicrobial activity of lysozyme against bacteria involved in food spoilage and food-borne disease. *Applied and Environmental Microbiology, 53*(9), 2165-2170.

Husain, Q. (2010). *β*-Galactosidases and their potential applications: a review. *Critical Reviews in Biotechnology, 30*(1), 41-62.

Ichikawa, Y., Look, G. C., & Wong, C. H. (1992). Enzyme-catalyzed oligosaccharide synthesis. *Analytical Biochemistry, 202*(2), 215-238.

Iliev, D., & Wuthrich, B. (1998). Occupational protein contact dermatitis with type I allergy to different kinds of meat and vegetables. *International Archives of Occupational and Environmental Health, 71*, 289-292.

Israelachvili, J. (1991) *Intermolecular and Surface Forces* 2nd ed., (pp. 176-311). San Diego: Academic Press.

Jacobson, R. H., Zhang, X. J., DuBose, R. F., & Matthews, B. W. (1994). Three-dimensional structure of *β*-galactosidase from *E. coli*. *Nature, 369*(6483), 761-766.

Jakas, A., Katić, A., Bionda, N., & Horvat, Š. (2008). Glycation of a lysine-containing tetrapeptide by D-glucose and D-fructose - influence of different reaction conditions on the formation of Amadori/Heyns products. *Carbohydrate Research, 343*(14), 2475-2480.

Jegouic, M., Grindberg, V., Guingant, A., & Haertle, T. (1997). Baric oligomerization of *α*-lactalbumin/*β*-lactoglobulin mixtures. *Journal of Agricultural and Food Chemistry, 45*, 19-22.

Jenkins, N., & Curling, E. M. A. (1994). Glycosylation of Recombinant Proteins - Problems and Prospects. *Enzyme and Microbial Technology, 16*(5), 354-364.

Jiménez-Castaño, L., Villamiel, M., & López-Fandiño, R. (2007). Glycosylation of individual whey proteins by Maillard reaction using dextran of different molecular mass. *Food Hydrocolloids, 21*(3), 433-443.

Jiménez-Castaño, L., Villamiel, M., Martín-Álvarez, P. J., Olano, A., & López-Fandiño, R. (2005). Effect of the dry-heating conditions on the glycosylation of *β*-lactoglobulin with dextran through the Maillard reaction. *Food Hydrocolloids, 19*(5), 831-837.

Jiménez-Saiz, R., Belloque, J., Molina, E., & López- Fandiño, R. (2011). Human immunoglobulin E (IgE) binding to heated and glycated ovalbumin and ovomucoid before and after in vitro digestion. *Journal of Agricultural and Food Chemistry, 59*, 10044-10051.

Jindal, S., & Naeem, A. (2013). Consequential secondary structure alterations and aggregation during prolonged casein glycation. *Journal of Fluorescence, 23*(3), 367-374.

Jing, H., Yap, M., & Wong, P. Y. Y. (2011). Comparison of physicochemical and antioxidant properties of egg-white proteins and fructose and inulin Maillard reaction products. *Food Bioprocess Technology, 4*, 1489-1496.

Johansson, E., Hedbys, L., & Larsson, P. O. (1991). Enzymatic synthesis of monosaccharide-amino acid conjugates. *Enzyme and Microbial Technology, 13*(10), 781-787.

Johansson, E., Hedbys, L., Mosbach, K., & Larsson, P. O. (1989). Studies of reversed *α*-mannosidase reaction in high concentrations of mannose. *Enzyme and Microbial Technology, 11*, 347-353.

Joubran, Y., Mackie, A., & Lesmes, U. (2013). Impact of the Maillard reaction on the antioxidant capacity of bovine lactoferrin. *Food Chemistry, 141*, 3796-3802.

Juers, D. H., Heightman, T. D., Vasella, A., McCarter, J. D., Mackenzie, L., Withers, S. G., & Matthews, B. W. (2001). A structural view of the action of *Escherichia coli* (lacZ) *β*-galactosidase. *Biochemistry, 40*(49), 14781-14794.

Juers, D. H., Jacobson, R. H., Wigley, D., Zhang, X. J., Huber, R. E., Tronrud, D. E., & Matthews, B. W. (2000). High resolution refinement of *β*-galactosidase in a new crystal form reveals multiple metal-binding sites and provides a structural basis for *α*-complementation. *Protein Science, 9*(9), 1685-1699.

Karplus, M., & McCammon, A. (2002). Molecular dynamics simulations of biomolecules. *Nature Structural Biology, 9*, 646-652.

Kasran, M., Cui, S. W., & Goff, H. D. (2013). Emulsifying properties of soy whey protein isolate-fenugreek gum conjugates in oil-in-water emulsion model system. *Food Hydrocolloids, 30*, 691-697.

Kato, A. (2000). Maillard-type protein polysaccharide conjugates. In G. Doxastakis & V. Kiosseoglou (Eds.), *Novel Macromolecules in Food Systems*. Amsterdam, Holland: Elsevier Science Ltd.

Kato, A. (2002). Industrial applications of Maillard-type protein-polysaccharide conjugates. *Food Science and Technology Research, 8*, 193-199.

Kato, A., & Kobayashi, K. (1991). Excellent emulsifying properties of protein dextran conjugates. In *Microemulsions and Emulsions in Foods*, vol. 448 (pp. 213-229).

Kato, A., Mifuru, R., Matsudomi, N., & Kobayashi, K. (1992). Functional casein-polysaccharide conjugates prepared by controlled dry heating. *Bioscience, Biotechnology, and Biochemistry, 56*(4), 567-571.

Kato, A., Minaki, K., & Kobayashi, K. (1993). Improvement of emulsifying properties of egg-white proteins by the attachment of polysaccharide through Maillard reaction in a dry state. *Journal of Agricultural and Food Chemistry, 41*(4), 540-543.

Kato, A., Nakamura, S., Takasasi, H., & Maki, S. (1996). Novel functional properties of glycosylated lysozyme constructed by chemical and genetic modifications. . In *Macromolecular Interactions in Food Technology*, (pp. 242-256).

Kato, A., Sasaki, Y., Furuta, R., & Kobayashi, K. (1990). Functional protein polysaccharide conjugate prepared by controlled dry-heating of ovalbumin dextran mixtures. *Agricultural and Biological Chemistry, 54*(1), 107-112.

Kato, Y., Matsuda, T., Kato, N., & Nakamura, R. (1998). Browning and protein polymerization induced by amino-carbonyl reaction of ovalbumin with glucose and lactose. *Journal of Agricultural and Food Chemistry, 36*, 806-809.

Kato, Y., Matsuda, T., Kato, N., Watanabe, K., & Nakamura, R. (1986). Browning and insolubilization of ovalbumin by the Maillard reaction with some aldohexoses. *Journal of Agricultural and Food Chemistry, 34*, 351-355.

Keller, A., Nesvizhskii, A. I., Kolker, E., & Aebersold, R. (2002). Empirical statistical model to estimate the accuracy of peptide identifications made by MS/MS and database search. *Analytical Chemistry, 74*(20), 5383-5392.

Kester, J. J., & Richardson, T. (1984). Modification of whey proteins to improve functionality. *Journal of Dairy Science, 67*(11), 2757-2774.

Khan, M. A. S., Babiker, E. F. E., Azakami, H., & Kato, A. (1999). Molecular mechanism of the excellent emulsifying properties of phosvitin-galactomannan conjugate. *Journal of Agricultural and Food Chemistry, 47*, 2262-2266.

Khmelnitsky, Y. L. (2004). Current strategies for in vitro protein glycosylation. *Journal of Molecular Catalysis B-Enzymatic, 31*(4-6), 73-81.

Kiefer, F., Arnold, K., Künzli, M., Bordoli, L., & Schwede, T. (2009). The SWISS-MODEL repository and associated resources. *Nucleic Acids Research, 37*, 387-392.

Kinsella, J. E. (1979). Functional properties of soy proteins. *Journal of American Oil Chemists Society, 56*, 242-258.

Kinsella, J. E., & Melachouris, N. (1976). Functional properties of proteins in foods: A survey. *Critical Reviews in Food Science and Nutrition, 7*(3), 219-280.

Klibanov, A. M. (1989). Enzymatic catalysis in anhydrous organic solvents. *Trends in Biochemical Sciences, 14*(4), 141-144.

Komarnytsky, S., Cook, A., & Raskin, I. (2011). Potato protease inhibitors inhibit food intake and increase circulating cholecystokinin levels by a trypsin-dependent mechanism. *International Journal of Obesity, 35*, 236-243.

Kong, J., & Yu, S. (2007). Fourier transform infrared spectroscopic analysis of protein secondary structures. *Acta Biochimica et Biophysica Sinica, 39*(8), 549-559.

Koppelman, S. J., van Koningsveld, G. A., Knulst, A. C., Gruppen, H., Pigmans, I. G. A. J., & de Jongh, H. H. J. (2002). Effect of heat-induced aggregation on the IgE binding of patatin (*Sol t 1*) is dominated by other potato proteins. *Journal of Agricultural and Food Chemistry, 50*, 1562-1568.

Kosters, H. A., Broersen, K., De Groot, J., Simons, J.-W. F. A., Wierenga, P. A., & De Jongh, H. H. J. (2003). Chemical processing as a toold to generate ovalbumin variants with changed stability. *Biotechnology and Bioengineering, 84*, 61-70.

Krause, R., Knoll, K., & Henle, T. (2003). Studies on the formation of furosine and pyridosine during acid hydrolysis of different Amadori products *European Food Research and Technology, 216*, 277-283.

Krimm, S., & Bandekar, J. (1986). Bibrational spectroscopy and conformation of peptides, polypeptides, and proteins. *Advanced Protein Chemistry, 38*, 181-364.

Kristinsson, H. G., & Rasco, B. A. (2000). Fish protein hydrolysates: Production, biochemical, and functional properties. *Critical Reviews in Food Science and Nutrition, 40*(1), 43-81.

Kroh, L. W., Jalyschko, W., & Häseler, J. (1996). Non-volatile reaction products by heat-induced degradation of α-glucans. Part I: Analysis of oligomeric maltodextrins and anhydrosugars. *Starch-Starke, 48*(11-12), 426-433.

Labuza, T. P., & Baisier, W. M. (1992). The kinetics of nonenzymatic browning. In H. G. Schwartzberg & R. W. Hastel (Eds.), *Physical Chemistry of Foods*, (pp. 595-689).

Labuza, T. P., & Saltmarch, M. (1981). Kinetics of browning and protein quality loss in whey powders during steady state and non-steady state storage conditions. *Journal of Food Science, 47*, 92-96, 113.

Laemmli, U. K. (1970). Cleavage of structural proteins during the assembly of the head of bacteriophage T4. *Nature, 227*, 680-685.

Lapolla, A., Fedele, D., Garbeglio, M., Martano, L., Tonani, R., Seraglia, R., Favretto, D., Fedrigo, M. A., & Traldi, P. (2000). Matrix-assisted laser desorption/ionization mass spectrometry, enzymatic digestion, and molecular modeling in the study of nonenzymatic glycation of IgG. *Journal of the American Society for Mass Spectrometry, 11*(2), 153-159.

Layer, A., & Fischer, F. (2006). Enzymatic *o*-galactosylation of protected serine and threonine by *β*-galactosidase employing high lactose concentrations. *Industrial & Engineering Chemistry Research, 45*, 6619-6621.

Lederer, M. O., Gerum, F., & Severin, T. (1998). Cross-linking of proteins by Maillard processes - Model reactions of D-glucose or methylglyoxal with butylamine and guanidine derivatives. *Bioorganic & Medicinal Chemistry, 6*, 993-1002.

Ledl, F., & Schleicher, E. (1990). New Aspects of the Maillard Reaction in Foods and in the Human-Body. *Angewandte Chemie-International Edition, 29*(6), 565-594.

Leparoux, S., Padrines, M., Fortun, Y., & Colas, B. (1996). O-glycosylation of dipeptides using *β*-galactosidase activity of *Achatina achatina* digestive juice. *Biotechnology Letters, 18*(2), 135-138.

Lesnierowski, G., & Kijowski, J. (2007). Lysozyme. In R. Huopalahti, R. López Fandiño, M. Anton & R. Schade (Eds.), *Bioactive Egg Compounds*, (pp. 33-42): Springer.

Li, Y., Lu, F., Luo, C., Chen, Z., Mao, J., Shoemaker, C., & Zhong, F. (2009). Functional properties of the Maillard reaction products of rice protein with sugar. *Food Chemistry, 117*(1), 69-74.

Li, Y., Zhong, F., Ji, W., Yokoyama, W., Shoemaker, C. F., Zhu, S., & Xia, W. (2013). Functional properties of Maillard reaction products of rice protein hydrolysates with mono-, oligo- and polysaccharides. *Food Hydrocolloids, 30*, 53-60.

Liu, J., Ru, Q., & Ding, Y. (2012a). Glycation a promising method for food protein modification: Physicochemical properties and structure, a review. *Food Research International, 49*, 170-183.

Liu, Y.-W., Han, C.-H., Lee, M.-H., Hsu, F.-L., & Hou, W.-C. (2003). Patatin, the tuber storage protein of potato (*Solanum tuberosum* L.), exibits antioxidant activity in vitro. *Journal of Agricultural and Food Chemistry, 51*, 4389-4393.

Liu, Y., Zhao, G., Zhao, M., Ren, J., & Yang, B. (2012b). Improvement of functional properties of peanut protein isolate by conjugation with dextran through Maillard reaction. *Food Chemistry, 131*, 901-906.

Liyanage, R., Han, K.-H., Watanabe, S., Shimada, K., Mitsuo, S., Ohba, K., Tokuji, Y., Ohnishi, M., Shibayama, S., Nakamori, T., & Fukushima, M. (2008). Potato and soy peptide diets modulate lipid metabolism in rats. *Bioscience Biotechnology and Biochemistry, 72*(4), 943-950.

Lonsdale, R., Ranaghan, K. E., & Mulholland, A. J. (2010). Computational enzymology. *Chemical Communications, 46*, 2354-2372.

Ma, X. J., Chen, H. B., Gao, J. Y., Hu, C. Q., & Li, X. (2013). Conformation affects the potential allergenicity of ovalbumin after heating and glycation. *Food Additives & Contaminants, Part A: Chemistry, Analysis, Control, Exposure & Risk Assessment, 30*(10), 1684-1692.

Mann, M., & Jensen, O. N. (2003). Proteomic analysis of post-translational modifications. *Nature Biotechnology, 21*, 255-261.

Manzocco, L., Calligaris, S., Mastrocola, D., Nicoli, M. C., & Lerici, C. R. (2000). Review of non-enzymatic browning and antioxidant capacity in processed foods. *Trends in Food Science & Technology, 11*(9-10), 340-346.

Marceau, E., & Yaylayan, A. V. (2009). Profiling of α-dicarbonyl content of commercial honeys from different botanical origins: Identification of 3,4-dideoxyglucoson-3-ene (3,4-DGE) and related compounds. *Journal of Agricultural and Food Chemistry, 57*, 10837-10844.

Marconi, E., Carboni, M. F., Messia, M. C., & Panfili, G. (2002). Furosine: a suitable marker for assessing the freshness of royal jelly. *Journal of Agricultural and Food Chemistry, 50*, 2825-2829.

Martinez-Bilbao, M., & Huber, R. E. (1994). Substitutions for Gly-794 show that binding interactions are important determinants of the catalytic action of *b*-galactosidase (*Escherichia coli*). *Biochemistry and Cell Biology, 72*(7-8), 313-319.

Martins, S. I. F. S., Jongen, W. M. F., & van Boekel, M. A. J. S. (2000). A review of Maillard reaction in food and implications to kinetic modelling. *Trends in Food Science & Technology, 11*(9-10), 364-373.

Matemu, A. O., Kayahara, H., Murasawa, H., & Nakamura, S. (2009). Importance of size and charge of carbohydrate chains in the preparation of functional glycoproteins with excellent emulsifying properties from tofu whey. *Food Chemistry, 114*(4), 1328-1334.

Matsudomi, N., Tsujimoto, T., Kato, A., & Kobayashi, K. (1994). Emulsifying and bactericidal properties of a protamine-galactomannan conjugate prepared by dry heating. *Journal of Food Science, 59*, 428-431.

Matthews, B. W. (2005). The structure of *E. coli* b-galactosidase. *Comptes Rendus Biologies, 328*, 549-556.

Mauron, J. (1990). Influence of processing on protein quality. *Journal of Nutritional Science and Vitaminology, 36*(4), S57-S69.

McClements, D. J. (2004). Protein-stabilized emulsions. *Current Opinion in Colloid & Interface Science, 9*, 305-313.

Meade, S. J., Miller, A. G., & Gerrard, J. A. (2003). The role of dicarbonyl compounds in non-enzymatic crosslinking: a structure-activity study. *Bioorganic & Medicinal Chemistry, 11*(6), 853-862.

Medrano, A., Abirached, C., Panizzolo, L., Moyna, P., & Añón, M. C. (2009). The effect of glycation on foam and structural properties of *β*-lactoglobulin. *Food Chemistry, 113*, 127-133.

Miller, A. G., Meade, S. J., & Gerrard, J. A. (2003). New insights into protein crosslinking via the Maillard reaction: structural requirements, the effect on enzyme function, and predicted efficacy of crosslinking inhibitors as anti-ageing therapeutics. *Bioorganic & Medicinal Chemistry, 11*(6), 843-852.

Miralles, B., Martínez-Rodríguez, A., Santiago, A., van de Lagemaat, J., & Heras, A. (2007). The occurence of a Maillard-type protein-polysaccharide reaction between *β*-lactoglobulin and chitosan. *Food Chemistry, 100*(3), 1071-1075.

Mohammed, Z. H., Hill, S. E., & Mitchell, J. R. (2008). Covalent crosslinking in heated protein systems. *Food Science, 65*, 221-226.

Montgomery, D. C. (2008). *Design and Analysis of Experiments* (7 ed.): Wiley.

Morales, J. F., Romeo, C., & Jimenez-Perez, S. (1996). Fluorescence associated with Maillard reaction in milk-resembling systems. *Food Chemistry, 57*(3), 423-428.

Moreaux, V., & BirlouezAragon, I. (1997). Degradation of tryptophan in heated beta-lactoglobulin-lactose mixtures is associated with intense Maillard reaction. *Journal of Agricultural and Food Chemistry, 45*(5), 1905-1910.

Moreno, F. J., López-Fandiño, R., & Olano, A. (2002). Characterization and functional properties of lactosyl caseinomacropeptide conjugates. *Journal of Agricultural and Food Chemistry, 50*(18), 5179-5184.

Moreno, F. J., Quintanilla-Lopez, J. E., Lebron-Aguilar, R., Olano, A., & Sanz, M. L. (2008). Mass spectrometric characterization of glycated beta-lactoglobulin peptides derived from galacto-oligosaccharides surviving the in vitro gastrointestinal digestion. *Journal of the American Society for Mass Spectrometry, 19*(7), 927-937.

Morgan, F., Leonil, J., Molle, D., & Bouhallab, S. (1999a). Modification of bovine beta-lactoglobulin by glycation in a powdered state or in an aqueous solution: Effect on association behavior and protein conformation. *Journal of Agricultural and Food Chemistry, 47*(1), 83-91.

Morgan, F., Molle, D., Henry, G., Venien, A., Leonil, J., Peltre, G., Levieux, D., Maubois, J. L., & Bouhallab, S. (1999b). Glycation of bovine beta-lactoglobulin: effect on the protein structure. *International Journal of Food Science and Technology, 34*(5-6), 429-435.

Morris, G. M., Goodsell, D. S., Halliday, R. S., Huey, R., Hart, W. E., Belew, R. K., & Olson, A. J. (1998). Automated docking using a Lamarckian generic algorithm and an empirical binding free energy function. *Journal of Computational Chemistry, 19*, 1639-1662.

Morris, G. M., & Lim-Wilby, M. (2008). Molecular docking. In A. Kukol (Ed.), *Molecular Modeling of Proteins*, vol. 443 (pp. 390). Totowa, NJ: Humana Press.

Mossine, V. V., Glinsky, G. V., & Feather, M. S. (1994). The preparation and characterization of some amadori compounds (1-amino-deoxy-D-fructose derivatives) derived from a series of aliphatic omega-amino acids. *Carbohydrate Research, 262*(2), 257-270.

Motoki, M., & Kumazawa, Y. (2000). Recent trends in transglutaminase technology for food processing. *Food Science and Technology Research, 6*, 151-160.

Myers, R., & Montgomery, D. C. (1995). *Response surface methodology: Process and product optimization using designed experiments*. New York: Wiley.

Nacka, F., Chobert, J. M., Burova, T., Leonil, J., & Haertle, T. (1998). Induction of new physicochemical and functional properties by the glycosylation of whey proteins. *Journal of Protein Chemistry, 17*, 495-503.

Nagaraj, R. H., Sarkar, P., Mally, A., Biemel, K. M., Lederer, M. O., & Padayatti, P. S. (2002). Effect of pyridoxamine on chemical modification of proteins by carbonyls in diabetic rats: characterization of a major product from the reaction of pyridoxamine and methylglyoxal. *Archives of Biochemistry and Biophysics, 402*(1), 110-119.

Nagaraj, R. H., Shipanova, I., & Faust, F. M. (1996). Protein cross-linking by the Maillard reaction. Isolation, characterization, and *in vivo* detection of a lysine-lysine cross-link derived from methylglyoxal. *Journal of Biological Chemistry, 271*, 19338-19345.

Nakamura, A., Watanabe, K., Ojima, T., Ahn, D.-H., & Saeki, H. (2005). Effect of Maillard reaction on allergenicity of scallop tropomyosin. *Journal of Agricultural and Food Chemistry, 53*, 2559-2564.

Nakamura, S., Kato, A., & Kobayashi, K. (1991). New antimicrobial characteristics of lysozyme-dextran conjugate. *Journal of Agricultural and Food Chemistry, 39*, 647-650.

Nakamura, S., Kato, A., & Kobayashi, K. (1992). Bifunctional Lysozyme Galactomannan Conjugate Having Excellent Emulsifying Properties and Bactericidal Effect. *Journal of Agricultural and Food Chemistry, 40*(5), 735-739.

Nakamura, S., Kobayashi, K., & Kato, A. (1994). Role of positive charge of lysozyme in the excellent emulsifying properties of Maillard-type lysozyme-polysaccharide conjugate. *Journal of Agricultural and Food Chemistry, 42*(12), 2688-2691.

Nakamura, S., Takasaki, H., Kobayashi, K., & Kato, A. (1993). Hyperglycosylation of hen egg white lysozyme in yeast. *Journal of Biological Chemistry, 268*, 12706-12712.

Namchuk, M. N., McCarter, J. D., Becalski, A., Andrews, T., & Withers, S. G. (2000). The role of sugar substituents in glycoside hydrolysis. *Journal of American Chemical Society, 122*(7), 1270-1277.

Naranjo, G. B., Malec, L. S., & Vigo, M. S. (1998). Reducing sugar effect on available lysine loss of casein by moderate heat treatment. *Food Chemistry, 62*, 309-313.

Nasiri, R., Field, M. J., Zahedi, M., & Moosavi-Movahedi, A. A. (2011). Cross-linking mechanisms of arginine and lysine with α,*β*-dicarbonyl compounds in aqueous solution. *Journal of Physical Chemistry A, 115*(46), 13542-13555.

Nesvizhskii, A. I., Keller, A., Kolker, E., & Aebersold, R. (2003). A statistical model for identifying proteins by tandem mass spectrometry. *Analytical Chemistry, 75*(17), 4646-4658.

Nilsson, K. G. I. (1988). Enzymatic-Synthesis of Oligosaccharides. *Trends in Biotechnology, 6*(10), 256-264.

Nishimura, K., Murakoshi, M., Katayama, S., & Saeki, H. (2011). Antioxidative ability of chicken myofibrillar protein developed by glycosylation and changes in the solubility and thermal stability. *Bioscience Biotechnology and Biochemistry, 75*(2), 247-254.

Niu, L.-Y., Jiang, S.-T., Pan, L.-J., & Zhai, Y.-S. (2011). Characteristics and functional properties of wheat germ protein glycated with saccharides through Maillard reaction. *International Journal of Food Science and Technology, 46*(10), 2197-2203.

Nursten, H. E. (2005). Introduction. In *The Maillard reaction: Chemistry, Biochemistry and Implications*). UK: Royal Society of Chemistry.

O'Regan, J., & Mulvihill, D. M. (2010). Sodium caseinate-maltodextrin conjugate hydrolysates: Preparation, characterisation and some functional properties. *Food Chemistry, 123*, 21-31.

Ogawa, T., Tsuji, H., Bando, N., Kitamura, K., Hirano, H., & Nishikawa, H. (1993). Identification of the soybean allergenic protein gly m Bd 30K with the soybean seed 34 kDa oilbody-associated protein. *Bioscience Biotechnology and Biochemistry, 57*, 1030-1033.

Oimomi, M., Igaki, N., Sakai, M., Ohara, T., Babu, S., & Kato, H. (1989). The effects of aminoguanidine on 3-deoxyglucosone in the Maillard reaction. *Agricultural and Biological Chemistry, 53*, 1727-1728.

Olden, K., Parent, J. B., & White, S. L. (1982). Carbohydrate moieties of glycoproteins a re-evaluation of their function. *Reviews on Biomembranes, 650*(4), 209-232.

Oliver, C. M., Melton, L. D., & Stanley, R. A. (2006a). Creating proteins with novel functionality via the Maillard reaction: A review. *Critical Reviews in Food Science and Nutrition, 46*(4), 337-350.

Oliver, C. M., Melton, L. D., & Stanley, R. A. (2006b). Glycation of caseinate by fructose and fructo-oligosaccharides during controlled heat treatment in the 'dry' state. *Journal of the Science of Food and Agriculture, 86*(5), 722-731.

Oliyai, C., Patel, J. P., Carr, L., & Borchardt, R. T. (1994). Chemical pathways of peptide degradation. VII Solid state chemical instability of an aspartyl residue in a model hexapeptide. *Pharmaceutical Research, 11*(6), 901-908.

Park, S. K., Bae, D. H., & Rhee, K. C. (2000). Soy protein biopolymers cross-linked with glutaraldehyde. *Journal of American Oil Chemists Society, 77*, 879-884.

Pérez-Sánchez, M., Cabrera, Á. C., García-Martín, H., Sinisterra, J. V., García, J. I., & Hernáiz, M. J. (2011). Improved synthesis of disaccharides with *Escherichia coli* b-galactosidase using bio-solvents derived from glycerol. *Tetrahedron, 67*(40), 7708-7712.

Petersen, B., Petersen, T. N., Andersen, P., Nielsen, M., & Lundegaard, C. (2009). A generic method for assignment of reliability scores applied to solvent accessibility predictions. *BMC Structural Biology, 9*, 51.

Pots, A. M., De Jongh, H. H. J., Gruppen, H., Hamer, R. J., & Voragen, A. G. J. (1998). Heat-induced conformational changes of patatin, the major potato tuber protein. *European Journal of Biochemistry, 252*, 66-72.

Pots, A. M., Gruppen, H., Hessing, M., van Boekel, M. A. J. S., & Voragen, A. G. J. (1999a). Isolation ad characterization of patatin isoforms. *Journal of Agricultural and Food Chemistry, 47*, 4587-4592.

Pots, A. M., Gruppen, H., van der Lee, J. J., van Boekel, M. A., Wijngaards, G., & Voragen, A. G. J. (1999b). The effect of storage of whole potatoes of three cultivars on the patatin and protease inhibitor content; a study using capillary electrophoresis and MALDI-TOF mass spectrometry. *Journal of the Science of Food and Agriculture, 79*, 1557-1564.

Pouvreau, L., Gruppen, H., Piersma, S. R., van den Broek, L. A. M., van Koningsveld, G. A., & Voragen, A. G. J. (2001). Relative abundance and inhibitory distribution of protease inhibitors in potato juice from cv. Elkana. *Journal of Agricultural and Food Chemistry, 49*, 2864-2874.

Povey, J. F., Howard, M. J., Williamson, R. A., & Smales, C. M. (2008). The effect of peptide glycation on local secondary structure. *Journal of Structural Biology, 161*, 151-161.

Quan, C., Alcala, E., Petkovska, I., Matthews, D., Canova-Davis, E., Taticek, R., & Ma, S. (2008). A study in glycation of a therapeutic recombinant humanized monoclonal antibody: Where it is, how it got there, and how it affects charge-based behavior. *Analytical Biochemistry, 373*(2), 179-191.

Ralet, M.-C., & Gueguen, J. (1999). Les protéines de pomme de terre: composition, isolement et propriétés fonctionnelles. *Science des Aliments, 19*, 147-165.

Ralet, M.-C., & Gueguen, J. (2000). Fractionation of potato proteins: solubility, thermal coagulation and emulsifying properties. *Lebensmittel-Wissenschaft und-Technologie, 33*, 380-387.

Ralet, M.-C., & Gueguen, J. (2001). Foaming properties of potato raw proteins and isolated fractions. *Lebensmittel-Wissenschaft und-Technologie, 34*, 266-269.

Requena, J. R., Vidal, P., & Cabezas-Cerrato, J. (1993). Aminoguanidine inhibits protein browning without extensive Amadori carbonyl blocking. *Diabetes Research and Clinical Practice, 19*, 23-30.

Resmini, P., Pellegrino, L., & Batelli, G. (1990). Accurate quantification of furosine in milk and dairy products by a direct HPLC method. *Italian Journal of Food Science, 2*(3), 173-183.

Rodríguez Patino, J. M., Carrera, C., & Rodríguez Niño, M. R. (2008). Implications of interfacial characteristics of food forming agents in foam formulations. *Advances in Colloid and Interface Science, 140*, 95-113.

Royer, C. A. (2006). Probing protein folding and conformational transitions with fluorescence. *Chemical Reviews, 106*, 1769-1784.

Rye, C. S., & Withers, S. G. (2000). Glycosidase mechanisms. *Current Opinion in Chemical Biology, 4*, 573-580.

Saeki, H., & Inoue, K. (1997). Improved solubility of carp myofibrillar proteins in low ionic strength medium by glycosylation. *Journal of Agricultural and Food Chemistry, 45*, 3419-3422.

Sakia, R. M. (1992). The Box-Cox transformation technique: a review. *Statistician, 41*, 169-178.

Sanz, M. L., Corzo-Martinez, M., Rastall, R. A., Olano, A., & Moreno, F. J. (2007). Characterization and in vitro digestibility of bovine beta-lactoglobulin glycated with galactooligosaccharides. *Journal of Agricultural and Food Chemistry, 55*(19), 7916-7925.

Sanz, M. L., Polemis, N., Morales, V., Corzo, N., Drakoularakou, A., Gibson, G. R., & Rastall, R. A. (2005). In vitro investigation into the potential prebiotic activity of honey oligosaccharides. *Journal of Agricultural and Food Chemistry, 53*(8), 2914-2921.

Sarabia-Sainz, H. M., Armenta-Ruiz, C., Sarabia-Sainz, J. A., Guzmán-Partida, A. M., Ledesma-Osuna, A. I., Vázquez-Moreno, L., & Montfort, G. R.-C. (2013). Adhesion of enterotoxigenic *Escherichia coli* strains to neoglycans synthesised with prebiotic galactooligosaccharides. *Food Chemistry, 141*, 2727-2734.

Sathe, S. K., Teuber, S. S., & Roux, K. H. (2005). Effects of food processing on the stability of food allergens. *Biotechnology Advances, 23*(6), 423-429.

Sauerbrei, B., & Thiem, J. (1992). Galactosylation and glucosylation by use of *β*-galactosidase. *Tetrahedron Letters, 33*(2), 201-204.

Scaman, C., Nakai, S., & Aminlari, M. (2006). Effect of pH, temperature and sodium bisulfite or cysteine on the level of Maillard-based conjugation of lysozyme with dextran, galactomannan and mannan. *Food Chemistry, 99*(2), 368-380.

Schwarz, R. T., & Datema, R. (1982). The lipid pathway of protein glycosylation and its inhibitors: the biological significance of protein-bound carbohydrates. *Advanced Carbohydrate Chemistry and Biochemistry, 40*, 287-379.

Seo, S., & Karboune, S. (2014). Investigation of the use of Maillard reaction inhibitors for the production of patatin:carbohydrate conjugates. *Bioconjugate Chemistry,* (To be submitted).

Seo, S., Karboune, S., & Archelas, A. (2014a). Production and characterization of potato patatin-galactose, galatooligosaccharides, and galactan conjugates of great potential as functional ingredients. *Food Chemistry, 158*(1), 480-489.

Seo, S., Karboune, S., L'Hocine, L., & Yaylayan, V. (2013). Characterization of glycated lysozyme with galactose, galactooligosaccharides and galactan: Effect of glycation on structural and functional properties of conjugates. *LWT - Food Science and Technology, 53*(1), 44-53.

Seo, S., Karboune, S., Yaylayan, V. A., & L'Hocine, L. (2012). Glycation of lysozyme with galactose, galactooligosaccharides and potato galactan through the Maillard reaction and optimization of the production of prebiotic glycoproteins. *Process Biochemistry, 47*(2), 297-304.

Seo, S., L'Hocine, L., & Karboune, S. (2014b). Allergenicity of potato proteins and of their conjugates with galactose, galactooligosaccharides, and galactan in native, heated, and digested forms. *Journal of Agricultural and Food Chemistry*. *62*(16), 3591-3598..

Seppala, U., Alenius, H., Turjanmaa, K., Reunala, T., Palosuo, T., & Kalkkinen, N. (1999). Identification of patatin as a novel allergen for children with positive skin prick test responses to raw potato. *Journal of Allergy and Clinical Immunology, 103*, 165-171.

Seppala, U., Majamaa, H., Turjanmaa, K., Helin, J., Reunala, T., Kalkkinen, N., & Palosuo, T. (2001). Identification of four novel potato (*Solanum tuberosum*) allergens belonging to the family of soybean trypsin inhibitors. *Allergy, 56*, 619-626.

Sharma, N., Gruszewski, H. A., Park, S.-W., Holm, D. G., & Vivanco, J. M. (2004). Purification of an isoform of patatin with antimicrobial activity against *Phytophthora infestans*. *Plant Physiology and Biochemistry, 42*, 647-655.

Shepherd, R., Robertson, A., & Ofman, D. (2000). Dairy glycoconjugate emulsifiers: casein-maltodextrins. *Food Hydrocolloids, 14*, 281-286.

Shevchenko, A., Wilm, M., Vorm, O., & Mann, M. (1996). Mass spectrometric sequencing of proteins from silver-stained polyacrylamide gels. *Analytical Chemistry, 68*, 850-858.

Shieber, A., Stintzing, F. C., & Carle, R. (2001). By-products of plant food processing as a source of functional compounds. Recent developments. *Trends in Food Science & Technology, 12*, 401.

Shu, Y.-W., Sahara, S., Nakamura, S., & Kato, A. (1996). Effects of the length of polysaccharide chains on the functional properties of the Maillard-type lysozyme-polysaccharide conjugate. *Journal of Agricultural and Food Chemistry, 44*(9), 2544-2548.

Singh, H. (1991). Modification of food proteins by covalent crosslinking. *Trends in Food Science & Technology, 2*, 196-200.

Sinnott, M. L. (1990). Catalytic Mechanisms of Enzymatic Glycosyl Transfer. *Chemical Reviews, 90*(7), 1171-1202.

Song, Y., Babiker, E. E., Usui, M., Saito, A., & Kato, A. (2002). Emulsifying properties and bactericidal action of chitosan-lysozyme conjugates. *Food Research International, 35*(5), 459-466.

Stierand, K., Maab, P., & Rarey, M. (2006). Molecular complexes at a glance: Automated generation of two-dimentional complex diagrams. *Bioinformatics, 22*, 1710-1716.

Suarez, G., Etlinger, D. J., Maturana, J., & Weitman, D. (1995). Fructated protein is more resistant to ATP-dependent proteolysis than glucated protein possibly as a result of higher content of Maillard fluorophores. *Archives of Biochemistry and Biophysics, 321*(1), 209-213.

Suarez, G., Maturana, J., Oronsky, A. L., & Raventos-Suarez, C. (1991). Fructose induced fluoresence generation of reductively methylated glycated bovine serum albumin: evidence for nonenzymatic glycation of Amadori products. *Biochimica and Biophysica Acta, 1075*, 12-19.

Sun, Y., Hayakawa, S., Chuamanochan, M., Fujimoto, M., Innun, A., & Izumori, K. (2006). Antioxidant effects of Maillard reaction products obtained from ovalbumin and different D-aldohexoses. *Bioscience Biotechnology and Biochemistry, 70*, 598-605.

Sun, Y., Jiang, L., & Wei, D. (2013). Partial characterization, *in vitro* antioxidant and antiproliferative activities of patatin purified from potato fruit juice. *Food & Function, 4*, 1502-1511.

Surewicz, W. K., & Mantsch, H. H. (1988). New insight into protein secondary structure from resolution-enhanced infrared spectra. *Biochimica and Biophysica Acta, 952*, 115-130.

Susi, H., & Byler, D. M. (1983). Protein structure by fourier transform infrared spectroscopy: Second derivative spectra. *Biochemical and Biophysical Research Communications, 115*, 391-397.

Susi, H., & Byler, D. M. (1986). Resolution-enhanced Fourier transform spectroscopy of enzymes. *Methods in Enzymology, 130*, 290-311.

Tagami, U., Akashi, S., Mizukoshi, T., Suzuki, E., & Hirayama, K. (2000). Structural studies of the Maillard reaction products of a protein using ion trap mass spectrometry. *Journal of Mass Spectrometry, 35*, 131-138.

Taheri-Kafrani, A., Gaudin, J.-C., Rabesona, H., Nioi, C., Agarwal, D., Drouet, M., Chobert, J.-M., Bordbar, A.-K., & Haertlé, T. (2009). Effects of heating and glycation of *β*-lactoglobulin on its recognition by IgE of sera from cow milk allergy patients. *Journal of Agricultural and Food Chemistry, 57*(11), 4974-4982.

Takahashi, K., Lou, X. F., Ishii, Y., & Hattori, M. (2000). Lysozyme-glucose stearic acid monoester conjugate formed through the Maillard reaction as an antibacterial emulsifier. *Journal of Agricultural and Food Chemistry, 48*(6), 2044-2049.

Taylor, R. D., Jewsbury, P. J., & Essex, J. W. (2002). A review of protein-small molecule docking methods. *Journal of Computer-Aided Molecular Design, 16*(3), 151-166.

Teleman, A., Tenkanen, M., Jacobs, A., & Dahlman, O. (2002). Characterization of *O*-acetyl-(4-*O*-methylglucurono)xylan isolated from birch and beech. *Carbohydrate Research, 337*(4), 373-377.

ter Haar, R., Schols, H. A., & Gruppen, H. (2011). Effect of saccharide structure and size on the degree of substitution and product diversity of α-lactalbumin glycated via the Maillard reaction. *Journal of Agricultural and Food Chemistry, 59*, 9378-9385.

Tessier, F. J., Monnier, V. M., Sayre, L. M., & Kornfield, J. A. (2003). Triosidines: novel Maillard reaction products and cross-links from the reaction of triose sugars with lysine and arginine residues. *Biochemical Journal, 369*, 705-719.

Thornalley, P., Wolff, S., Crabbe, J., & Stern, A. (1984). The autoxidation of glyceraldehyde and other simple monosaccharides under physiological conditions catalysed by buffer ions. *Biochimica and Biophysica Acta, 797*(2), 276-287.

Thornalley, P. J., Langborg, A., & Minhas, H. S. (1999). Formation of glyoxal, methylglyoxal and 8-deoxyglucosone in the glycation of proteins by glucose. *Biochemical Journal, 344*, 109-116.

Thornalley, P. J., Yurek-George, A., & Argirov, O. K. (2000). Kinetics and mechanism of the reaction of aminoguanidine with the α-oxoaldehydes glyoxal, methylglyoxal, and 3-deoxyglucosone under physiological conditions. *Biochemical Pharmacology, 60*(1), 55-65.

Tomizawa, H., Yamada, H., & Imoto, T. (1994). The mechanism of irreversible inactivation of lysozyme at pH 4 and 100°C. *Biochemistry, 33*(44), 13032-13037.

Toone, E. J., Simon, E. S., Bednarski, M. D., & Whitesides, G. M. (1989). Enzyme-Catalyzed Synthesis of Carbohydrates. *Tetrahedron, 45*(17), 5365-5422.

Tovchigrechiko, A., & Vakser, I. A. (2006). GRAMM-X public web server for protein-protein docking. *Nucleic Acids Research, 34*, W310-W314.

Trofimova, D., & de Jongh, H. H. J. (2004). Modification of *β*-lactoglobulin by oligofructose: Impact on protein adsorption at the air-water interface. *Langmuir, 20*, 5544-5552.

Trott, O., & Olson, A. J. (2010). AutoDock Vina: Improving the speed and accuracy of docking with a new scoring function, efficient optimization, and multithreading. *Journal of Computational Chemistry, 31*(2), 455-461.

Turgeon, S. L., Schmitt, C., & Sanchez, C. (2007). Protein-polysaccharide complexes and coarcervates. *Current Opinion in Colloid & Interface Science, 12*, 166-178.

Udatha, D. B. R. K. G., Sugaya, N., Olsson, L., & Panagiotou, G. (2012). How well do the substrates KISS the enzyme? Molecular docking program selection for feruloyl esterases. *Scientific Reports, 2*, 1-8.

Usui, M., Tamura, H., Nakamura, K., Ogawa, T., Muroshita, M., Azakami, H., Kanuma, S., & Kato, A. (2004). Enhanced bactericidal action and masking of allergen structure of soy protein by attachment of chitosan through Maillard-type protein-polysaccharide conjugation. *Nahrung, 48*, 69-72.

Usui, T., Yanagisawa, S., Ohguchi, M., Yoshino, M., Kawabata, R., Kishimoto, J., Arai, Y., Aida, K., Watanabe, H., & Hayase, F. (2007). Identification and determination of *α*-dicarbonyl compounds formed in the degradation of sugars. *Bioscience, Biotechnology, and Biochemistry, 71*(10), 2465-2472.

van Boekel, M. A. (2001). Kinetic aspects of the Maillard reaction: a critical review. *Nahrung, 45*(3), 150-159.

Vissers, Y. M., Blanc, F., Skov, P. S., Johnson, P. E., Rigby, N. M., Przybylski-Nicaise, L., Bernard, H., Wal, J.-M., Ballmer-Weber, B., Zuidmeer-Jongejan, L., Szepfalusi, Z., Ruinemans-Koerts, J., Jansen, A. P. H., Savelkoul, H. F. J., Wichers, H. J., Mackie, A. R., Mills, C. E. N., & Adel-Patient, K. (2011). Effect of heating and glycation on the allergenicity of 2S albumins (Ara h 2/6) from peanut. *PLoS One, 6*(8), e23998.

Voziyan, P. A., Metz, T. O., Baynes, J. W., & Hudson, B. G. (2002). A post-Amadori inhibitor pyridoxamine also inhibits chemical modification of proteins by scavenging carbonyl

intermediates of carbohydrate and lipid degradation. *Journal of Biological Chemistry, 277*(5), 3397-3403.

Waglay, A., Karboune, S., & Alli, I. (2014). Potato protein isolates: Recovery and characterization of their properties. *Food Chemistry, 142*, 373-382.

Wahl, R., Lau, S., Maasch, H. J., & Wahn, U. (1990). IgE mediated allergic reactions to potatoes. *International Archives of Allergy and Immunology, 92*(2), 168-174.

Wang, Q., & Ismail, B. (2012). Effect of Maillard-induced glycosylation on the nutritional quality, solubility, thermal stability and molecular configuration of whey protein. *International Dairy Journal, 25*, 112-122.

Watkins, N. G., Negliafisher, C. I., Dyer, D. G., Thorpe, S. R., & Baynes, J. W. (1987). Effect of phosphate on the kinetics and specificity of glycation of protein. *Journal of Biological Chemistry, 262*(15), 7207-7212.

Welinder, K. G., & Jørgensen, M. (2009). Covalent structures of potato tuber lipases (patatins) and implications for vacuolar import. *Journal of Biological Chemistry, 284*(15), 9764-9769.

Wells-Knecht, K. J., Zyzak, D. V., Litchfield, J. E., Thorpe, S. R., & Baynes, J. W. (1995). Mechanism of autoxidative glycosylation: Identification of glyoxal and arabinose as intermediates in the autoxidative modification of proteins by glucose. *Biochemistry, 34*, 3702-3709.

Wijewickreme, A. N., Kitts, D. D., & Durance, T. D. (1997). Reaction conditions influence the elementary composition and metal chelating affinity of non-dialyzable model Maillard reaction products. *Journal of Agricultural and Food Chemistry, 45*(12), 4577-4583.

Wong, B. T., Day, L., & Augustin, M. A. (2011). Deamidated wheat protein-dextran Maillard conjugates: Effect of size and location of polysaccharide conjugated on steric stabilization of emulsions at acidic pH. *Food Hydrocolloids, 25*(6), 1424-1432.

Wooster, T. J., & Augustin, M. A. (2006). beta-Lactoglobulin-dextran Maillard conjugates: Their effect on interfacial thickness and emulsion stability. *Journal of Colloid and Interface Science, 303*(2), 564-572.

Wooster, T. J., & Augustin, M. A. (2007). Rheology of whey protein-dextran conjugate films at the air/water interface. *Food Hydrocolloids, 21*, 1072-1080.

Wu, H., Govidarajan, S., Smith, T., Rosen, J. D., & Ho, C.-T. (1990). Glucose-lysozyme in a restricted water environment. In P. A. Finot, H. U. Aeschbacher, R. F. Hurrel & R. Liardon (Eds.), *The Maillard Reaction in Food Processing, Human Nutrition and Physiology*, (pp. 85-90). Basel: Birkhauser Verlag.

Xu, Q. P., Tao, W. Y., & Ao, Z. H. (2007). Antioxidant activity of vinegar melanoidins. *Food Chemistry, 102*(3), 841-849.

Yang, L., Dordick, J. S., & Garde, S. (2004). Hydration of enzyme in nonaqueous media is consistent with solvent dependence of its activity. *Biophysical Journal, 87*, 812-821.

Yaylayan, A. V., & Huyghues-Despointes, A. (1994). Chemistry of Amadori rearrangement products: analysis, synthesis, kinetics, reactions and spectroscopic properties. *Critical Reviews in Food Science and Nutrition, 34*(4), 321-369.

Yaylayan, A. V., Ismail, A. A., & Mandeville, S. (1993). Quantitative determination of the effect of pH and temperature on the keto form of D-fructose by FTIR spectroscopy. *Carbohydrate Research, 248*, 355-360.

Yeboah, A., & Yaylayan, A. V. (2001). Analysis of glycated proteins by mass spectrometric techniques: qualitative and quantitative aspects. *Nahrung, 45*, 164-171.

Yeboah, F. K., Alli, I., & Yaylayan, V. A. (1999). Reactivities of D-glucose and D-fructose during glycation of bovine serum albumin. *Journal of Agricultural and Food Chemistry, 47*(8), 3164-3172.

Yeboah, F. K., Alli, I., Yaylayan, V. A., Konishi, Y., & Stefanowicz, P. (2000). Monitoring glycation of lysozyme by electrospray ionization mass spectrometry. *Journal of Agricultural and Food Chemistry, 48*(7), 2766-2774.

Yeboah, F. K., Alli, I., Yaylayan, V. A., Yasuo, K., Chowdhury, S. F., & Purisima, E. O. (2004). Effect of limited solid-state glycation on the conformation of lysozyme by ESI-MSMS peptide mapping and molecular modeling. *Bioconjugate Chemistry, 15*, 27-34.

Yoo, J., & Medina-Franco, J. L. (2011). Homology modeling, docking and structure-based pharmacophore of inhibitors of DNA methyltransferase. *Journal of Computer-Aided Molecular Design, 25*(6), 555-567.

Yoshida, T., & Lee, Y. C. (1994). Glycamine formation via reductive amination of oligosaccharides with benzylamine: efficient coupling of oligosaccharides to protein. *Carbohydrate Research, 251*, 175.

Zheng, Z., Luo, Y., Yao, L., Lu, J., & Bu, G. (2013). Effects of Maillard reaction conditions on the functional properties of WPI chitosan oligosaccharide conjugates. *Journal of Food Science and Technology*, 1-9.

Zhong, J. Z., Xu, Y. J., Liu, W., Liu, C. M., Luo, S. J., & Tu, Z. C. (2013). Antigenicity and functional properties of *β*-lactoglobulin conjugated with fructo-oligosaccharides in relation to conformational changes. *Journal of Dairy Science, 96*, 2808-2815.